REAL-TIME MONITORING OF NITRIC OXIDE RELEASE

A THESIS

SUBMITTED IN PARTIAL FULFILMENT OF THE

REQUIREMENTS

OF THE DEGREE OF

DOCTOR OF PHILOSOPHY

BY

RAVIKUMAR. G

20133239

INDIAN INSTITUTE OF SCIENCE EDUCATION AND

RESEARCH PUNE – 411 008

2018

Dedicated to…

My Mother

भारतीयविज्ञानशिक्षाएवंअनुसंधानसंस्थान, पुणे
INDIAN INSTITUTE OF SCIENCE EDUCATION AND RESEARCH (IISER), PUNE
(An Autonomous Institution, Ministry of Human Resource Development, Govt. of India)
900 NCL Innovation Park Dr Homi Bhabha Road Pune 411008

Harinath Chakrapani, Ph.D.
Associate Professor – Chemistry
www.iiserpune.ac.in/~harinath/

CERTIFICATE

Certified that, the work incorporated in the thesis entitled, "***Real-time Monitoring of Nitric oxide Release***" submitted by ***Ravikumar. G*** was carried out by the candidate, under my supervision. The work presented here or any part of it has not been included in any other thesis submitted previously for the award of any degree or diploma from any other University or institution.

Date: 30th July 2018 **Dr. Harinath Chakrapani**

Pune (MH), India.

DECLARATION

I declare that this written submission represents my ideas in my own words and where others' ideas have been included; I have adequately cited and referenced the original sources. I also declare that I have adhered to all principles of academic honesty and integrity and have not misrepresented or fabricated or falsified any idea/data/fact/source in my submission. I understand that violation of the above will be cause for disciplinary action by the Institute and can also evoke penal action from the sources which have thus not been properly cited or from whom proper permission has not been taken when needed.

Date: 30th July 2018 **Ravikumar. G**

Pune (MH), India. **20133239**

Table of Contents

General remarks

- ^{1}H NMR spectra were recorded on JEOL ECX 400 MHz spectrometer using tetramethylsilane (TMS) as an internal standard. Chemical shifts are expressed in ppm units downfield to TMS.
- ^{13}C NMR spectra were recorded on JEOL ECX 100 MHz spectrometer.
- Mass spectra were obtained using HRMS-ESI-Q-Time of Flight LC-MS (Synapt G2, Waters) or MALDI TOF/TOF Analyser (Applied Biosystems 4800 Plus).
- FT-IR spectra were obtained using NICOLET 6700 FT-IR spectrophotometer as KBr disc or Bruker Alpha-FT-IR spectrometer and reported in cm^{-1}.
- All reactions were monitored by Thin-Layer Chromatography carried out on precoated Merck silica plates (F254, 0.25 mm thickness); compounds were visualized by UV light.
- All reactions were carried out under nitrogen or argon atmosphere with freshly dried solvents under anhydrous conditions and yields refer to chromatographically homogenous materials unless otherwise stated.
- All evaporators were carried out under reduced pressure on Büchi and Heildoph rotary evaporator below 45 °C unless otherwise specified.
- Silica gel (60-120) and (100-200) mesh were used for column chromatography.
- Materials were obtained from commercial suppliers and were used without further purification.
- Semi-preparative HPLC purification was performed using high performance liquid chromatography (HPLC), Dionex ICS-3000 model and preparative HPLC with C-18 preparative column (21.2 mm × 250 mm, 10 μm; Kromasil C18).
- HPLC analysis data was obtained using Agilent Technologies 1260 Infinity, C18 reversed phase column (4.6 mm × 250 mm, 5 μm).
- NO was detected using Sievers Nitric Oxide Analyzer (NOA 280i).
- Spectrophotometric and fluorimetric measurements were performed using Thermo Scientific Varioscan microwell plate reader.
- Scheme, Figure and Compound numbers in abstract and individual chapters are different.

Abbreviations

Ac – Acetyl

ACN – Acetonitrile

AcOH – Acetic acid

Ac_2O – Acetic anhydride

AIBN – Azobisisobutyronitrile

au – Arbitrary unit

BH_4 – Biopterin

BRET – Bioluminescence resonance energy transfer

bs – Broad singlet

^tBuOH – Tertiary-butanol

Bu_3SnH – Tributyl tin hydride

Calcd – Calculated

CaM – Calmodulin

$CDCl_3$ – Chloroform-D

$CHCl_3$ – Chloroform

c-PTIO – 2-(4-carboxyphenyl)-4,4,5,5-tetramethylimidazoline-1-oxyl-3-oxide potassium salt

Ctrl – Control

$Cu(OAc)_2$ – Copper acetate

CV – Cyclic voltammetry

DAPI – 4', 6-Diamidino-2-phenylindole

dd – Doublet of doublet

DCM – Dichloromethane

DMAP – *N*, *N*-Dimethylaminopyridine

DMEM – Dulbecco's Modified Eagle's Medium

DMF – *N*, *N*'-Dimethyl formamide

DMSO – Dimethyl sulfoxide

DNA – Deoxyribonucleic acid

DPBS – Dulbecco's Phosphate-Buffered Saline

DSBs – Double strand breaks

dt – Doublet of triplet

DT-D – DT-Diaphorase

DTPA – Diethylene triamine pentaacetic acid

δ – Delta (in ppm)

E. coli – Escherichia coli

equiv. – Equivalents

ES – Esterase

ESI – Electron spray ionization

Et_3N – Triethylamine

EtOH – Ethanol

EtOAc – Ethyl acetate

Et_2O – Diethyl ether

FACS – Fluorescence Activated Cell Sorting

FAD – Flavin-adenine-dinucleotide

FBS – Fetal bovine serum

FMN – Flavin-mononucleotide

g – Gram

GDEPT – Gene Directed Enzyme Prodrug Therapy

GFP – Green fluorescence protein

GSH – Glutathione

GS-T – Glutathione S-Transferase

h – Hours

HBSS – Hank's Balanced Salt Solution

HCl – Hydrochloric acid

HEK – Human embryonic kidney

HIF – Hypoxia Inducible Factor

H_2O – Water

H_2O_2 – Hydrogen peroxide

HNO_3 – Nitric acid

HPLC – High performance liquid chromatography

HRMS – High-resolution mass spectrometry

Hz – Hertz

IC_{50} – Half maximal inhibitory concentration

IR – Infrared

J – Coupling constant

K_2CO_3 – Potassium carbonate

LB – Luria-Bertani

λ_{ex} – Excitation wavelength

λ_{em} – Emission wavelength

m – Multiplet

MALDI – Matrix-Assisted Laser Desorption Ionization

MDR – Multidrug resistant

Me – Methyl

MeOH – Methanol

mg – Milligram

MIC – Minimum inhibitory concentration

Min. – Minutes

MHz – Megahertz

mL – Millilitre

MMC – Mitomycin C

mM – Millimolar

mmol – Millimoles

m.p. – Melting point

MRP – Multidrug resistant proteins

MS – Mass spectrum

M. smeg – Mycobacterium smegmatis

Mtb – Mycobacterium tuberculosis

MTT – 3-(4,5-Dimethylthiazol-2-yl)-2,5-diphenyltetrazolium bromide

MW – Molecular weight

m/z – Mass to Charge ratio

µM – Micromolar

$NaBH_4$ – Sodium borohydride

NAcCys – *N*-acetyl cysteine

NADPH – Reduced nicotinamide-adenine-dinucleotide phosphate

NaH – Sodium hydride

$NaHCO_3$ – Sodium bicarbonate

NaI – Sodium iodide

$NaIO_4$ – Sodium periodate

$NaNO_2$ – Sodium nitrite

NaOCl – Sodium hypochlorite

Na_2SO_4 – Sodium sulphate

NBS – *N*-Bromosuccinimide

NH_4Cl – Ammonium chloride

n-BuLi – *n*-Butyllithium

NMO – *N*-Methyl morpholine *N*-oxide

NMR – Nuclear magnetic resonances

NO – Nitric oxide

NO^{2-} – Nitrite

NO^{3-} – Nitrate

NOA – Nitric oxide analyser

NOS – Nitric oxide synthase

nM – Nanomolar

NTR – Nitroreductase

O.D – Optical density

$^{\bullet}OH$ – Hydroxyl radical

$O_2^{\bullet-}$ – Superoxide radical

$ONOO^-$ – Peroxynitrite

OsO_4 – Osmium tetraoxide

PBr_3 – Phosphorous tribromide

PBS – Phosphate buffered saline

Pd – Palladium

$Pd(OAc)_2$ – Palladium acetate

$Pd(PPh_3)$ – Tetrakis(triphenylphosphine)palladium(0)

PET – Photo induced electron transfer

pH – Potential of hydrogen

Ph – Phenyl

$POCl_3$ – Phosphorous oxychloride

PPh_3 – Triphenyl phosphine

Py – Pyridine

ppm – Parts per million

% – Per cent

RFI – Relative fluorescence intensity

R*f* – Retention factor

Rluc – *Renilla* luciferase

RNS − Reactive nitrogen species

ROS – Reactive oxygen species

RPMI Medium – Roswell Park Memorial Institute Medium

RT – Room temperature

s – Singlet

SA – *Staphylococcus aureus*

sGC – soluble guanylate cyclase

SOD – Superoxide dismutase

SiO_2 – Silica

SNAP – *S*-Nitroso-*N*-acetylpenicillamine

SNP– Sodium nitroprusside

t – Triplet

TBHP – *tert*-butyl hydroperoxide

TEA – Triethylamine

TEMPO – 2,2,6,6-tetramethylpiperidinyloxy

TFA – Trifluoroacetic acid

THF – Tetrahydrofuran

TLC – Thin layer chromatography

TMS – Tetramethylsilane

TRIS – Tris(hydroxymethyl)aminomethane

UV – ultraviolet

µg – Microgram

µmol– Micromolar

µL – Microliter

µm – Micrometre

XRD – X-ray diffraction

WT – Wild type

Zn – Zinc

Acknowledgements

First of all, I would like to express my heartfelt gratitude to my supervisor, Associate Professor Dr. Harinath Chakrapani, for his immeasurable intellectual input, constant guidance, valuable suggestions, unparalleled encouragement and efficient support throughout my years of study. I have been extremely lucky to have a supervisor who cared so much about my work, and who responded to my questions and queries so promptly. He acted as a positive catalyst in my professional as well as personal life to reach this milestone.

I would like to express my gratitude to RAC members Dr. D. Srinivasa Reddy (NCL Pune), Prof. Manickam Jayakannan (IISER Pune, chair of chemistry) for their valuable suggestions and feedback during RAC evaluations. I wish to express many thanks to our collaborators Dr. Deepak Saini kumar (IISc) and Dr. Siddhesh Kamat (IISER Pune) for their efficient research support. Special thanks to Dr. Meisam Bagheri for motivating me towards new projects. I thank all the IISER Pune chemistry faculty members for their constant support and encouragement.

I would like to extend my thanks to my colleagues in the Hari's group. Dr. Satish Malwal, Dr. A. T. Dharmaraja, Dr. Kavitha Sharma, Dr. Vinayak, Dr. Viraj, Dr. Kundan (Kundan Sir), Dr. Ritu, Dr. Vijay, R. Sankar, Abhijeet, Rohan, Charu, Sushma, Sharath, Charu, Abhishek, Shreyas, Amogh, Preeti, Ajay, Bandana, Prerona, Harsha, Shweta, Komal, Mrutunjay (MJ), Mrs. Beula, Anand, Pooja, Laxman, Ashwin, Suman, Gaurav, Bhakti, Minhaj, Dr. Amol, Sourab. They all have made my life in IISER happier and memorable. It has been a really enjoyable experience to work in this friendly group.

In IISER, I was fortunate to make good friends and I express my gratitude to all of them. Special thanks to Dr. Manikandan and Dr. Trimbak Mete, S. Balamurugan, Dr. S. Ananth Raj, Dr. Shivaji A. Thadke, Dr. Mothukuri Ganesh Kumar, Dr. Sandip Jadhav, Vijayakanth, Dr. Karnati Narsimha, Rajasekar, Manoharan, Alagar Raja, Nandha Kumar, Dr. Kiran reddy, Dr. Nagesh More, Sudeshna Manna, Sopan Shinde, Metikoti Jagadeeswararao, Veeresh, Shiva Shankar, Aamod V. Desai, Nilesh Deshpande, Bijoy Mishra, Mahesh Neralkar, Dinesh Mullangi, Rajkumar, Yashwant Kumar.

I wish to thank Ankitha Shetty, Simran Kaur, Libi Anandi for giving their time and teaching me biology.

A special thanks to Mayuresh, Mahesh, Yathish, Nayna, Tushar, and Prabhas for their administrative help throughout my doctoral study. Swati (MALDI-TOF), Swati, Nayna and Sandip (HRMS), Deepali, Chinmay, Pooja and Nitin (NMR), Archana (XRD), Ganesh (IR), Vijay vithal (Confocal), Suresh Kumar (IT).

I wish to thank all my teachers at various stages of my education, especially Prof. S. Perumal, Prof. S. Muthusubramanian, Dr. R. Ranjith Kumar (MSc, Madurai Kamaraj University) and Dr. V. Senthilkumar (BSc, Govt. Arts College, Salem) for motivating me at all the times for pursuing science.

My science journey started because of Dr. A. P. J. Aabdul kalam, an excellent scientist and former President of India, my sincere thanks to him for inspiring me always.

Sports is one of my enjoyment other than research, I would like to thank all the "ALCHEMIST" team players for giving opportunity to play enjoyable cricket.

My special thanks to my best friends Mr. S. Vellaiyadevan, Mr. Angamuthu, Dr. Manikandan, Dr. Trimbak mete, my brother Dr. Dharmaraja, my sisters Dr. Kavita Sharma, Dr. Dhanalakshmi and Preeti chauhan. These are the people always encouraged and supported me in my research as well as personal life.

Finally, I would like to acknowledge the most important people in my life - my mother Malliga Govindan, my wife Kavitha Ravikumar and my uncle Mr. Sanmugam, Mr. Seenivasan for everything.

Ravikumar

****

ABSTRACT

Nitric oxide (NO) is an endogenously produced gaseous signalling molecule with cancer therapeutic potential. Since NO is unstable under ambient conditions, it is difficult to generate as well as reliably detect this gas. Although a number of methodologies for enhancement as well as detection of NO are available, these events are typically mutually exclusive. The most common problem during NO delivery and concomitant detection is consumption of NO. Thus, a strategy where a small molecule can generate NO in a controlled manner to the cancer cells selectively along with a fluorescence reporter for NO would be useful for NO based cancer therapy. As a proof-of-concept, we first designed and synthesized FLUORO/NO, a new class of triggerable NO donors with an in-built fluorescence reporter. Upon activation by an esterase enzyme the compound produces NO as well as a fluorescence signal simultaneously, without NO consumption. Cellular studies with a FLUORO/NO derivative revealed a dose-dependent enhancement of NO as well as fluorescence. Next, in order to deliver NO selectively to cancer cells, a second stimulus for activation was chosen: hydrogen peroxide (H_2O_2), a reactive oxygen species (ROS). As ROS is frequently found to be elevated in rapidly dividing cells such as cancers, H_2O_2 has been previously used to specifically activate prodrugs and latent fluorophores (as imaging agents) in cancers. Boronate ester is known to react with H_2O_2 to produce an alcohol; hence this functional group was chosen as the metabolic stimulus. We designed and synthesized a series of arylboronate ester based diazeniumdiolates (BORO/NO). Having established that BORO/NO derivatives are capable of generating NO when triggered by H_2O_2, next we synthesized Thera/NO, a H_2O_2 activated NO donor with fluorescence reporter. Upon activation by H_2O_2 in buffer, a nearly quantitative correlation between fluorescence signal and NO generation is observed. When encountered with cellular situations with varying ROS levels, Thera/NO is observed to preferentially generate NO in cell lines with elevated ROS levels. Together, we have developed a convenient tool to enhance NO selectively in cancer cells and allows real-time monitoring of NO release without collateral consumption of NO. Further adaption of this technology to better direct NO to cancers is possible.

In addition to NO, a number of other redox active reactive species have important biological roles. Controlled generation as well as reliable detection of these species is

challenging. In order to assess the generality of the method developed herein, we aimed to develop a ROS generator with a fluorescence reporter. This tool would be useful to deliver and real-time monitor ROS generation in cells without the need for secondary assays.

CHAPTER 1: Introduction

1.1. Nitric oxide

Nitric oxide (NO) is a colourless paramagnetic free radical gas, discovered by Joseph Priestley in 1772. NO, initially considered as a toxic and carcinogenic air pollutant produced from fuel burning, became the 'molecule of the year' in 1992 on the cover story of *Science* due to the discovery of its wide range of biological functions, including smooth muscle relaxation, inhibition of platelet aggregation, neurotransmission and host defense mechanisms.[1-5] This remarkable discovery was honoured with the Nobel Prize in the field of Medicine and Physiology to Ferid Murad, Loius J. Ignarro and Robert F. Furchgott for discovering NO as major signalling molecule in the cardiovascular system. Subsequently, extensive research started in order to explore the role of NO in physiological processes other than cardiovascular system. It is the first gaseous molecule that acts as a biological messenger in mammals.[3,6,7]

1.2. Biosynthesis of nitric oxide

NO is produced in nearly all the living cells and mediates numerous physiological processes.[8] It is endogenously synthesized by a class of enzyme called nitric oxide synthases (NOS), through the stepwise oxidation of L-arginine into L-citrulline, during this process NO is produced (Scheme 1.1).[2,3,9] In mammalian cells, there are three major distinct isoforms of NOS are present: endothelial NOS (eNOS or NOS 3), neuronal NOS (nNOS or NOS 1) and inducible NOS (iNOS or NOS 2). The eNOS and nNOS are constitutively expressed in the endothelial cells and in the neuronal cells, respectively and release NO in nanomolar range (calcium-dependent isoforms). Whereas, iNOS is expressed upon stimulation of immune cells and produce a burst of NO in micromolar range for long time (calcium-independent isoform). The catalytic activity of NOS depending on the availability of several cofactors and cosubstrates, such as nicotinamide adenine dinucleotide phosphate (NADPH), flavin adenine dinucleotide (FAD), and tetrahydrobiopterin (BH_4).[8,10]

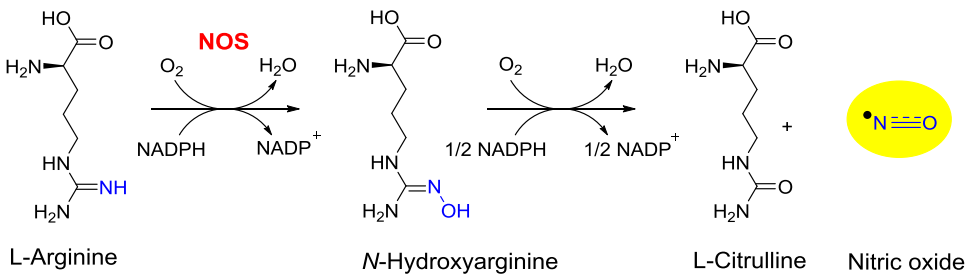

Scheme 1.1. Biosynthesis of nitric oxide from L -arginine

Under hypoxia, reduction of nitrite (NO_2^-) can provide an alternative, oxygen-independent source of low levels of NO (Scheme 1.2).[10,11]

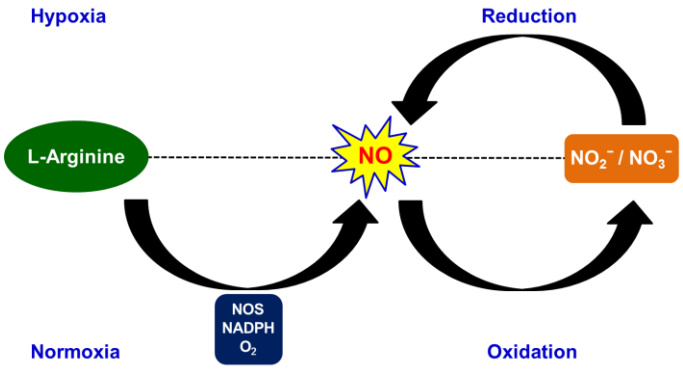

Scheme 1.2. Biosynthesis of nitric oxide. NO is generated from L-arginine by the enzyme NOS under normoxic conditions. Under these conditions, NO is oxidized to nitrite and nitrate. Under hypoxia, nitrite is reduced to NO in a NOS-independent pathway.

1.3. Biological effects of nitric oxide

NO mediates various physiological processes in the body, and its effects are largely concentration-dependent.[8] The biological effects of NO are divided into direct and indirect effects, which highly rely on the concentration of NO (Figure 1.1). At low concentrations, NO exerts direct effects on cellular systems. One of the most important biochemical effects of NO is the activation of soluble guanylate cyclase (sGC), which catalyzes the conversion of guanosine triphosphate (GTP) to 3′,5′-cyclic guanosine monophosphate (cGMP), a secondary messenger. This, in turn, leads to the activation of cGMP-dependent protein kinases, phosphodiesterases and cyclic nucleotide gated ion channels, which ultimately promote the main biological functions of NO, including vasodilation, inhibition of platelet aggregation and smooth muscle relaxation.[12]

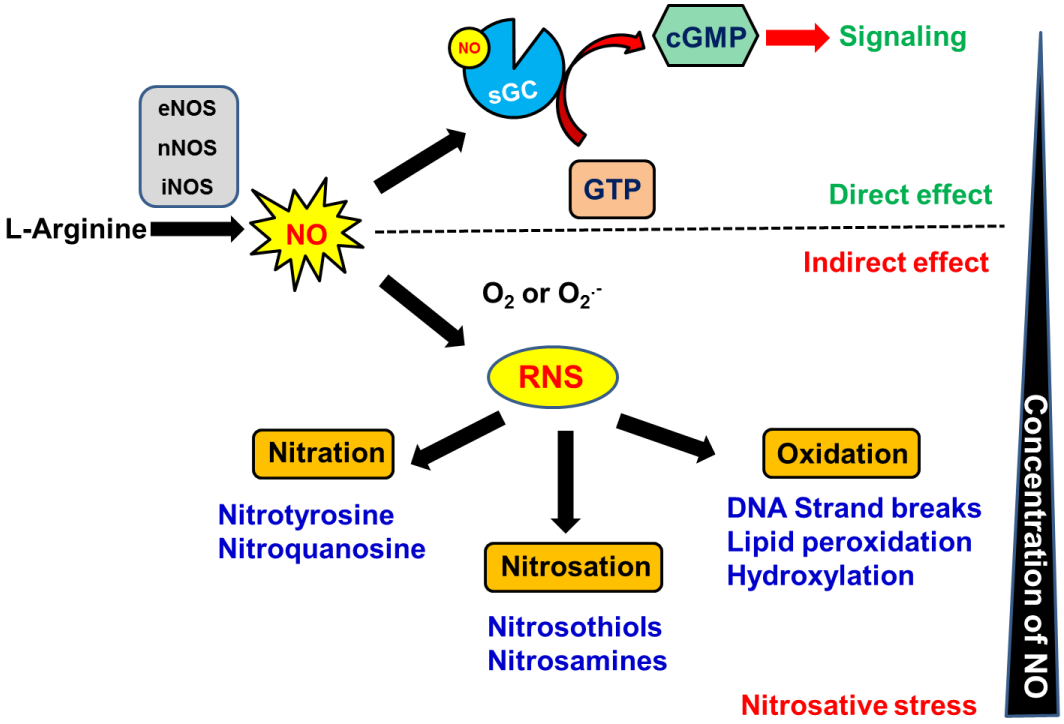

Figure 1.1. Concentration dependent biological effects of NO

In contrast, at higher concentration, NO reacts with various reactive oxygen species (ROS) to produce reactive nitrogen species (RNS), which exert indirect effects such as, oxidation, nitration and nitrosation (Figure 1.1 and 1.2).[7,8,10,12-14] For example,

1) The reaction of NO with molecular oxygen (O_2) forms nitrogen dioxide (NO_2), which further reacts with NO to form unstable species dinitrogen trioxide (N_2O_3). In physiological media N_2O_3 forms nitrosonium ion (NO^+) and nitrite (NO_2^-). Thus, nitrosonium ion can nitrosylate nucleophiles in cells like thiols, metals, secondary amines and can form oxidized species like S-nitrosothiols, metal-nitrosyl complexes, N-nitrosamines.
2) NO reacts with superoxide anion ($O_2^{\bullet-}$) in a diffusion-controlled manner to form a strong oxidant species, peroxynitrite ($ONOO^-$), which is short-lived molecule (<10 ms) in aqueous medium, forms peroxynitrous acid (ONOOH) and is rapidly oxidized to nitrite ($NO_2^{\bullet}$) and hydroxyl ($^{\bullet}OH$) radicals. The nitrite radical can lead to nitrate biomolecules especially nitration of protein that contain tyrosine. On the other hand, the formation of hydroxyl radical ($^{\bullet}OH$) leads to hydroxylation, peroxidation of lipids and DNA damage.

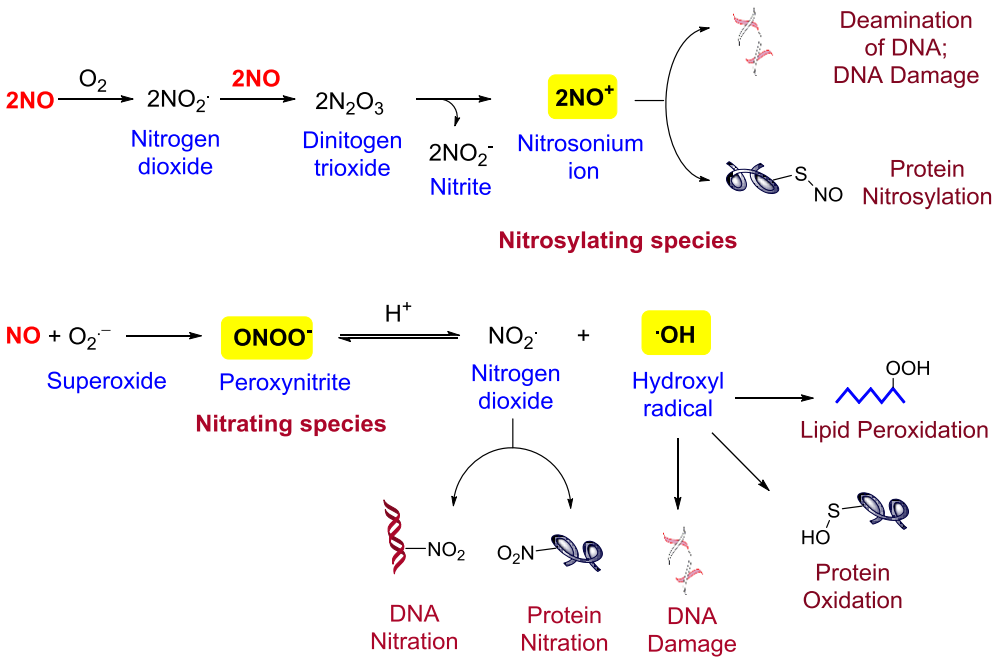

Figure 1.2. Cytotoxic effects of NO mediated by reactive nitrogen species (RNS).

1.4. Nitric oxide and cancer

The importance of nitric oxide (NO) in mediating numerous cellular processes is by now well established. The relationship between NO and cancer is complex and is largely dependent on the location, concentration, duration of release as well as the presence or lack thereof of other reactive entities.[8,9,13,15] Several investigations have shown that low levels of NO promote cancer growth, while higher concentrations of NO induce cancer cell death.[16-18] Numerous studies have shown that cancers have elevated levels of NO in comparison with paired normal cells. So, the tumour cells required an optimal concentration of NO for its proliferation. However, very low levels of NO or very high levels of NO is toxic to tumour cells. This provide a therapeutic opportunity to target cancer either by lowering the concentration of NO using NOS inhibitors to inhibit tumor growth or by increasing the level of NO using NO donors to induce tumor cell death (Figure 1.3).[11] Thus, a number of studies have focused on dissipating NO within tumours by using inhibitors of NOS such as L-NAME.[19] Due to the decreased levels of NO, tumour growth is slowed. However, the use of NOS inhibitors requires long term, systemic administration that may result in hypertension and tumour regrowth if treatment is come to end prior to complete eradication.

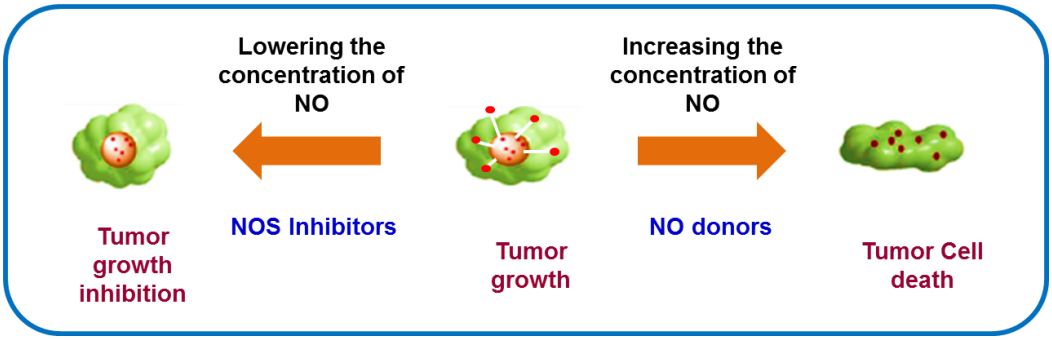

Figure 1.3. Concentration dependent effect of NO in tumor.

Meanwhile, numerous parallel studies focused on increasing NO concentrations at the tumor site to induce tumor cell death. Due to increased metabolism associated with rapidly dividing cells, tumors also have elevated levels of reactive oxygen species (ROS) including superoxide radical anion. Thus, enhancement of NO within cancers is expected to produce peroxynitrite ($ONOO^-$), a product of rapid combination of NO and superoxide anion radical, that may be highly toxic to cancers.[21-24] Furthermore, NO synergized with established drugs including doxorubicin and cis-platin and contributed to inhibition of drug efflux pumps that decreased intracellular availability of the drug. Multidrug resistance (MDR) is the one of the major problems associated with failure of cancer chemotherapy. [25-28] Cancer cells are known to overexpress efflux pumps that reduce the intracellular accumulation of a drug, which leads to MDR.[27,29] P-glycoprotein (P-gp), multidrug resistance related proteins (MRPs) and breast cancer resistance proteins (BCRP-1) are the primary efflux pumps involved in this process.[30-33] One of the strategies to reverse MDR is co-administration of anticancer drugs with efflux pump inhibitors. These agents inhibit the efflux pump thus allowing the intracellular accumulation of the anticancer drug, which consequently restores the antitumoral activity in resistance cell lines. These complex molecules belong to the third generation of P-gp inhibitors that have been studied in clinical trials.[34] P-gp inhibitors have some limitations including immunosuppressive effects and cardiovascular effects.[35-37] NO has been reported to inhibit efflux pumps and may therefore become an alternative to these P-gp inhibitors.[38] Extensive studies confirm that the antitumor effect of cancer chemotherapy agents was enhanced by the use of NO donors. The major reason is that NO donors generate reactive nitrogen species, which nitrate tyrosine residue of the efflux pumps which leads to increased intracellular drug accumulation and enhanced anticancer effect against drug resistant cancer cells.[38-40] Solid tumours have significant regions where oxygen concentration is diminished, hypoxia.[41,42] This condition is rather difficult to treat and hypoxic cells have an increased propensity to develop resistance to doxorubicin, for example NO can reverse this resistance.[43]

Furthermore, NO can also act as a hypoxic radiosensitizer, due to low oxygen concentrations, solid tumors becomes less sensitivity towards radiation therapy. NO mimics the oxygen role and sensitize solid tumors to the radiation therapy.

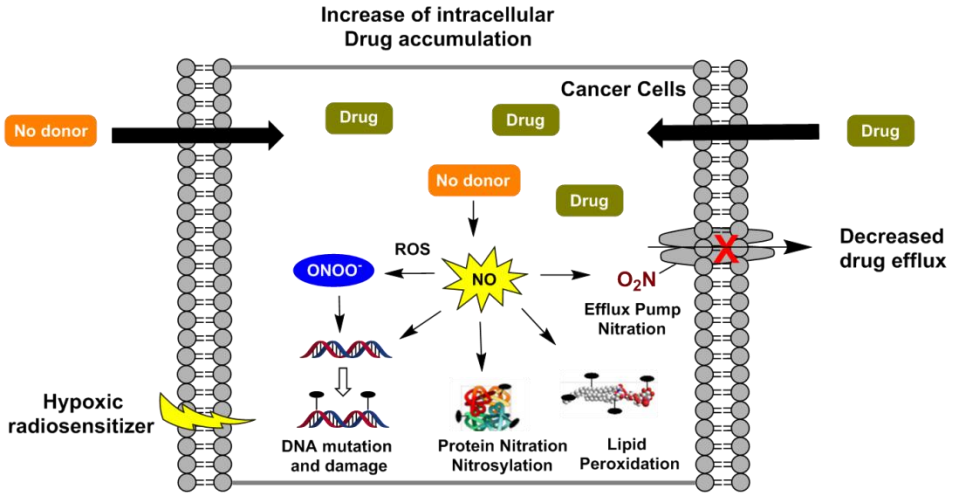

Figure 1.4. Cellular effects of nitric oxide

1.5. NO Delivery system

The relationship between NO and cancer is complex and depends on the concentration of NO and duration of release.[8] A number of efforts towards delivering NO to cancer cells as a tumoristatic agent are in development, which is mainly consists of iNOS gene therapy and NO donors (alone or in combination or in hybridization with an anticancer drug) based therapy.

1.5.1. iNOS gene therapy

Enhancement of intracellular NO can be achieved by increased expression of NOS. Transfection of the relevant gene should result in increased NOS levels. Among the isoforms of NOS, iNOS has the capacity to increase high levels of NO.[44,45] Efforts have been made to encapsulate the plasmid encoding the iNOS protein. Delivery and subsequent expression of this protein will produce NO within cells.[46-48] Exposure of such cancer cells to cytotoxic agents including doxorubicin revealed the enhanced sensitivity of drug-resistant cells to doxorubicin. Subsequent studies have shown nitration of tyrosine residues in drug efflux pumps results in decreased efflux capacity resulting in larger accumulation of the drug within cells. Currently, many types of vectors have been employed for iNOS gene delivery, including adenoviral vectors, cationic liposomes, bioinspired recombinant vectors, and retroviral vectors. The effects of iNOS gene therapy have been demonstrated on various cancer cells and numerous animal models.[49-55] Although iNOS gene therapy is highly

effective in enhancing NO in cancer, this strategy must overcome many problems such as selectivity, toxicity and the requirement of cofactors for NOS.[56-60] Furthermore, the concentration of NO produced may be difficult to control and may present challenges.

1.5.2. NO donors based therapy

NO is unstable under ambient conditions, it is difficult to generate NO directly within cells. Other strategy of NO delivery is use of exogenous donors to generate NO within cells. Different classes of NO donors are available to enhance NO in cells, including organic nitrates, metal-NO complexes, S-nitrosothiols, furoxans, sydnonimines and diazeniumdiolates (Figure 1.5).[15,47,61-63] These NO donors have been investigated as potential medicinal agents for cardiovascular, cancer, antibacterial, and wound healing. Among the current NO donors, only organic nitrates and sodium nitroprusside (SNP) are available for clinical use.[64,65] However, taking nitrates for long-term showed side effect such as hypotension, headache and evolving tolerance. The metal nitrosyl complex SNP is a potent vasodilator but prolonged administration of SNP leads to cyanide accumulation in the body.[13,15,66] Recently, 1-Bromoacetyl-3,3-dinitroazetidine (**2**) releases high levels of NO selectively under hypoxic conditions at a sustained but accelerated speed to exert potent antitumor activity.[67-70] Several lines of evidence suggest that the antitumor effect of certain cancer chemotherapy agents enhanced by nitric oxide treatment. However, the use of co-treatment with NO donors and an anticancer drug while effective may again suffer for differences in bio distribution of the NO donor and the drug. The NO donor must co-localize in the tumour and must be able to produce NO concurrently with the drug and only in the tumour. This may be challenging, which can be overcome by covalent modification of NO donor with anticancer drugs called NO donor-drug hybrids. This approach has numerous advantages including delivery of NO at the site of drug action. The challenges would be to localize the conjugate at the tumour site and future work will focus on directed delivery of drug conjugates. For therapeutic purpose, need a triggerable NO donors, should release NO in a controlled and sustained manner selectively at cancer site to avoid the drawbacks associated with traditional NO donors. Therefore, researchers are actively looking for a new NO donor vehicles capable of delivering precise NO doses directly to specific tissues for improved therapeutic output and reduced side effects.

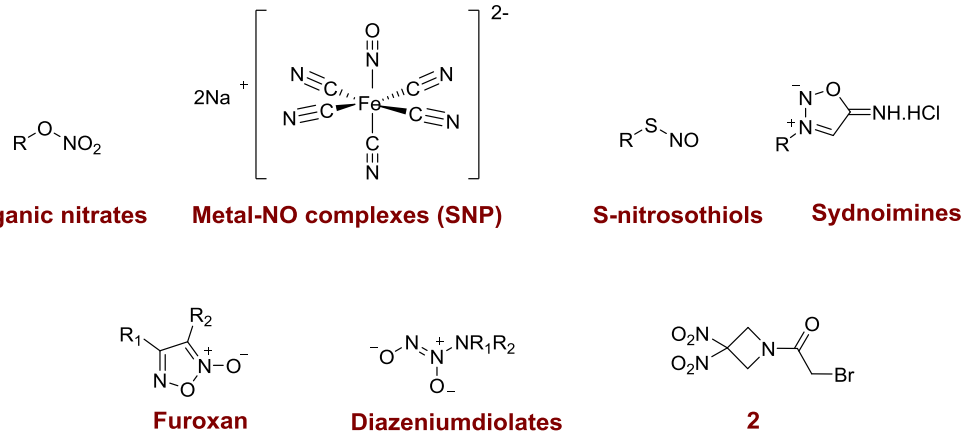

Figure.1.5. Structural representation of various classes of NO donors

1.6. Cancer targeted delivery of NO

As NO is a free radical, short-lived, highly diffusible and reactive gas that easily gets oxidized to inactive forms, namely, nitrate and nitrite, therefore delivering NO within the target is a challenging job. Although, number of NO donors has been reported to enhance NO, diazeniumdiolates are the highly efficient, reliable and versatile class of NO donors over others. Each molecule of diazeniumdiolate spontaneously generates upto two moles of NO under physiological conditions with half-lives ranging from a few seconds to several hours depending on the groups present on the amine nitrogen.[47,61,71] The different rates of NO release of these salts could be leveraged to develop NO donors for very specific needs. Diazeniumdiolates release NO in a non-specific manner in aqueous solution, which cannot be used to selectively deliver NO within cancer due to their non-specific activation which may result in systemic side-effects. In order to overcome this problem, the O^2-protected diazeniumdiolates are developed by derivatizing the terminal oxygen with a protecting group (Scheme 1.3). Generally, the protecting groups incorporated for derivatizing diazeniumdiolates are substrates for cellular enzymes. Thus, unlike free diazeniumdiolates, the protected diazeniumdiolates are more stable in physiological solutions. Further, the O^2-protected diazeniumdiolates are converted into an active NO-donor by specific enzymes present within cells and thus ensure intracellular release of NO (Scheme 1.3).[23]

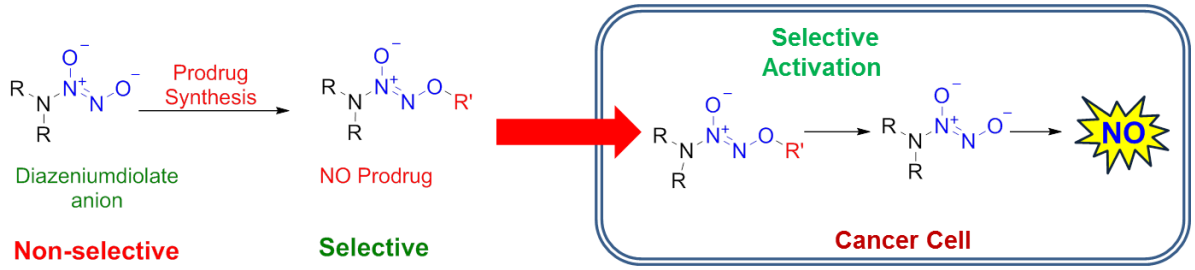

Scheme 1.3. Mechanism of activation of O^2-protected diazeniumdiolates based NO prodrug by specific trigger for delivery of NO within cells

For cancer target delivery, need to select an appropriate protecting group, which should be metabolically removed by enzymes that are highly overexpressed in cancer cells. Based on this concept number of O^2-protected diazeniumdiolates based NO-prodrugs have been reported to deliver NO to the cancer site. For example, NO donors that are activated by esterase (**2a**)[72], β-galactosidase[73-75], and DT-diaphorase[76] are known (Figure 1.6). Although some of these enzymes are over-expressed in tumours, cancer-selectivity data for these NO donors are not available. Lastly, glutathione/glutathione S-transferase (GSH/GST) NO prodrugs such as JS-K[77] and PABA/NO[78] are reported (Figure 1.6). Although these thiol-activated NO donors have limited cancer specificity, they have potent anti-proliferative activity in animal models, supporting the further development of NO as a tumoristatic agent.

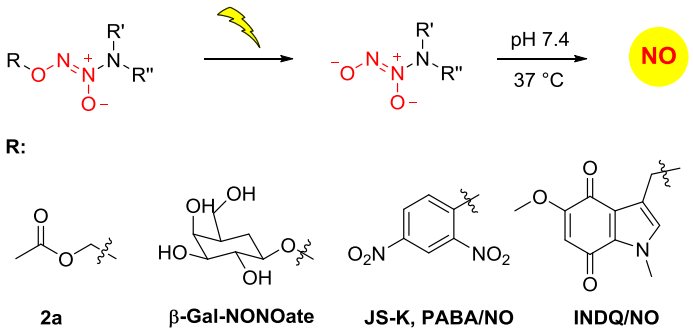

Figure 1.6. Selective examples of diazeniumdiolate based NO donors R' and R" = various groups

However, in order to infer the production of NO from these NO donors, secondary assays are required.[79-81] In addition to the site directed NO delivery, real-time monitoring of NO in cells is another important challenge needs to be addressed, which will be discussed in the following section.

1.7. Monitoring of NO in cells

Since the concentration, and spatial and temporal information of NO in living cells are crucial for its functions, enormous efforts have been directed towards the development of sensitive methods to analyse NO generation and distribution in living cells. NO is a short lived (lifetime in seconds)[82], highly diffusible (diffusion coefficients approaching 3300 $\mu m^2.s^{-1}$ in physiological buffer)[83,84] and highly reactive towards biomolecules, precise detection of NO in a biological systems is highly challenging. For example, the colorimetric Griess assay is the most popular method for the analysis of NO. First developed in 1879, the Griess assay measures NO indirectly as nitrite (NO_2^-), a product of NO's autooxidation.[85] NO produced from the compound is converted into nitrite, which subsequently reacts with the Griess reagent (i.e., Sulfanilamide and *N*-(1-napthyl) ethylene diamine) to form an azo dye with an absorbance maximum at 540 nm which can be detected using conventional UV-visible absorption spectroscopy (Figure 1.7).[79,86-88] The amount of nitrite released was estimated from a standard calibration curve generated using sodium nitrite ($NaNO_2$) solution.

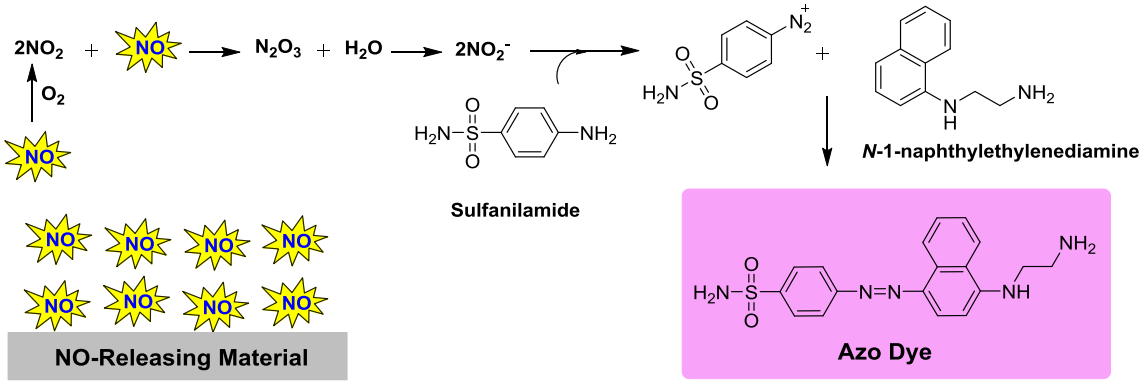

Figure 1.7. The reaction of nitrite (NO_2^-) with Griess assay reagents forms an azo dye.

Although inexpensive, readily available commercially, and useful for the indirect determination of NO totals, the limit of detection for Griess is only ~2.5 µM. Proteins and other additives interfere with the Griess assay, acting as either positive or negative interferents. For example, positive interferents such as NOS and hemoglobin absorb light around 540 nm. Nitrite can react with cysteine, tyrosine, ascorbate, and NADPH which leads to negative interference to the assay. Additionally, NO and nitrite are readily oxidized to nitrate resulting in superficially low NO values. Furthermore, acidic environment is required to perform this assay, which is not biocompatible.[79,86,89] Real-time analysis of NO generation using the Griess assay is not possible. Despite such drawbacks, the commercial availability of

reagent kits and the ability to employ high throughput 96-well microtiter plates make it a useful method for studying NO release.

Several other methods such as chemiluminescence, electron paramagnetic resonance (EPR) spectroscopy, amperometry and magnetic resonance imaging (MRI) have been applied for NO detection *in vivo*, but they suffer from low spatial resolution and in some cases require complicated instrumentation.[86,88,90-93] Furthermore, all the above methods require invasive procedures to detect NO in *in vivo*. Compared to all other NO detection techniques, fluorescence imaging has many advantages in view of its sensitivity, selectivity, spatiotemporal resolution, and experimental feasibility. Furthermore, this method can provide *in vivo* and *in situ* visualization of NO in cells and tissues in a non-invasive way.[94] Therefore, fluorogenic methods have been recognized as a reliable approach for the monitoring of NO.

Nagano's group first developed a series of *o*-diamine functional groups containing fluorescence probes.[95-98] This probes work based on the principle of photo induced electron transfer (PET). Here *o*-diamine acts as a fluorescence quencher. Under aerobic condition NO reacts with *o*-diamine to produce an electron deficient triazole adduct, which dissipates the PET pathway and restores the fluorescence (Figure 1.8).[99]

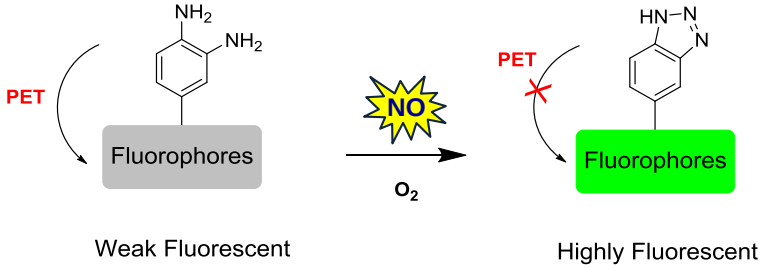

Figure 1.8. Mechanism of fluorescence response of *o*-diamine based NO probe

Based on this concept, number of *o*-diamine probes were developed and applied to detect NO in living cells, including *o*-diaminofluoresceins (DAFs), *o*-diaminorhodamine (DARs), DAMBO and *o*-diaminocyanines (DACs) (Figure 1.9).[96]

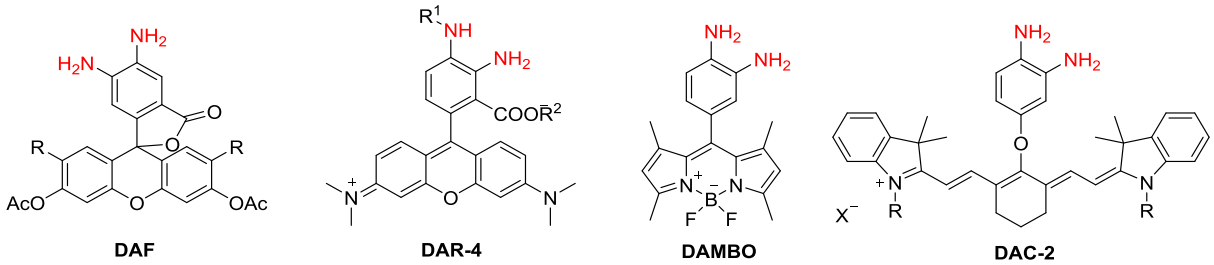

Figure 1.9. Structure of *o*-diamine based NO probes

Among these probes, DAF is a commercially available and frequently used secondary assay to measure intracellular NO. In this assay, the cells were treated with weakly fluorescent DAF-2 DA dye, which gets hydrolysed upon its entry inside cells to form a weakly fluorescent species DAF-2. DAF-2 reacts with oxidized product of NO (N_2O_3) and forms a highly fluorescent triazole moiety, DAF-2T (Figure 1.10).

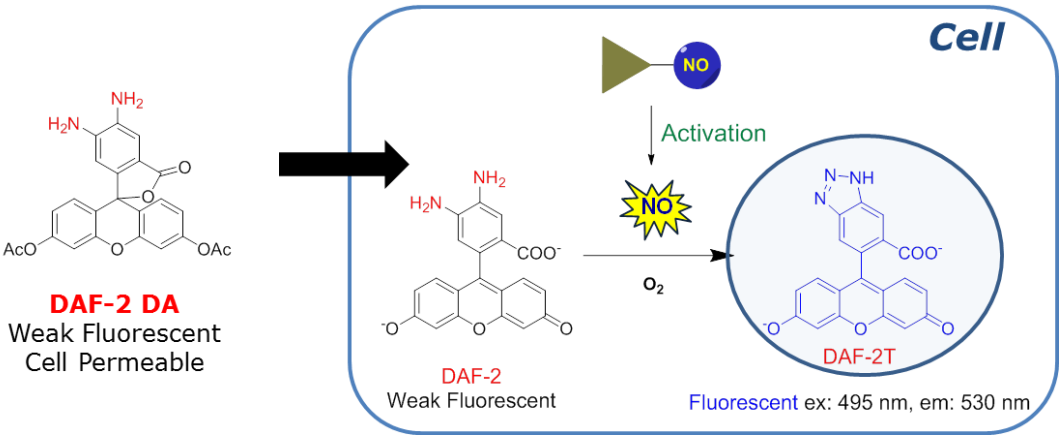

Figure 1.10. Detection of intracellular NO using a fluorescence based DAF assay

Major limitation with *o*-diamine based probes is that, these probes react with oxidized NO products and not with NO itself, resulting in the inability to reflect real-time NO production (Figure 1.11). Diaminofluorescein probes are susceptible to the interference by both oxidants and antioxidants such as dehydroascorbic acid (DHA), ascorbic acid (AA), glutathione, certain phenolic compounds, possibly due to the highly electron rich *o*-diaminophenyl group. Efflux of DAF-2 was commonly seen in cultured endothelial cells, which is another limitation of this probe. [100]

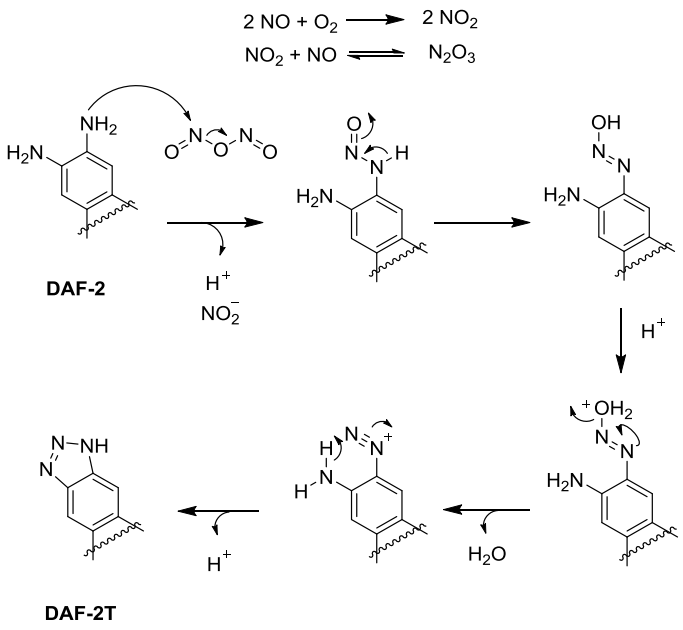

Figure 1.11. Mechanism for triazole formation

In order to address this limitation, Lippard and coworkers have developed a copper (CuFL) based fluorescence probes for selective image NO in living cells (Figure 1.12).[101] This probe is non-toxic, cell permeable and rapidly reacts with NO in a selective manner compared to a wide range of ROS, RNS and other additives. This probe showed an excellent fluorescent property as well.

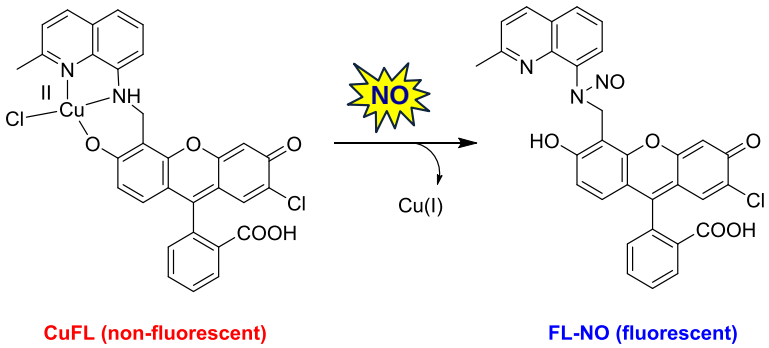

Figure 1.12. CuFL based fluorescence probes for NO

1.8. NO donor with a fluorescence reporter

The therapeutic value of NO is well documented, and a complete realisation of its potential relies on precise spatiotemporal control over NO generation.[8,21] Exogenous sources of NO ("NO donors") are used for this.[61,71] Some NO donors spontaneously dissociate to produce NO, whereas others are triggered intracellularly and dissociate to produce NO (Scheme 1.x).[76,102-109] However, in order to infer the production of NO, secondary assays are used,

typically fluorescence-based cellular assays for reactive nitrogen species (Scheme 1.4.a).[80,100,101,110] Since, NO is a free radical and highly reactive species, once released inside the cell, it can react with different molecules that are present inside cell, as a result of which measurement of NO by secondary assays might be inaccurate. All the secondary dyes are used to detect only free NO (unbound) in living cells and treatment of cells with these secondary dyes often renders them unsuitable for further study. Furthermore, measurement of NO with these secondary dyes invariably associated with consumption of NO. Enhancement of NO within cells as well as simultaneous detection is cumbersome. So real-time monitoring of NO in cells is challenging. One possibility to address this task is to introduce a fuorescent reporter in the NO donor. Thus, a strategy where a small molecule can generate NO along with a fluorescence reporter, for the produced NO would be useful (Scheme 1.4.b), which will eliminates the need for the secondary assays to monitor the release of NO.

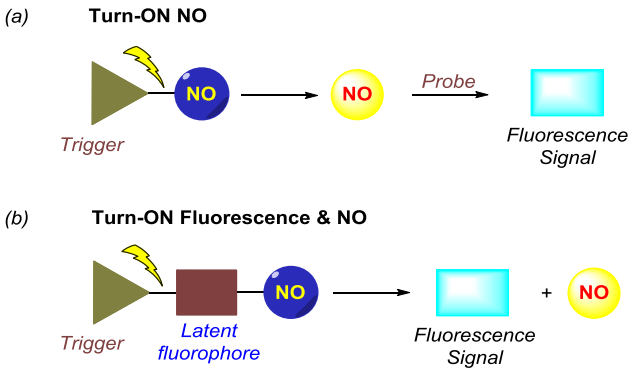

Scheme 1.4. (a) Stimuli responsive nitric oxide generation by a NO donor requires a secondary probe for detection of NO produced. (b) Incorporation of a latent fluorophore in the donor eliminates the need for the secondary probe for monitoring of NO.

It is therefore necessary to develop a reporter linked NO donors. A photochemical trigger offers a high degree of spatiotemporal control over NO generation and useful for ON-Demand NO generation.[111-117] A number of methodologies for light-activated generation of NO with a fluorescence reporter are known. For example, Mascharak and coworkers have developed a light-triggered ruthenium based NO donors with fluorescencent reporter (resorufin or dansyl chromophores) to track NO in cells (Figure 1.13).[118,119] However, this system displays turn-OFF fluorescence signal upon NO release.

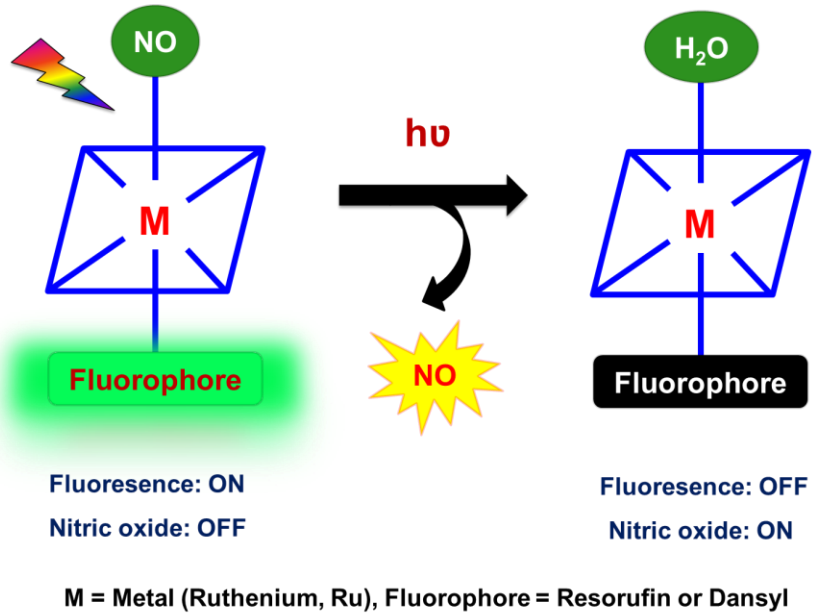

Figure 1.13. Photosensitive Metal-based NO donor with a fluorescence reporter

For real-time monitoring of NO, turn ON fluorescence signal would be useful. Same group developed a turn ON system to track NO release in cells. But because of the fluorescence bands (metal bound and free dye) overlapping, monitoring of NO in cells is difficult with this method.[120] Next, Sortino and coworkers have developed a light activated NO donor with fluorescence reporter.[121-126] Although, this system is fluorescence turn ON type, nitroaniline derivative was used as a NO donor, which is not an efficient NO donor. Recently, a nanoplatform for light triggered target specific NO delivery methods also reported but this system generates NO as well as singlet oxygen.[127] Several materials-based methods for NO generation are known, but they have limitations, such as consumption of NO or being a turn-off fluorescence methodology.[128,129] However, all the above methods required light as a trigger, most optically triggered approaches utilize UV light, which limits tissue permeability and triggers toxic side effects. A nitric oxide delivery system with a fluorescence reporter for broad applicability is not yet available.

Therefore, we need a new NO donor, which should have the following characteristics,

1) It should be a triggerable NO donor
2) The trigger should be cancer selective
3) Fluorescence reporter signal should be turn ON type
4) Fluorophore should not consume NO during its detection
5) It should release NO in a controlled and sustained manner at a cancer site

Weinstein *et al*. reported real-time monitoring of drug release using a reporting drug delivery system (RDDS) where a 7-hydroxycoumarin linker was used as a fluorescent reporter. 7-hydroxylcoumarin derivative was attached to the peptidase substrate to one end and to the drug molecule on the other end. Upon activation of RDDS, a spontaneous 1, 8- elimination reaction takes place and release the drug and reporter molecule (Figure 1.14).[130]

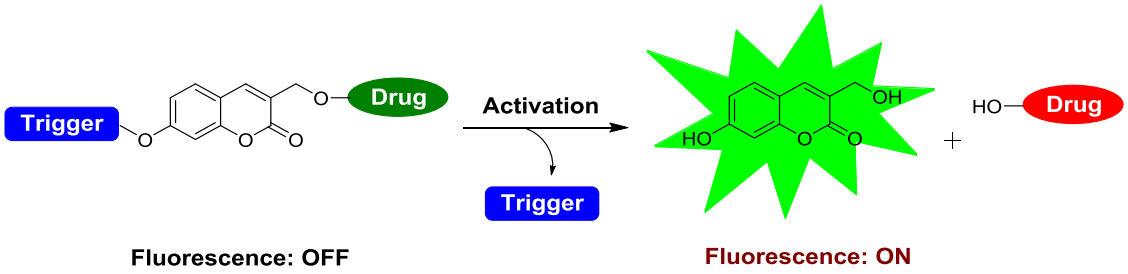

Figure 1.14. 7-Hydroxycoumarin was used as a fluorescence reporter for real time monitoring of drug release

Therefore, based on the above strategy of real-time monitoring of drug release, in **Chapter 2**, we propose FLUORO/NO, a nitric oxide donor with fluorescence reporter. In the presence of esterase it produces NO and fluorescence signal without consumption of NO during its detection. The trigger that we had is esterase, which is present in nearly all cells, and therefore the compound will be suitable for a range of cell biology studies. In order to study the precise role of NO in cancer, we need a cancer specific trigger. Since cancer cells produce higher level of H_2O_2 compared with normal cells, as a proof of concept in **Chapter 3**, we propose BORO/NO, a NO donor without fluorescence reporter, which are capable of generating NO when triggered by H_2O_2. Next, in **Chapter 4**, we propose Thera/NO, a H_2O_2 activated NO donor that can be used for selectively delivering and monitoring the release of NO in cancer cells.

The versatility of this scaffold for real-time monitoring of NO release was demonstrated by incorporating two distinct triggers and can, in principle, be extended to other stimuli of interest as well. Altogether, the results presented in this thesis address important problems associated with real-time monitoring of NO in cells and site-specific delivery of NO as well. It is anticipated that these tools will find use in interrogating NO biology, which is yet to be completely understood.

Finally, Superoxide is also endogenously generated by NADPH oxidase and further single electron reduction produces H_2O_2, which converts into highly toxic hydroxyl radial in the presence of metals ions. Superoxide and hydrogen peroxide and hydroxyl radial are collectively called reactive oxygen species (ROS).[24,131,132] During immune response both

ROS and NO are produced to counter pathogens.[10,24,133-135] NO and ROS are interconnected with each other and plays very important role in the biological system.[136,137] Like NO, reactive oxygen species are short half-life, highly unstable under ambient condition. Controlled and localized generation of ROS in cells is challenging. Number of ROS donors have been reported, however in order to infer the production of ROS in cells, multiple independent assays are required.[138-140] Finally, in **chapter 5**, using the coumarin based strategy, we proposed an esterase sensitive ROS donor with a fluorescent reporter**.** This tool would be useful to deliver and real-time monitor ROS release in cells without the need for secondary assays.

1.9. References

(1) Culotta, E.; Koshland, D. E., Jr. *Science (New York, N.Y.)* **1992**, *258*, 1862.

(2) Palmer, R. M. J.; Ferrige, A. G.; Moncada, S. *Nature* **1987**, *327*, 524.

(3) Ignarro, L. J. *Angew. Chem. Int. Ed.* **1999**, *38*, 1882.

(4) Ignarro, L. J. *Biochem. Pharmacol.* **1991**, *41*, 485.

(5) Andrew, P. J.; Mayer, B. *Cardiovasc. Res.* **1999**, *43*, 521.

(6) Ferid, M. *Angew. Chem. Int. Ed.* **1999**, *38*, 1856.

(7) Heinrich, T. A.; da Silva, R. S.; Miranda, K. M.; Switzer, C. H.; Wink, D. A.; Fukuto, J. M. *Br. J. Pharmacol.* **2013**, *169*, 1417.

(8) Thomas, D. D.; Ridnour, L. A.; Isenberg, J. S.; Flores-Santana, W.; Switzer, C. H.; Donzelli, S.; Hussain, P.; Vecoli, C.; Paolocci, N.; Ambs, S.; Colton, C. A.; Harris, C. C.; Roberts, D. D.; Wink, D. A. *Free Radic. Biol. Med.* **2008**, *45*, 18.

(9) Thomas, D. D.; Ridnour, L. A.; Isenberg, J. S.; Flores-Santana, W.; Switzer, C. H.; Donzelli, S.; Hussain, P.; Vecoli, C.; Paolocci, N.; Ambs, S.; Colton, C. A.; Harris, C. C.; Roberts, D. D.; Wink, D. A. *Free Radical Biol. Med.* **2008**, *45*, 18.

(10) Wink, D. A.; Hines, H. B.; Cheng, R. Y. S.; Switzer, C. H.; Flores-Santana, W.; Vitek, M. P.; Ridnour, L. A.; Colton, C. A. *J Leukoc Biol.* **2011**, *89*, 873.

(11) Oronsky, B.; Fanger, G. R.; Oronsky, N.; Knox, S.; Scicinski, J. *Transl. Oncol* **2014**, *7*, 167.

(12) Hanafy, K. A.; Krumenacker, J. S.; Murad, F. *Med. Sci. Monit.* **2001**, *7*, 801.

(13) Huang, Z.; Fu, J.; Zhang, Y. *J. Med. Chem.* **2017**, *60*, 7617.

(14) Basudhar, D.; Ridnour, L. A.; Cheng, R.; Kesarwala, A. H.; Heinecke, J.; Wink, D. A. *Coord. Chem. Rev.* **2016**, *306*, 708.

(15) Carpenter, A. W.; Schoenfisch, M. H. *Chem. Soc. Rev.* **2012**, *41*, 3742.

(16) Fukumura, D.; Kashiwagi, S.; Jain, R. K. *Nat. Rev. Cancer* **2006**, *6*, 521.

(17) Bonavida, B.; Khineche, S.; Huerta-Yepez, S.; Garbán, H. *Drug Resist. Updates* **2006**, *9*, 157.

(18) Wink, D. A.; Vodovotz, Y.; Cook, J. A.; Krishna, M. C.; Kim, S.; Coffin, D.; DeGraff, W.; Deluca, A. M.; Liebmann, J.; Mitchell, J. B. *Biochemistry. Biokhimiia* **1998**, *63*, 802.

(19) Tozer, G. M.; Prise, V. E.; Chaplin, D. J. *Cancer research* **1997**, *57*, 948.

(20) #xed; te; #x10d; ek, J.; Lojek, A.; #xed; Valacchi, G.; Kubala, L.; #xe1; #x161 *Mediators of Inflammation* **2012**, *2012*, 22.

(21) Szabo, C. *Nat. Rev. Drug. Discov.* **2016**, *15*, 185.

(22) Szabó, C. *Toxicol. Lett.* **2003**, *140–141*, 105.

(23) Sharma, K.; Chakrapani, H. *Nitric Oxide* **2014**, *43*, 8.

(24) Szabo, C.; Ischiropoulos, H.; Radi, R. *Nat. Rev. Drug Discov.* **2007**, *6*, 662.

(25) Szakacs, G.; Paterson, J. K.; Ludwig, J. A.; Booth-Genthe, C.; Gottesman, M. M. *Nature Rev. Drug Discovery* **2006**, *5*, 219.

(26) Gottesman, M. M.; Fojo, T.; Bates, S. E. *Nature Rev. Cancer* **2002**, *2*, 48.

(27) Sarkadi, B.; Homolya, L.; Szakács, G.; Váradi, A. *Physiol. Rev.* **2006**, *86*, 1179.

(28) Wilson, T. R.; Johnston, P. G.; Longley, D. B. *Curr. Cancer Drug Targets* **2009**, *9*, 307.

(29) Simon, S. M.; Schindler, M. *PNAS* **1994**, *91*, 3497.

(30) Cole, S.; Bhardwaj, G.; Gerlach, J.; Mackie, J.; Grant, C.; Almquist, K.; Stewart, A.; Kurz, E.; Duncan, A.; Deeley, R. *Science (New York, N.Y.)* **1992**, *258*, 1650.

(31) Uchida, S.; Shimada, Y.; Watanabe, G.; Li, Z. G.; Hong, T.; Miyake, M.; Imamura, M. *Br. J. Cancer* **1999**, *79*, 1168.

(32) Doyle, L. A.; Yang, W.; Abruzzo, L. V.; Krogmann, T.; Gao, Y.; Rishi, A. K.; Ross, D. D. *PNAS* **1998**, *95*, 15665.

(33) Eckford, P. D. W.; Sharom, F. J. *Chem. Rev.* **2009**, *109*, 2989.

(34) Abdallah, H. M.; Al-Abd, A. M.; El-Dine, R. S.; El-Halawany, A. M. *Journal of Advanced Research* **2015**, *6*, 45.

(35) Planting, A. S. T.; Sonneveld, P.; van der Gaast, A.; Sparreboom, A.; van der Burg, M. E. L.; Luyten, G. P. M.; de Leeuw, K.; de Boer-Dennert, M.; Wissel, P. S.; Jewell, R. C.; Paul, E. M.; Purvis, N. B.; Verweij, J. *Cancer Chemother. Pharmacol.* **2005**, *55*, 91.

(36) Kuppens, I. E. L. M.; Witteveen, E. O.; Jewell, R. C.; Radema, S. A.; Paul, E. M.; Mangum, S. G.; Beijnen, J. H.; Voest, E. E.; Schellens, J. H. M. *Clin. Cancer Res.* **2007**, *13*, 3276.

(37) Pusztai, L.; Wagner, P.; Ibrahim, N.; Rivera, E.; Theriault, R.; Booser, D.; Symmans, F. W.; Wong, F.; Blumenschein, G.; Fleming, D. R.; Rouzier, R.; Boniface, G.; Hortobagyi, G. N. *Cancer* **2005**, *104*, 682.

(38) Riganti, C.; Miraglia, E.; Viarisio, D.; Costamagna, C.; Pescarmona, G.; Ghigo, D.; Bosia, A. *Cancer Res.* **2005**, *65*, 516.

(39) Chegaev, K.; Riganti, C.; Lazzarato, L.; Rolando, B.; Guglielmo, S.; Campia, I.; Fruttero, R.; Bosia, A.; Gasco, A. *ACS Med. Chem. Lett.* **2011**, *2*, 494.

(40) Riganti, C.; Rolando, B.; Kopecka, J.; Campia, I.; Chegaev, K.; Lazzarato, L.; Federico, A.; Fruttero, R.; Ghigo, D. *Mol. Pharmaceutics* **2013**, *10*, 161.

(41) Wilson, W. R.; Hay, M. P. *Nat. Rev. Cancer.* **2011**, *11*, 393.

(42) Shannon, A. M.; Bouchier-Hayes, D. J.; Condron, C. M.; Toomey, D. *Cancer Treat Rev.* **2003**, *29*, 297.

(43) Evig, C. B.; Kelley, E. E.; Weydert, C. J.; Chu, Y.; Buettner, G. R.; Patrick Burns, C. *Nitric Oxide* **2004**, *10*, 119.

(44) Wang, Z.; Cook, T.; Alber, S.; Liu, K.; Kovesdi, I.; Watkins, S. K.; Vodovotz, Y.; Billiar, T. R.; Blumberg, D. *Cancer Res.* **2004**, *64*, 1386.

(45) Knowles, R. G.; Moncada, S. *Biochem J.* **1994**, *298 (Pt 2)*, 249.

(46) Singh, S.; Gupta, A. K. *Cancer Chemother Pharmacol.* **2011**, *67*, 1211.

(47) Huerta, S.; Chilka, S.; Bonavida, B. *Int. J. Oncol.* **2008**, *33*, 909.

(48) Xu, W.; Liu, L. Z.; Loizidou, M.; Ahmed, M.; Charles, I. G. *Cell Res.* **2002**, *12*, 311.

(49) Wang, Z.; Cook, T.; Alber, S.; Liu, K.; Kovesdi, I.; Watkins, S. K.; Vodovotz, Y.; Billiar, T. R.; Blumberg, D. *Cancer research* **2004**, *64*, 1386.

(50) N., S. M.; P., B.; K., B.; G., L.; A., R. B.; S., L. *J. Gene Med.* **2000**, *2*, 344.

(51) McCarthy, H. O.; Zholobenko, A. V.; Wang, Y.; Canine, B.; Robson, T.; Hirst, D. G.; Hatefi, A. *Int. J. Pharm.* **2011**, *405*, 196.

(52) Ye, S.; Yang, W.; Wang, Y.; Ou, W.; Ma, Q.; Yu, C.; Ren, J.; Zhong, G.; Shi, H.; Yuan, Z.; Su, X.; Zhu, W. *Int. J. Mol. Med.* **2013**, *31*, 33.

(53) Singh, S.; Gupta, A. K. *Cancer Chemother. Pharmacol.* **2011**, *67*, 1211.

(54) Tan, J.; Zeng, Q.; Jiang, X.-Z.; He, L.-Y.; Wang, J.-R.; Yao, K.; Wang, C.-H. *Chin. J. Cancer Res.* **2013**, *25*, 593.

(55) Jenny, W.; O., M. H.; Eimear, B.; Catherine, A.; Tracy, R.; G, H. D. *J. Gene Med.* **2004**, *6*, 673.

(56) Mocellin, S.; Bronte, V.; Nitti, D. *Med. Res. Rev.* **2007**, *27*, 317.

(57) Lehrman, S. *Nature* **1999**, *401*, 517.

(58) Lehrman, S. *Nature* **1999**, *401*, 517.

(59) Simone, M.; Vincenzo, B.; Donato, N. *Med. Res. Rev.* **2007**, *27*, 317.

(60) Tzeng, E.; Yoneyama, T.; Hatakeyama, K.; Shears, L. L.; Billiar, T. R. *Surgery* **1996**, *120*, 315.

(61) Wang, P. G.; Xian, M.; Tang, X.; Wu, X.; Wen, Z.; Cai, T.; Janczuk, A. J. *Chem. Rev.* **2002**, *102*, 1091.

(62) Hrabie, J. A.; Keefer, L. K. *Chem. Rev.* **2002**, *102*, 1135.

(63) Bonavida, B.; Baritaki, S. *Nitric Oxide* **2011**, *24*, 1.

(64) Ning, S.; Bednarski, M.; Oronsky, B.; Scicinski, J.; Knox, S. J. *Biochem. Biophys. Res. Commun.* **2014**, *447*, 537.

(65) Yang, L.; Lan, C.; Fang, Y.; Zhang, Y.; Wang, J.; Guo, J.; Wan, S.; Yang, S.; Wang, R.; Fang, D. *Int. Immunopharmacol.* **2013**, *17*, 383.

(66) Ignarro, L. J.; Napoli, C.; Loscalzo, J. *Circ. Res.* **2002**, *90*, 21.

(67) Reid, T.; Oronsky, B.; Scicinski, J.; Scribner, C. L.; Knox, S. J.; Ning, S.; Peehl, D. M.; Korn, R.; Stirn, M.; Carter, C. A.; Oronsky, A.; Taylor, M. J.; Fitch, W. L.; Cabrales, P.; Kim, M. M.; Burris, H. A.; Lao, C. D.; Abrouk, N. E. D.; Fanger, G. R.; Infante, J. R. *Lancet Oncol.* **2015**, *16*, 1133.

(68) Carter, C. A.; Oronsky, B.; Caroen, S.; Scicinski, J.; Degesys, A.; Cabrales, P.; Reid, T. R.; Brzezniak, C. *Case Rep. Oncol.* **2016**, *9*, 285.

(69) Carter, C. A.; Oronsky, B.; Caroen, S.; Scicinski, J.; Cabrales, P.; Degesys, A.; Brzezniak, C. *Respir. Med. Case Rep.* **2016**, *18*, 62.

(70) Ning, S.; Bednarski, M.; Oronsky, B.; Scicinski, J.; Saul, G.; Knox, S. J. *Cancer research* **2012**, *72*, 2600.

(71) Keefer, L. K. *ACS Chem. Biol.* **2011**, *6*, 1147.

(72) Saavedra, J. E.; Shami, P. J.; Wang, L. Y.; Davies, K. M.; Booth, M. N.; Citro, M. L.; Keefer, L. K. *J. Med. Chem.* **2000**, *43*, 261.

(73) Chen, C.; Shi, Y.; Li, S.; Qi, Q.; Gu, L.; Song, J.; Wang, P. G. *Arch. Pharm. Pharm. Med. Chem.* **2006**, *339*, 366.

(74) Valdez, C. A.; Saavedra, J. E.; Showalter, B. M.; Davies, K. M.; Wilde, T. C.; Citro, M. L.; Barchi, J. J.; Deschamps, J. R.; Parrish, D.; El-Gayar, S.; Schleicher, U.; Bogdan, C.; Keefer, L. K. *J. Med. Chem.* **2008**, *51*, 3961.

(75) Wu, X.; Tang, X.; Xian, M.; Wang, P. G. *Tetrahedron Lett.* **2001**, *42*, 3779.

(76) Sharma, K.; Iyer, A.; Sengupta, K.; Chakrapani, H. *Org. Lett.* **2013**, *15*, 2636.

(77) Shami, P. J.; Saavedra, J. E.; Wang, L. Y.; Bonifant, C. L.; Diwan, B. A.; Singh, S. V.; Gu, Y.; Fox, S. D.; Buzard, G. S.; Citro, M. L.; Waterhouse, D. J.; Davies, K. M.; Ji, X.; Keefer, L. K. *Mol. Cancer Ther.* **2003**, *2*, 409.

(78) Saavedra, J. E.; Srinivasan, A.; Buzard, G. S.; Davies, K. M.; Waterhouse, D. J.; Inami, K.; Wilde, T. C.; Citro, M. L.; Cuellar, M.; Deschamps, J. R.; Parrish, D.;

Shami, P. J.; Findlay, V. J.; Townsend, D. M.; Tew, K. D.; Singh, S.; Jia, L.; Ji, X.; Keefer, L. K. *J. Med. Chem.* **2006**, *49*, 1157.

(79) Coneski, P. N.; Schoenfisch, M. H. *Chem. Soc. Rev.* **2012**, *41*, 3753.

(80) Chan, J.; Dodani, S. C.; Chang, C. J. *Nat. Chem.* **2012**, *4*, 973.

(81) Miller, E. W.; Chang, C. J. *Curr. Opin. Chem. Biol.* **2007**, *11*, 620.

(82) Lowenstein, C. J.; Dinerman, J. L.; Snyder, S. H. *Ann. Intern. Med.* **1994**, *120*, 227.

(83) Lancaster, J. R. *Nitric Oxide* **1997**, *1*, 18.

(84) Malinski, T.; Taha, Z.; Grunfeld, S.; Patton, S.; Kapturczak, M.; Tomboulian, P. *Biochem. Biophys. Res. Commun.* **1993**, *193*, 1076.

(85) Peter, G. *Chem. Ber.* **1879**, *12*, 426.

(86) Hetrick, E. M.; Schoenfisch, M. H. *Annu. Rev. Anal. Chem. (Palo Alto Calif).* **2009**, *2*, 409.

(87) Sun, J.; Zhang, X.; Broderick, M.; Fein, H. *Sensors* **2003**, *3*, 276.

(88) Bryan, N. S.; Grisham, M. B. *Free Radical Biol. Med.* **2007**, *43*, 645.

(89) Hunter, R. A.; Storm, W. L.; Coneski, P. N.; Schoenfisch, M. H. *Anal. Chem.* **2013**, *85*, 1957.

(90) Bates, J. N. *Neuroprotocols* **1992**, *1*, 141.

(91) Privett, B. J.; Shin, J. H.; Schoenfisch, M. H. *Chem. Soc. Rev.* **2010**, *39*, 1925.

(92) Fethi, B.; Nicole, V. *Electroanalysis* **2003**, *15*, 5.

(93) Yoshimura, T.; Yokoyama, H.; Fujii, S.; Takayama, F.; Oikawa, K.; Kamada, H. *Nat. Biotechnol.* **1996**, *14*, 992.

(94) Chen, X.; Tian, X.; Shin, I.; Yoon, J. *Chem. Soc. Rev.* **2011**, *40*, 4783.

(95) Kojima, H.; Nakatsubo, N.; Kikuchi, K.; Kawahara, S.; Kirino, Y.; Nagoshi, H.; Hirata, Y.; Nagano, T. *Anal. Chem.* **1998**, *70*, 2446.

(96) Nagano, T. *J. Clin. Biochem. Nutr.* **2009**, *45*, 111.

(97) Nakatsubo, N.; Kojima, H.; Kikuchi, K.; Nagoshi, H.; Hirata, Y.; Maeda, D.; Imai, Y.; Irimura, T.; Nagano, T. *FEBS Lett.* **1998**, *427*, 263.

(98) Kojima, H.; Sakurai, K.; Kikuchi, K.; Kawahara, S.; Kirino, Y.; Nagoshi, H.; Hirata, Y.; Nagano, T. *Chem. Pharm. Bull. (Tokyo)* **1998**, *46*, 373.

(99) Nagano, T.; Yoshimura, T. *Chem. Rev.* **2002**, *102*, 1235.

(100) Li, H.; Wan, A. *Analyst* **2015**, *140*, 7129.

(101) Lim, M. H.; Xu, D.; Lippard, S. J. *Nat. Chem. Biol.* **2006**, *2*, 375.

(102) Cai, T. B.; Lu, D. N.; Landerholm, M.; Wang, P. G. *Org. Lett.* **2004**, *6*, 4203.

(103) Saavedra, J. E.; Shami, P. J.; Wang, L. Y.; Davies, K. M.; Booth, M. N.; Citro, M. L.; Keefer, L. K. *J. Med. Chem.* **2000**, *43*, 261.

(104) Chakrapani, H.; Maciag, A. E.; Citro, M. L.; Keefer, L. K.; Saavedra, J. E. *Org. Lett.* **2008**, *10*, 5155.

(105) Chakrapani, H.; Showalter, B. M.; Kong, L.; Keefer, L. K.; Saavedra, J. E. *Org. Lett.* **2007**, *9*, 3409.

(106) Chakrapani, H.; Showalter, B. M.; Citro, M. L.; Keefer, L. K.; Saavedra, J. E. *Org. Lett.* **2007**, *9*, 4551.

(107) Sharma, K.; Sengupta, K.; Chakrapani, H. *Bioorg. Med. Chem. Lett.* **2013**, *23*, 5964.

(108) Barraud, N.; Kardak, B. G.; Yepuri, N. R.; Howlin, R. P.; Webb, J. S.; Faust, S. N.; Kjelleberg, S.; Rice, S. A.; Kelso, M. J. *Angew. Chem. Int. Ed.* **2012**, *51*, 9057.

(109) Yepuri, N. R.; Barraud, N.; Mohammadi, N. S.; Kardak, B. G.; Kjelleberg, S.; Rice, S. A.; Kelso, M. J. *Chem. Commun.* **2013**, *49*, 4791.

(110) McQuade, L. E.; Lippard, S. J. *Curr. Opin. Chem. Biol.* **2010**, *14*, 43.

(111) Nakagawa, H.; Hishikawa, K.; Eto, K.; Ieda, N.; Namikawa, T.; Kamada, K.; Suzuki, T.; Miyata, N.; Nabekura, J.-i. *ACS Chem. Biol.* **2013**, *8*, 2493.

(112) Kitamura, K.; Ieda, N.; Hishikawa, K.; Suzuki, T.; Miyata, N.; Fukuhara, K.; Nakagawa, H. *Bioorg. Med. Chem. Lett.* **2014**, *24*, 5660.

(113) Ieda, N.; Hotta, Y.; Miyata, N.; Kimura, K.; Nakagawa, H. *J. Am. Chem. Soc.* **2014**, *136*, 7085.

(114) Kitamura, K.; Kawaguchi, M.; Ieda, N.; Miyata, N.; Nakagawa, H. *ACS Chem. Biol.* **2016**.

(115) Rose, M. J.; Olmstead, M. M.; Mascharak, P. K. *J. Am. Chem. Soc.* **2007**, *129*, 5342.

(116) Heilman, B.; Mascharak, P. K. *Philos. Transac. Royal Soc.London A: Math. Phys. Engineer. Sci.* **2013**, *371*.

(117) Sortino, S. *Chem. Soc. Rev.* **2010**, *39*, 2903.

(118) Rose, M. J.; Fry, N. L.; Marlow, R.; Hinck, L.; Mascharak, P. K. *J. Am. Chem. Soc.* **2008**, *130*, 8834.

(119) Rose, M. J.; Mascharak, P. K. *Chem. Commun.* **2008**, 3933.

(120) Fry, N. L.; Wei, J.; Mascharak, P. K. *Inorg. Chem.* **2011**, *50*, 9045.

(121) Vittorino, E.; Sciortino, M. T.; Siracusano, G.; Sortino, S. *ChemMedChem.* **2011**, *6*, 1551.

(122) Fraix, A.; Sortino, S. *Chem. Asian J.* **2015**, *10*, 1116.

(123) Fraix, A.; Kandoth, N.; Gref, R.; Sortino, S. *Asian J. Org. Chem.* **2015**, *4*, 256.

(124) Kirejev, V.; Kandoth, N.; Gref, R.; Ericson, M. B.; Sortino, S. *J. Mater. Chem. B* **2014**, *2*, 1190.

(125) Deniz, E.; Kandoth, N.; Fraix, A.; Cardile, V.; Graziano, A. C. E.; Lo Furno, D.; Gref, R.; Raymo, F. M.; Sortino, S. *Chem. Eur. J.* **2012**, *18*, 15782.

(126) Kandoth, N.; Malanga, M.; Fraix, A.; Jicsinszky, L.; Fenyvesi, É.; Parisi, T.; Colao, I.; Sciortino, M. T.; Sortino, S. *Chem. Asian J.* **2012**, *7*, 2888.

(127) Giancane, G.; Valli, L.; Sortino, S. *ChemPhysChem.* **2009**, *10*, 3077.

(128) Tan, L.; Wan, A.; Li, H. *Analyst* **2013**, *138*, 879.

(129) Liu, S.; Jin, L.; Chronakis, I. S.; Li, X.; Ge, M. *Mater. Lett.* **2014**, *123*, 104.

(130) Weinstain, R.; Segal, E.; Satchi-Fainaro, R.; Shabat, D. *Chem. Commun.* **2010**, *46*, 553.

(131) Winterbourn, C. C. *Nat. Chem. Biol.* **2008**, *4*, 278.

(132) Stadtman, E. R. *Free Radic. Res.* **2006**, *40*, 1250.

(133) Fang, F. C. *Nat. Rev. Microbiol.* **2004**, *2*, 820.

(134) West, A. P.; Shadel, G. S.; Ghosh, S. *Nat. Rev. Immunol.* **2011**, *11*, 389.

(135) Yang, Y.; Bazhin, A. V.; Werner, J.; Karakhanova, S. *Int. Rev. Immunol.* **2013**, *32*, 249.

(136) Kohchi, C.; Inagawa, H.; Nishizawa, T.; Soma, G. *Anticancer Res.* **2009**, *29*, 817.

(137) Dickinson, B. C.; Chang, C. J. *Nat. Chem. Biol.* **2011**, *7*, 504.

(138) Wardman, P. *Free Radic Biol Med.* **2007**, *43*, 995.

(139) Wrona, M.; Patel, K.; Wardman, P. *Free Radic. Biol. Med.* **2005**, *38*, 262.

(140) Miller, E. W.; Tulyathan, O.; Isacoff, E. Y.; Chang, C. J. *Nat. Chem. Biol.* **2007**, *3*, 263.

CHAPTER 2: FLUORO/NO: A Nitric Oxide Donor with a Fluorescence Reporter

2.1. Introduction

Nitric oxide (NO) is a key biomolecule that is produced in nearly all cells and can mediate numerous cellular processes including vasodilation, neurotransmission and immune response.[1,2] The therapeutic value of NO is well documented, and a complete realisation of its potential relies on precise spatiotemporal control over NO generation.[3] Exogenous sources of NO ("NO donors") are used for this.[4,5] Some NO donors spontaneously dissociate to produce NO, whereas others are triggered intracellularly and dissociate to produce NO (Scheme 2.1.a).[6-12] However, in order to infer the production of NO, assays are used, typically fluorescence-based cellular assays for reactive nitrogen species (Scheme 2.1.a).[13,14] As NO and its derivatives are short lived and highly reactive towards biomolecules, precise detection of NO in biological systems is highly challenging. Furthermore, the measurement of NO is invariably associated with consumption of NO.[15] Thus, a strategy where a small molecule can generate NO along with a fluorescence reporter, for the produced NO would be useful (Scheme 2.1.b), which will eliminates the need for the secondary assays to monitor the release of NO.

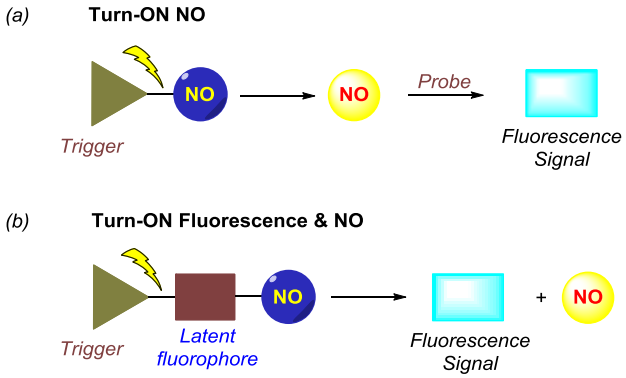

Scheme 2.1. (a) Stimuli responsive nitric oxide generation by a NO donor requires a secondary probe for detection of NO produced. (b) Incorporation of a latent fluorophore in the donor eliminates the need for the secondary probe for monitoring of NO.

Derivatives of 7-hydroxycoumarins have been previously used as latent fluorophores suitable for drug delivery as well as imaging.[16,17] Here, when substituted by an alkyl or aryl group, fluorescence of the compound is diminished. However, upon cleavage of the group to produce a free alcohol, a significant increase in fluorescence is seen. Using this property, a number of probes for a variety of analytes have been designed and developed (Scheme 2.2).[18-20]

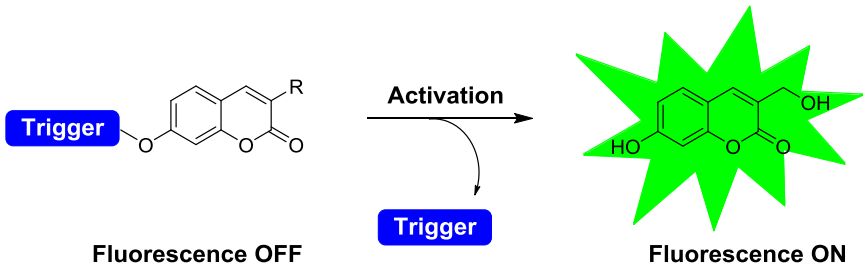

Scheme 2.2. 7-Hydroxycoumarin was used as a latent fluorophore in drug delivery as well as imaging of various analytes

In addition, substitution at the 3-position of 7-Hydroxycoumarin with a methylene functionality containing a suitable leaving group has been reported to undergo rearrangement to release the leaving group. For example, Weinstein *et al*. reported real-time monitoring of drug release using a reporter where 7-hydroxycoumarin derivative was used as a fluorescent reporter. The phenolic alcohol of 7-hydroxycoumarin derivative was connected to the trigger and the hydroxymethyl substituent was attached to the drug molecule. Upon trigger activation, a spontaneous 1,8-elimination reaction takes place, leading to the release of drug and generation of coumarin quinone-methide. Addition of water molecule to the reactive quinone methide leads to the formation of the highly fluorescent coumarin derivative (Scheme 2.3).[16]

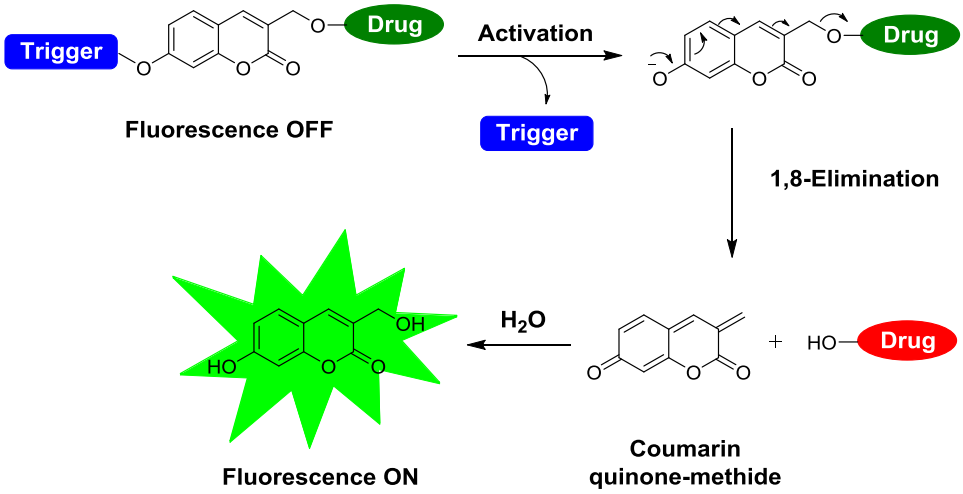

Scheme 2.3. 7-Hydroxycoumarin was used as a fluorescence reporter for real time monitoring of drug release

Using the coumarin-based strategy, FLUORO/NO (**5**) was designed the compound was expected to permeate cells to be cleaved by esterase to produce the highly fluorescent **12** and the nitric oxide-releasing **DEA/NO**. If the release of NO and the fluorescent **12** is nearly concurrent, a secondary assay for NO would not be necessary to monitor NO generation

(Scheme 2.4). The triggers that we chose were metabolically relevant, esterases are present in nearly all cells, and therefore the trigger would have broad relevance.

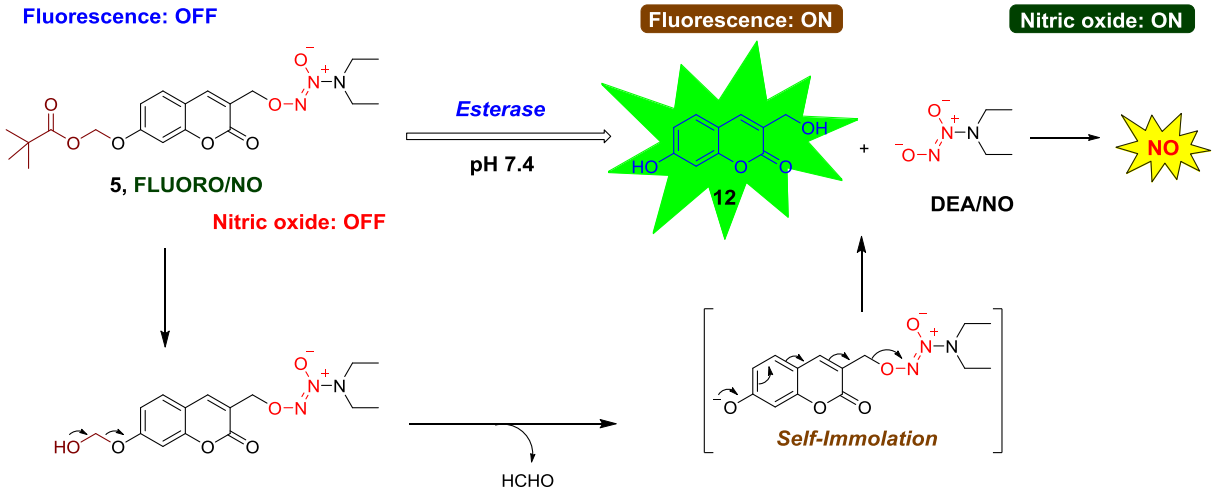

Scheme 2.4. FLUORO/NO (**5**), a class of triggerable nitric oxide donors with an in-built fluorescence reporter. FLUORO/NO is expected to have diminished fluorescence. Upon activation by esterase, followed by self-immolation and reaction with water will produce **12**, which is highly fluorescent and DEA/NO, which dissociates in pH 7.4 buffer to produce NO.

2.2. Results and Discussion

2.2.1. Synthesis

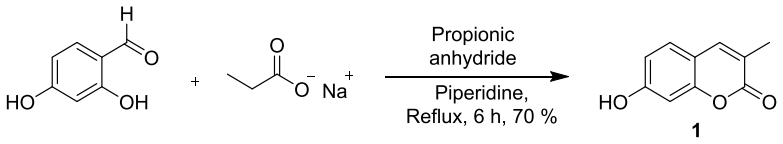

Scheme 2.5. Synthesis of **1**

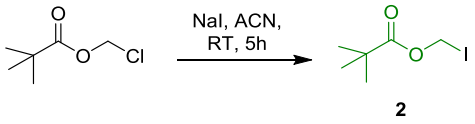

Scheme 2.6. Synthesis of **2**

In order to test this hypothesis, esterase activated NO donor with a fluorescence reporter was synthesized in five steps. Compound **1** and **2** were synthesized using previously reported methodology where 2,4-dihydroxy benzaldehyde was reacted with sodium propionate in the presence of propionic anhydride with catalytic amount of piperidine to produce compound **1** in 70% yield (Scheme 2.5).[21] Next, Iodomethylpivalate (**2**) was synthesized from cholorometh ylpivalate using sodium iodide in quantitative yield (Scheme 2.6).[22] Reaction of

3-methylumbelliferone (**1**) with iodomethylpivalate (**2**) in the presence of K_2CO_3 produced **3** in excellent yield. Next, **3** was reacted with *N*-bromosuccinamide (NBS) in the presence of a radical initiator azo-isobutyronitrile (AIBN) in carbon tetrachloride to produce corresponding bromide **4** in 75% yield, which was then reacted with sodium N, N-(diethylamino)diazen-1-ium-1,2-diolate (DEA/NO) in THF in the presence of 15-crown-5 to afford desired compound **5**, in 24% yield (Scheme 2.7).

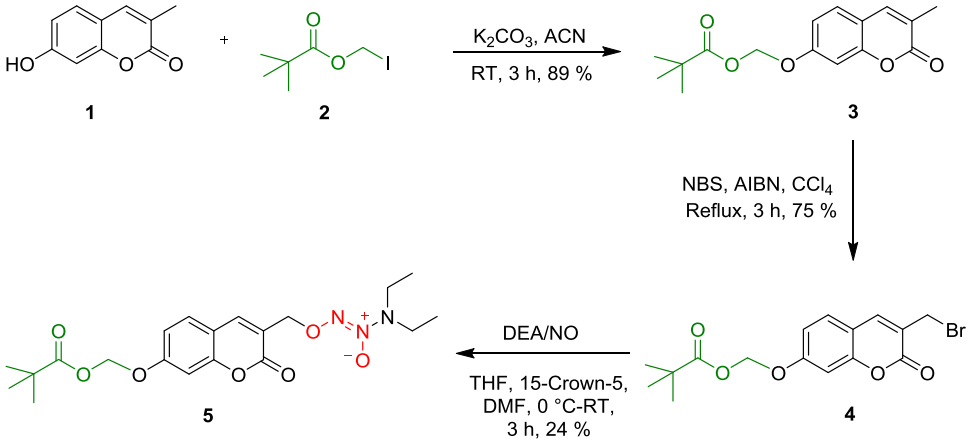

Scheme 2.7. Synthesis of **FLUORO/NO** (**5**)

In addition, esterase sensitive NO donor **6** was synthesized as a control compound, which upon activation by esterase, produces NO without enhancing fluorescence. The reaction of DEA/NO with **2** afforded **6** in 15% yield (Scheme 2.8).[23]

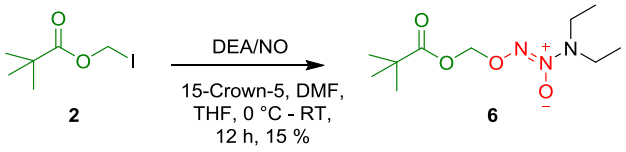

Scheme 2.8. Synthesis of control compound **6**

Based on the proposed mechanism, compound **12** is expected to be formed from **5** upon activation by esterase. Compound **12** was synthesized by the reported procedure.[16] 2,4-dihydroxy benzaldehyde was reacted with diethyl glutaconate to form the compound **7** in 85% yield (Scheme 2.9), which was acetylated using acetic anhydride to give compound **8** in 94% yield. Next, olefin **8** was oxidized to diol **9** by using osmium tetraoxide (OsO_4) in the presence of *N*-methyl morpholine *N*-oxide (NMO). The resulting diol **9** was cleaved by sodium periodate ($NaIO_4$) to obtain corresponding aldehyde **10** in 97% yield. Deacetylation of **10** was achieved using NH_4OH to get compound **11** in 63% yield, which on further reduction by a reducing agent $NaBH_4$ gave compound **12** in excellent yield (Scheme 2.9). After confirming the product formation by NMR, the fluorescence quantum yield (Φ_F) of

compound **12** in buffer (Φ_F = 0.50) was determined, 2-Aminopurin (Φ_F = 0.68) was used as a standard in this experiment (Table 2.1). Compound **12** was found to be highly fluorescent.

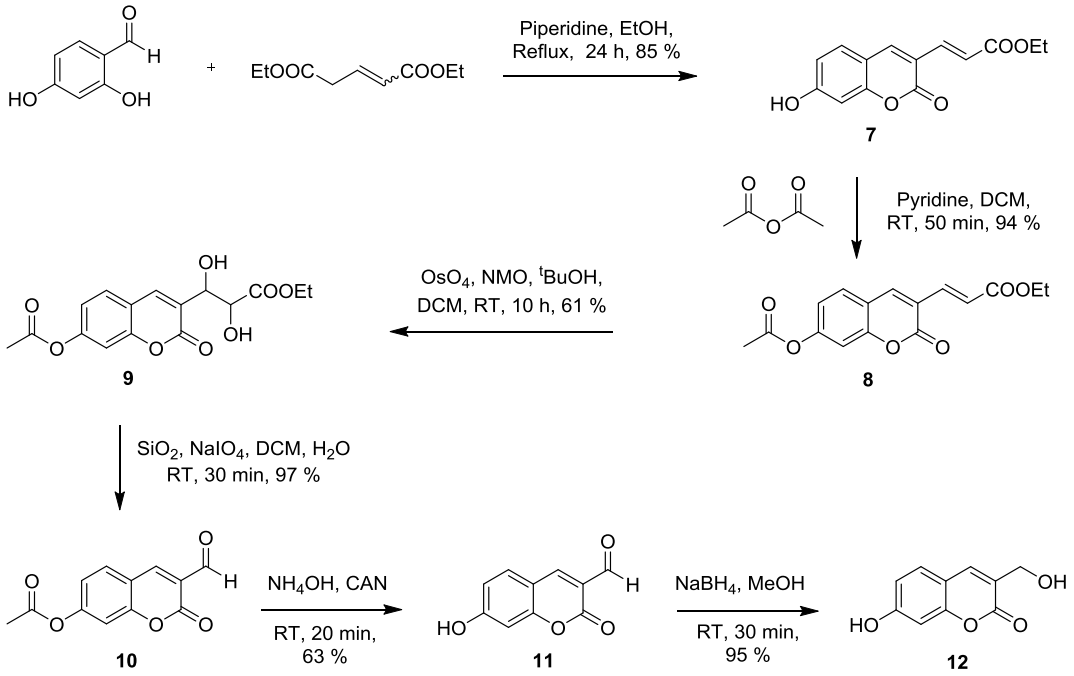

Scheme 2.9. Synthesis of fluorophore **12**

2.2.2. Nitric oxide release and fluorescence emission in buffer

2.2.2.1. Nitric oxide release from 5

The ability of compound **5** to produce NO was tested using a chemiluminescence based Nitric Oxide Analyzer (NOA). In this assay, nitric oxide that is produced from the compound is then carried by continuously flowing stream of inert gas (argon) to a reaction cell within the chemiluminescence instrument. In the reaction cell NO reacts with ozone (O_3) that is generated in situ to form nitrogen dioxide (NO_2*) in its excited state. The subsequent decay of NO_2* to its ground state results in the emission of a photon between 600-800 nm, the emitted photons are measured by chemiluminescence detector.[24] Compound **5** was dissolved in phosphate buffer (10 mM, pH 7.4), and an aliquot was analyzed by NOA, as expected no evidence for NO generation. Whereas, in the presence of esterase, a signal attributable to NO was seen confirming the ability of **5** to produce NO (Figure 2.1). The amount of NO released was estimated using a standard calibration curve generated using sodium nitrite ($NaNO_2$) solution (Figure 2.13). The yield of NO in this experiment was found as 93%. When similar experiment was conducted with 2-(4-carboxyphenyl)-4,4,5,5-tetramethylimidazoline-1-oxyl-3-oxide potassium salt (c-PTIO, a known quencher of NO)[25], nearly complete disappearance

of NO signal was observed (Figure 2.1). Together, these data show that **5** generated NO upon activation by esterases.

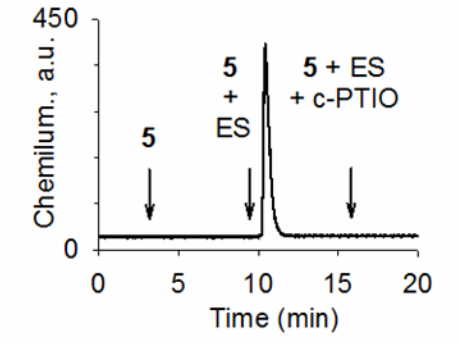

Figure 2.1. Nitric oxide produced during incubation of **5** (25 μM) alone or in the presence of esterase (ES, 0.5 U/mL), with and without c-PTIO (250 μM) in phosphate buffer pH 7.4 solution at 37 °C; analysis was conducted after 10 min incubation and arrow indicates approximate point of injection of analyte.

2.2.2.2. Fluorescence response from 5

Next, in order to study if this compound was capable of fluorescing upon cleavage by esterase, fluorescence emission spectra of **5** with and without esterase was recorded in buffer using fluorescence spectrophotometer (excitation 315 nm; emission 325 to 600 nm). In the absence of esterase, no significant fluorescence signal was seen at 460 nm (Figure 2.2.a). When incubated with esterase, we found a significant increase in fluorescence signal at 460 nm attributable to **12** (Figure 2.2.a). The yield of **12** in this assay was found to nearly quantitative, which was estimated through a calibration curve generated using authentic **12** (Figure 2.2.d), suggesting an efficient conversion of **5** to **12** (Scheme 2.4) in the presence of esterase. When the concentration of **5** was varied, a dose-dependent increase in fluorescence signal was observed (Figure 2.2.b). Together these experiments suggest that this compound was cleaved by esterase to turn on fluorescence.

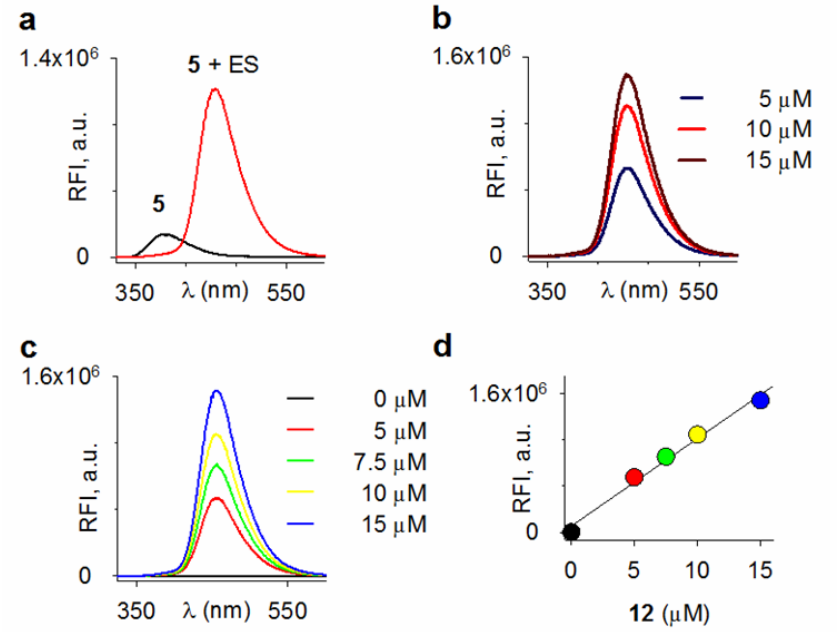

Figure 2.2. (a) Fluorescence emission spectra of **5** (10 μM) recorded in the absence and presence of ES (0.5 U/mL) in buffer; analysis was conducted after 10 min. (b) Enhancement of fluorescence signal at 460 nm with different concentration of **5** in the presence of ES (0.5 U/mL) in buffer; analysis was conducted after 10 min. (c), (d) Calibration curve with authentic **12** in buffer (All the experiments were conducted in phosphate buffer pH 7.4 at 37 °C, excitation 315 nm; emission 325 to 460 nm).

2.2.2.3. Time course of NO generation and fluorescence emission

Having established that compound **5** is able to enhance NO and fluorescence signal in the presence of ES, next time course of NO generation and fluorescence enhancement were independently monitored. The fluorescence signal at 460 nm was measured using fluorescence spectrophotometer, while NO released was measured using a nitric oxide analyzer. The time course of NO generation corresponded well with the time course of fluorescence enhancement (Figure 2.3), thus suggesting that once the pivaloyl group is cleaved, the rearrangement of the ensuing intermediate to produce DEA/NO and **12** is rapid (Scheme 2.4). Hence, once the fluorescence signal is seen, NO generation can be expected nearly instantaneously. Together, these data demonstrate that fluorescence emission at 460 nm is a convenient signal for NO release.

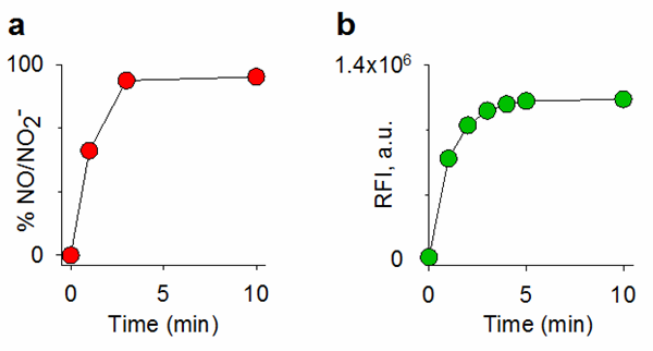

Figure 2.3. (a) Time-course of NO generation from **5** with ES (0.5 U/mL) in buffer (b) Time-course of fluorescence enhancement from **5** with ES (0.5 U/mL) in buffer (All the experiments were conducted in phosphate buffer pH 7.4 at 37 °C, excitation 315 nm; emission 325 to 460 nm).

2.2.2.4. Stability of compound 5 in RPMI media

Before performing the cellular study, first we tested the stability of compound **5** in RPMI media (10 % FBS) through measuring the level of NO release by nitric oxide analyser (NOA). When compound **5** (25 µM) was incubated for 30 min in RPMI media (10 % FBS), and an aliquot was analysed using NOA. As expected there was no significant level of NO observed in the absence of ES, thus supporting the stability of **5** in media (Figure 2.4).

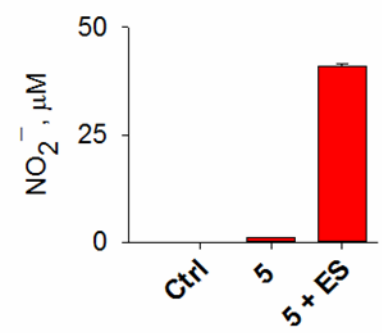

Figure 2.4. Stability of compound **5** in RPMI medium at 37 °C

2.2.3. Nitric oxide release and fluorescence emission in cells

In order to study the capability of compound **5** to enhance fluorescence signal as well as NO within the cells, HeLa cells were treated with 25 µM of compounds (**4**, **5** and **6**). After 30 min, the fluorescence signal at 460 nm was measured using a micro-well plate reader, while nitrite release was measured by Griess assay (Figure 2.5). In this Griess assay, NO produced from the compound is converted into nitrite, which subsequently reacts with the Griess reagent (i.e., Sulfanilamide and *N*-(1-napthyl) ethylene diamine) to form an azo dye with an absorbance maximum at 540 nm.[24] The amount of nitrite released was estimated from a standard calibration curve generated using sodium nitrite ($NaNO_2$) solution (Figure 2.14).

With a control compound **4** (does not contain diazeniumdiolate), an increase in the fluorescence signal was seen but no significant NO generation (Figure 2.5.a, 2.5.b); and with a control compound **6** (does not contain coumarin), an increase in extracellular nitrite was observed with no significant fluorescence signal (Figure 2.5.a, 2.5.b). Whereas, compound **5** is able to enhance both fluorescence signal as well as NO was observed (Figure 2.5.a, 2.5.b). When the dose of **5** was varied, as expected, a dose-dependent increase in fluorescence signal as well as nitrite was observed (Figure 2.5.c), thus supporting the suitability of **5** to enhance NO as well as fluorescence within cells. Thus, when cells are treated with **5** and the fluorescence signal at 460 nm is a reporter for NO generated.

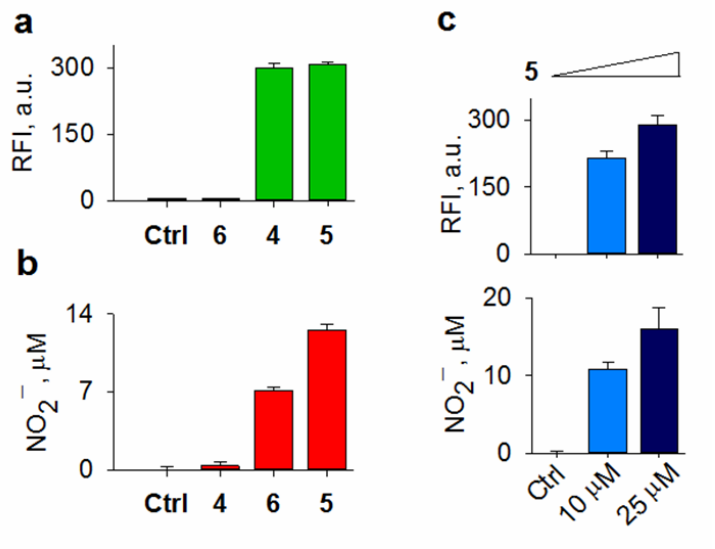

Figure 2.5. Comparison of fluorescence intensity attributable to **12** (a) and (b) extracellular nitrite release upon incubation of HeLa cells with 25 μM of **4**, **5** or **6**. (c) Comparison of fluorescence intensity attributable to **12** and extracellular nitrite release during incubation of HeLa cells with **5** at 0, 10 and 25 μM after 30 min at 37 °C (excitation 315 nm; emission 460 nm).

2.2.4. Consumption of NO during its detection

Liji Jin and coworkers reported an *O*-diamine based fluorogenic probe **15**, which is highly sensitive to NO, and two-photon excitable ability.[26] This probe works based on the principle of photo induced electron transfer (PET). Here *O*-diamine acts as a fluorescence quencher, in the presence of NO, due to the formation of triazole adduct the PET process gets blocked, which leads to enhancement in the fluorescence (Scheme 2.10).

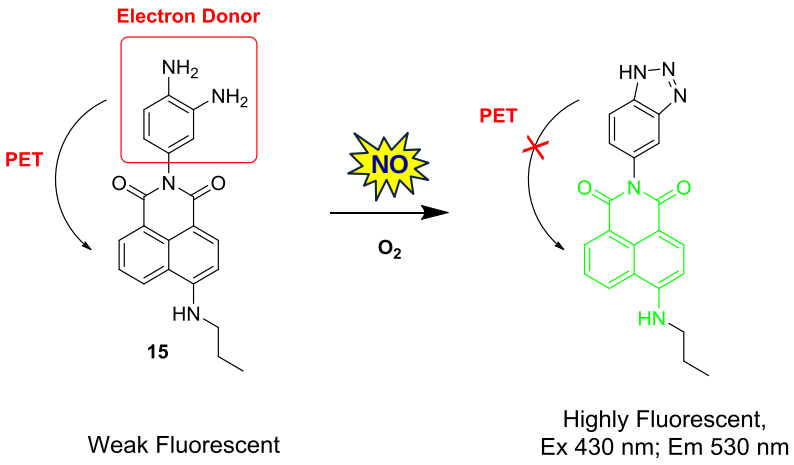

Scheme 2.10. Formation of the highly fluorescent triazole product from **15** in the presence of NO

The most common problem during NO delivery and concomitant detection is consumption of NO. In order to demonstrate that, an *O*-diamine based fluorogenic probe **15** was synthesized by reported procedure in three steps (Scheme 2.11).[26] Wherein, 1,4-Diamino-2-nitrobenzene was reacted with 4-bromo-1,8-naphthalic anhydride to form the compound **13** in 90% yield, which was then reacted with propylamine gave compound **14** in good yield. Reduction of **14** gave the desired fluorophore **15** with an excellent yield (Scheme 2.11).

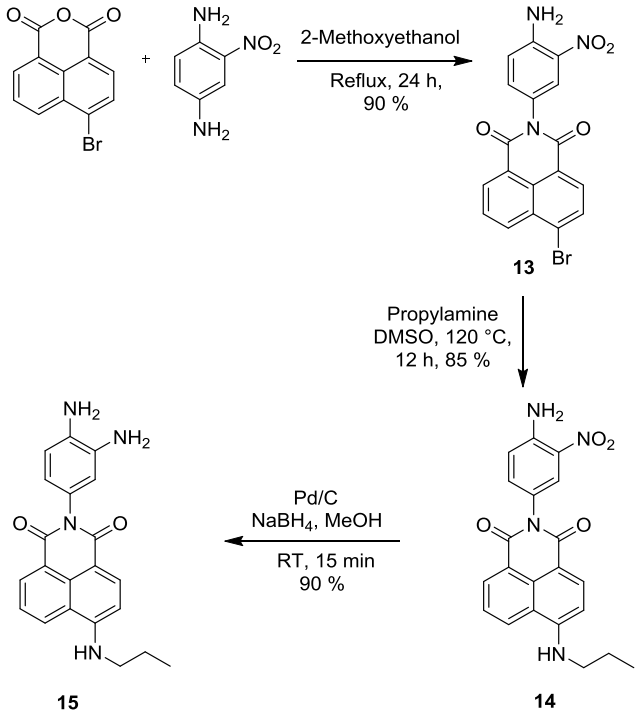

Scheme 2.11. Synthesis of NO probe **15**

An esterase sensitive NO donor **6** was synthesized (Scheme 2.8) which produces NO in the presence of ES. Compound **6** was treated with ES in buffer, and nitrite release from **6** was

measured by Griess assay, a signal attributable to NO was observed. Similar experiment was conducted in the presence of probe **15**, a diminished colorimetric signal was observed when compared with **6**+ES (Figure 2.6.a). At similar time point, when we performed the fluorescence study, a fluorescence signal at 530 nm attributable to the formation of triazole adduct was observed (Figure 2.6.b), which confirmed that the diminished colorimetric signal is due to the formation of highly fluorescent triazole adduct. In a cellular assay, co-treatment of **6** along with probe **15** resulted in diminished yield of nitrite when compared with a similar concentration of **6** alone (Figure 2.6.c). Together, these data show that using a NO donor along with a probe for NO invariably leads to collateral consumption of NO during detection. This major limitation is overcome by the use of FLUORO/NO (**5**) as NO is released along with a fluorescence signal at 460 nm in buffer, without collateral consumption of NO.

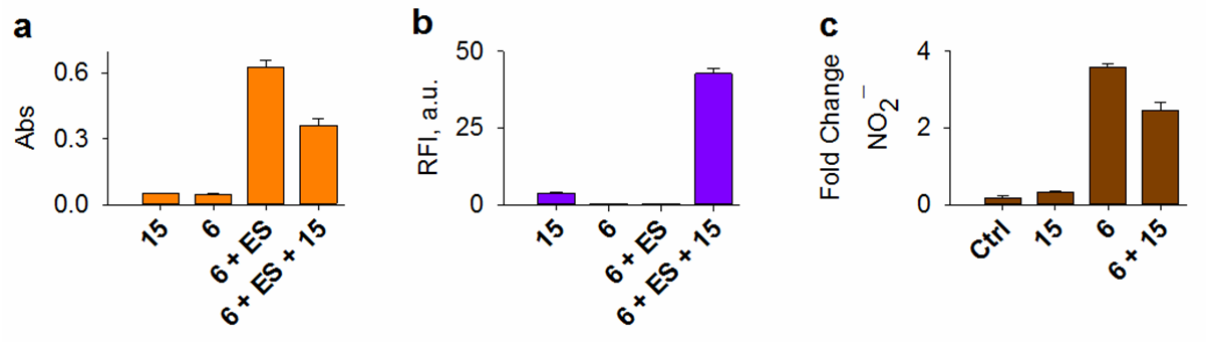

Figure 2.6. (a) Griess assay for the formation of nitrite upon incubation of **6** in the presence/absence of ES, and with and without NO dye **15** in buffer (pH 7.4) at 37 °C. (b) Detection of NO by **15** during incubation in buffer (pH 7.4) at 37 °C (excitation 430 nm; emission 530 nm). (c) Griess assay for the formation of nitrite upon incubation of **6** with and without NO dye **15** in HeLa cells.

2.2.5. Intracellular activation of 5

2.2.5.1. Confocal microscopy imaging

Having established that **5** is a reliable source of NO within cells, the fluorescence signal at 460 nm can now be used as a surrogate for NO generation. In order to study the cellular uptake of **5**, HeLa cells were treated with different concentrations of **5** for 30 min and the fluorescence signal attributable to the formation of **12** at 460 nm was monitored by confocal microscopy. A dose-dependent increase in fluorescence signal was observed (Figure 2.7). The fluorescence signal was nearly uniformly distributed within cells, possibly due to the ubiquitous nature of esterase. These results supporting that, the compound **5** permeate cells and get activated by cellular esterase to produce fluorescence signal attributable to **12**.

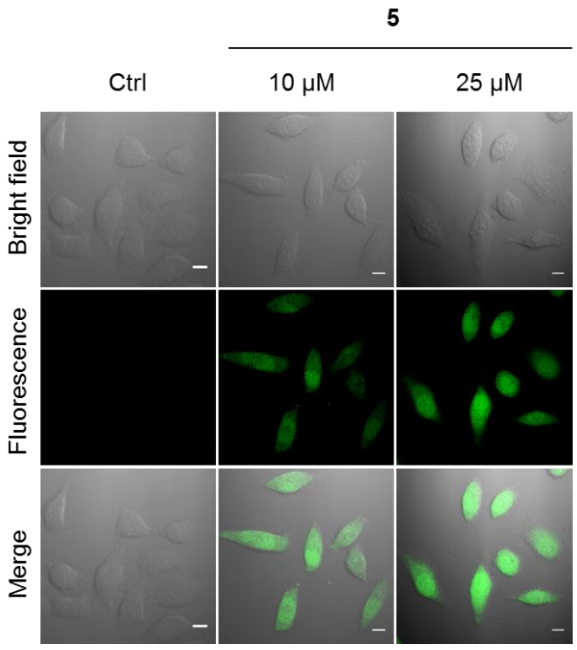

Figure 2.7. Confocal microscopy images of HeLa cells treated with **5** (10 and 25 μM) after 30 min at 37 °C. The excitation and emission channels were 405 nm and 460 nm respectively. Scale bar = 10 μm.

2.2.5.2. Two-photon microscopy imaging

The release of NO is reported by a fluorescent signal attributable to **12** at 460 nm, which is sufficient to monitor the release of NO *in vitro*. In one photon imaging, shorter wavelength was used to excite the coumarin derivative **12**, which is associated with less tissue penetration, auto fluorescence and photo-toxicity. In order to infer the production of NO *in vivo* model, longer wavelength excitation would be useful. Since two-photon imaging tool has more advantages over the one-photon ones, such as localized excitation, increased tissue penetration, decreased light scattering, reduced tissue auto-fluorescence, photo-bleaching and therefore, we adopted the two-photon fluorescent spectroscopy tool for cellular imaging.[27] As coumarin-based fluorophores are compatible with two-photon excitation microscopy, we carried out live-cell imaging experiment with **5** (Figure 2.8).[28] HeLa cells were treated with different concentration of **5** and the fluorescence signal attributable to **12** was monitored by two-photon microscopy. As expected, we found a dose-dependent increase in the fluorescence signal at 460 nm with 740 nm excitation (Figure 2.8). Thus, this compound is expected to have deep tissue penetration and reduced phototoxicity during imaging of NO in *in vivo* model.

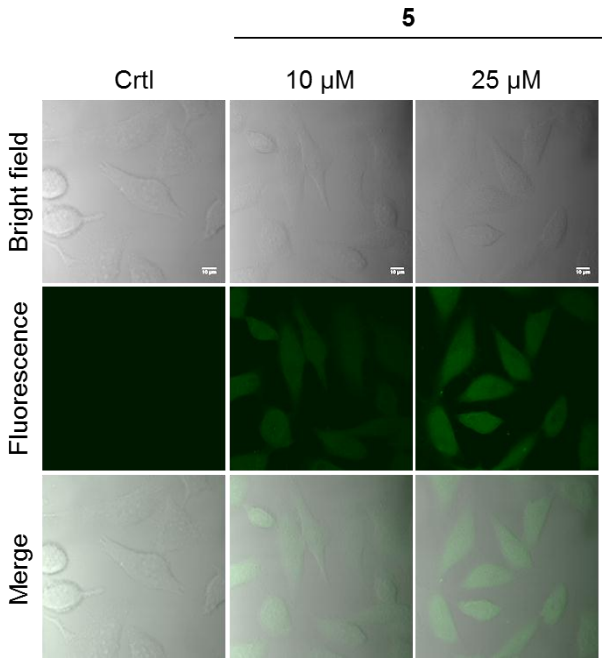

Figure 2.8. Two photon microscopy images of HeLa cells treated with **5** (10 and 25 µM) after 30 min. The excitation and emission channels were 740 nm and 460 nm respectively. Scale bar = 10 µm.

2.2.5.3. Fluorescence-activated cell sorting (FACS)

Next, in order to further verify the intracellular activation of **5**, we used fluorescence-activated cell sorting (FACS) to track the release of **12** within the cells. FACS analysis of HeLa cells treated with **5** (0, 10, 25 µM), similarly showed a dose-dependent increase in fluorescence signal attributable to **12** (Figure 2.9). Together, these results suggest the suitability of **5** in flow-cytometry as well as live-cell imaging experiments.

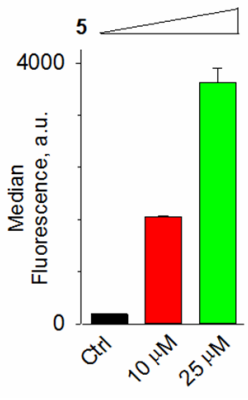

Figure 2.9. FACS analysis of HeLa cells incubated with **5** (0, 10 and 25 µM) after 30 min at 37 °C (excitation 355 nm; emission 460 nm).

2.2.6. Activation of cGMP by NO released from 5

One of the most important biological roles of NO is activation of soluble guanylate cyclase (sGC), which results in the production of secondary messenger cGMP from GTP, which ultimately promotes the main biological functions of NO, including smooth muscle relaxation, platelet aggregation and gene expression. In order to test if **5** was capable of activating sGC within cells, cGMP levels were measured by using a bioluminescence resonance energy transfer (BRET) assay in human embryonic HEK293T cells.[29] BRET is based on energy transfer between luminescence donor and fluorescent acceptor proteins, for example, *Renilla* luciferase (Rluc) and green fluorescence protein (GFP). Here, the ratio between GFP fluorescence and chemiluminescence was determined. An increase in the BRET ratio is an indication of the conformational change that occurred in the GAF domain on cGMP binding (Figure 2.10). First, a known NO donor, sodium nitroprusside (SNP, 50 µM) was tested as the positive control and a significant enhancement in cGMP levels was observed (Figure 2.11). When a similar assay was conducted with **5** (25 µM), as expected, a signal for cGMP was observed. This assay was conducted with the negative control compound **4** and as expected no significant enhancement in cGMP levels was observed (Figure 2.11). Thus, other than NO, the by-products produced during decomposition of **5** were incapable of inducing NO-like signalling. This result suggesting that **FLUORO/NO** (**5**) was suitable for use as a tool to enhance NO for cellular signalling studies.

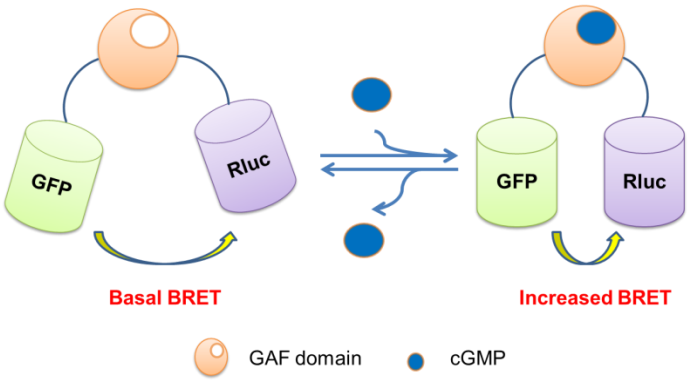

Figure 2.10. The BRET sensor consists of the cGMP binding sites (GAF domain) GFP and Rluc. Binding of cGMP to GAF domain leads to a conformational change, decreasing the distance between Rluc and GFP, which results in an enhanced BRET signal.

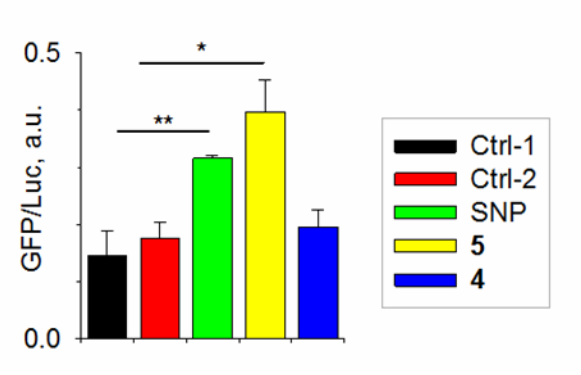

Figure 2.11. Formation of NO in cells was inferred by measurement of cyclic GMP, a secondary messenger for NO, by a BRET assay at 37 °C. *p value = 0.022; **p value = 0.007. Control 1=cells only, Control 2=cells containing DeepBlueC (luciferase substrate) without any treatment. Data provided by Meisam Bagheri & Deepak Saini, IISc Bangalore.

2.2.7. DNA damage induced by NO released from 5

Nitric oxide and reactive nitrogen species (RNS) are well known to induce DNA damage, especially double strand breaks (DSBs).[30] 53BP1 is one of the DNA damage response proteins that is recruited very efficiently to sites of DNA double-strand breaks. Its recruitment can be visualized by monitoring live cells expressing 53BP1 fused to green fluorescent protein (GFP). Therefore, we monitored the ability of **5** to induce DNA damage by monitoring 53BP1 foci, which are markers of double strand breaks and accumulate as nuclear foci.[31] HeLa cells stably expressing 53BP1 fused to GFP were seeded on glass-bottom dishes and independently treated with **5** and **4**, and imaged 24 h post-treatment. As expected, we found a dose-dependent increase in DNA damage induced by **5** as evidenced by increased foci, increased foci are indicative of enhanced DNA damage response (Figure 2.12). Furthermore, **4** did not induce the same level of damage, which indicated that **5** induced DNA double strand breaks presumably as a result of released NO (Figure 2.12).

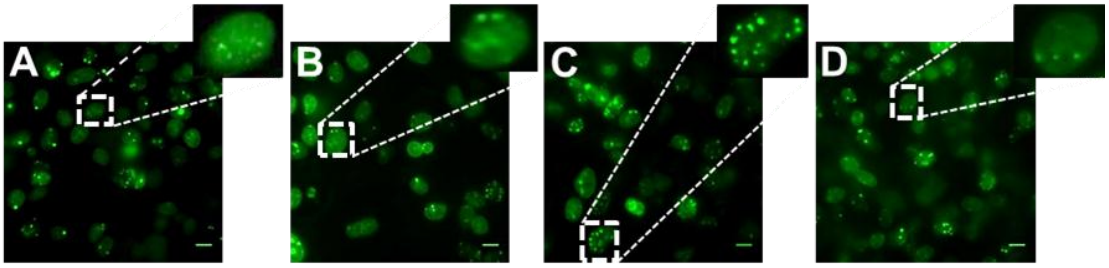

Figure 2.12. Formation of 53BP1 foci at 37 °C upon exposure of A) control, B) 5 μM **5**, C) 10 μM **5**, or D) 10 μM **4**. Scale bar: 10 μm. Increased foci are indicative of enhanced DNA damage response. Data provided by Meisam Bagheri & Deepak Saini, IISc Bangalore.

Recently, Prof. Pradeep Singh's lab has developed a coumarin-based strategy for real-time monitoring of NO release with light as a trigger (Scheme 2.12).[32]

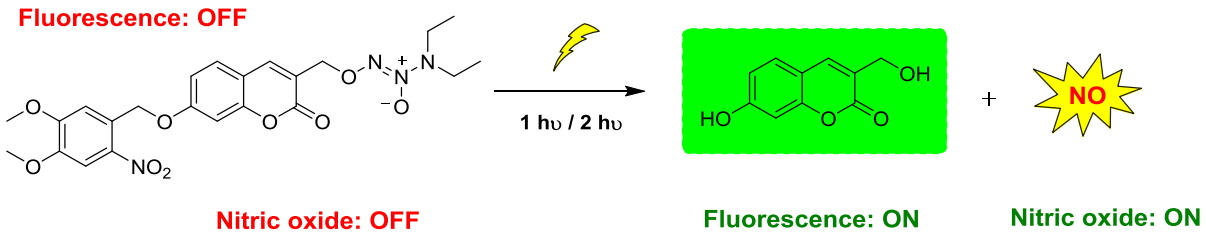

Scheme 2.12. Light triggerable NO donor with a fluorescence reporter for real-time monitoring of NO in cells.

2.3. Summary

In this chapter, we report FLUORO/NO, a NO donor with a fluoresence reporter for studying NO biology that eliminates the need for secondary assays to report the formation of NO. The collateral consumption of NO that is associated with NO delivery and concomitant detection can be avoided by the use of FLUORO/NO. The versatility of this scaffold for real-time monitoring of NO released was demonstrated with an esterase and can, in principle, be extended to other stimuli of interest as well. This compound will be useful for cellular studies in microwells, confocal microscopy for imaging or flow cytometry. The compatibility of the fluorophore for use in two-photon imaging where longer wavelength excitation indicates the possibility of use of FLUORO/NO for *in vivo* imaging as well. The by-products of decomposition do not show NO-like activity in signalling as well as DNA damage assays suggesting the suitability of this compound for NO delivery. To the best of our knowledge, this is the first example of a small molecule that, when incubated in the presence of an enzyme, simultaneously produces NO as well as a fluorescence signal without collateral NO consumption. It is anticipated that this tool will find use in interrogating NO biology, which is yet to be completely understood.

2.4. Experimental Section

2.4.1. Synthesis and characterization

Compounds **1**[21], **2**[22], **6**[23], **7-12**[16] and **13-15**[26] were synthesized using previously reported procedures, and the analytical data that we collected were consistent with the reported values.

((3-Methyl-2-oxo-*2H*-chromen-7-yl)oxy)methyl pivalate (3):

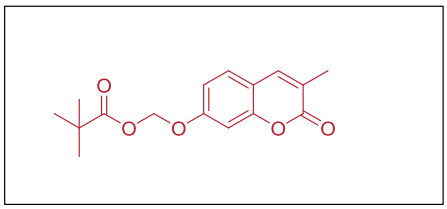

To a solution of compound **1** (50 mg, 0.28 mmol) in ACN (3 mL), K_2CO_3 (118 mg, 0.85 mmol) was added followed by a solution of **2** (103 mg, 0.42 mmol) in ACN (1mL). The reaction mixture was stirred for 3 h under a nitrogen atmosphere at room temperature. Upon completion of reaction (TLC analysis), the solvent was removed under reduced pressure. The residue was purified by silica gel column chromatography using EtOAc/pet ether (0 → 25 %) as the eluent to obtain **3** (73 mg, 89 %) as a white solid: m.p. 98 – 100 °C; FT-IR (ν_{max}, cm^{-1}): 2969, 1755, 1709, 1615, 1505; ^{1}H NMR ($CDCl_3$, 400 MHz): δ 7.46 (s, 1H), 7.34 (d, *J* = 8.6 Hz, 1H), 7.00 (d, *J* = 2.4 Hz, 1H), 6.92 (dd, *J* = 8.4, 2.4 Hz, 1H), 5.79 (s, 2H), 2.18 (d, *J* = 1.3 Hz, 3H), 1.20 (s, 9H); ^{13}C NMR ($CDCl_3$, 100 MHz): δ 177.3, 162.4, 158.9, 154.6, 139.2, 128.1, 123.5, 114.8, 113.6, 103.2, 85.2, 39.1, 27.0, 17.2; HRMS (ESI) for $C_{16}H_{18}O_5$ $[M+H]^+$: Calcd., 291.1232, Found., 291.1234.

((3-(Bromomethyl)-2-oxo-*2H*-chromen-7-yl)oxy)methyl pivalate (4):

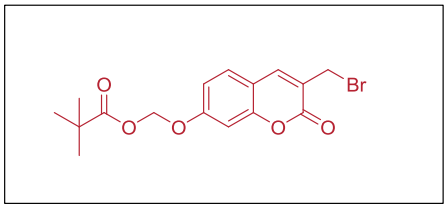

To a solution of compound **3** (50 mg, 0.17 mmol) in CCl_4 (6 mL), NBS (34 mg, 0.19 mmol) was added along with a trace amount of AIBN. The reaction mixture was refluxed for 3 h under a nitrogen atmosphere. After cooling to room temperature, the solvent was removed under reduced pressure. Then the residue was purified by column chromatography using EtOAc/Pet ether (0 → 30 %) as the eluent to obtain **4** (48 mg, 75 %) as a white solid: mp 124 – 126 °C; FT-IR (ν_{max}, cm^{-1}): 2978, 1751, 1725, 1612, 1502; ^{1}H NMR ($CDCl_3$, 400 MHz): δ 7.80 (s, 1H), 7.44 (d, *J* = 8.6 Hz, 1H), 7.02 (d, *J* = 2.4 Hz, 1H), 6.97 (dd, *J* = 8.6, 2.5 Hz, 1H), 5.81 (s, 2H), 4.42 (s, 2H), 1.20 (s, 9H); ^{13}C NMR ($CDCl_3$, 100 MHz): δ 177.2, 160.2, 160.1, 155.3, 142.0, 129.4, 123.1, 114.1, 114.0, 103.2, 84.9, 39.1, 28.0, 27.0; HRMS (ESI) for $C_{16}H_{17}BrO_5$ $[M+H]^+$: Calcd., 369.0337, Found., 369.0336.

(*Z*)-3,3-diethyl-1-((2-oxo-7-((pivaloyloxy)methoxy)-*2H*-chromen-3-yl)methoxy)triaz-1 ene 2-oxide (5):

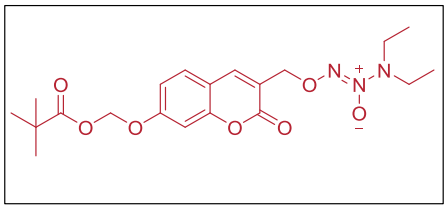

To a solution of **DEA/NO** (100 mg, 0.65 mmol) in THF (3 mL) under ice, 15-crown-5 (12 µL) was added and the mixture stirred at 0 ºC for 5 min under a nitrogen atmosphere. A solution of **4** (200 mg, 0.54 mmol) in DMF (1 mL) was added to the reaction mixture at 0 ºC and stirred at room temperature for 3 h. The solvent was evaporated under reduced pressure, diluted with 10 mL of water and the aqueous solution was extracted with EtOAc (3×5 mL). The combined organic layer was washed with brine, dried over Na_2SO_4 (5 g), filtered and the filtrate was concentrated to give a crude compound. This crude was initially purified by silica gel column chromatography using EtOAc/pet ether (0 → 40 %) as the eluent. The resulting mixture was further purified using semi-preparative HPLC with C-18 semi-preparative column (9.4 mm × 250 mm, 5 µm; ZORBAX ODS), using a gradient of ACN and water (60 – 80 %), under ambient temperature with a flow rate of 2.5 mL/min to obtain **5** (55 mg, 24 %) as a white solid: mp 81 – 83 °C; FT-IR (ν_{max}, cm^{-1}): 2980, 1752, 1726, 1614, 1571, 1508, 1392; ^1H NMR ($CDCl_3$, 400 MHz): δ 7.71 (s, 1H), 7.40 (d, *J* = 8.6 Hz, 1H), 7.02 (d, *J* = 2.4 Hz, 1H), 6.96 (dd, *J* = 8.7, 2.5 Hz, 1H), 5.81 (s, 2H), 5.22 (d, *J* = 1.1 Hz, 2H), 3.16 (q, *J* = 7.2 Hz, 4H), 1.20 (s, 9H), 1.09 (t, *J* = 7.1 Hz, 6H); ^{13}C NMR ($CDCl_3$, 100 MHz): δ 177.2, 160.2, 159.9, 155.0, 140.2, 129.2, 121.2, 114.0, 113.9, 103.2, 85.0, 70.0, 48.6, 39.1, 27.0, 11.6; HRMS (ESI) for $C_{20}H_{27}N_3O_7$ $[M+Na]^+$: Calcd., 444.1746, Found, 444.1743.

2.4.2. NO release and fluorescence emission in Buffer

2.4.2.1. Nitric oxide detection from 5

A 1 mM stock solution of compound **5** in DMSO and a 1 U/mL stock solution of porcine liver esterase (Sigma-Aldrich) in phosphate buffer pH 7.4 were prepared. A typical reaction mixture consisted of compound **5** (25 µM) and esterase (0.5 U/mL) was prepared by mixing **5** (12.5 µL, 1 mM) and 250 µL of esterase from the stock solutions with 237.5 µL of pH 7.4 phosphate buffer (10 mM) at 37 ºC. An aliquot of the reaction mixture (10 µL) from the reaction vial was injected into a Sievers nitric oxide analyzer (NOA 280i) using argon as the carrier gas.[33] For the experiment with the NO scavenger 2-(4-carboxyphenyl)-4,4,5,5-tetramethylimidazoline-1-oxyl-3-oxide potassium salt (250 µM, 10 eq., c-PTIO), an aliquot of the reaction mixture (10 µL) was injected into the NOA chamber. The amount of NO released was estimated using a standard calibration curve generated using sodium nitrite

($NaNO_2$) solution of concentration from 0 – 100 μM using NOA Analyzer (Y = 68.84X; R^2 = 0.998).

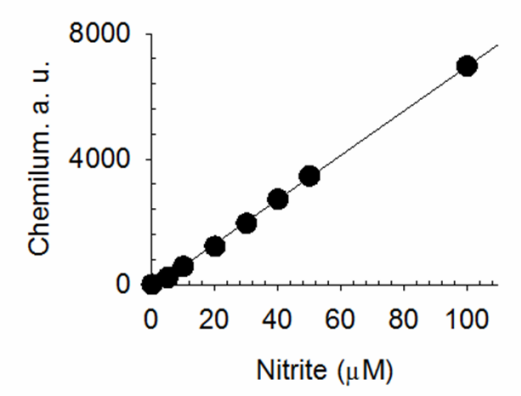

Figure 2.13. Calibration curve for nitrite in phosphate buffer pH 7.4 solution at 37 °C

2.4.2.2. Fluorescence emission spectra

Compounds **5** or **12** in phosphate buffer pH 7.4 (10 mM) was excited at respective lowest energy absorption maximum with an excitation slit width of 1 nm and emission slit width of 1 nm, and the emission profile was recorded. A solution contained 1% of DMSO. Fluorescence experiments were performed in a micro fluorescence cell (Hellma, path length 1.0 cm) on a HORIBA Jobin Yvon, Fluorolog fluorescence spectrophotometer.

2.4.2.3. Quantum yield determination

For determination of fluorescence quantum yield (Φ_F) of compound **12**, 2-Aminopurine in water ($\Phi_{F(s)}$ = 0.68) was used as a standard.[34] The $\Phi_{F(x)}$ value was calculated according to eq. 1.

$$\Phi_{F(x)} = (A_s/A_x)\,(F_x/F_s)\,(n_x/n_s)^2\,\Phi_{F(s)} \qquad \textbf{eq. 1}$$

Where s is the standard, x is the compound **12**, A is the absorbance at excitation wavelength, F is the area under the emission curve, n is the refractive index of the solvent and Φ_F is the quantum yield.

Table 2.1. Comparison of the quantum yields.

Sample	λ_{abs} (nm)	A	λ_{em} (nm)	F	Φ_F
2-Amino purine (s)	324	0.0345	377	2.21×10^7	0.68
Compound **12** (x)	324	0.1605	456	6.87×10^7	0.50

2.4.2.4. Stability of compound 5 in RPMI medium

A 1 mM stock solution of compound **5** in DMSO was prepared and 12.5 µL of **5** (25 µM) was incubated with 487.5 µL of RPMI medium (10 % FBS) with and without esterase (0.5 U/mL) at 37 ºC. After 30 min, an aliquot of the reaction mixture (10 µL) from the reaction vial was injected into a Sievers Nitric Oxide Analyzer (NOA 280i) using argon as the carrier gas. The amount of nitrite release was estimated using a standard calibration curve generated using sodium nitrite ($NaNO_2$) solution of concentration from 0 – 100 µM using NOA Analyzer (Y = 68.84X; R^2 = 0.998). The data represented here is average of 3 repeats.

2.4.3. Nitric oxide collateral consumption assay

The nitric oxide donor **6** and NO-sensitive fluorophore **15** was used to demonstrate collateral consumption of NO during its detection. Here, **6** (25 µM) and **15** (75 µM) was incubated in pH 7.4 buffer at 37 ºC for 15 min with and without esterase (0.5 U/mL) and fluorescence emission was measured using a Thermo Scientific Varioscan microwell plate reader (excitation 430 nm; emission 530 nm). For nitrite measurement, after 15 min incubation, Griess reagent (14 µL for 200 µL reaction mixture, Sigma Aldrich) was added, and incubated at 37 ºC for 25 min before measuring OD at 535 nm using a Thermo Scientific Varioscan microwell plate reader. The data represented here is average of 3 repeats.

2.4.4. NO release and fluorescence emission in cells

2.4.4.1. Fluorescence emission and nitrite release in cells

Cells were suspended in PBS (1X) and plated in a 96-well plate (0.5 x 10^5 cells/100 µL). Compound **4**, **5** and **6** in DMSO was added to the cell suspension. Cells were incubated at 37 ºC for 30 min and fluorescence emission was measured using a Thermo Scientific Varioscan microwell plate reader (excitation 315 nm; emission 460 nm). For nitrite measurement, after 30 min incubation, Griess reagent (14 µL for 200 µL reaction mixture, Sigma Aldrich) was added, and incubated at 37 ºC for 25 min before measuring OD at 540 nm using a Thermo Scientific Varioscan microwell plate reader. The amount of nitrite release was estimated using a standard calibration curve generated using sodium nitrite $NaNO_2$ solution of concentration from 0 – 50 µM (Y = 0.0145 X; $R2$ = 0.998). The data represented here is average of 3 repeats.

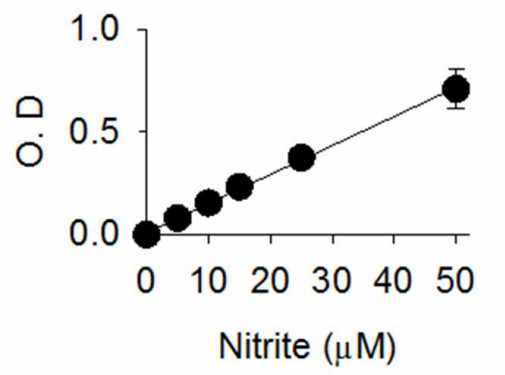

Figure 2.14. Calibration curve for nitrite in HBSS Buffer at 37 °C (O.D = Optical Density).

2.4.4.2. Confocal Image of HeLa cells with 5

HeLa cells were seeded at 1×10^5 cells/well in 4-well chamber for overnight in DMEM medium supplemented with 10% FBS (fetal bovine serum) and 1% antibiotic solution in an atmosphere of 5% CO_2 at 37 °C. After incubation, old media was removed and the cells were washed with 500 µL of PBS (1X) buffer. Then 500 µL of fresh DMEM media was added along with compound **5** (10, 25 µM) and cells were incubated for 30 minutes at 37 °C. After 30 minutes, old media was removed, cells were washed twice with 200 µL of PBS (1X) and then cells were imaged on a Zeiss LSM 710 confocal microscopy with 405 nm (740 nm was used for two photon) laser lines at 2% power using a 63X oil immersion objective. Images were analysed by ImageJ software.

2.4.4.3. FACS analysis for 5

HeLa cells were seeded at 1×10^5 cells/well in 6 well plate for overnight in DMEM media supplemented with 10% FBS (fetal bovine serum) and 1% antibiotic solution in an atmosphere of 5% CO_2 at 37°C. After incubation, old media was removed and the cells were washed with 1 mL of PBS (1X) buffer. Then 1 mL of fresh DMEM media was added along with compound **5** (10, 25 µM) and cells were incubated for 30 minutes at 37 °C. After 30 minutes, media was removed, cells were washed with 1 mL of PBS (1X) and cells were detached by trypsination. Cells were centrifuged at 1000 rpm, 22 °C for 5 min. Supernatant were removed and 500 µL of PBS (1X) was added to the cell pellet. Samples were illuminated with a UV laser at 355 nm on a Flowcytometry (BD LSRFortessa SORP cell analyser, performed at NCL Innovation Park, Pune). The data represented here is average of 2 repeats.

2.4.4.4. cGMP measurement[29]

Human embryonic kidney (HEK) 293T cells were maintained in DMEM with fetal calf serum (10%), penicillin (100 mg L^{-1}) and streptomycin (100 mg L^{-1}) at 37 °C in a 5% CO_2 humidified incubator. HEK 293T cells were transfected with pGFP2-GAFa-Rluc, in a 12-well plate using Turbofect (Thermo Fisher Scientific) according to the manufacturer's protocol. After 48 h, cells were harvested, and reseeded (10^5 cells per well) in a 96-well plate in Live Cell Imaging Solution (Invitrogen) and treated with various compounds (as indicated). After 10 min, DeepBlueC (5 μM, ThermoFisher, USA) was added and BRET (Bioluminescence Resonance Energy Transfer) measurements were made in an Infinite M1000 PRO plate reader (Tecan, Austria) at the channel of BLUEI (luminescence) and Green1 (fluorescence). The data represented here is average of 3 repeats and statistical analysis was done using t-test.

2.4.4.5. 53BP1 foci formation assay

HeLa cells stably expressing GFP-53BP1 were used for live imaging experiments.[35] The cells were treated with different concentrations of **5** and/or **4** for 5 days and imaged prior to and after treatment. For imaging, cells were seeded in glass-bottom dishes and treated with indicated compounds and imaged in an IX83 inverted fluorescence microscope (Olympus) using 60X objective and data was analysed using Slidebook 6.0 software (Intelligent Imaging Innovations, Denver, CO). Images were taken in the GFP channel with fixed acquisition settings.

2.5. Spectral charts

^{1}H-NMR Spectrum (400 MHz, $CDCl_3$) of Compound **3**

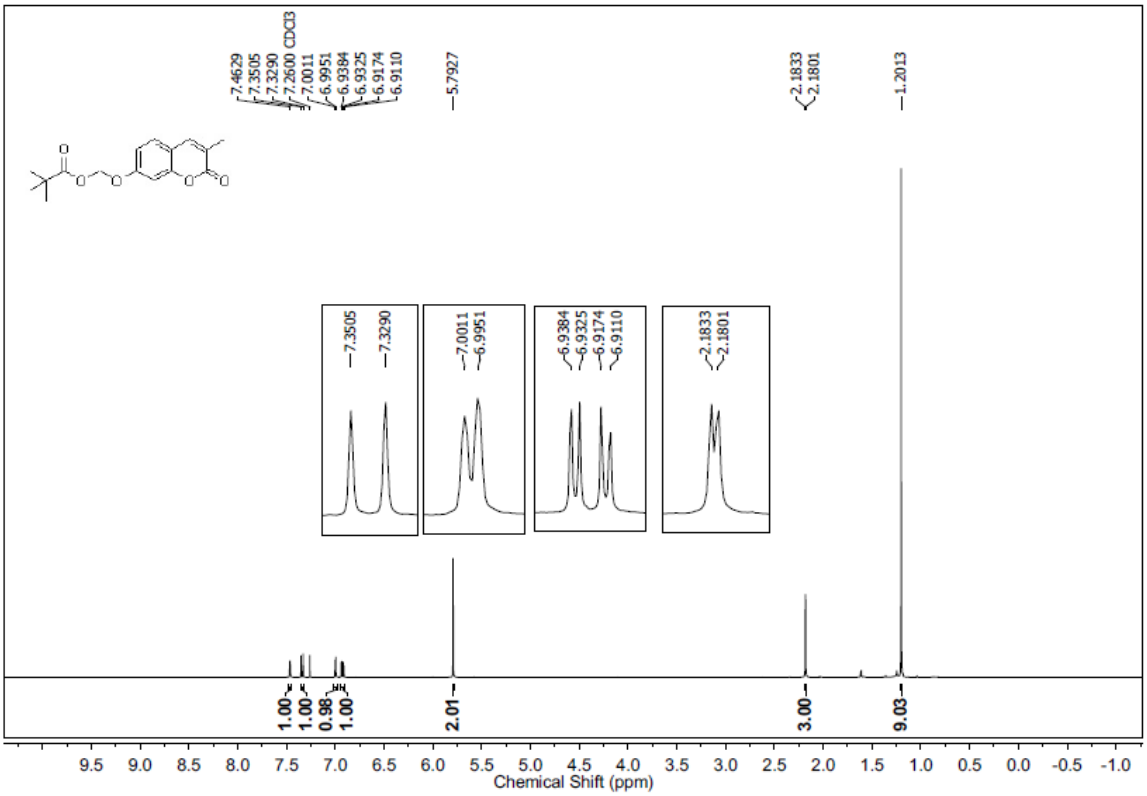

^{13}C NMR Spectrum (100 MHz, $CDCl_3$) of Compound **3**

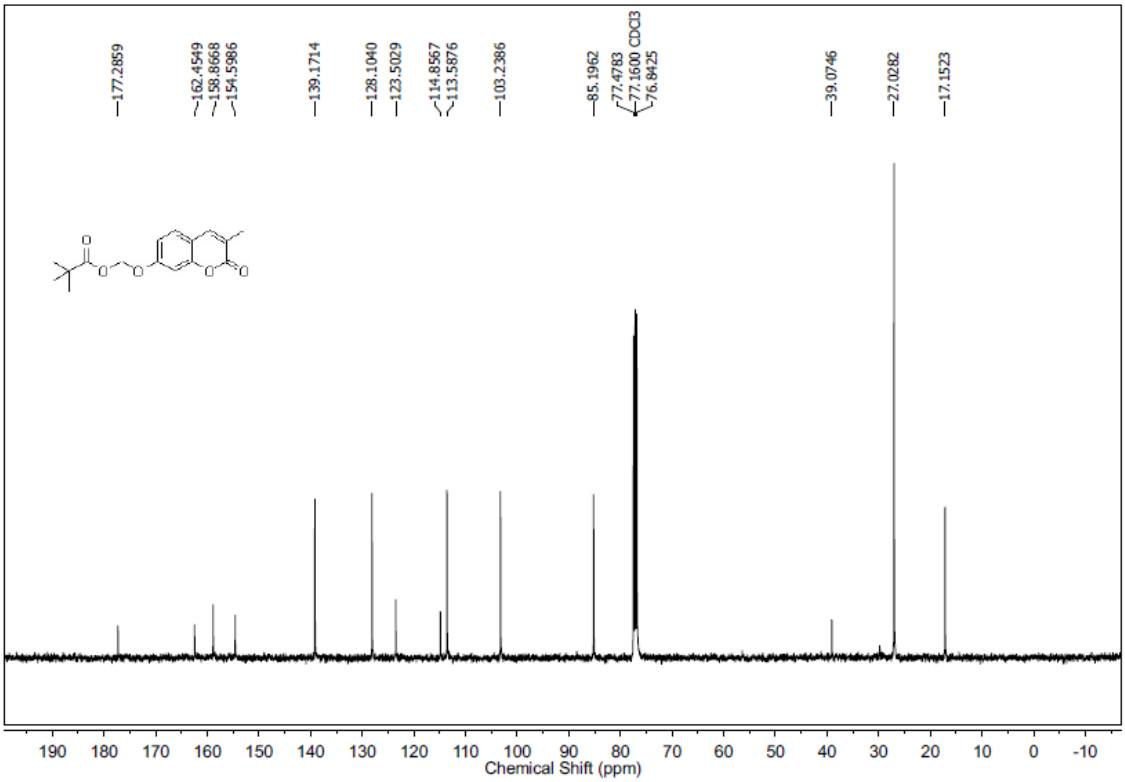

^{1}H-NMR Spectrum (400 MHz, $CDCl_3$) of Compound **4**

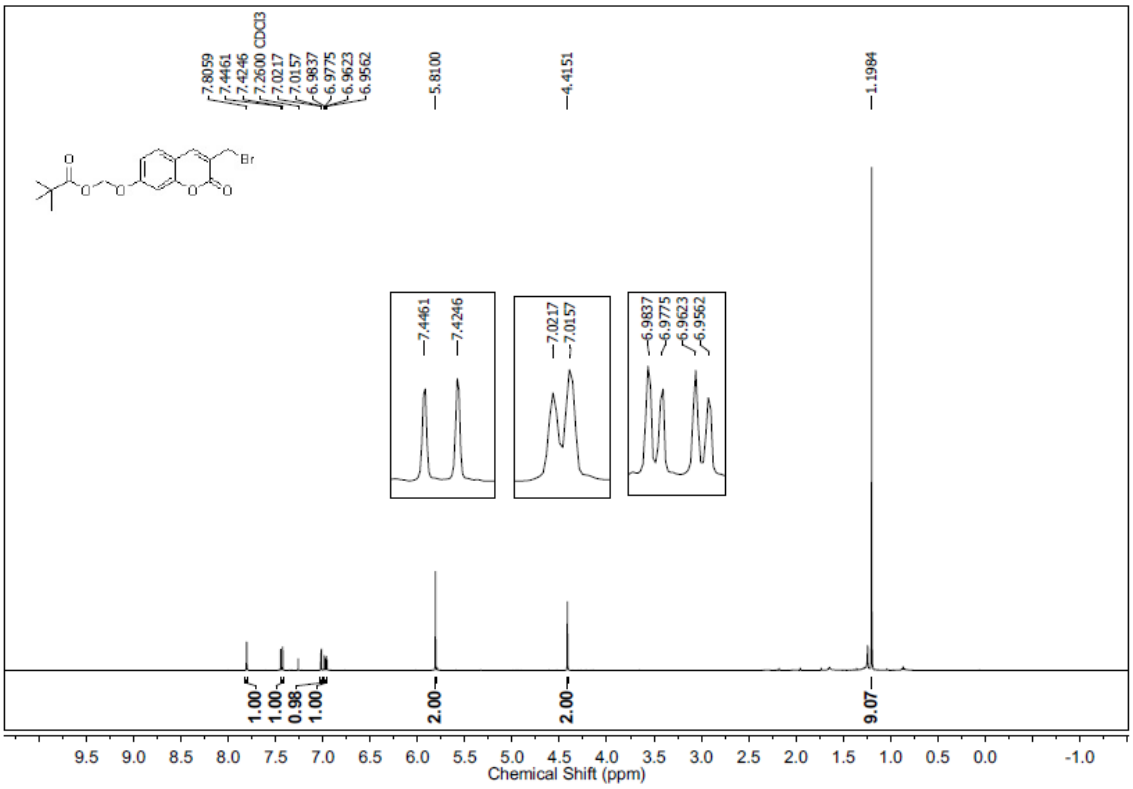

^{13}C NMR Spectrum (100 MHz, $CDCl_3$) of Compound **4**

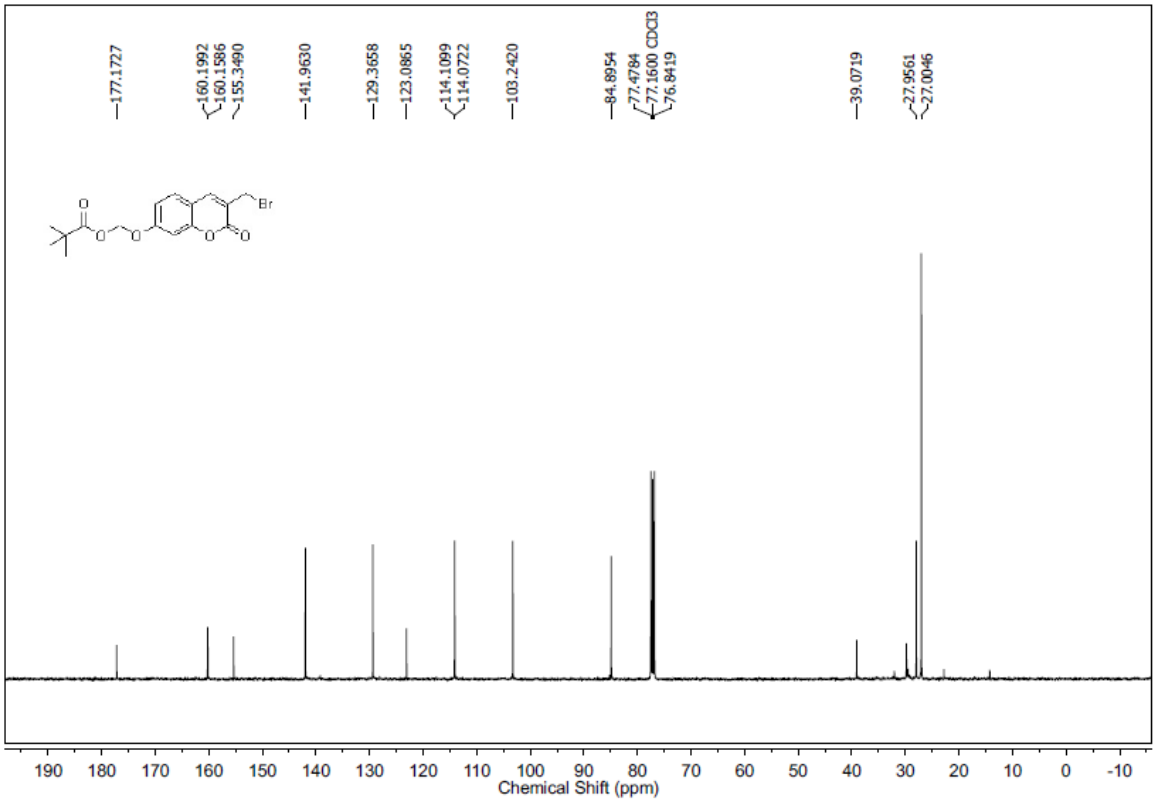

^{1}H-NMR Spectrum (400 MHz, $CDCl_3$) of Compound **5**

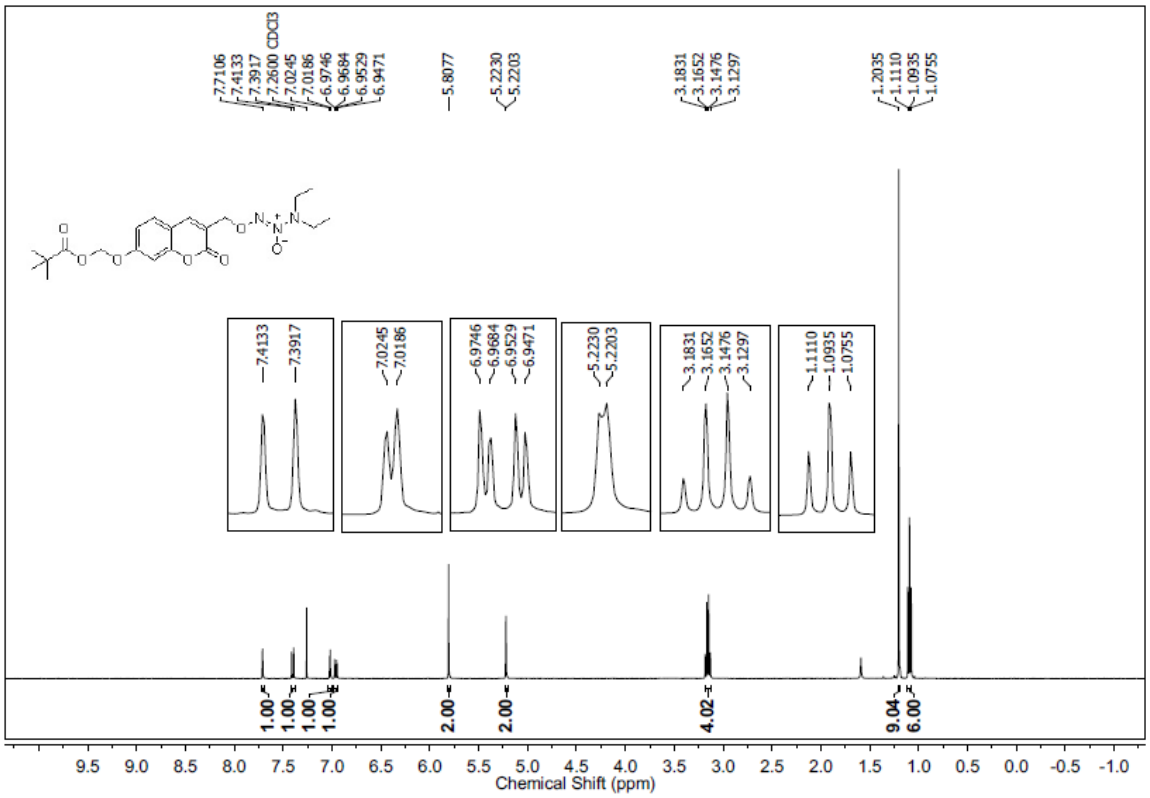

^{13}C NMR Spectrum (100 MHz, $CDCl_3$) of Compound **5**

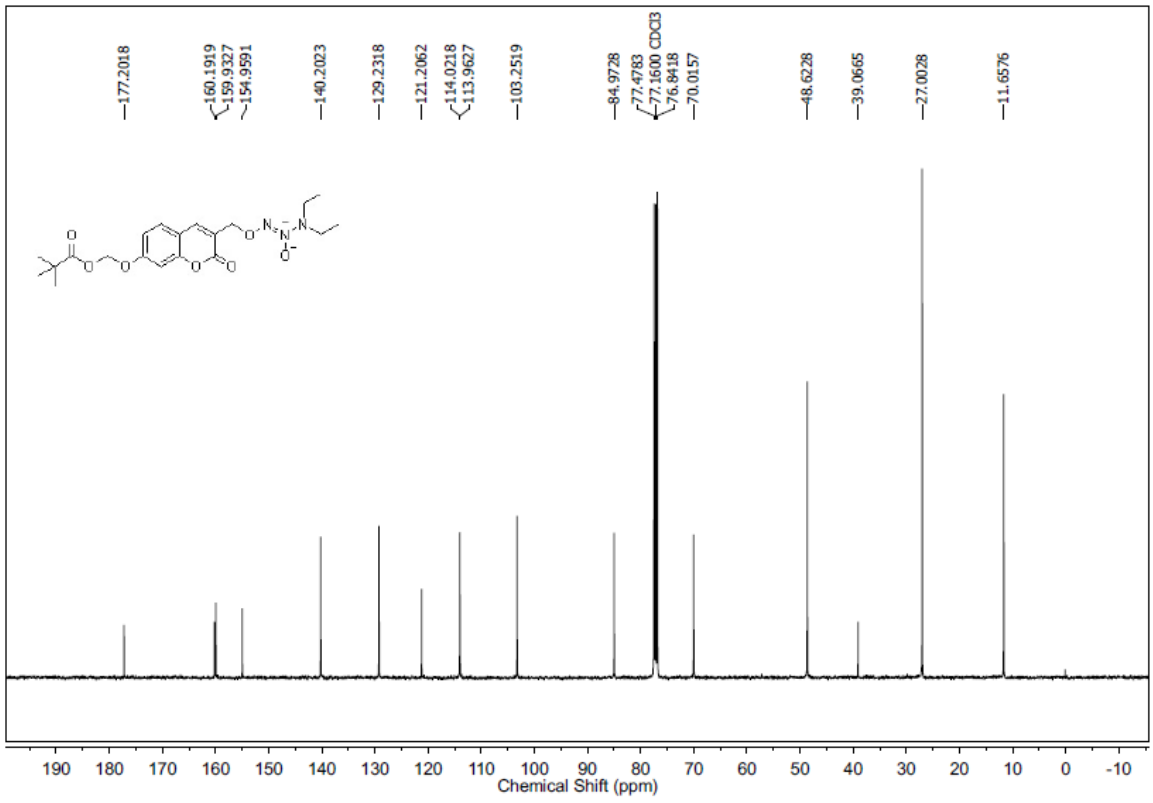

2.6. References

(1) Ignarro, L. J. *Angew. Chem. Int. Ed.* **1999**, *38*, 1882.

(2) Wink, D. A.; Hines, H. B.; Cheng, R. Y.; Switzer, C. H.; Flores-Santana, W.; Vitek, M. P.; Ridnour, L. A.; Colton, C. A. *J. Leukoc. Biol.* **2011**, *89*, 873.

(3) Szabo, C. *Nat. Rev. Drug. Discov.* **2016**, *15*, 185.

(4) Wang, P. G.; Xian, M.; Tang, X.; Wu, X.; Wen, Z.; Cai, T.; Janczuk, A. J. *Chem. Rev.* **2002**, *102*, 1091.

(5) Keefer, L. K. *ACS Chem. Biol.* **2011**, *6*, 1147.

(6) Cai, T. B.; Lu, D. N.; Landerholm, M.; Wang, P. G. *Org. Lett.* **2004**, *6*, 4203.

(7) Saavedra, J. E.; Shami, P. J.; Wang, L. Y.; Davies, K. M.; Booth, M. N.; Citro, M. L.; Keefer, L. K. *J. Med. Chem.* **2000**, *43*, 261.

(8) Chakrapani, H.; Maciag, A. E.; Citro, M. L.; Keefer, L. K.; Saavedra, J. E. *Org. Lett.* **2008**, *10*, 5155.

(9) Chakrapani, H.; Showalter, B. M.; Kong, L.; Keefer, L. K.; Saavedra, J. E. *Org. Lett.* **2007**, *9*, 3409.

(10) Chakrapani, H.; Showalter, B. M.; Citro, M. L.; Keefer, L. K.; Saavedra, J. E. *Org. Lett.* **2007**, *9*, 4551.

(11) Sharma, K.; Iyer, A.; Sengupta, K.; Chakrapani, H. *Org. Lett.* **2013**, *15*, 2636.

(12) Sharma, K.; Sengupta, K.; Chakrapani, H. *Bioorg. Med. Chem. Lett.* **2013**, *23*, 5964.

(13) Nagano, T.; Yoshimura, T. *Chem. Rev.* **2002**, *102*, 1235.

(14) Chan, J.; Dodani, S. C.; Chang, C. J. *Nat Chem* **2012**, *4*, 973.

(15) Hunter, R. A.; Storm, W. L.; Coneski, P. N.; Schoenfisch, M. H. *Anal. Chem.* **2013**, *85*, 1957.

(16) Weinstain, R.; Segal, E.; Satchi-Fainaro, R.; Shabat, D. *Chem. Commun.* **2010**, *46*, 553.

(17) Kim, E.-J.; Bhuniya, S.; Lee, H.; Kim, H. M.; Cheong, C.; Maiti, S.; Hong, K. S.; Kim, J. S. *J. Am. Chem. Soc.* **2014**, *136*, 13888.

(18) Choi, M. G.; Hwang, J.; Moon, J. O.; Sung, J.; Chang, S.-K. *Org. Lett.* **2011**, *13*, 5260.

(19) Li, J.; Zhang, C.-F.; Ming, Z.-Z.; Yang, W.-C.; Yang, G.-F. *RSC Adv.* **2013**, *3*, 26059.

(20) Li, K.; Xu, H.-R.; Yu, K.-K.; Hou, J.-T.; Yu, X.-Q. *Anal. Methods* **2013**, *5*, 2653.

(21) Leonetti, F.; Favia, A.; Rao, A.; Aliano, R.; Paluszcak, A.; Hartmann, R. W.; Carotti, A. *J. Med. Chem.* **2004**, *47*, 6792.

(22) Bandgar, B. P.; Sarangdhar, R. J.; Viswakarma, S.; Ahamed, F. A. *J. Med. Chem.* **2011**, *54*, 1191.

(23) Bensel, N.; Reymond, M. T.; Reymond, J.-L. *Chem. Eur. J.* **2001**, *7*, 4604.

(24) Coneski, P. N.; Schoenfisch, M. H. *Chem. Soc. Rev.* **2012**, *41*, 3753.

(25) Goldstein, S.; Russo, A.; Samuni, A. *J. Biol. Chem.* **2003**, *278*, 50949.

(26) Yu, H.; Xiao, Y.; Jin, L. *J. Am. Chem. Soc.* **2012**, *134*, 17486.

(27) Helmchen, F.; Denk, W. *Nat. Methods* **2005**, *2*, 932.

(28) Maiti, S.; Park, N.; Han, J. H.; Jeon, H. M.; Lee, J. H.; Bhuniya, S.; Kang, C.; Kim, J. S. *J. Am. Chem. Soc.* **2013**, *135*, 4567.

(29) Biswas, K. H.; Sopory, S.; Visweswariah, S. S. *Biochemistry* **2008**, *47*, 3534.

(30) Kiziltepe, T.; Hideshima, T.; Ishitsuka, K.; Ocio, E. M.; Raje, N.; Catley, L.; Li, C.-Q.; Trudel, L. J.; Yasui, H.; Vallet, S.; Kutok, J. L.; Chauhan, D.; Mitsiades, C. S.; Saavedra, J. E.; Wogan, G. N.; Keefer, L. K.; Shami, P. J.; Anderson, K. C. *Blood* **2007**, *110*, 709.

(31) Zgheib, O.; Pataky, K.; Brugger, J.; Halazonetis, T. D. *Mol. Cell. Biol.* **2009**, *29*, 1050.

(32) Behara, K. K.; Rajesh, Y.; Venkatesh, Y.; Pinninti, B. R.; Mandal, M.; Singh, N. D. P. *Chem. Commun.* **2017**, *53*, 9470.

(33) Dharmaraja, A. T.; Ravikumar, G.; Chakrapani, H. *Org. Lett.* **2014**, *16*, 2610.

(34) Fery-Forgues, S.; Lavabre, D. *J. Chem. Educ.* **1999**, *76*, 1260.

(35) Bagheri, M.; Nair, R. R.; Singh, K. K.; Saini, D. K. *Biochim. Biophys. Acta Mol. cell Res.* **2017**, *1864*, 177.

CHAPTER 3: BORO/NO, a Class of Hydrogen Peroxide Inducible Nitric Oxide (NO) Donors

3.1. Introduction

In chapter 2, we have reported FLUORO/NO, a nitric oxide donor with fluorescence reporter. In the presence of esterase it produces NO and fluorescence signal without consumption of NO during its detection.[1] The trigger that we had is esterase, which is present in nearly all cells, and therefore the compound will be suitable for a range of cell biology studies. In order to study the precise role of NO in cancer, we need a specific trigger to target cancer. The tumour micro environment is different from normal tissues; one feature that has been widely reported is the high levels of reactive oxygen species (ROS).[2-6] These are reduced forms of oxygen that mediate certain signalling events within the cell but are harmful at elevated concentrations and damage bio-macromolecules including DNA, proteins and RNA. The most common ROS include superoxide anion ($O_2^{\bullet -}$), hydrogen peroxide (H_2O_2), and hydroxyl radical ($HO^{\bullet}$). Among these, H_2O_2 was found to be more stable due to its uncharged in nature and generation of H_2O_2 in several cancer cell lines has been estimated to be 0.5 nM per 10^4 cells per h, which are significantly higher than those in normal cells.[2] Keeping this in mind, H_2O_2 has been used as a specific agent to activate prodrugs[7-12] and latent fluorophores[13-15] (as imaging agents) in cancers. A functional group that has been widely used is the arylboronate ester, which is known to react with H_2O_2 to produce phenol (Scheme 3.1).

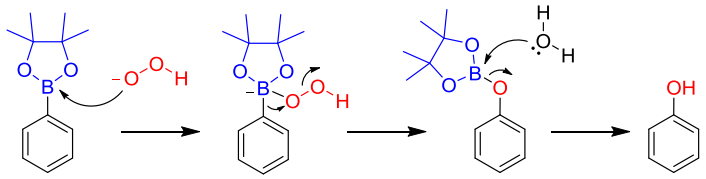

Scheme 3.1. Reaction of boronate ester with H_2O_2

For example, Chang's group has used boronic acid and esters for the development of H_2O_2 activated fluorescent probes for imaging H_2O_2 *in vitro* and *in vivo* (Scheme 3.2).[14]

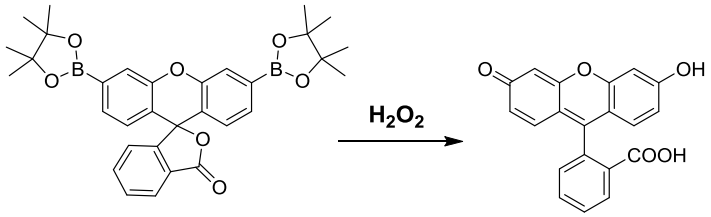

Fluorescence: OFF Fluorescence: ON

Scheme 3.2. Boronate-based fluorescent probe for H_2O_2 imaging

In 2011, Peng and coworkers reported, a first anticancer prodrug, which is activated by H_2O_2 and releases DNA cross linking agent selectively to cancer cells over normal cells (Scheme 3.3).[7]

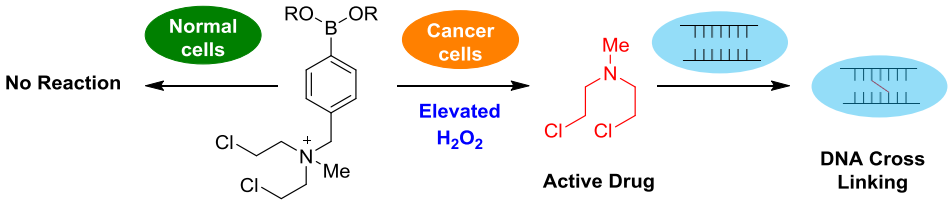

Scheme 3.3. Hydrogen peroxide inducible DNA cross-linking agent

Hence, this functional group was chosen as a substrate for the metabolic stimulus, *i.e.* H_2O_2 to specifically generate NO in cancer cells. Furthermore, due to the complexity associated with the detection of NO, the presence of a "turn on" fluorescence reporter for NO would be an additional feature which will be useful for studying possible cancer therapeutic outcomes of NO in a systematic manner. As a proof of concept, first we have designed a H_2O_2 activated NO donor without fluorescence reporter and studied in this chapter. Arylboronate ester based diazeniumdiolates (BORO/NO), a class of diazeniumdiolate derivatives that are attached to a pinacolboronate ester through a self-immolative aryl linker were considered as H_2O_2 activated NO donors (Scheme 3.4). Reaction of BORO/NO with H_2O_2 should produce the phenolate intermediate **I**, which could rearrange to produce the diazeniumdiolate anion, which in pH 7.4 releases NO (Scheme 3.4).

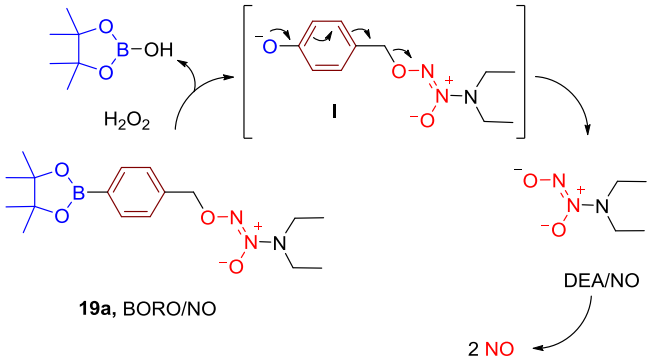

Scheme 3.4. Proposed mechanism of activation of **19a** by hydrogen peroxide to produce nitric oxide

3.2. Results and Discussion

3.2.1. Synthesis

In order to test our hypothesis of H_2O_2 activated NO donor, compound **19a** was synthesized in four steps starting from 4-bromotoluene. First, treatment of 4-bromotoluene with *n*-BuLi in THF at -78 °C to formed lithiated intermediate *in situ*, which was then reacted with trimethyl borate and followed by acid hydrolysis to give compound **16** in 85% yield (Scheme 3.5). Next, the boronic acid (**16**) was protected using pinacol to form compound **17** in 90% yield. Then, compound **17** was reacted with *N*-bromosuccinamide (NBS) in the presence of a radical initiator azobisisobutyronitrile (AIBN) in carbon tetrachloride to produce the corresponding bromide (**18**), which was then reacted with **DEA/NO** (**1a**) to give the desired compound **19a** (Scheme 3.5).

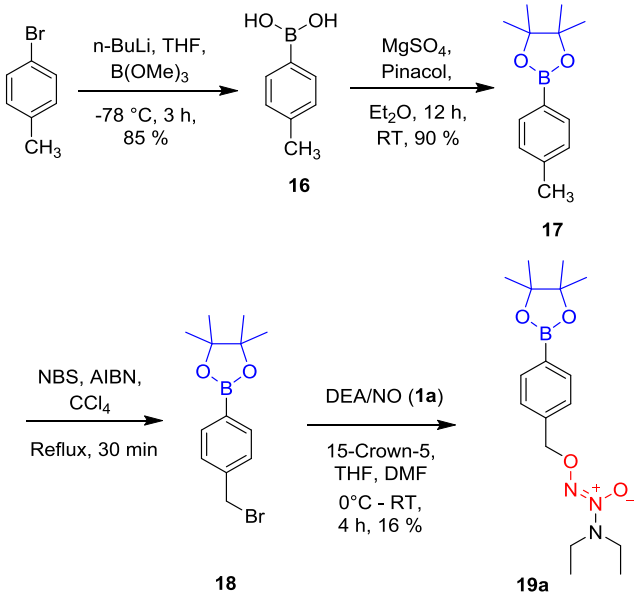

Scheme 3.5. Synthesis of **19a**

In addition compound **20** was synthesized as a control compound by reported procedure. Treatment of diethylamine with **18** afforded **20** in quantitative yield (Scheme 3.6). Compound **20** which contained the boronate ester but do not have DEA/NO functional group. Next, another control compound **21** was prepared, by reacting DEA/NO with benzyl bromide (Scheme 3.6), which contained the NO donating functional group DEA/NO, but do not have boronate ester moiety.

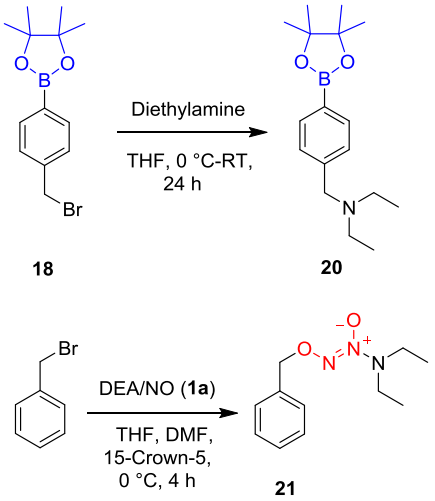

Scheme 3.6. Synthesis of control compounds (**20** and **21**)

3.2.2. H_2O_2 activated NO generation in buffer

The ability of compound **19a** to produce NO was tested using a chemiluminescence based Nitric oxide analyser (NOA). The compound **19a** was dissolved in buffer, and an aliquot was analysed by NOA, as expected no evidence for NO generation for several hours, whereas in the presence of H_2O_2, a signal attributable to NO was seen confirming the ability of **19a** to produce NO. When similar experiment was conducted with 2-(4-carboxyphenyl)-4,4,5,5-tetramethylimidazoline-1-oxyl-3-oxide potassium salt (c-PTIO, a known quencher of NO), nearly complete disappearance of NO signal was observed (Figure 3.1.a). These results suggest that, the compound **19a** is stable in buffer and the boronate moiety gets converted into hydroxyl group by H_2O_2, generates NO.

Next, compounds **17**, **20** and **21** were incubated in buffer and treated with H_2O_2 (10 eq.) and generation of NO was monitored using NOA. The amount of NO released from these compounds were estimated using a standard calibration curve generated using sodium nitrite ($NaNO_2$) solution (Figure 3.1.b). Compound **17** and **20** contained boronate ester functional group but do not have NO donating functional group DEA/NO. Similarly, compound **21** contained NO donating functional group but do not have boronate ester functional group. As expected, we found no evidence for NO generation from these compounds. When similar experiment was performed with **19a**, a signal attributable to NO was observed. Together these results suggest that, both the diazeniumdiolate as well as the boronate ester functional groups are required for NO production (Figure 3.1.c).

Next, the stimuli responsiveness of compound **19a** toward H_2O_2 was studied, wherein, compound **19a** was treated with increasing concentration of H_2O_2 and the release of NO was

monitored by NOA. A dose-dependent increase in nitric oxide release was observed (Figure 3.1.d). Thus, when encountered with cellular situations with varying ROS levels, **19a** is expected to preferentially generate NO in cell lines where ROS levels are relatively higher. Since cancer cells produce higher level of H_2O_2 compared with normal cells, we expect this compound **19a** will produce more NO selectively in cancer cells over normal cells.

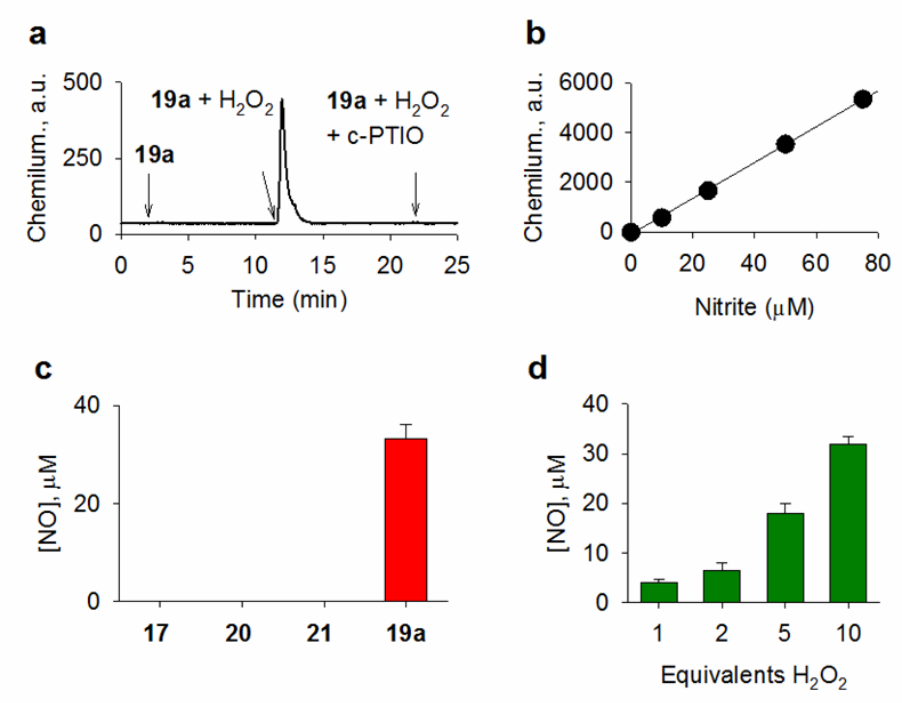

Figure 3.1. (a) Nitric oxide produced during incubation of **19a** (25 μM) alone or in the presence of hydrogen peroxide (H_2O_2, 250 μM), with and without c-PTIO (250 μM) in buffer; analysis was conducted after 10 min incubation and arrow indicates approximate point of injection of analyte. (b) Calibration curve generated using sodium nitrite in buffer. (c) Nitric oxide analysis of **17**, **19a**, **20** and **21** (25 μM) in the presence of H_2O_2 (250 μM) in buffer after 10 min incubation. (d) NO generated by **19a** (25 μM) with increasing equivalents of H_2O_2 (All the experiments were conducted in 10 mM pH 7.4 phosphate buffer containing 100 μM of diethylene triamine pentaacetic acid (DTPA), a metal ion chelating agent at 37 ºC).

3.2.3. Selectivity of 19a towards H_2O_2

In order to deliver NO selectively to cancer over normal cells, the compound should be selectively activated by H_2O_2 over other common reactive species that are present in cells. In order to verify that, selectivity of **19a** towards activation by H_2O_2 was investigated in the presence of number of biologically relevant nucleophiles, reductants and oxidants. The compound **19a** was incubated in buffer and treated with 10 equivalents of different reactive species and an aliquot was analysed by NOA for NO. The compound **19a** generates NO only

in the presence of H_2O_2 and no significant levels of NO generation was observed in the presence of biologically relevant thiols, metal ions, antioxidants and other common reactive oxygen species (Figure 3.2), which suggesting the selectivity of the functional group towards activation by H_2O_2 in a physiological condition. The observed specificity of boronate ester functional group towards H_2O_2 was consistent with previous reports.[7,13]

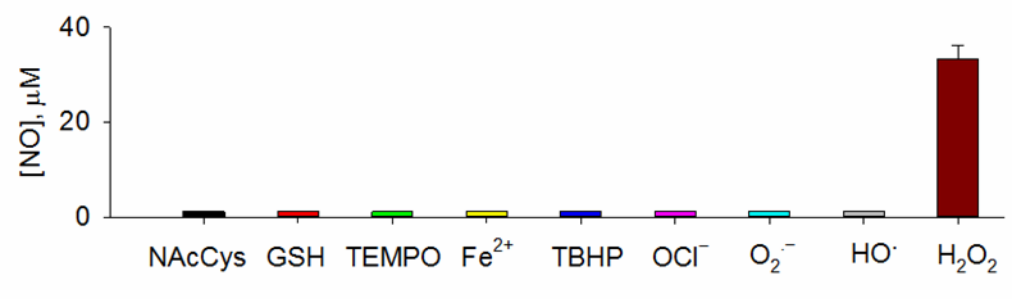

Figure 3.2. Nitric oxide analysis of **19a** (25 µM) with various reactive species (250 µM) at 37 °C in pH 7.4 phosphate buffer after 10 min incubation, NAcCys: N-acetyl cysteine; GSH: glutathione; TEMPO: 2,2,6,6-tetramethylpiperidinyloxy; Fe (II): $FeCl_2$; TBHP: *tert*-butyl hydroperoxide; OCl^-: sodium hypochlorite; $O_2^{\bullet-}$: generated using hypoxanthine/xanthine oxidase; $HO^{\bullet}$ was generated using H_2O_2 and Fe(II) mixed at a 1:10 ratio; H_2O_2.

Having established that compound **19a** was capable of generating NO when triggered by H_2O_2, a series of 4-BORO/NO compounds was synthesized with different diazeniumdiolates. A similar procedure (Scheme 3.5) was used to synthesize **19b-19d** by the reaction of the bromide **18** with the corresponding diazeniumdiolate salts, **1b-1d** (Scheme 3.7).

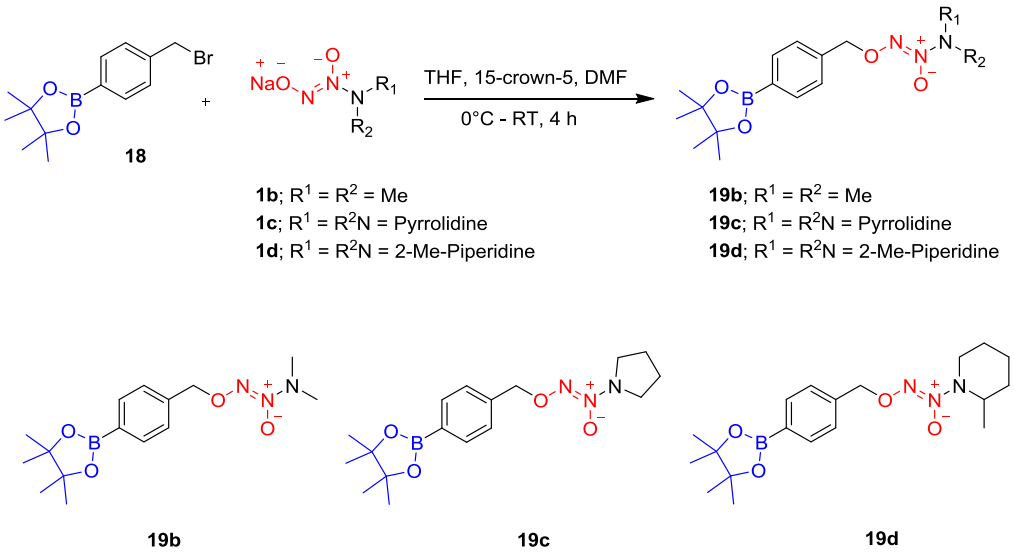

Scheme 3.7. Synthesis of **4-BORO/NO** derivatives

In order to study possible differences in 1,4- versus 1,2-elimination of the phenolate intermediate generated during hydrogen peroxide activated NO release from this class of

compounds, derivatives **1a**, **1b**, and **1d** were reacted with the corresponding 2-(pinacol boronate ester)benzyl bromides (Synthesized from 2-bromotoluene derivatives, procedure similar to Scheme 3.5) to produce **24a-24d** (Scheme 3.8).

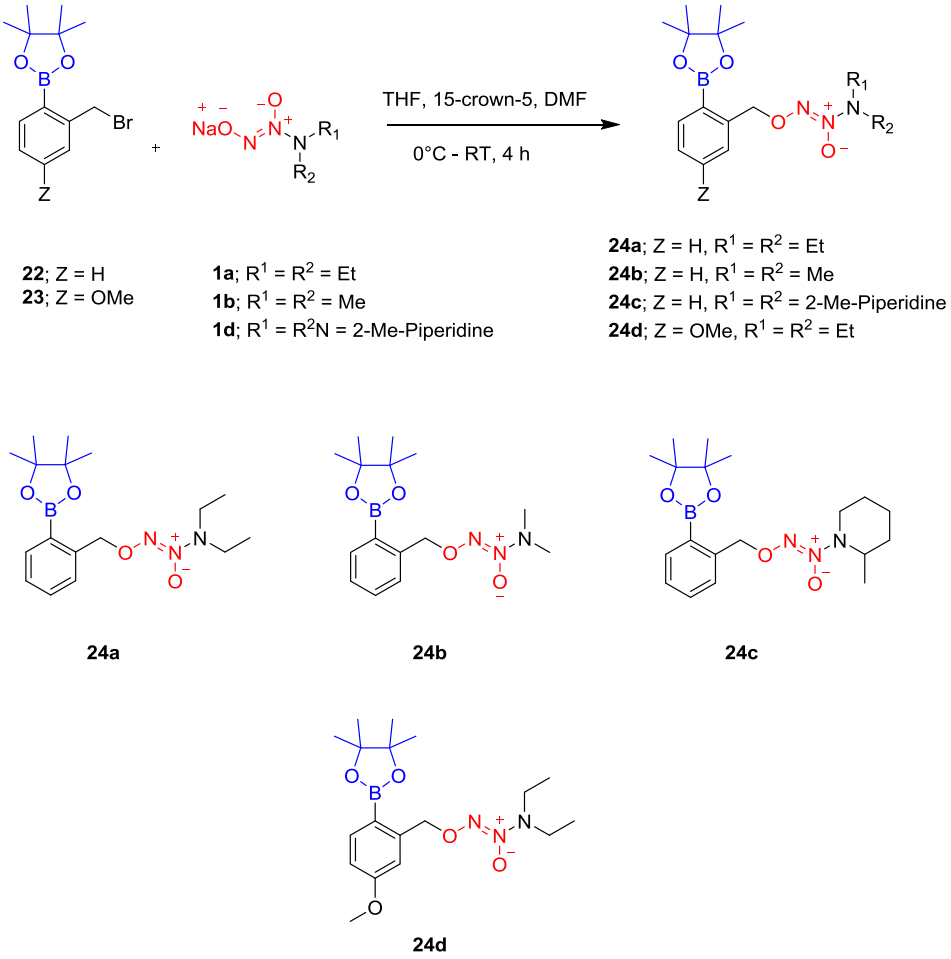

Scheme 3.8. Synthesis of **2-BORO/NO** derivatives

3.2.4. NO generation from BORO/NO derivatives

After confirmation of products, the ability of all analogues of BORO/NO derivatives **19b-19d** and **24a-24d** to produce NO was investigated. The compounds **19b-19d** and **24a-24d** (25 µM) were independently incubated with H_2O_2 (250 µM) in pH 7.4 buffer for 10 min and an aliquot was analysed by NOA for NO. We found all the compounds were stable and generated nitric oxide only when exposed to H_2O_2 and the yields of NO (Figure 3.3) were comparable or lower than the yield of NO produced during incubation of **19a** under similar conditions. And we found, the release of NO from **19a** and **24a** was comparable (Figure 3.3).

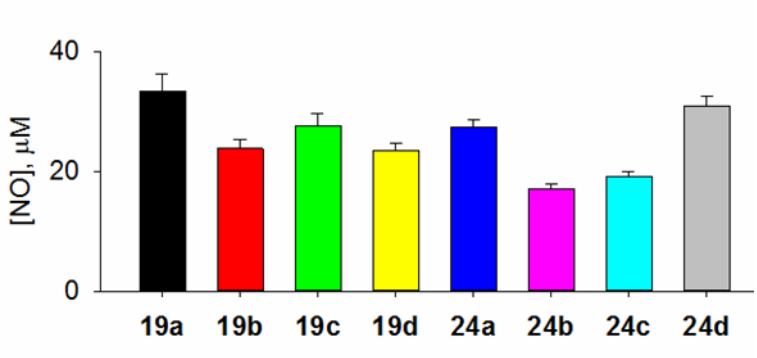

Figure 3.3. Nitric oxide analysis of BORO/NO derivatives **19a-19d** and **24a-24d** (25 μM) in the presence of H_2O_2 (10 eq.) in buffer after 10 min incubation (Experiments were conducted in 10 mM pH 7.4 phosphate buffer containing 100 μM of diethylene triamine pentaacetic acid (DTPA), a metal ion chelating agent at 37 ºC).

3.3. Summary

In this chapter, as a proof of concept, we have designed and synthesized a series of an arylboronate ester based diazeniumdiolates (BORO/NO), a class of hydrogen peroxide inducible nitric oxide (NO) donors. Using nitric oxide analyser (NOA), we have demonstrated NO generation from these compounds. When BORO/NO was incubated in pH 7.4 buffer, no signal for NO generation was observed. In the presence of H_2O_2, a signal corresponding to NO generation was found. Next, when BORO/NO was treated with increasing concentration of H_2O_2, a dose dependent increase in the NO release was seen. Lastly, we showed the selectivity of BORO/NO towards H_2O_2 over other biologically relevant nucleophiles, reductants, and oxidants. To the best of our knowledge, this is the first example of a small molecule that produces NO in the presence of H_2O_2. Since, cancer cells produce higher level of H_2O_2 over their normal counterparts, this tool would be useful to deliver NO in a selective and control manner at a cancer site.

3.4. Experimental Section

3.4.1. Synthesis and characterization

Compounds **18**[16], **20**[17], **21**[18], **22**[19] and **23**[19] were synthesized using a previously reported procedure and the analytical data that we collected were consistent with the reported values.

General procedure for the synthesis of 19 and 24

To an ice cold solution of Diazeniumdiolates (1.2 mmol) in THF (3 mL), 15-crown-5 (0.01 mL) was added and the mixture stirred at 0 ºC for 5 min under a nitrogen atmosphere. A solution of corresponding 2-(pinacol boronate ester)benzylbromides (1 mmol) in DMF (1 mL) was added to the reaction mixture at 0 ºC and stirred at room temperature for 4 h. The solvent was evaporated under reduced pressure, diluted with 25 mL of water and the aqueous solution was extracted with DCM (3×5 mL). The combined organic layer was washed with brine, dried over Na_2SO_4 (5 g), filtered and the filtrate was concentrated to give a crude compound, which was passed through silica gel (60-120 mesh) column chromatography using ethyl acetate (1→5 %) and petroleum ether solvent system to obtain a crude product. The mixture was further purified using semi-preparative HPLC with C-18 semi-preparative column, eluent consisting a gradient of acetonitrile (ACN) and water (40 – 80%), under ambient temperature with a flow rate of 2.5 mL/min for a 25 min program to obtain pure material.

1-((4,4,5,5-tetramethyl-1,3,2-dioxaborolan-2-yl)phenyl)-4-methyl-[1-(N,N-diethylamino) diazen-1-ium-1,2-diol-2-ate] (19a):

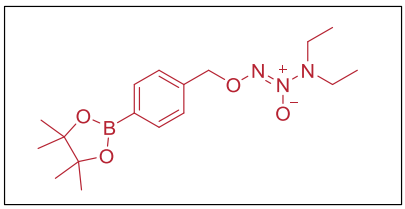

Starting from compound **1a** (125 mg, 0.81 mmol) product (**19a**, 38 mg, 16%) was isolated as a pink oil: FT-IR (ν_{max}, cm^{-1}): 2979, 2929, 1614, 1508, 1360, 1146, 1084; ^1H NMR ($CDCl_3$, 400 MHz): δ 7.78 (d, J = 8.1 Hz, 2H), 7.37 (d, J = 8.0 Hz, 2H), 5.28 (s, 2H), 3.06 (q, J = 7.1 Hz, 4H), 1.34 (s, 12H), 1.01 (t, J = 7.1 Hz, 6H); ^{13}C NMR ($CDCl_3$, 100 MHz): δ 138.9, 135.1, 127.6, 84.0, 75.6, 48.9, 25.0, 11.6; HRMS (ESI) for $[C_{17}H_{28}BN_3O_4+Na]^+$: Calcd., 372.2070, Found, 372.2071.

1-((4,4,5,5-tetramethyl-1,3,2-dioxaborolan-2-yl)phenyl)-4-methyl-[1-(N,N-dimethylamino) diazen-1-ium-1,2-diol-2-ate] (19b):

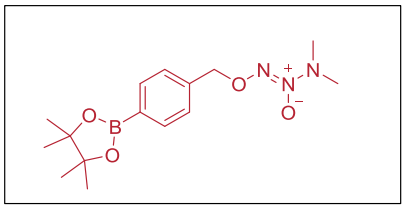

Starting from compound **1b** (205 mg, 1.62 mmol) a white solid (**19b**, 19 mg, 4%) was isolated: FT-IR (ν_{max}, cm^{-1}): 2978, 2924, 1617, 1493, 1360, 1208, 1143, 1087; ^1H NMR

($CDCl_3$, 400 MHz): δ 7.80 (d, *J* = 8.0 Hz, 2H), 7.38 (d, *J* = 8.0 Hz, 2H), 5.22 (s, 2H), 2.96 (s, 6H), 1.34 (s, 12H); ^{13}C NMR ($CDCl_3$, 100 MHz): δ 139.0, 135.1, 127.8, 84.0, 75.4, 43.0, 25.0; HRMS (ESI) for $[C_{15}H_{24}BN_3O_4+Na]^+$: Calcd., 344.1757, Found, 344.1768.

1-((4,4,5,5-tetramethyl-1,3,2-dioxaborolan-2-yl) phenyl)-4-methyl-[1-(pyrrolidynyl)diazen-1-ium-1,2-diol-2-ate] (19c):

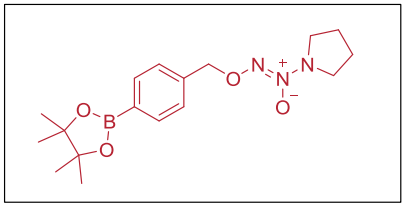

Starting from compound **1c** (247 mg, 1.62 mmol) a yellow oil was obtained (**19c**, 19 mg, 4%): FT-IR (ν_{max}, cm^{-1}): 2978, 2928, 2861, 1657, 1612, 1478, 1360, 1272, 1144, 1085; ^1H NMR ($CDCl_3$, 400 MHz): δ 7.79 (d, *J* = 7.9 Hz, 2H), 7.38 (d, *J* = 8.0 Hz, 2H), 5.18 (s, 2H), 3.48 (t, *J* = 6.7 Hz, 4H), 1.91 (q, *J* = 3.4 Hz, 4H), 1.34 (s, 12H); ^{13}C NMR ($CDCl_3$, 100 MHz): δ 139.3, 135.0, 127.8, 84.0, 75.1, 51.0, 25.0, 22.9; HRMS (ESI) for $[C_{17}H_{26}BN_3O_4+Na]^+$: Calcd., 370.1913, Found, 370.1911.

1-((4,4,5,5-tetramethyl-1,3,2-dioxaborolan-2-yl)phenyl)-4-methyl-[2-methylpiperidinyl) diazen-1-ium-1,2-diol-2-ate] (19d):

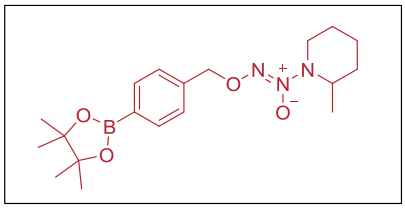

Starting from compound **1d** (115 mg, 0.64 mmol) a pale yellow oil (**19d**, 24 mg, 12%) was obtained: FT-IR (ν_{max}, cm^{-1}): 2974, 2929, 1624, 1503, 1362, 1148, 1086, 1017; ^1H NMR ($CDCl_3$, 400 MHz): δ 7.78 (d, *J* = 8.0 Hz, 2H), 7.37 (d, *J* = 8.0 Hz, 2H), 5.29 (s, 2H), 3.22-3.14 (m, 3H), 1.78-1.63 (m, 6H), 1.34 (s, 12H), 0.94 (d, *J* = 6.1 Hz, 3H); ^{13}C NMR ($CDCl_3$, 100 MHz): δ 138.8, 135.1, 127.5, 84.0, 75.6, 56.8, 54.1, 33.0, 25.2, 25.0, 23.3, 18.4; HRMS (ESI) for $[C_{19}H_{30}BN_3O_4+K]^+$: Calcd., 414.1966, Found, 414.1956.

1-((4,4,5,5-tetramethyl-1,3,2-dioxaborolan-2-yl)phenyl)-2-methyl-[1-(N,N-diethylamino) diazen-1-ium-1,2-diol-2-ate] (24a):

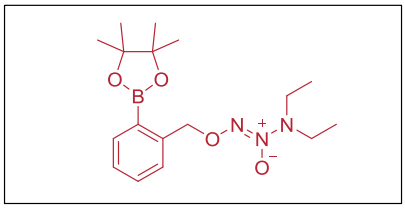

Starting from compound **1a** (125 mg, 0.81 mmol) a pale yellow oil was obtained (**24a**, 34 mg, 14%): FT-IR (ν_{max}, cm^{-1}): 2982, 1505, 1360, 1268, 1146; ^1H NMR ($CDCl_3$, 400 MHz): δ 7.82 (d, *J* = 7.3 Hz, 1H), 7.43-7.41 (m, 2H), 7.31-7.27 (m, 1H), 5.63 (s, 2H), 3.06 (q, *J* = 7.1 Hz, 4H), 1.34 (s, 12H), 1.03 (t, *J* = 7.1 Hz, 6H); ^{13}C NMR ($CDCl_3$, 100 MHz): δ 142.2, 136.1, 131.2, 127.8, 127.4, 83.9, 75.1, 49.0, 25.0, 11.7; HRMS (ESI) for $[C_{17}H_{28}BN_3O_4+Na]^+$: Calcd., 372.2070, Found, 372.2073.

1-((4,4,5,5-tetramethyl-1,3,2-dioxaborolan-2-yl)phenyl)-2-methyl-[1-(N,N-dimethylamino) diazen-1-ium-1,2-diol-2-ate] (24b):

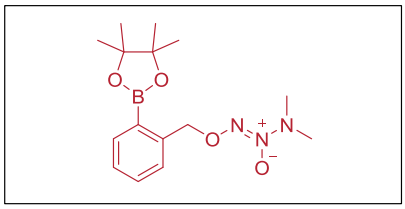

Starting from compound **1b** (205 mg, 1.62 mmol) a pale yellow semi solid was obtained (**24b**, 10 mg, 2%): FT-IR (ν_{max}, cm^{-1}): 3446, 2983, 2921, 1653, 1499, 1352, 1144, 1014; ^1H NMR ($CDCl_3$, 400 MHz): δ 7.82 (d, J = 7.3 Hz, 1H), 7.43-7.41 (m, 2H), 7.33-7.28 (m, 1H), 5.56 (s, 2H), 2.96 (s, 6H), 1.34 (s, 12H); ^{13}C NMR ($CDCl_3$, 100 MHz): δ 142.3, 136.1, 131.2, 128.1, 127.4, 83.9, 74.9, 43.2, 25.0; HRMS (ESI) for $[C_{15}H_{24}BN_3O_4+Na]^+$: Calcd., 344.1757, Found, 344.1758.

1-((4,4,5,5-tetramethyl-1,3,2-dioxaborolan-2-yl)phenyl)-2-methyl-[2-methylpiperidinyl) diazen-1-ium-1,2-diol-2-ate] (24c):

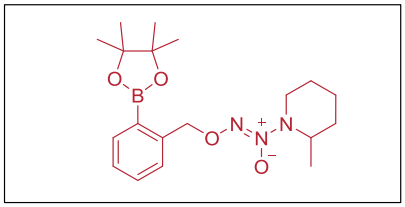

Starting from compound **1d** (293 mg, 0.81 mmol) a pale yellow oil was obtained (**24c**, 10 mg, 2%): FT-IR (ν_{max}, cm^{-1}): 2936, 2856, 1502, 1445, 1352, 1147, 1020; ^1H NMR ($CDCl_3$, 400 MHz): δ 7.82 (d, J = 7.4 Hz, 1H), 7.42 (d, J = 4.1 Hz, 2H), 7.30-7.28 (m, 1H), 5.63 (s, 2H), 3.17-3.19 (m , 3H), 1.79-1.68 (m , 6H), 1.33 (s, 12H), 0.98 (d, J = 6.1 Hz, 3H); ^{13}C NMR ($CDCl_3$, 100 MHz): δ 142.1, 136.2, 131.1, 127.6, 127.4, 83.9, 75.2, 56.8, 54.3, 33.1, 25.3, 25.0, 23.4, 18.6; HRMS (ESI) for $[C_{19}H_{30}BN_3O_4+Na]^+$: Calcd., 398.2226, Found, 398.2225.

1-((5-methoxy-1-(4,4,5,5-tetramethyl-1,3,2-dioxaborolan-2-yl) phenyl)-4- [1-(N,N-diethylamino)diazen-1-ium-1,2-diol-2-ate] (24d):

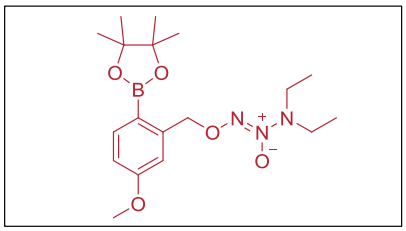

Starting from compound **1a** (185 mg, 0.59 mmol) a colorless oil was obtained (**24d**, 11 mg, 3%): FT-IR (ν_{max}, cm^{-1}): 2983, 1607, 1507,1452, 1359, 1233, 1145, 1029; ^1H NMR ($CDCl_3$, 400 MHz): δ 7.76, (d, J = 8.3 Hz, 1H), 6.98 (d, J = 2.5 Hz, 1H), 6.80 (dd, J = 8.3, 2.5 Hz, 1H), 5.62 (s, 2H), 3.80 (s, 3H), 3.07 (q, J = 7.1 Hz, 4H), 1.32 (s, 12H), 1.05 (t, J = 7.1 Hz, 6H); ^{13}C NMR ($CDCl_3$, 100 MHz): δ 162.2, 144.8, 138.1, 113.0, 112.8, 83.7, 74.9, 55.3, 49.0, 25.0, 11.7; HRMS (ESI) for $[C_{18}H_{30}BN_3O_5+Na]^+$: Calcd., 402.2176, Found, 402.2180.

3.4.2. Hydrogen peroxide activated NO release in Buffer

3.4.2.1. Nitric oxide detection from compounds

A 10 mM stock solution of compounds in DMSO and a 100 mM stock solution of H_2O_2 in water were prepared. A typical reaction mixture consisted of compound (25 μM, 1 eq) and H_2O_2 (250 μM, 10 eq) were prepared by mixing 1.25 μL of compound and 1.25 μL of H_2O_2 from the stock solutions with 497.5 μL of pH 7.4 phosphate buffer (10 mM buffer containing 100 μM of diethylene triamine pentaacetic acid (DTPA), a metal ion chelating agent) at 37 ºC. An aliquot of the reaction mixture (10 μL) from the reaction vial was injected into a Sievers nitric oxide analyzer (NOA 280i) using argon as the carrier gas. For the experiment with the NO scavenger 2-(4-carboxyphenyl)-4,4,5,5- tetramethylimidazoline-1-oxyl-3-oxide potassium salt (250 μM, 10 eq., c-PTIO), an aliquot of the reaction mixture (10 μL) was injected into the NOA chamber.

3.4.2.2. NO generation from 19a with different equivalents of H_2O_2

A 10 mM stock solution of **19a** in DMSO and 100 mM stock solution of H_2O_2 in water were prepared for quantifying amount of NO release from H_2O_2 mediated decomposition of **19a**. A reaction mixture of **19a** (25 μM, 1 eq.,) and H_2O_2 (0 -250 μM, 1 - 10eq) were prepared by mixing 1.25 μL of **19a** and respective volume of H_2O_2 from the stock solutions to 500 μL with of pH 7.4 phosphate buffer (10 mM containing 100 μM of DTPA) at 37 ºC. Reaction mixture (10 μL) and blank were injected after 10 min into a Sievers Nitric Oxide Analyzer (NOA 280i) containing reducing mixture using argon as the carrier gas. The amount of NO released was estimated using a standard calibration curve generated using sodium nitrite ($NaNO_2$) solution of concentration from 0 – 75 μM using NOA (R^2 = 0.999).

3.4.2.3. Selectivity studies of 27 with oxidants and reductants

Compound **19a** was prepared as mentioned earlier and reacted with different reactive species. Reactive oxygen species (10 eq., 100 μM) were administered to **19a** in 10 mM phosphate buffer (pH 7.4, containing 100 μM of DTPA (except for Fe^{2+} and $HO^{\bullet}$), at 37 °C) as follows. Stock solutions of (10 mM) H_2O_2 (30%), *tert*-butylhydroperoxide (TBHP, 70%), and hypochlorite (NaOCl, 10%) were prepared from commercial sources. Hydroxyl radical ($HO^{\bullet}$), was generated by reaction of 10 mM Fe^{2+} with 1 mM H_2O_2. Superoxide ($O_2^{\bullet-}$) was delivered from the enzymatic reaction of xanthine oxidase (0.02 unit/mL) and hypoxanthine 10 mM (in phosphate buffer pH 7.4).[20] *N*-acetylcysteine, glutathione solutions (10 mM) were prepared in de-ionized water. 2,2,6,6-Tetramethylpiperidinyloxy (TEMPO) solutions (10

mM) were prepared in DMSO. After 10 min of incubation at 37 °C reaction mixture was analyzed for NO.

3.4.2.4. Real-time monitoring of nitric oxide release from 19a

To a reaction chamber connected to nitric oxide analyzer **19a** (50 μM) in phosphate buffer (10 mM, pH 7.4, 7 mL) was purged with argon for baseline stabilization, H_2O_2 (10 eq.) was injected to the reaction mixture and NO release was monitored over a period of 1 h using NOA (low sensitivity mode).

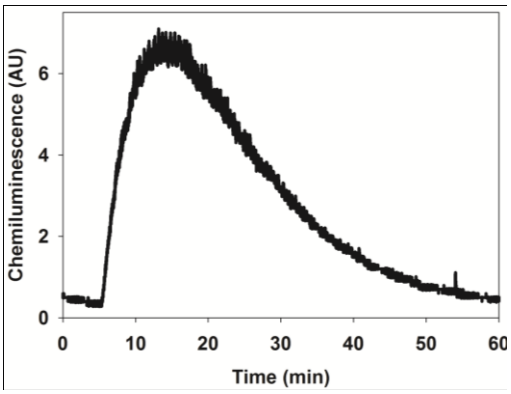

Figure 3.4. Real-time nitric oxide analysis from **19a** (50 μM) with 10 equivalent of H_2O_2 in buffer

3.5. Spectral charts:

^{1}H-NMR Spectrum (400 MHz, $CDCl_3$) of Compound **19a**

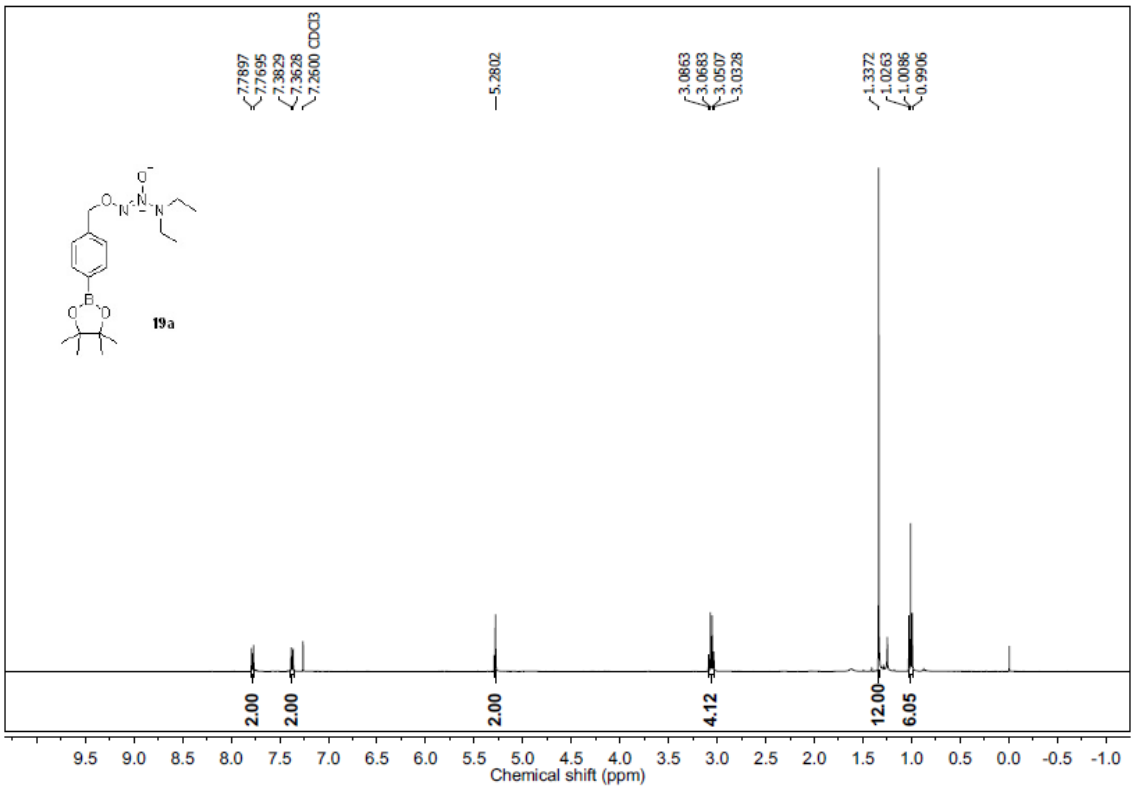

^{13}C NMR Spectrum (100 MHz, $CDCl_3$) of Compound **19a**

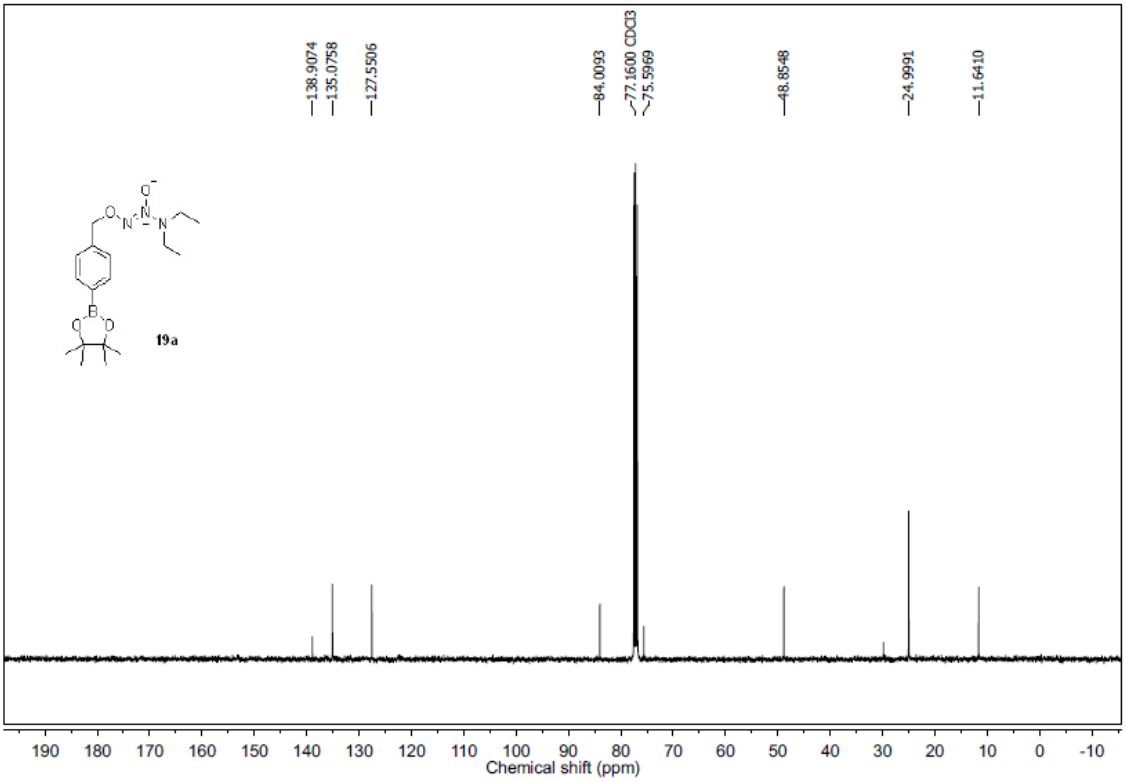

^{1}H-NMR Spectrum (400 MHz, $CDCl_3$) of Compound 19b

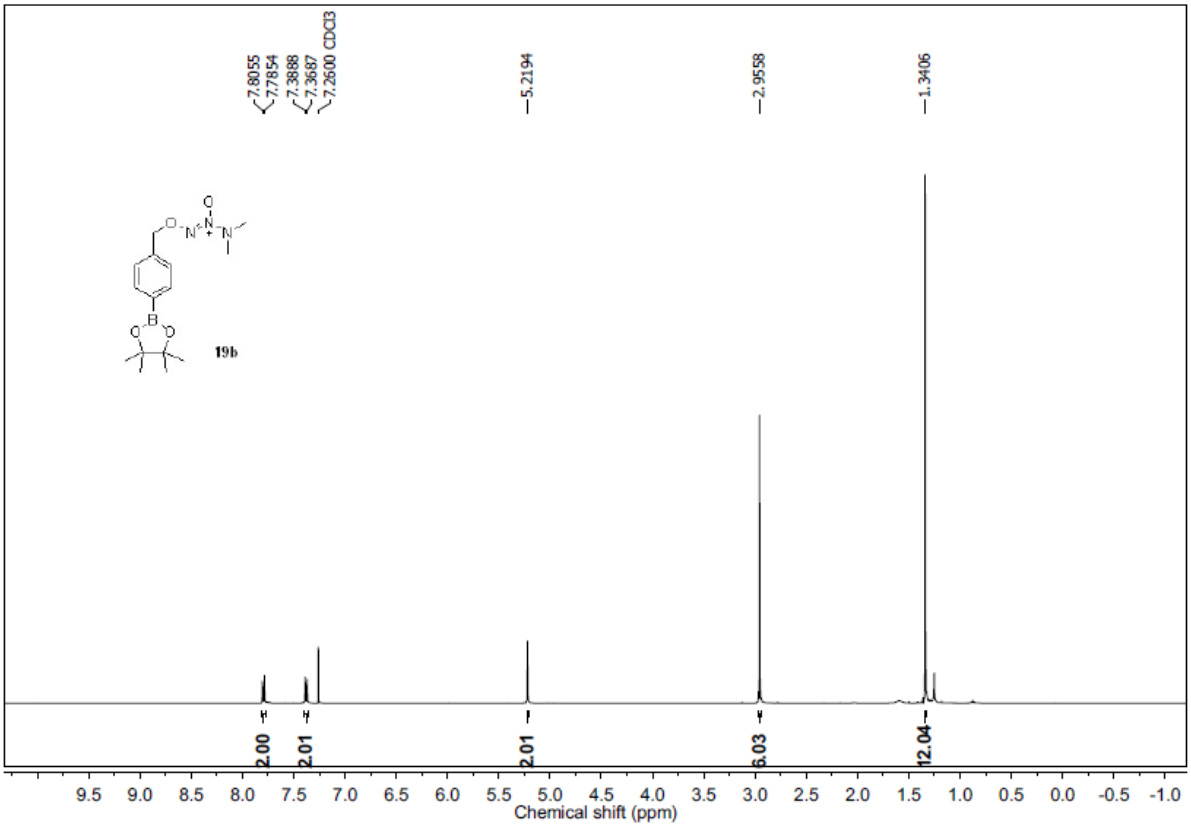

^{13}C NMR Spectrum (100 MHz, $CDCl_3$) of Compound 19b

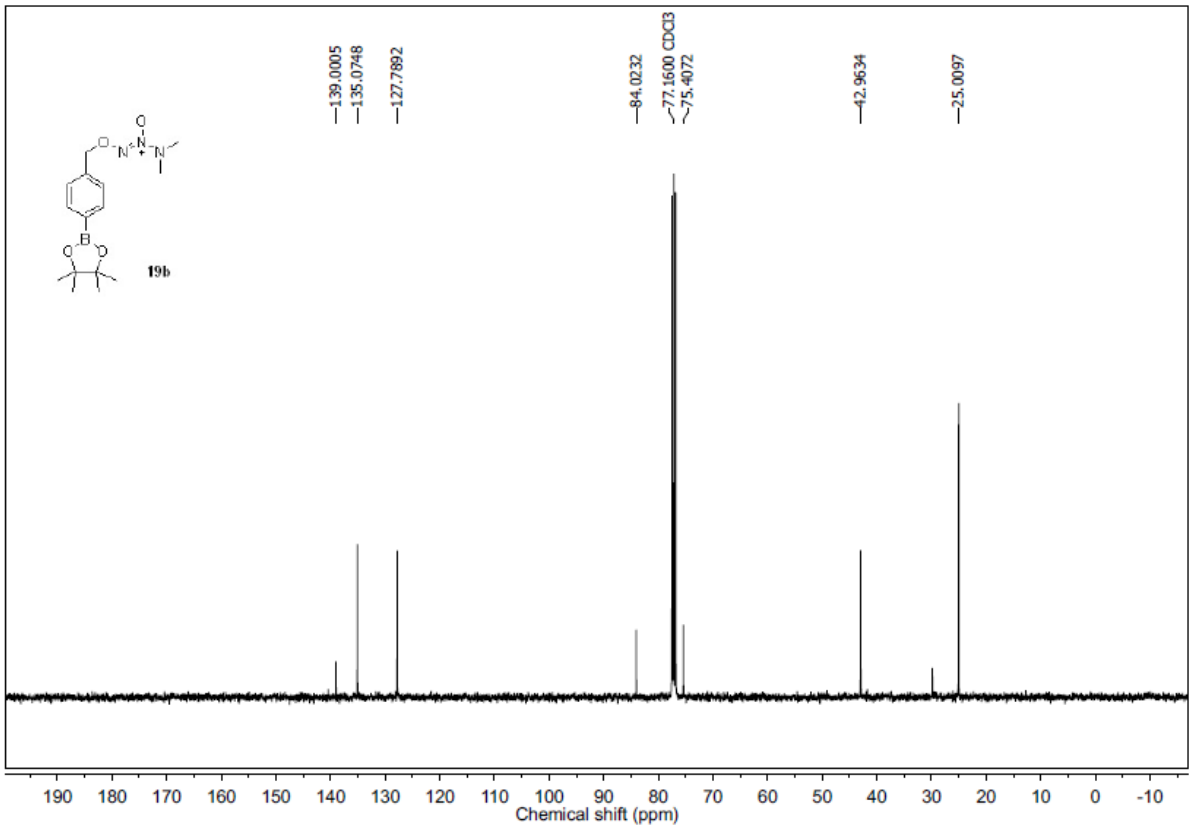

^{1}H-NMR Spectrum (400 MHz, $CDCl_3$) of Compound 19c

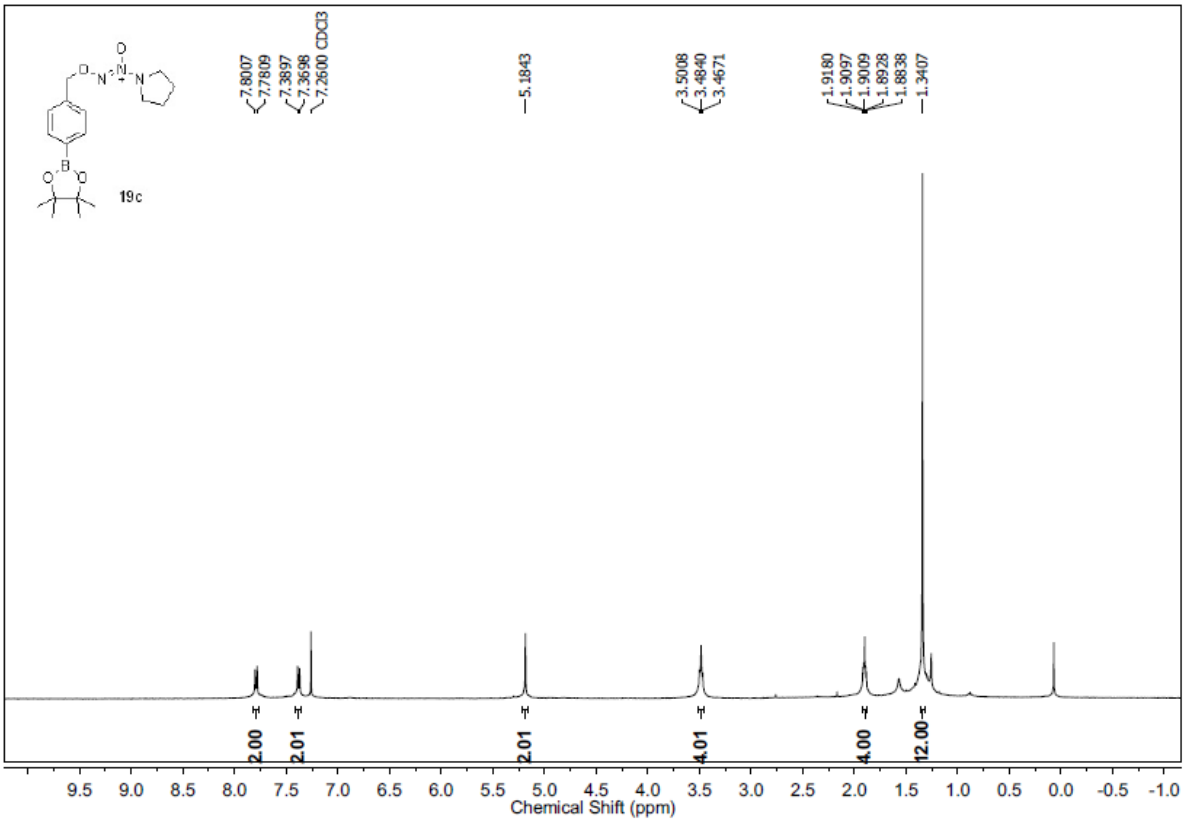

^{13}C NMR Spectrum (100 MHz, $CDCl_3$) of Compound 19c

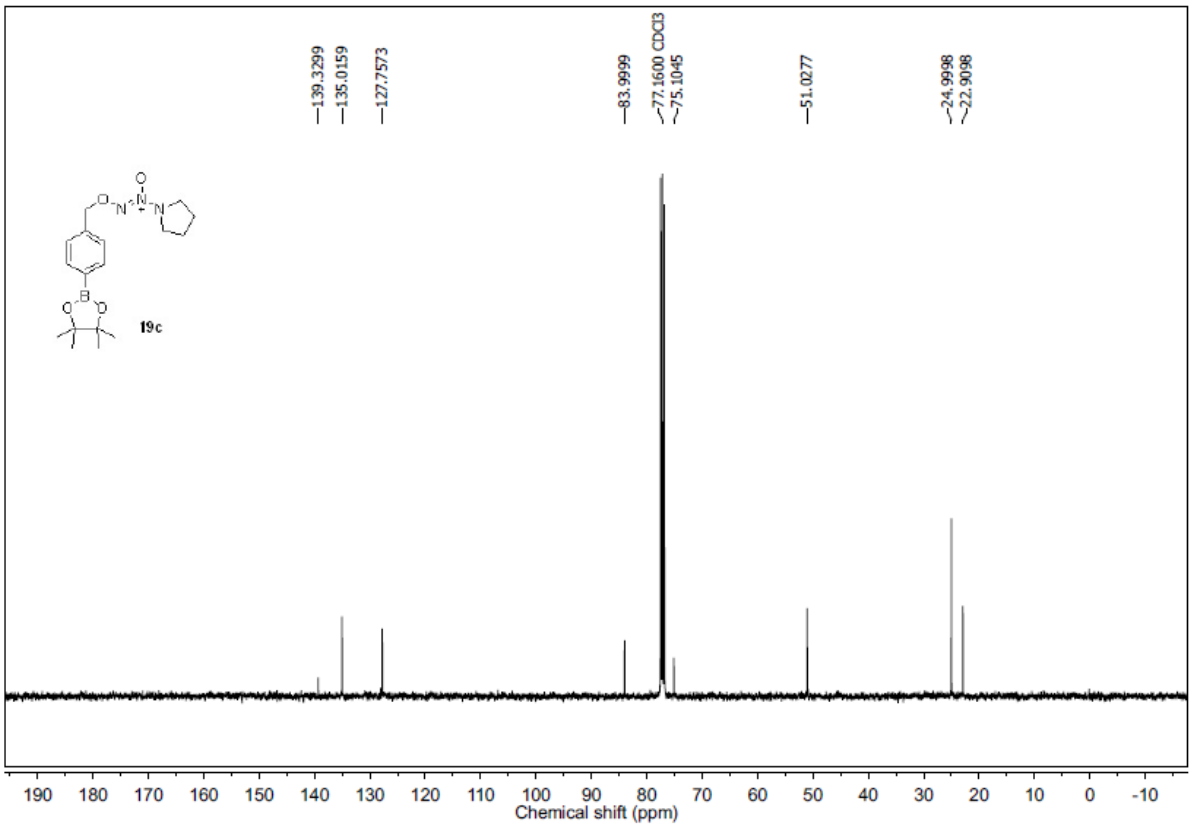

^{1}H-NMR Spectrum (400 MHz, $CDCl_3$) of Compound 19d

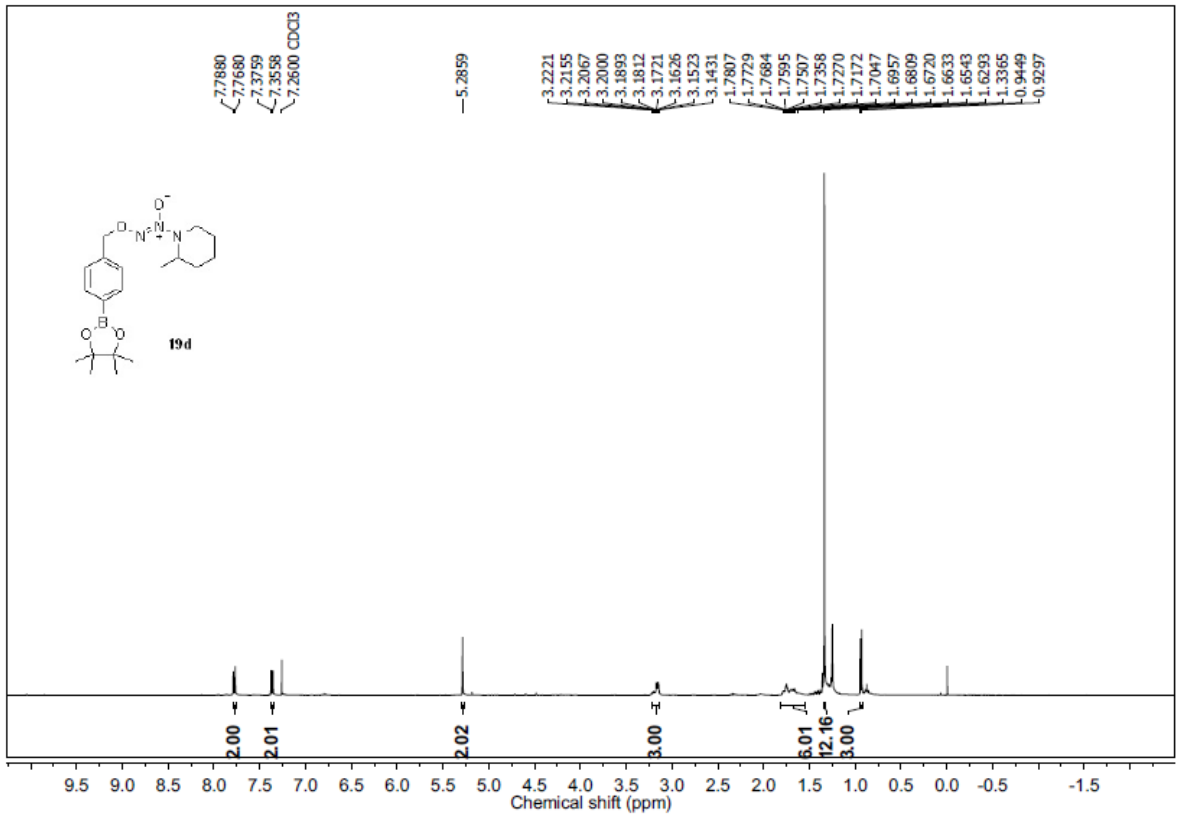

^{13}C NMR Spectrum (100 MHz, $CDCl_3$) of Compound 19d

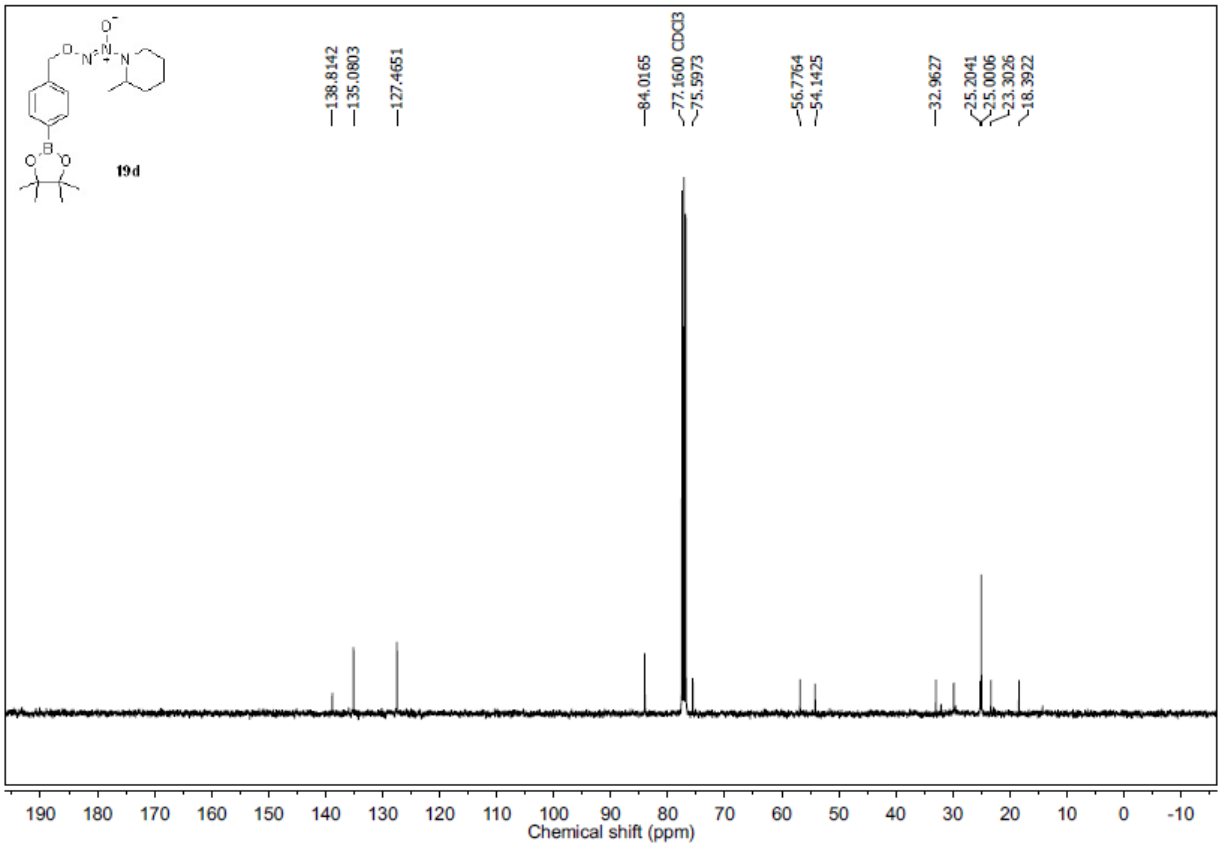

^{1}H-NMR Spectrum (400 MHz, $CDCl_3$) of Compound 24a

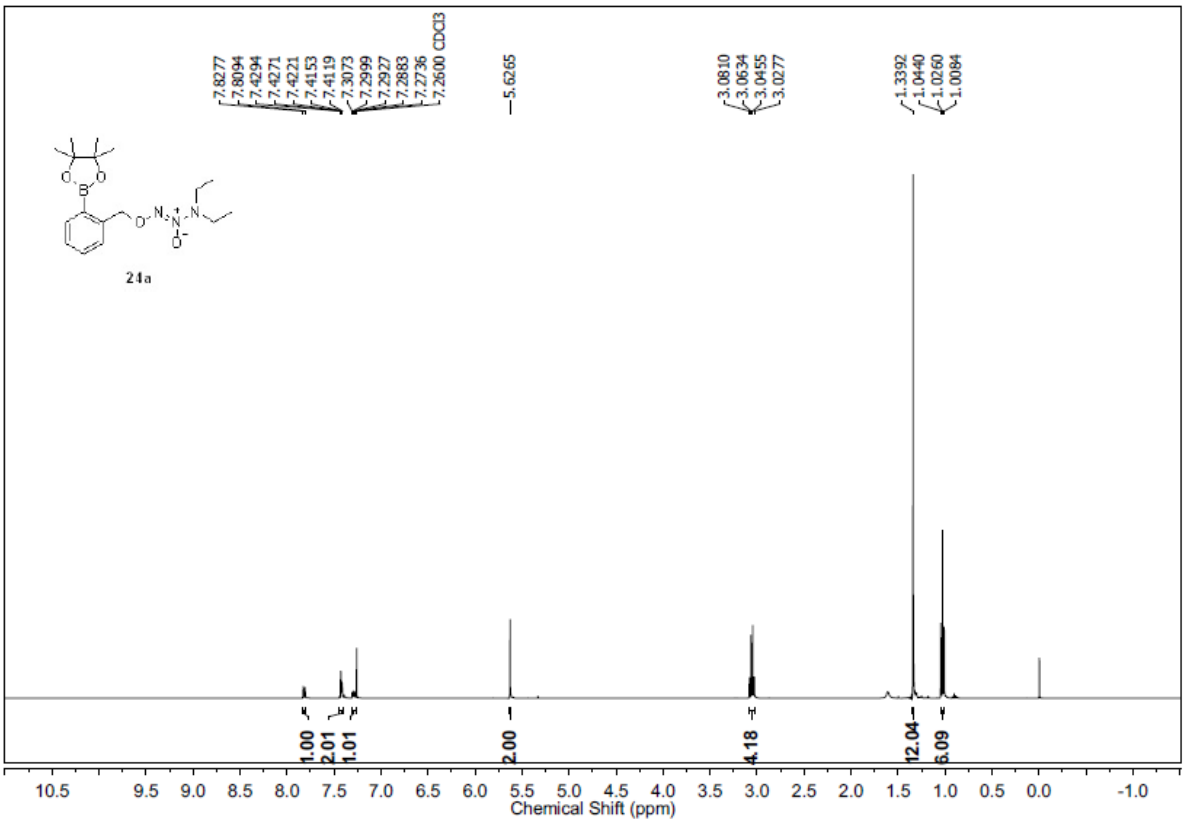

^{13}C NMR Spectrum (100 MHz, $CDCl_3$) of Compound 24a

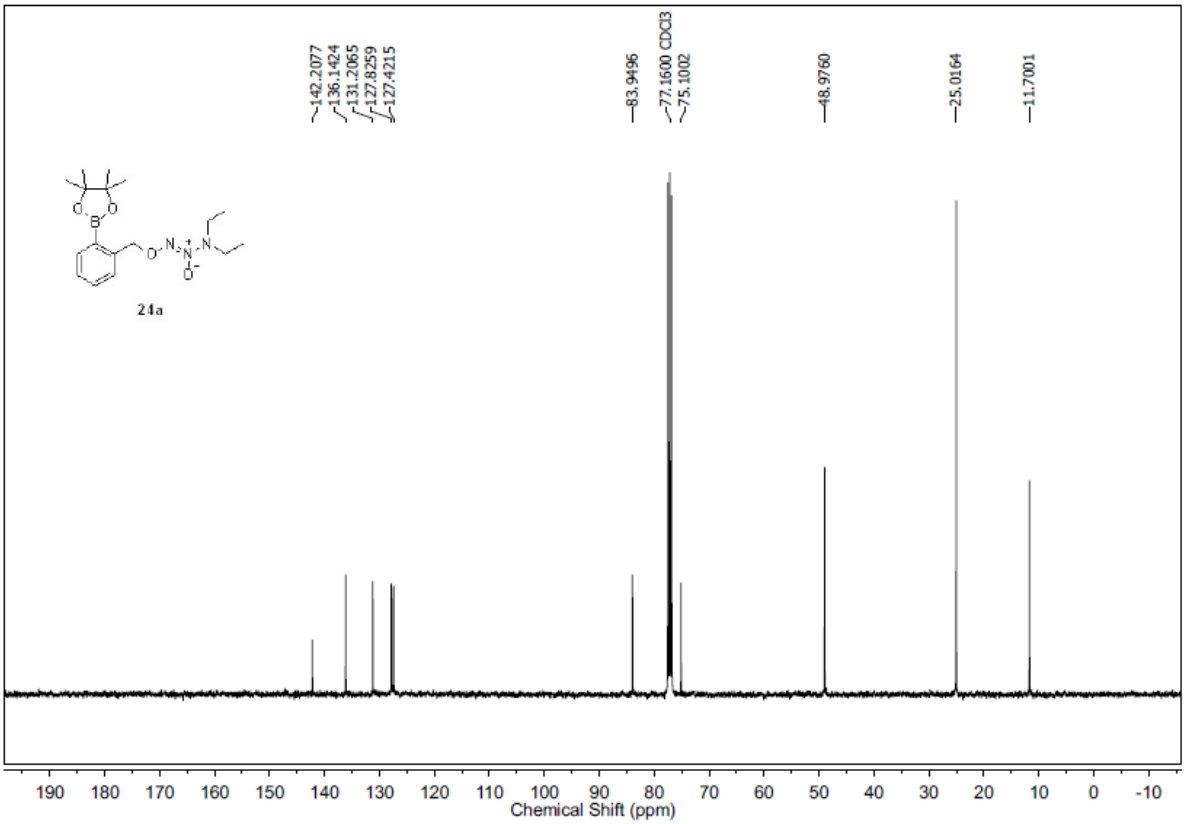

^{1}H-NMR Spectrum (400 MHz, $CDCl_3$) of Compound 24b

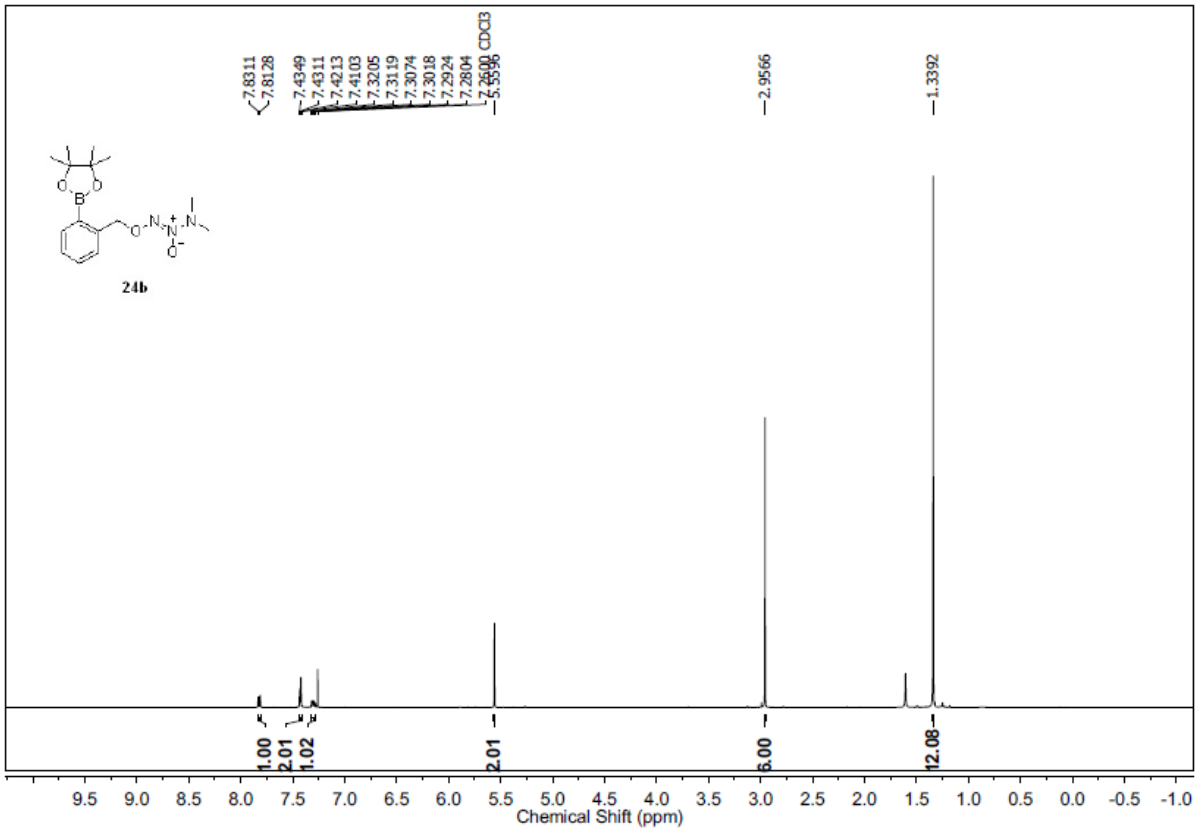

^{13}C NMR Spectrum (100 MHz, $CDCl_3$) of Compound 24b

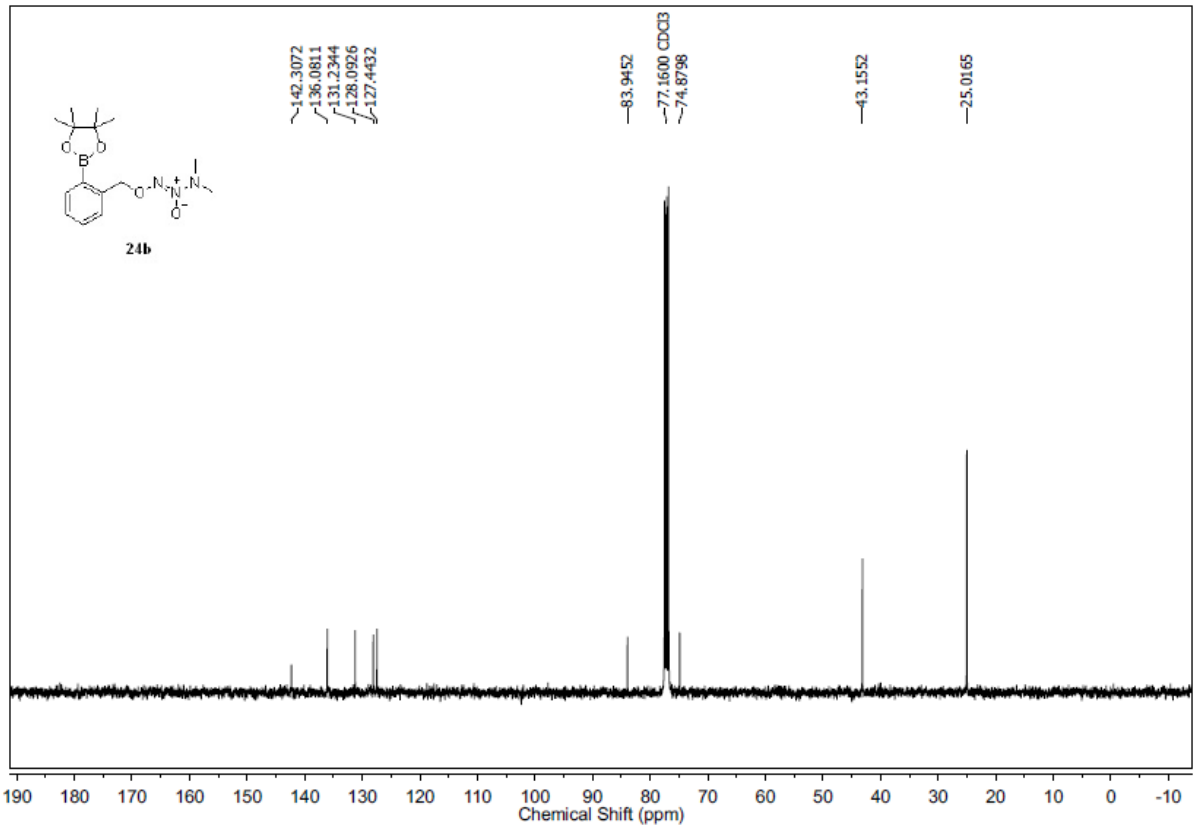

^{1}H-NMR Spectrum (400 MHz, $CDCl_3$) of Compound 24c

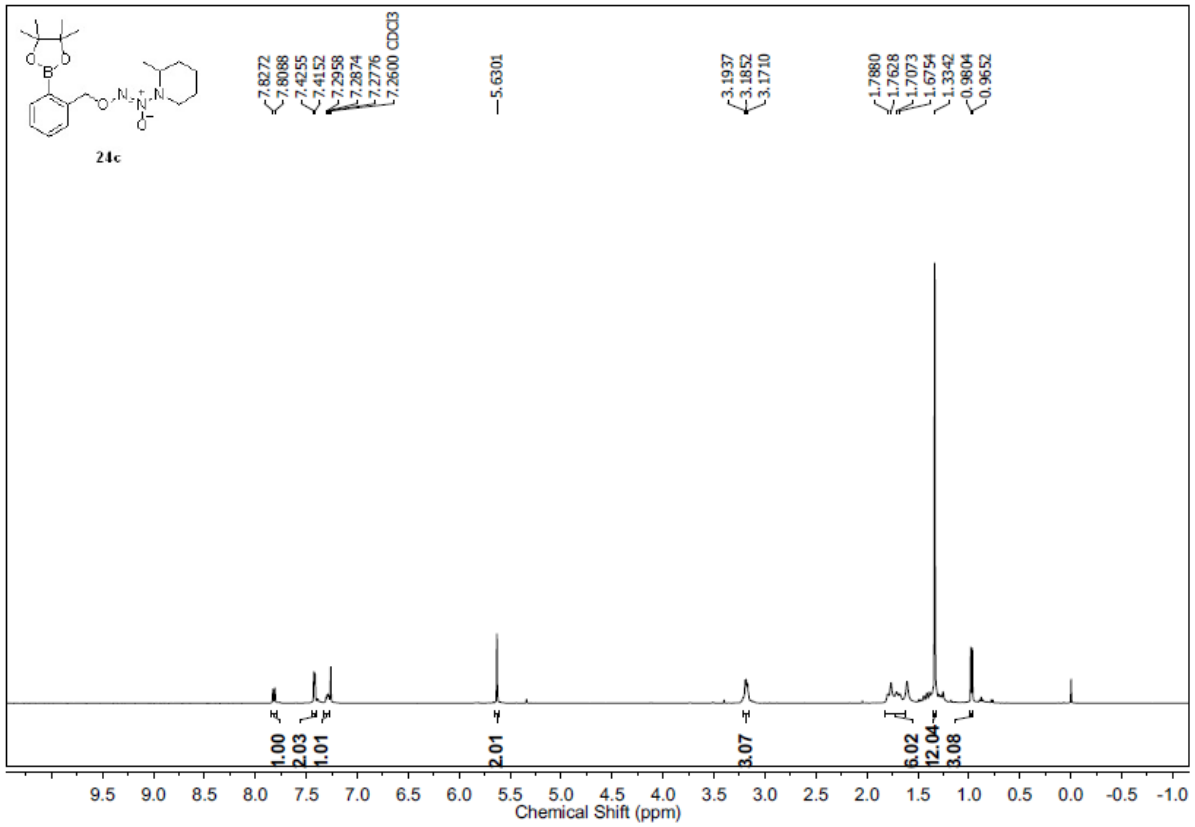

^{13}C NMR Spectrum (100 MHz, $CDCl_3$) of Compound 24c

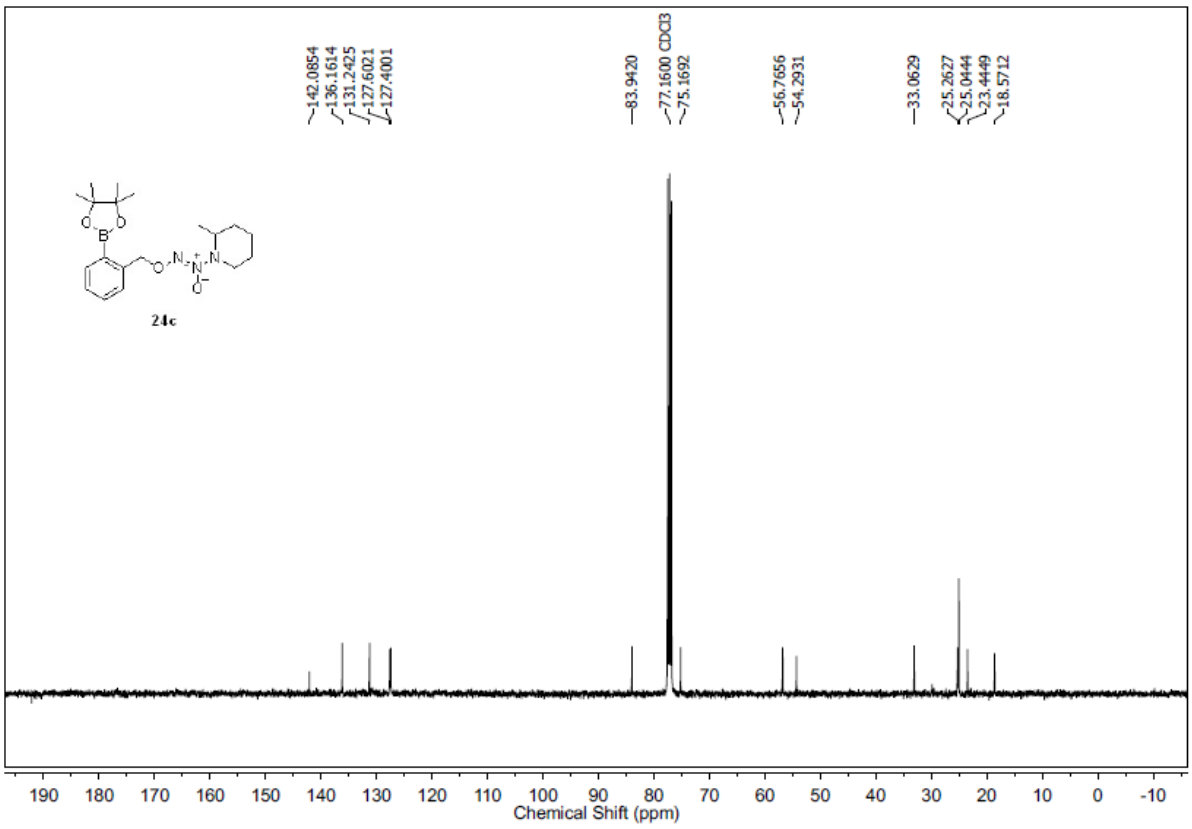

^{1}H-NMR Spectrum (400 MHz, $CDCl_3$) of Compound 24d

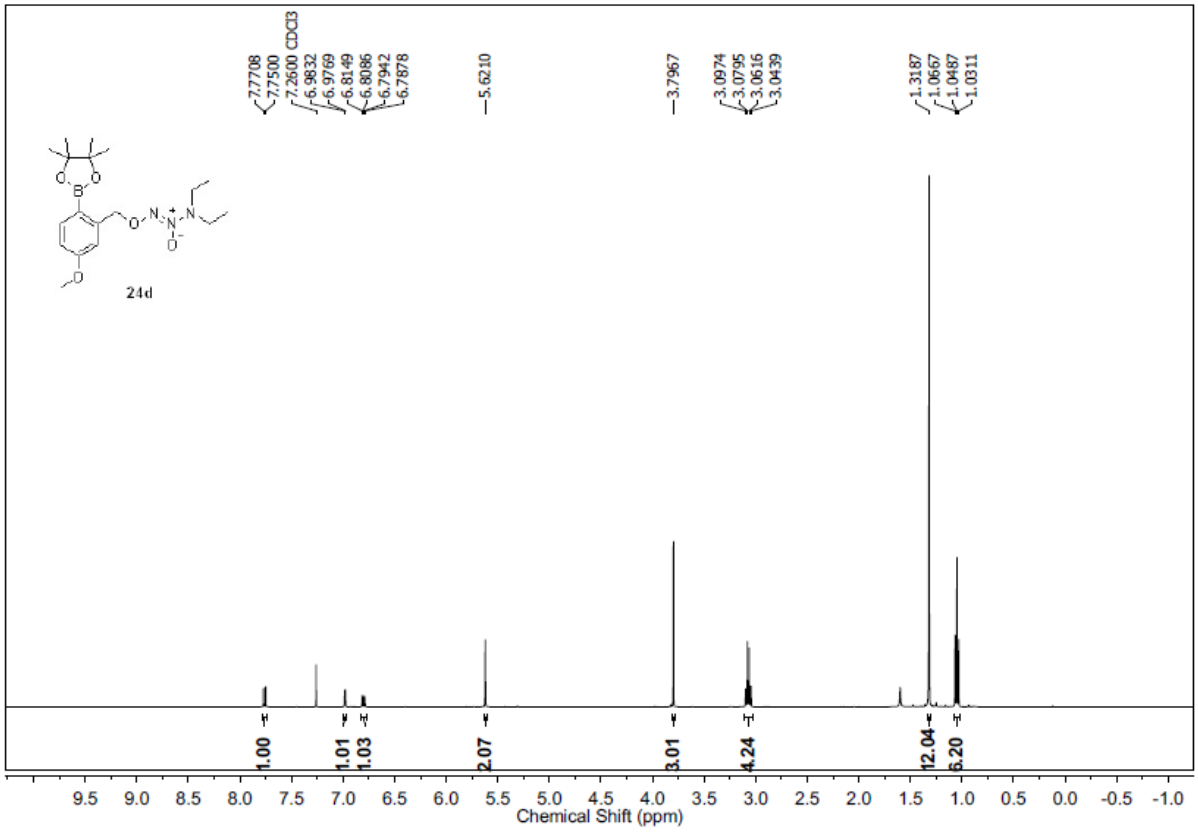

^{13}C NMR Spectrum (100 MHz, $CDCl_3$) of Compound 24d

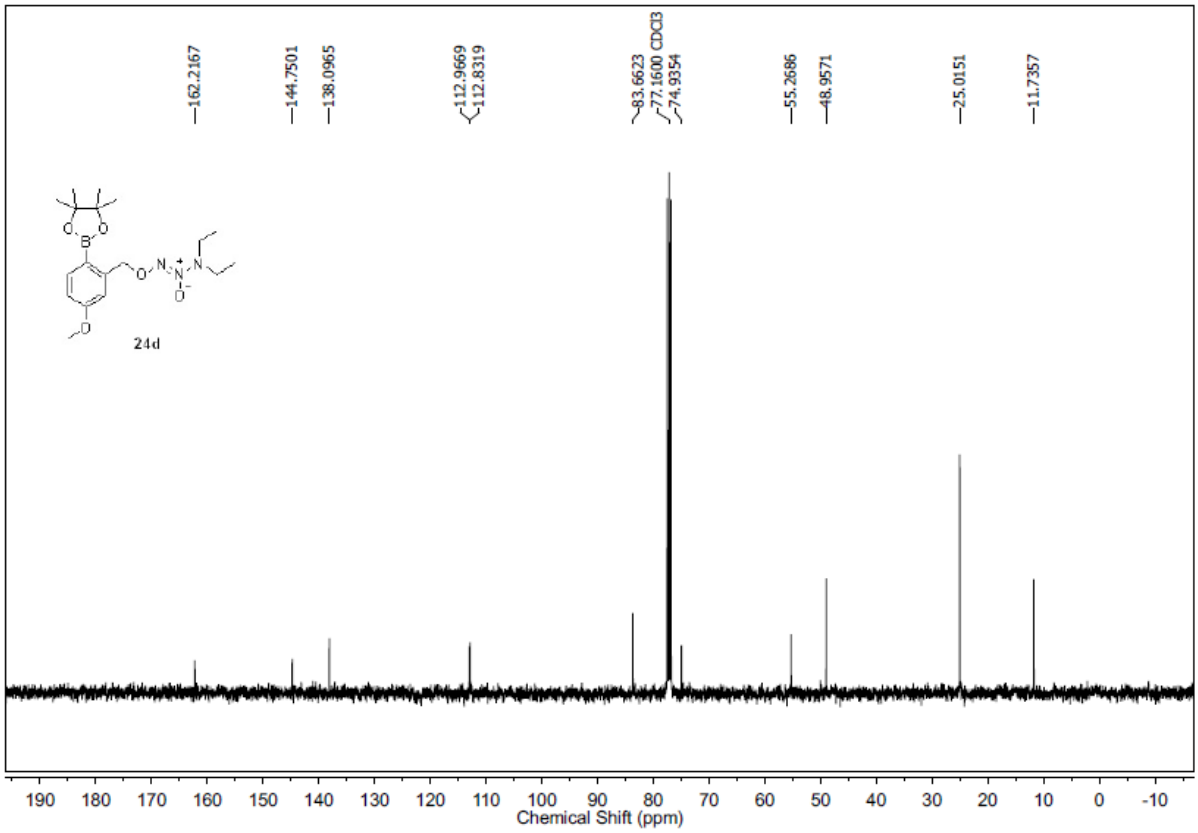

3.6. References

(1) Ravikumar, G.; Bagheri, M.; Saini, D. K.; Chakrapani, H. *ChemBioChem* **2017**, *18*, 1529.

(2) Szatrowski, T. P.; Nathan, C. F. *Cancer Res.* **1991**, *51*, 794.

(3) Lim, S. D.; Sun, C.; Lambeth, J. D.; Marshall, F.; Amin, M.; Chung, L.; Petros, J. A.; Arnold, R. S. *Prostate* **2005**, *62*, 200.

(4) Khandrika, L.; Kumar, B.; Koul, S.; Maroni, P.; Koul, H. K. *Cancer Lett.* **2009**, *282*, 125.

(5) Trachootham, D.; Alexandre, J.; Huang, P. *Nat. Rev. Drug Discov.* **2009**, *8*, 579.

(6) Antunes, F.; Cadenas, E. *FEBS Lett.* **2000**, *475*, 121.

(7) Kuang, Y.; Balakrishnan, K.; Gandhi, V.; Peng, X. *J. Am. Chem. Soc.* **2011**, *133*, 19278.

(8) Chen, W.; Balakrishnan, K.; Kuang, Y.; Han, Y.; Fu, M.; Gandhi, V.; Peng, X. *J. Med. Chem.* **2014**, *57*, 4498.

(9) Peng, X.; Gandhi, V. *Ther. Deliv.* **2012**, *3*, 823.

(10) Marzenell, P.; Hagen, H.; Sellner, L.; Zenz, T.; Grinyte, R.; Pavlov, V.; Daum, S.; Mokhir, A. *J. Med. Chem.* **2013**, *56*, 6935.

(11) Kumar, R.; Han, J.; Lim, H.-J.; Ren, W. X.; Lim, J.-Y.; Kim, J.-H.; Kim, J. S. *J. Am. Chem. Soc.* **2014**, *136*, 17836.

(12) Kim, E.-J.; Bhuniya, S.; Lee, H.; Kim, H. M.; Cheong, C.; Maiti, S.; Hong, K. S.; Kim, J. S. *J. Am. Chem. Soc.* **2014**, *136*, 13888.

(13) Dickinson, B. C.; Chang, C. J. *J. Am. Chem. Soc.* **2008**, *130*, 9638.

(14) Miller, E. W.; Tulyathan, O.; Isacoff, E. Y.; Chang, C. J. *Nat. Chem. Biol.* **2007**, *3*, 263.

(15) Miller, E. W.; Albers, A. E.; Pralle, A.; Isacoff, E. Y.; Chang, C. J. *J. Am. Chem. Soc.* **2005**, *127*, 16652.

(16) White, J. R.; Price, G. J.; Schiffers, S.; Raithby, P. R.; Plucinski, P. K.; Frost, C. G. *Tetrahedron Lett.* **2010**, *51*, 3913.

(17) Spencer, J.; Baltus, C. B.; Patel, H.; Press, N. J.; Callear, S. K.; Male, L.; Coles, S. J. *ACS Comb. Sci.* **2011**, *13*, 24.

(18) Srinivasan, A.; Kebede, N.; Saavedra, J. E.; Nikolaitchik, A. V.; Brady, D. A.; Yourd, E.; Davies, K. M.; Keefer, L. K.; Toscano, J. P. *J. Am. Chem. Soc.* **2001**, *123*, 5465.

(19) Sheng, C.; Robin, C.; Xiaohua, P. *Chem. Eur. J.* **2013**, *19*, 9050.

(20) Chung, C.; Srikun, D.; Lim, C. S.; Chang, C. J.; Cho, B. R. *Chem. Commun.* **2011**, *47*, 9618.

CHAPTER 4: Hydrogen peroxide Activated NO Donor with a Fluorescence Reporter

4.1. Introduction

In chapter 2, as a proof-of-concept, we designed and synthesized **FLUORO/NO**, a new class of triggerable NO donors with an in-built fluorescence reporter. Upon activation by an esterase enzyme the compound produces NO as well as a fluorescence signal simultaneously, without NO consumption.[1] Due to the ubiquitous expression of esterases, the donor **FLUORO/NO** would uniformly enhance NO in nearly all cells. Next, in order to deliver NO selectively to cancer cells, a second stimulus for activation was chosen: hydrogen peroxide (H_2O_2), a reactive oxygen species (ROS). As ROS is frequently found to be elevated in rapidly dividing cells such as cancers,[2-6] H_2O_2 has been previously used to specifically activate prodrugs[7-9] and latent fluorophores[10] (as imaging agents) in cancers. Boronate ester is known to react with H_2O_2 to produce an alcohol;[7,11] hence this functional group was chosen as the metabolic stimulus. In chapter 3, we designed and synthesized a series of arylboronate ester based diazeniumdiolates (**BORO/NO**), established that **BORO/NO** derivatives are capable of generating NO when triggered by H_2O_2. Using these templates we designed **27**, a H_2O_2 activated NO donor that can be used for selectively delivering and monitoring the release of NO in cancer cells (Scheme 4.1).

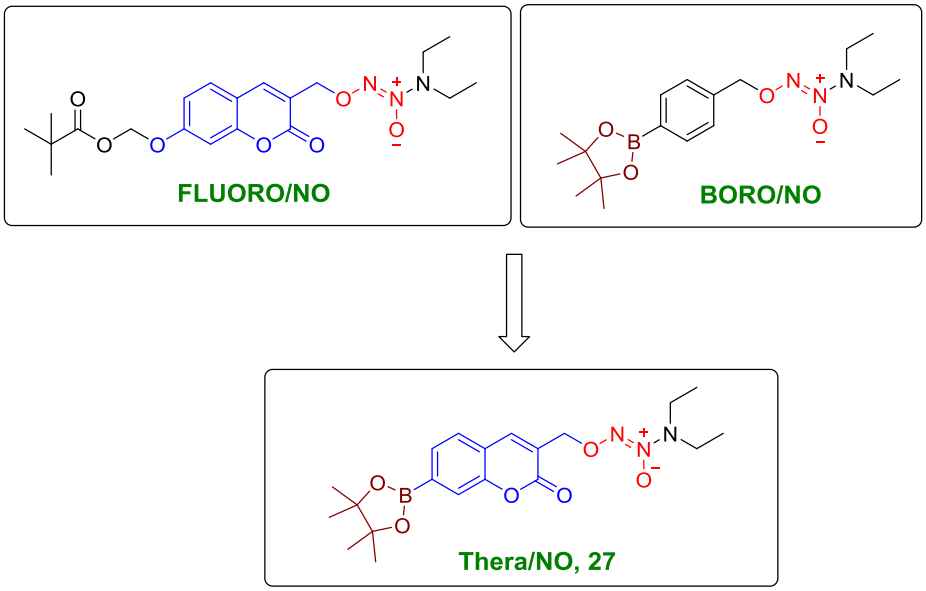

Scheme 4.1. Proposed model for the real-time monitoring of NO release in cancer cells

The proposed mechanism of activation of the reporter probe, **27** is as follows. Upon activation of **27** by H_2O_2, self-immolation and reaction with water produces **12** and DEA/NO, which rapidly dissociates at pH 7.4 to produce NO (Scheme 4.2).

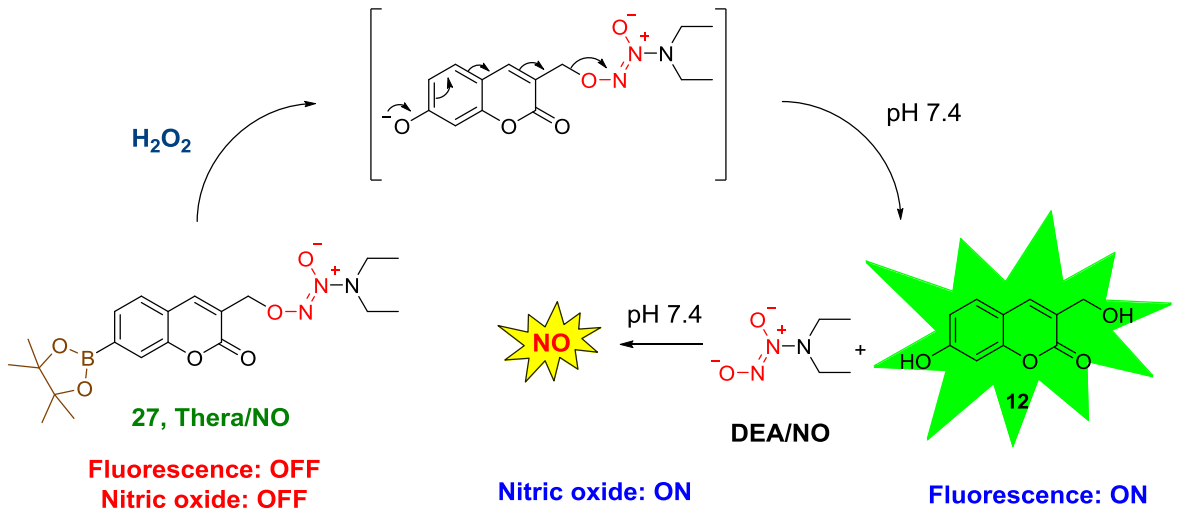

Scheme 4.2. Proposed mechanism of activation of **27** by hydrogen peroxide to produce **12** and NO

4.2. Results and Discussion

4.2.1. Synthesis

In order to test our hypothesis of H_2O_2 activated NO donor with fluorescence reporter, compound **27** was synthesized in three steps starting from compound **1** (Scheme 4.3). Briefly, 3-Methyl-umbelliferone (**1)** was reacted with trifluromethanesulfonic anhydride in the presence of pyridine to form compound **25** in 86% yield. Next**,** Pd (II) catalyzed borylation of compound **25** provided compound **26** in 65% yield. The synthesis of compounds **1** and **26** were performed using reported procedures.[12,13] Then**,** compound **26** was reacted with *N*-bromosuccinamide (NBS) in the presence of a radical initiator azobisisobutyronitrile (AIBN) in carbon tetrachloride to produce the corresponding bromide, which was then reacted with **DEA/NO** to give the desired compound **27** (Scheme 4.3).

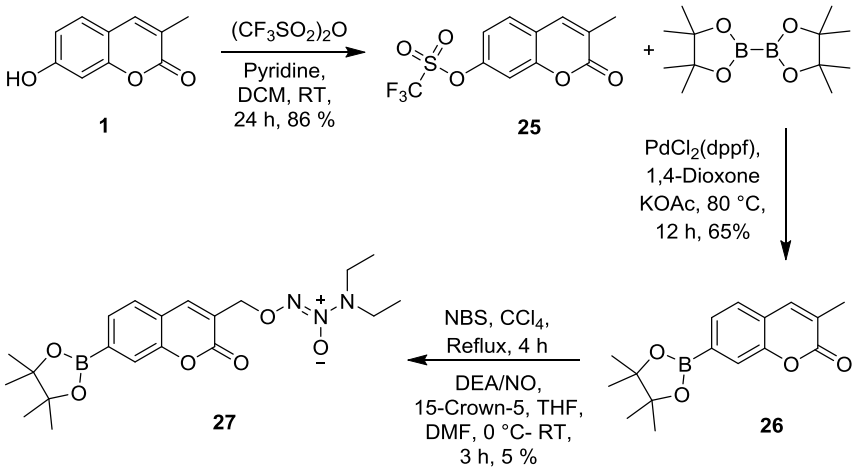

Scheme 4.3. Synthesis of **27**

4.2.2. Selectivity of 27 towards H_2O_2

First, the selectivity of **27** towards activation by H_2O_2 was investigated in the presence of number of biologically relevant nucleophiles, reductants, and oxidants. Compound **27** was incubated in buffer and treated with 10 equivalent of different reactive species and fluorescence signal attributable to **12** was monitored using a microwell plate reader after 30 min. Compound **27** was found to be highly selective toward activation by H_2O_2 and no significant increase in fluorescence signal was observed in the presence of biologically relevant thiols, metal ions, antioxidants, and other common reactive oxygen species (Figure 4.1.a). The observed selectivity of the boronate ester functional group towards H_2O_2 was consistent with previous reports.[7,10,14] Next, when compound **27** was treated with increasing concentration of H_2O_2, we found a dose-dependent increase in fluorescence signal at 460 nm (Figure 4.1.b). Together these results suggest the selectivity of the functional group towards activation by hydrogen peroxide in a physiological condition.

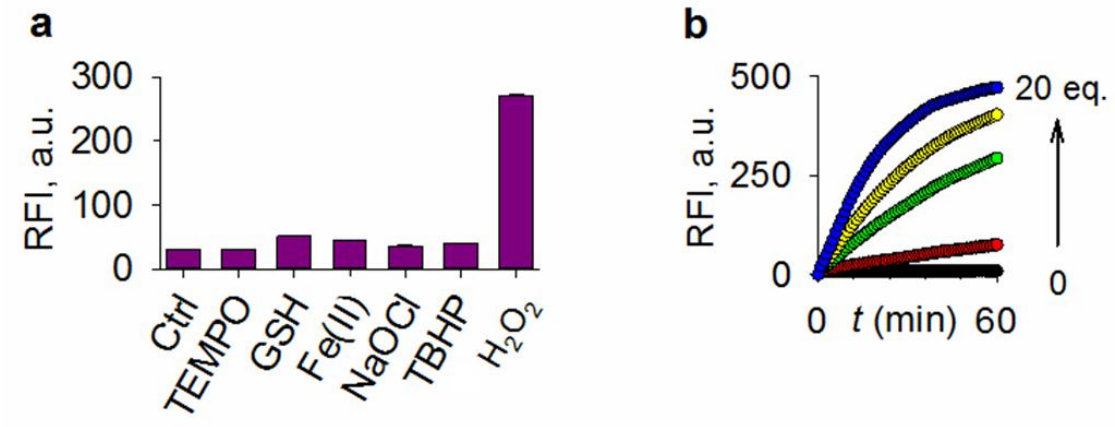

Figure 4.1. (a) Fluorescence response of **27** (10 μM) with various reactive species (100 μM) at 37 °C in pH 7.4 buffer after 30 min incubation. Ctrl: buffer; TEMPO: 2,2,6,6-tetramethylpiperidinyloxy; GSH: glutathione; Fe(II): $FeCl_2$; NaOCl: sodium hypochlorite; TBHP: *tert*-butyl hydroperoxide; H_2O_2. (b) Time course of fluorescence measurements during incubation of **27** (25 μM) in the presence of H_2O_2 at various concentrations (Excitation 315 nm; Emission 460 nm). (All the experiments were conducted in phosphate buffer pH 7.4 at 37 °C, excitation 315 nm; emission 460 nm).

4.2.3. NO release and fluorescence emission in Buffer

Next, the ability of the compound **27** to generate NO and fluorescence signal in phosphate buffer (pH 7.4, 10 mM) was evaluated. Compound **27** was treated with 10 eq. H_2O_2 and the fluorescence signal attributable to **12** as well as nitric oxide was independently monitored. The fluorescence signal at 460 nm was measured using a micro-well plate reader while nitric oxide released was measured by nitric oxide analyser (NOA). In the presence of H_2O_2, a

gradual increase in fluorescence signal attributable to **12** was observed during 50 min (Figure 4.2.a). However under similar conditions, there is no significant fluorescence signal was seen from **27** in the absence of H_2O_2.

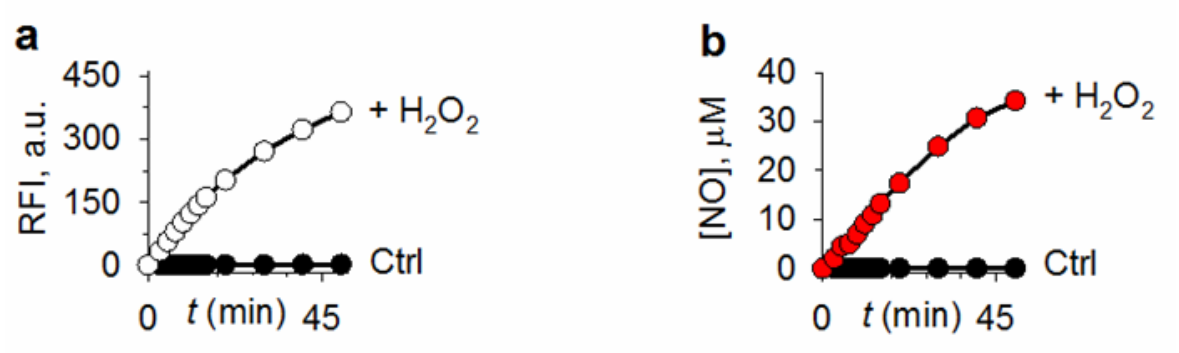

Figure 4.2. (a) Time course of enhancement of fluorescence signal (excitation 315 nm, emission 460 nm) attributable to **12** upon incubation of **27** (25 µM) with and without H_2O_2 (10 eq). (b) Time course of enhancement of NO upon incubation of **27** (25 µM) with and without H_2O_2 (10 eq). (All the experiments were conducted in phosphate buffer pH 7.4 at 37 °C, excitation 315 nm; emission 460 nm).

Similarly, when NO was monitored, we found that the compound generated NO only in the presence of H_2O_2 (Figure 4.2.b). The rate constant for the fluorescence signal k_{Fluor} was found to be 4×10^{-4} s^{-1}; while the rate constant for the formation of NO, k_{NO} under similar conditions was found to be comparable in magnitude: 2×10^{-4} s^{-1}. Next, the yield of **12** formed upon treatment of **27** with H_2O_2 was calculated through a calibration curve with authentic **12** (Scheme 4.2 and Figure 4.16). Using this quantitative data, the time course for formation of **12** was monitored by its fluorescence signal at 460 nm and independently, the formation of NO was also monitored under similar conditions. A close correlation between these two parameters was observed (Figure 4.3.a), suggesting that the aforementioned fluorescence signal and NO generation were nearly concurrent.

4.2.4. On-demand release of NO in Buffer

Next, the accumulation of hydrogen peroxide is localized during inflammation and tumour progression and provides for a chemical handle for spatiotemporal control. We used **27**, which is activated by a chemical trigger i.e. hydrogen peroxide to test if **27** can be used for generation of NO in a spatiotemporally controlled manner. First, the fluorescence signal as well as NO generated was monitored by first exposing the compound to 5 eq. (first arrow) of H_2O_2. A gradual increase in NO as well as fluorescence was observed (Figure 4.3.b). This situation mimics the normal tissue where accumulation of H_2O_2 is minimal. When this

solution was then exposed to 20 eq. (second arrow) of H_2O_2; this concentration perhaps represents situations of tumours where a large amount of ROS is present, a rapid increase in fluorescence as well as NO was observed (Figure 4.3.b). Thus, this compound is suitable to produce NO "On-demand".

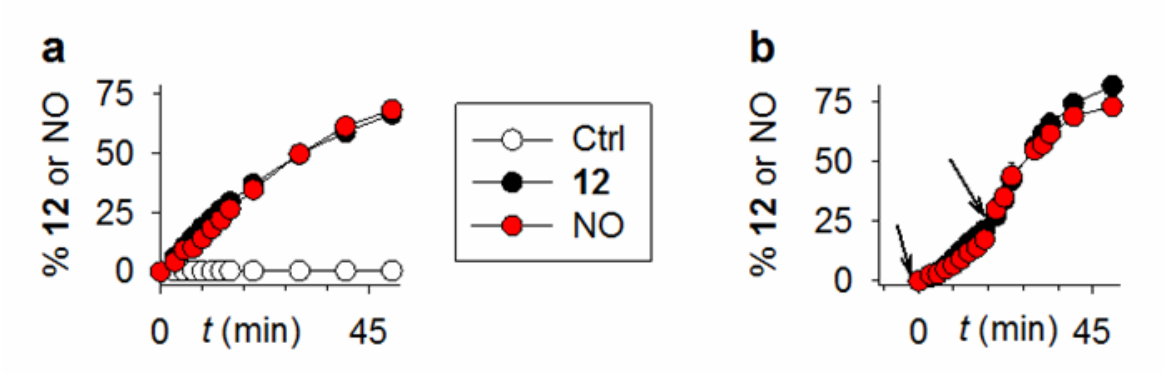

Figure 4.3. (a) Time course of enhancement of fluorescence signal attributable to **12** and time course of enhancement of NO upon incubation of **27** (25 μM) with and without H_2O_2 (10 eq). (Ctrl = **27** without H_2O_2). (b) Stimuli responsive fluorescence as well as NO generation during exposure to 5 and 20 eq. of H_2O_2 (All the experiments were conducted in phosphate buffer pH 7.4 at 37 °C, excitation 315 nm; emission 460 nm).

4.2.5. Fluorescence properties of 12 with excess of H_2O_2

The fluorescence properties of compound **12** towards excess of H_2O_2 was studied, where the compound **12** was incubated in buffer and treated with different equivalents of H_2O_2 and fluorescence signal at 460 nm was monitored using a microwell plate reader after 30 min. We found there is no significant change in the fluorescence signal. This result suggests that the fluorescence intensity attributable to **12** was not affected by increasing concentrations of hydrogen peroxide (Figure 4.4).

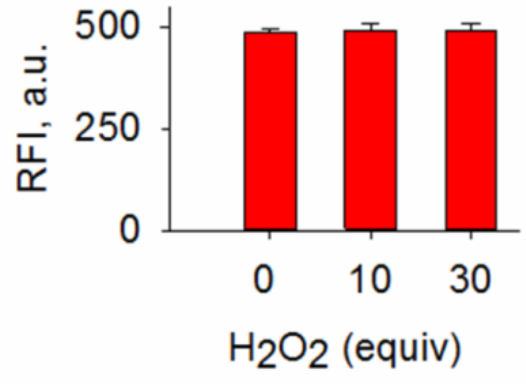

Figure 4.4. Fluorescence properties of compound **12** with different equivalents of H_2O_2 in pH 7.4 phosphate buffer at 37 °C (excitation 315 nm; emission 460 nm).

4.2.6. NO release and fluorescence emission in Cells

In order to study the capability of compound **27** to enhance fluorescence signal as well NO within the cells, HeLa cells were treated with **27** and exogenously H_2O_2 was added. The fluorescence signal at 460 nm was measured using a micro-well plate reader while nitrite released was measured by Griess assay and an increase in fluorescence and nitrite was observed (Figure 4.5). These results indicate that, the compound **27** gets activated by H_2O_2 within cells and produces NO and fluorescence signal.

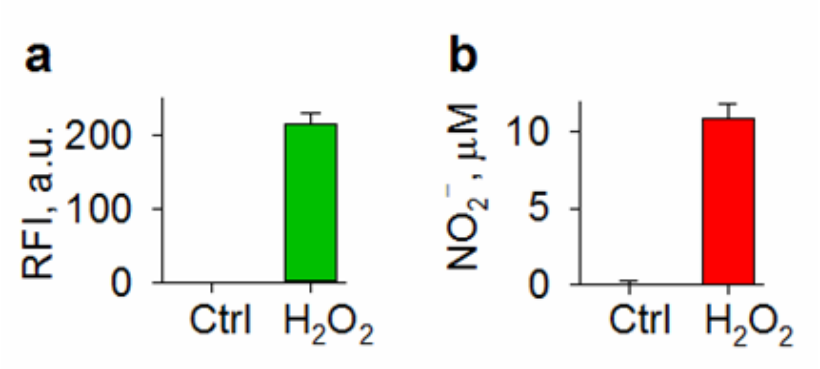

Figure 4.5. Comparison of the fluorescence signal attributable to **12** (a) and extracellular nitrite release (b) during incubation of HeLa cells when incubated with **27** (25 µM) alone (Ctrl) or HeLa cells pre-treated with H_2O_2 (100 µM) for 30 min followed by addition of **27** (25 µM) (excitation 315 nm; emission 460 nm).

4.2.7. Intracellular activation of 27

4.2.7.1. Fluorescence microscopy imaging

Having established that **27** is a reliable source of NO within cells, the fluorescence signal at 460 nm can now be used as a surrogate for NO generation. Fluorescence microscopy images of HeLa cells pretreated with **27** (25 µM) for 30 min and exposed to increasing concentrations of exogenous H_2O_2 for 30 min showed a dose-dependent increase in fluorescence signal at 460 nm (Figure 4.6), suggesting the reliability of this compound to permeate cells.

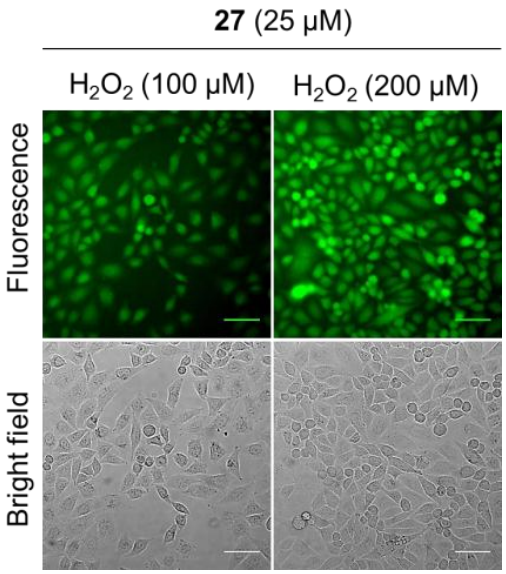

Figure 4.6. Fluorescence images of HeLa cells incubated with **27** (25 μM) with increasing concentration of H_2O_2 (100 and 200 μM). Images were taken using DAPI channel, pseudocolor (green) was given for better visualisation. Scale bar: 50 μm. Data provided by Meisam Bagheri & Deepak Saini, IISc Bangalore.

4.2.7.2. Fluorescence-activated cell sorting (FACS)

Next, in order to further verify the intracellular activation of **27**, we used fluorescence-activated cell sorting (FACS) to track the release of **12** within the cells. FACS analysis of HeLa cells pretreated with **27** (25 μM) for 30 min and exposed to increasing concentrations of exogenous H_2O_2 for 30 min showed a dose-dependent increase in fluorescence signal at 460 nm (Figure 4.7). These results supports that, the compound **27** permeate cells and get activated by H_2O_2 to produce fluorescence signal attributable to **12**.

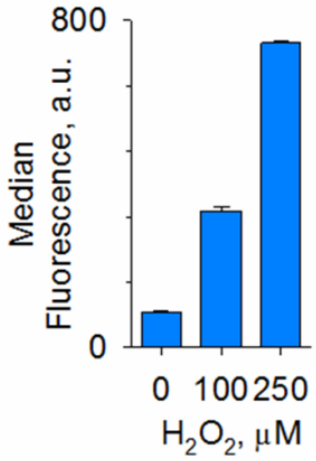

Figure 4.7. Flow cytometry analysis of HeLa cells incubated with **27** at 25 μM with increasing concentration of H_2O_2 (excitation 355 nm; emission 460 nm).

4.2.7.3. Cellular uptake and intracellular localization of 27

In order to study the cellular uptake and intracellular localization of **27**, confocal imaging was performed. Here, HeLa cells were treated with **27** followed by incubation with H_2O_2 and the cells were stained with LysoTracker green (fluorescence marker for Lysosome). A significant enhancement in the fluorescence signal, which overlapped with the fluorescence signal of LysoTracker green (Figure 4.8), was observed. This result suggested the preferential activation of **27** in lysosomes, which is along the lines of previous reports (It has been reported that intracellular hydrogen peroxide was mainly produced by mitochondria in the cells but it enters into lysosome via diffusion. Since, in contrast to cytoplasm, lysosomes do not contain hydrogen peroxide degrading enzymes such as catalase, H_2O_2 can get accumulated more in lysosomes than other part of cells).[9,15,16]

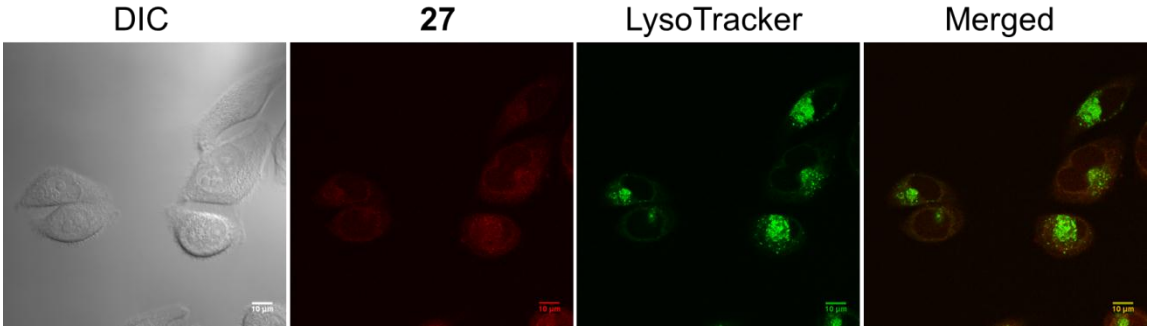

Figure 4.8. Subcellular localization of **27** in HeLa cells. Cells were treated with **27** (25 μM) for 30 min. Then, cells were treated with 100 μM H_2O_2 and further incubated for 30 min. Lysosomal localization was identified by LysoTracker-green. The excitation channel for **27** and LysoTracker were 405 and 488 nm, respectively. Scale bar: 10 μm.

4.2.8. Selective activation of 27 in catalase knockdown cells

Catalases are the highly efficient antioxidant enzymes, found in nearly all living organisms. It catalyses the conversion of hydrogen peroxide to water and molecular oxygen. Catalases protect the cells from oxidative stress by maintaining a safe level of H_2O_2 in cells.[17] In order to simulate increased ROS intracellularly, a catalase knockdown HeLa cell line (KD) was used. Here, due to the low level of catalase, which was confirmed by quantitative real-time PCR to check the mRNA levels (Figure 4.9) an increased level of ROS is expected. When intracellular ROS level was measured by $DCFH_2$-DA assay (fluorescence indicator for reactive oxygen species in cells), the catalase knockdown cell line (KD) showed higher DCF fluorescence (Figure 4.10.a) when compared with wild-type (WT).

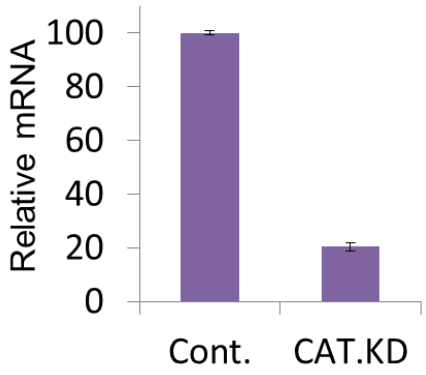

Figure 4.9. Relative mRNA level.

Both these cell lines were independently exposed to **27** and fluorescence signal corresponding to **12** was measured. We found that the relative increase in fluorescence signal was much higher in the case of KD when compared with WT (Figure 4.10.b). Thus, when encountered with cellular situations with varying ROS levels, **27** is preferentially activated in cell lines where ROS levels are relatively higher.

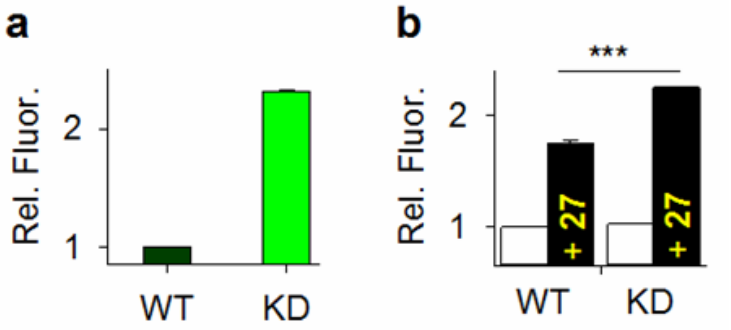

Figure 4.10. (a) Intracellular ROS enhancement was measured using a $DCFH_2$-DA assay in wild type (WT) and catalase expression knockdown (KD) cells. (b) Comparison of the relative fluorescence signal attributable to **12** in wild type (WT) and catalase expression knockdown (KD) cells after treatment with **27**. ***p-value = 0.006. Data provided by Meisam Bagheri & Deepak Saini, IISc Bangalore.

4.2.9. Selective activation of 27 in cancer cells

Since cancer cells produce higher level of H_2O_2 compared with normal cells, selective activation of **27** was expected in cancer cells than the normal cells. To validate it, compound **27** was treated with MRC5 (normal fibroblast) and cancer cell lines: A549, HeLa, MDA-MB-231 and the fluorescence response was evaluated by fluorescence microscopy imaging. As expected, we found enhancement in the fluorescence signal attributable to **12** in cancer cells compared with normal cells (Figure 4.11). Together these experiments suggest that **27** get selectively activated in cancer cells over normal cells.

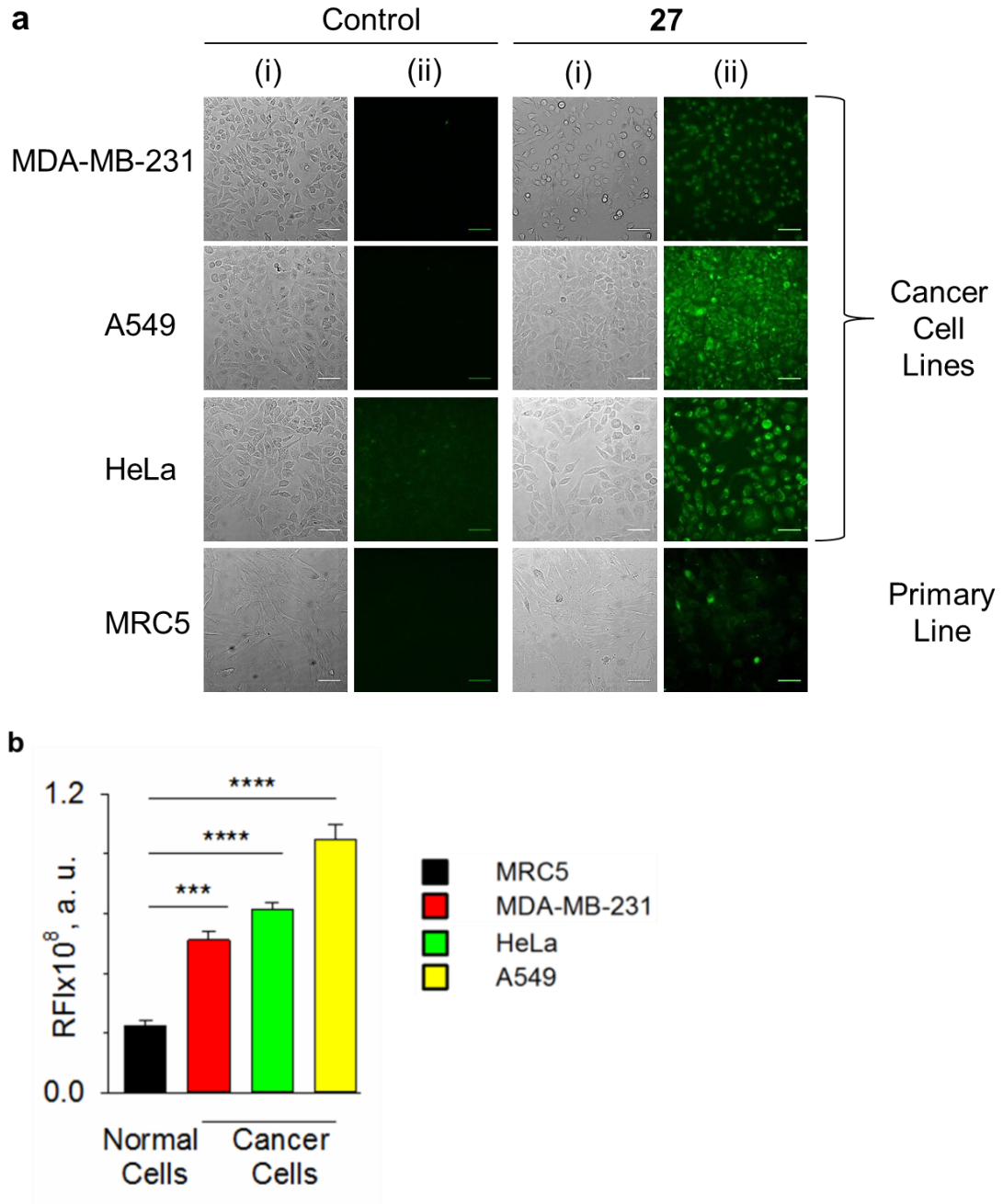

Figure 4.11. (a) Fluorescence images of different cells treated with **27** (25 μM) after 6 h at 37 °C. Images were taken using DAPI channel and pseudocolored (in green) for better visualisation. (i) Bright field image, (ii) Fluorescence image. Scale bar = 100 μm. All images were acquired with identical parameters (gain 3, intensification 200 and ND: 75). (b) Quantification of fluorescence intensity was done using ImageJ software and statistical analysis was done using t-test. ***p-value 0.0002, ****p-value < 0.0001. Data provided by Meisam Bagheri & Deepak Saini, IISc Bangalore.

4.2.10. Real-time monitoring of NO release and its effect-TheraNOstic

Nitric oxide and reactive nitrogen species (RNS) are well known to induce DNA damage, especially double strand breaks (DSBs).[18] 53BP1 is one of the DNA damage response proteins that is recruited very efficiently to sites of DNA double-strand breaks. Its recruitment can be visualized by monitoring live cells expressing 53BP1 fused to green fluorescent protein (GFP).[19] Therefore, we monitored the ability of **27** to induce DNA damage by monitoring 53BP1 foci, which are markers of double strand breaks and accumulate as nuclear foci. HeLa cells stably expressing 53BP1 fused to GFP were seeded on glass-bottom dishes and independently treated with **27** and imaged 6 h post-treatment. As expected, we found an increase in DNA damage induced by **27** as evidenced by increased foci, increased foci are indicative of enhanced DNA damage response (Figure 4.12) suggesting the involvement of reactive nitrogen species (RNS) in the observed phenotype.[20] When the concentration of **27** was varied, a dose-dependent increase in 53BP1 foci was observed (Figure 4.12). Under similar conditions, an increase in the fluorescence signal attributable to **12** in DAPI channel was also observed (Figure 4.13) suggesting the suitability of Thera/NO for real-time monitoring of NO.

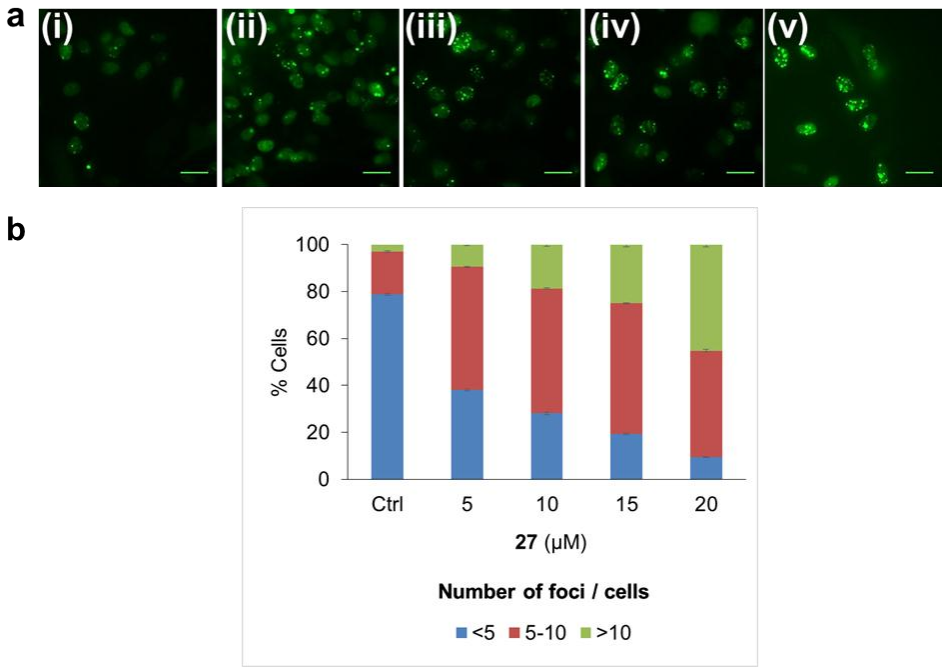

Figure 4.12. (a). Formation of 53BP1 foci upon exposure of (i) Control, (ii) 5 μM of **27**, (iii) 10 μM of **27**, (iv) 15 μM of **27**, (v) 20 μM of **27**. Images were taken in GFP channel. (b) Quantitation of 53BP1-GFP foci: Number of foci per cell were counted and the cells were classified in three categories (<5; 5-10; >10) based on number of foci per cell. Scale bar = 100 μm. All images were

acquired with identical parameters (Camera gain 3, intensification 200 and ND: 75). Data provided by Meisam Bagheri & Deepak Saini, IISc Bangalore.

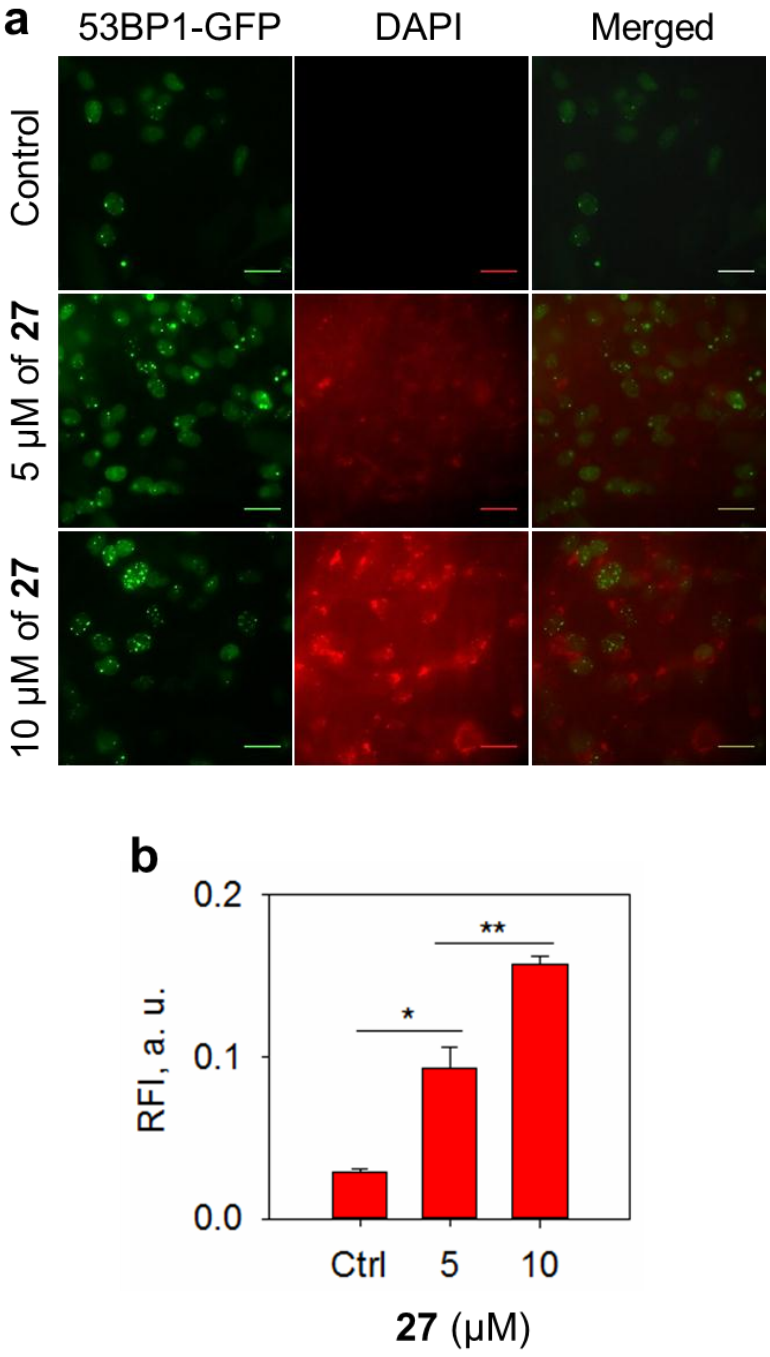

Figure 4.13. (a) Formation of 53BP1 foci and enhancement of fluorescence signal attributable to **12** upon exposure of **27** in HeLa cells. Images were taken in GFP channel (for foci) and DAPI channel (for **12**) with fixed acquisition settings. DAPI images have been pseudocolored (red) for better visualization. Scale bar 100 μm. All images were acquired with identical image acquisition parameters. (b) Quantification of fluorescence intensity was done using ImageJ software and

statistical analysis was done using t-test. *p-value 0.0112, **p-value 0.0086. Data provided by Meisam Bagheri & Deepak Saini, IISc Bangalore.

4.2.11. Cytotoxic effect of 27 with normal vs cancer cells

Finally, the cytotoxic effect of compound **27** was evaluated with MRC5 (normal fibroblast) and cancer cell lines: A549, HeLa, MDA-MB-231 by an Alamar blue assay, as expected we found compound **27** showed significant cytotoxic effect towards cancer cells compared with normal cells (Figure 4.14).

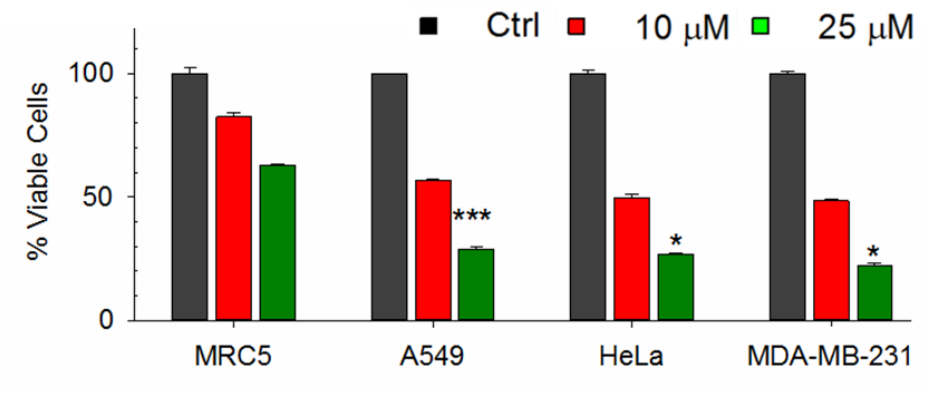

Figure 4.14. Comparison of cytotoxic effect of **27** (10 and 25 μM) on primary cell (MRC5) versus cancer cells (A549, HeLa and MDA-MB 231 cells) after incubation for 12 h. Statistical analysis at 25 μM: A549 vs MRC5, p-value 0.0096; HeLa vs MRC5, p-value 0.014; MDA-MB-231 vs MRC5, p-value 0.028. Data provided by Meisam Bagheri & Deepak Saini, IISc Bangalore.

4.3. Conclusion and outlook

In this chapter, we synthesized Thera/NO, a H_2O_2 activated NO donor with fluorescence reporter. Upon activation by H_2O_2 in buffer, a nearly quantitative correlation between fluorescence signal and NO generation was observed. When encountered with cellular situations with varying ROS levels, Thera/NO is observed to preferentially generate NO in cell lines with elevated ROS levels. Using cancer and primary cells, we showed that Thera/NO preferentially releases NO in cancer cells, which can trigger DNA damage and cell death in them. The coupled fluorescence signal facilitated tracking the NO release in living cells without use of secondary dyes for NO. Together, we have developed a convenient tool to enhance NO selectively in cancer cells and allows real-time monitoring of NO release without collateral consumption of NO. Further adaption of this technology to better direct NO to cancers is possible. For example, Thera/NO can be encapsulated with a polymer-nanoparticle carrier system, and due to the enhanced permeability and retention (EPR) effect, large amount of NO can be delivered selectively at the cancer site. The polymer backbone can be decorated with different targeting groups such as cancer targeting groups (folate, biotin), organelle targeting group (mitochondria, lysosomes), which offers an additional specificity to the NO delivery system. Furthermore, decorated NO donating nanoparticle system can be further encapsulate with an anticancer drugs and would be useful for the combination therapy.

The potential for use of NO in cancers is multifarious: (a) the vasodilatory effects of NO may improve blood circulation in the proximity of tumours; (b) the ability of NO to synergize with certain cancer drugs, especially, by inhibition of drug efflux pumps may be highly beneficial; and (c) NO can be a radiosensitizer facilitating radiation therapy. Thera/NO will lay the platform for exploiting the unique properties of NO in cancer therapy.

4.4. Experimental Section

4.4.1. Synthesis and characterization

Compounds **1**[12], **12**[21] and **26**[13] were synthesized using a previously reported procedure and the analytical data that we collected were consistent with the reported values.

(Z)-3,3-diethyl-1-((2-oxo-7-(4,4,5,5-tetramethyl-1,3,2-dioxaborolan-2-yl)-*2H*-chromen-3-yl)methoxy)triaz-1-ene 2-oxide (27):

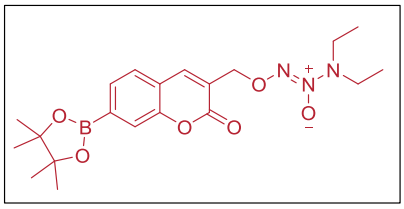

To a solution of compound **26** (200 mg, 0.70 mmol) in CCl_4 (5 mL), NBS (149 mg, 0.84 mmol) was added along with a trace amount of AIBN. The reaction mixture was refluxed for 4 h under nitrogen atmosphere. After cooling to room temperature, the solvent was removed under reduced pressure. The crude 3-(bromomethyl)-7-(4,4,5,5-tetramethyl-1,3,2-dioxaborolan-2-yl)-2H-chromen-2-one was taken for next reaction without further purification. To a solution of **DEA/NO** (102 mg, 0.66 mmol) in THF (3 mL) under ice, 15-crown-5 (12 µL) was added and the mixture stirred at 0 ºC for 5 min under nitrogen atmosphere. A solution of 3-(bromomethyl)-7-(4,4,5,5-tetramethyl-1,3,2-dioxaborolan-2-yl)-2H-chromen-2-one (crude, 200 mg, 0.55 mmol) in DMF (1 mL) was added to the reaction mixture at 0 ºC and stirred at room temperature for 3 h. The solvent was evaporated under reduced pressure, diluted with 10 mL of water and the aqueous solution was extracted with EtOAc (3×5 mL). The combined organic layer was washed with brine, dried over Na_2SO_4 (5 g), filtered and the filtrate was concentrated to give a crude compound. This crude was initially purified by silica gel column chromatography using EtOAc/pet ether (0 → 40 %) as the eluent. The resulting mixture was further purified using semi-preparative HPLC with C-18 semi-preparative column (9.4 mm × 250 mm, 5 µm; ZORBAX ODS), using a gradient of ACN and water (60 – 80 %), under ambient temperature with a flow rate of 2.5 mL/min to obtain **27** (12 mg, 5 %) as a semi solid; FT-IR (ν_{max}, cm^{-1}): 2923, 1723, 1550, 1508, 1359; ^{1}H NMR ($CDCl_3$, 400 MHz): δ 7.75 (s, 2H), 7.69 (d, J = 8.0 Hz, 1H), 7.46 (d, J = 7.7 Hz, 1H), 5.26 (d, J = 1.2 Hz, 2H), 3.17 (q, J = 7.1 Hz, 4H), 1.36 (s, 12H), 1.10 (t, J = 7.1 Hz, 6H); ^{13}C NMR ($CDCl_3$, 100 MHz): δ 160.1, 152.9, 139.6, 130.6, 127.3, 124.9, 122.7, 120.9, 84.6, 70.0, 48.6, 25.0, 11.7; HRMS (ESI) for $C_{20}H_{28}BN_3O_6$ $[M+Na]^+$: Calcd., 440.1968, Found, 440.1967.

4.4.2. NO release and fluorescence emission in Buffer

4.4.2.1. Nitric oxide detection from 27

A 1 mM stock solution of compound **27** in DMSO and 10 mM stock solution of H_2O_2 in water were prepared. A typical reaction mixture consisted of compound **27** (25 µM) and H_2O_2 (250 µM, 10 eq.) was prepared by mixing 12.5 µL of **27** and 12.5 µL of H_2O_2 from the stock solutions with 475 µL of pH 7.4 phosphate buffer (10 mM) at 37 ºC. An aliquot of the reaction mixture (10 µL) from the reaction vial was injected into a Sievers Nitric Oxide Analyzer (NOA 280i) using argon as the carrier gas. The amount of NO released was estimated using a standard calibration curve generated using sodium nitrite $NaNO_2$ solution of concentration from 0 – 50 µM using NOA Analyzer (Y = 140.2X; R^2 = 0.996). The data represented here is average of 3 repeats.

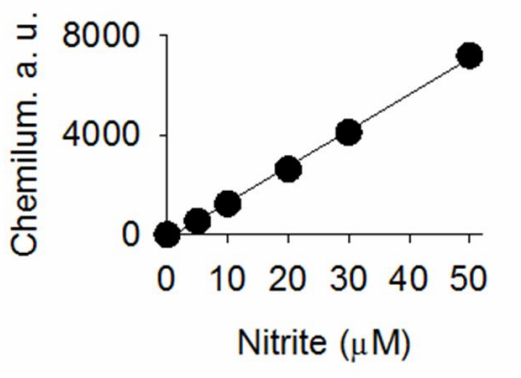

Figure 4.15. Calibration curve for nitrite in pH 7.4 phosphate buffer at 37 °C

4.4.2.2. Fluorescence measurement from 27

A 1 mM stock solution of compound **27** and a 10 mM stock solution of H_2O_2 in water were prepared. The experiment was performed in 96 well plate. In the control experiment, 2.5 µL of compound (25 µM) and 97.5 µL of phosphate buffer pH 7.4. In another set serving as H_2O_2 activated set 2.5 µL of compound **27** (25 µM) was added to 2.5 µL of H_2O_2 (final concentration of **27** was 25 µM in both blank and reaction; H_2O_2 used was 250 µM). The amount of **12** released was estimated using a standard calibration curve generated using authentic **12** solution of concentration varying from 0 – 25 µM (Y = 21.8X; R^2 = 0.994). Fluorescence was measured using a Thermo Scientific Varioskan Flash microwell plate reader (excitation 315 nm; emission 460 nm). The data represented here is average of 3 repeats.

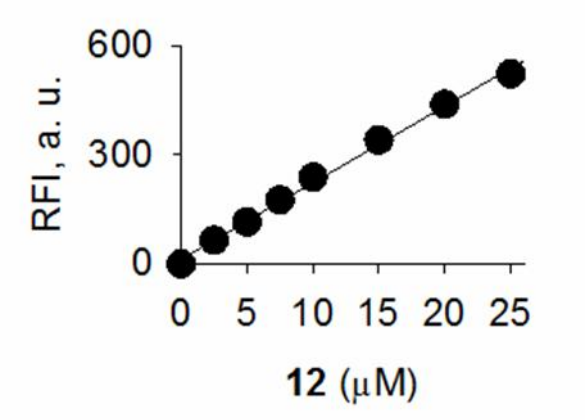

Figure 4.16. Calibration curve for compound **12** in pH 7.4 phosphate buffer at 37 °C

4.4.2.3. Selectivity studies of 27 with oxidants and reductants

A 1 mM stock solution of **27** in DMSO and 10 mM stock solution of various reactive species were prepared. A reaction mixture of **27** (10 μM, 1 eq.) and various analytes (100 μM, 10 eq.) were prepared by mixing 1 μL of **27** and 10 μL of analytes from the stock solutions to 89 μL of pH 7.4 phosphate buffer (10 mM) at 37 ºC. Fluorescence was measured using a Thermo Scientific Varioskan Flash microwell plate reader (excitation 315 nm; emission 460 nm). The data represented here is average of 3 repeats.

4.4.2.4. Fluorescence emission from 27 with different equivalents of H_2O_2

A 1 mM stock solution of **27** in DMSO and 10 mM stock solution of H_2O_2 in water were prepared. A reaction mixture of **27** (25 μM, 1 eq.) and H_2O_2 (0 - 500 μM, 0 - 20 eq.) were prepared by mixing 2.5 μL of **27** and respective volume of H_2O_2 from the stock solutions to pH 7.4 phosphate buffer (10 mM, final volume 100 μL) at 37 ºC. Fluorescence was measured using a Thermo Scientific Varioskan Flash microwell plate reader (excitation 315 nm; emission 460 nm). The data represented here is average of 3 repeats.

4.4.2.5. Fluorescence properties of compound 12

A 1 mM stock solution of compound **12** and a 100 mM stock solution of H_2O_2 in water were prepared. The experiment was performed in 96 well plates. In the control experiment, 2.5 μL of compound **12** (25 μM) was added to 97.5 μL of phosphate buffer pH 7.4. In another set serving as H_2O_2 activated set 2.5 μL of compound **12** (25 μM) was added to 0.25 μL and 0.75 uL of 100 mM H_2O_2 (For 10 and 30 eq. H_2O_2 respectively). Fluorescence was measured after 30 min using a Thermo Scientific Varioskan Flash microwell plate reader (excitation 315 nm; emission 460 nm). The data represented here is average of 3 repeats.

4.4.3. NO release and fluorescence emission in cells

4.4.3.1. Fluorescence emission and nitrite release from 27 in HeLa cells

Cells were suspended in HBSS medium and plated in a 96-well plate ($2.5x10^4$ cells/200 µL). A 10 mM stock solution of **27** in DMSO and 10 mM stock solution of H_2O_2 in water were prepared. In control experiment, compound **27** (25 µM) was added to the cell suspension. In another set serving as H_2O_2 activated set, cells were pre-treated with H_2O_2 (100 µM) for 30 min, followed by compound **27** was incubated for 30 min at 37 ºC and fluorescence emission was measured using a Thermo Scientific Varioskan Flash microwell plate reader (excitation 315 nm; emission 460 nm). For nitrite measurement, Griess reagent (14 µL for 200 µL reaction mixture, Sigma Aldrich) was added, and incubated at 37 ºC for 25 min before measuring OD at 540 nm using a Thermo Scientific Varioskan Flash microwell plate reader. The amount of nitrite release was estimated using a standard calibration curve generated using sodium nitrite $NaNO_2$ solution of concentration from 0 – 50 µM (Y = 0.0145 X; R^2 = 0.998). The data represented here is average of 3 repeats.

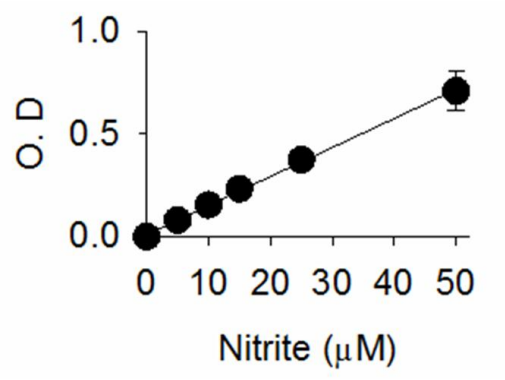

Figure 4.17. Calibration curve for nitrite in HBSS Buffer at 37 °C (O.D = Optical Density).

4.4.3.2. Fluorescence image of 27 activated by exogenous H_2O_2

HeLa cells were seeded at 50000 cells in 35cm glass bottom dishes for overnight in DMEM media supplemented with 10% FBS (fetal bovine serum) and 1% antibiotic solution in an atmosphere of 5% CO_2 at 37 °C. After incubation, old media was removed and the cells were washed with 1 mL of PBS (1X) buffer. Then 1 mL of fresh DMEM media was added along with compound (25 µM) and cells were incubated for 30 minutes at 37 °C. After 30 minutes, media was removed, cells were washed with 1 mL of PBS (1X). 1 mL of media was added along with H_2O_2 (100, 200 µM) and cells were incubated for 30 minutes. After 30 minutes, media was removed, cells were washed with 1 mL of PBS (1X) and 1 ml of live cell imaging solution (Invitrogen A14291DJ) was added and imaged by olympus IX83 fluorescence

microscopy. And the image was analysed by slide book 6.0 software (intelligent Imaging Innovations, Denver, CO).

4.4.3.3. FACS analysis of HeLa cells with 27

HeLa cells were seeded at 1×10^5 cells/well in 6 well plate for overnight in DMEM media supplemented with 10% FBS and 1% antibiotic solution in an atmosphere of 5% CO_2 at 37 °C. After incubation, old media was removed and the cells were washed with 1 mL of PBS (1X) buffer. Then 1 mL of fresh DMEM media was added along with compound **27** (25 μM) and cells were incubated for 30 minutes at 37 °C. After 30 minutes, media was removed, cells were washed with 1 mL of PBS (1X). 1 mL of fresh DMEM media was added along with H_2O_2 (100, 250 μM) and cells were incubated for 30 minutes. After 30 minutes, media was removed, cells were washed with 1 mL of PBS (1X) and cells were detached by trypsination. Cells were centrifuged at 1000 rpm, 22 °C for 5 min. Supernatant were removed and 500 μL of PBS (1X) was added to the cell pellet. Samples were illuminated with a UV laser at 355 nm on a Flowcytometry (BD LSRFortessa SORP cell analyser, performed at NCL Innovation Park, Pune). The data represented here is average of 2 repeats.

4.4.3.4. Confocal Image of HeLa cells with 27

HeLa cells were seeded at 0.5×10^5 cells/well in 4-well chamber for overnight in DMEM medium supplemented with 10% FBS and 1% antibiotic solution in an atmosphere of 5% CO_2 at 37 °C. After incubation, old media was removed and the cells were washed with 500 μL of PBS (1X) buffer. Then 500 μL of fresh DMEM media was added along with compound **27** (25 μM) and cells were incubated for 30 minutes at 37 °C. After 30 minutes, media was removed, cells were washed with 200 μL of PBS (1X). Then 500 μL of fresh DMEM media was added along with H_2O_2 (100 μM) and cells were incubated for 30 minutes. After 30 minutes, media was removed, cells were washed twice with 200 μL of PBS (1X) followed by cells were stained with LysoTracker for 5 min and imaged on a Zeiss LSM 710 confocal microscopy with 405 nm, 488 nm laser lines at 2% power using a 63X oil immersion objective (DAPI channel was used for **27** and LysoTracker Green DND-26 channel were used for LysoTracker). Images were analysed by ImageJ software. DAPI channel was used for **27** and pseudocolor (red) was given for the better visualisation.

4.4.3.5. Cell culturing and transfection

All cell lines were cultured in the modified Dulbecco's medium (DMEM) containing 3.7 g/l sodium bicarbonate, 110 mg sodium pyruvate, antibiotics (100 units/ml penicillin-

streptomycin) and 10% FBS. Cells were incubated at 37 °C in a humidified incubator in presence of 5% CO_2 and 20% oxygen for all experiments. For transfection, HeLa cells were seeded at density of 50,000 cells per 35 mm dish, and transfected using the Turbofect^{TM} Reagent (Thermofisher Inc., USA) as per the manufacturer's protocol.

4.4.3.6. Stable cell line generation

For shRNA knockdown (targeting catalase gene or the scrambled shRNA), plasmids encoding gene specific shRNAs from Broad Institute's TRC shRNA library (Sigma, USA) were used to generate the stable HeLa cell lines, which were selected on puromycin (3 µg/ml) for 48 hours before experiments.

4.4.3.7. Measurements of ROS with H_2DCFDA dye

ROS detection was performed using multimode fluorescence plate reader (Tecan, Austria). Briefly, the cells were washed with PBS (1X) and incubated with 10 µM H_2DCFDA (2′,7′-Dichlorofluorescin diacetate) for 30 minutes in dark. Subsequently the cells were washed and DCF (2′,7′-dichlorofluorescein) fluorescence was detected at excitation and emission wavelength as 495 nm and 525 nm respectively. The fluorescence value recorded was normalized to 10^3 cells.

4.4.3.8. Real-time quantitative PCR

Total RNA was isolated from treated and untreated cells using the RNA isolation Mini kit (RBC Bioscience Inc., UK). The cDNA was synthesized using random hexamers and RevertAid Reverse Transcriptase enzyme. Quantitative real time PCR was done using Power SYBR green master mix using Rotogene-Q real time cycler according to manufacturer's instructions. The β-actin expression was used as an internal control for expression normalization. Primers used for analysis are listed below.

Gene Name	
β -actin	Forward 5′CCAACCGCGAGAAGATGAC 3′
	Reverse 5′CAGAGGCGTACAGGGATAGC 3’
Catalase	Forward 5’ TGGGATCTCGTTGGAAATAACAC3’
	Reverse 5’ TCAGGACGTAGGCTCCAGAAG3’

4.4.3.9. Fluorescence response from 27 with WT and KD cells

2 x 10^4 cells were seeded in 24 well plate and incubated overnight. Cells were washed with PBS (1X) and treated with **27** (100 μM) in live cell imaging buffer at 37 °C for 30 minutes in dark. Subsequently the cells were washed with PBS (1X) and fluorescence was recorded using an excitation and emission wavelength of 315 nm and 460 nm respectively an Infinite M1000 PRO plate reader (Tecan, Austria). The data represented here is average of 3 repeats and statistical analysis was done using t-test.

4.4.4.0. Fluorescence imaging of 27 activated by endogenous H_2O_2

Four different cells, HeLa, A549, MRC5 and MDA-MB-231 were seeded at 1×10^5 in 35cm glass bottom dishes for overnight in DMEM media supplemented with 10% FBS and 1% antibiotic solution in an atmosphere of 5% CO_2 at 37 °C. After incubation, old media was removed and the cells were washed with 1 mL of PBS (1X) buffer. Then 1 mL of fresh DMEM media was added along with compound (25 μM) and cells were incubated for 6 h at 37 °C. After 6 h, old media was removed, cells were washed with 1 mL of PBS (1X) and 1 ml of live cell imaging solution (Invitrogen A14291DJ) was added and imaged using Olympus IX83 fluorescence microscope. And the image was analysed by slide book 6.0 software (Intelligent Imaging Innovations, Denver, CO).

4.4.4.1. 53BP1 (P53 Binding Protein 1) foci formation assay

HeLa cells stably expressing GFP-53BP1 were used for live cell imaging experiments.[19,20,22] The cells were treated with different concentrations of **27** for 6h while or before imaging. For imaging after the treatments, cells were seeded in glass bottomed dish and treated with indicated compounds and imaged in an IX83 inverted fluorescence microscope (Olympus) with Slidebook 6.0 software (intelligent Imaging Innovations, Denver, CO). Images were taken first in GFP channel and then in DAPI channel with fixed acquisition settings.

4.4.4.2. Cytotoxicity assay with normal vs cancer cells

Cytotoxicity assay was done using Alamar Blue cell viability assay, 2 x 10^4 cells were seeded in 24 well plate and incubated overnight. Cells were washed with PBS (1X) and treated with **27** (10 and 25 μM) in media and incubated at 37 °C for 12 hrours in dark. Subsequently the cells washed with PBS (1X) and Alamar Blue dye was added to each well as final concentration of 100 μM in media and incubated for 4 hours, Fluorescence was recorded using an excitation and emission wavelength of 590 nm and 600 nm respectively in an

Infinite M1000 PRO plate reader (Tecan, Austria). The data represented here is average of four repeats and statistical analysis was done using t-test.

4.5. Spectral charts

^{1}H-NMR Spectrum (400 MHz, $CDCl_3$) of Compound **27**

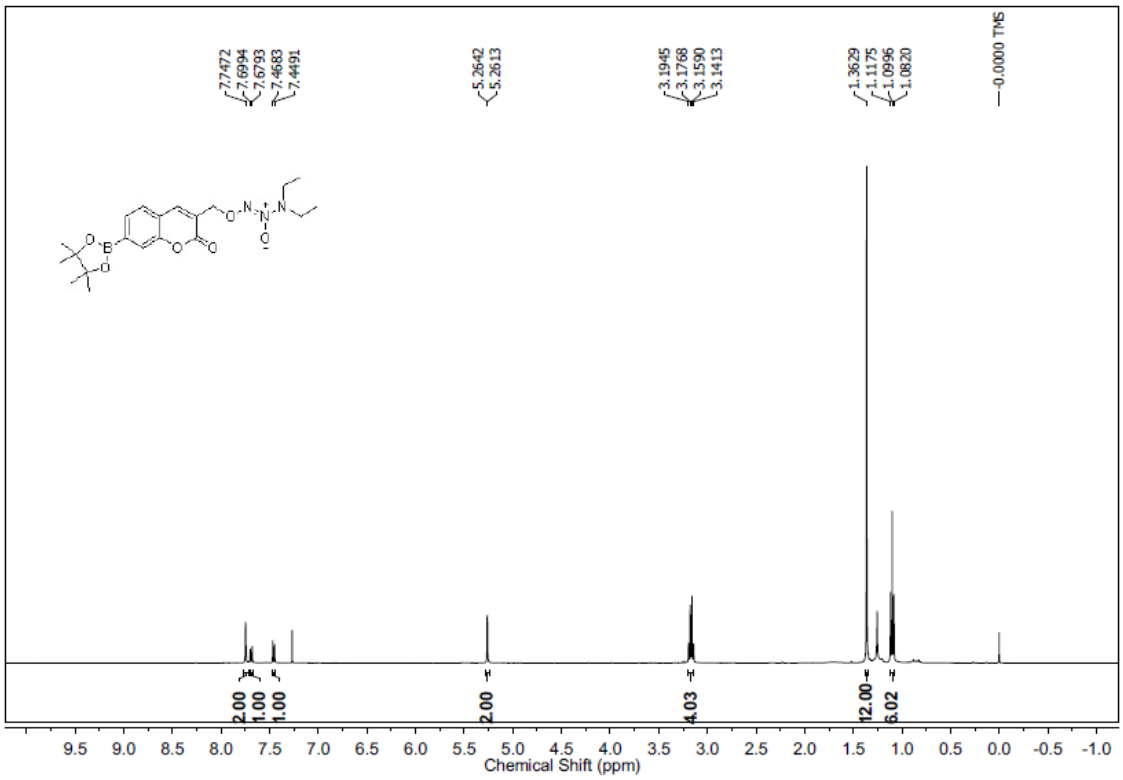

^{13}C NMR Spectrum (100 MHz, $CDCl_3$) of Compound **27**

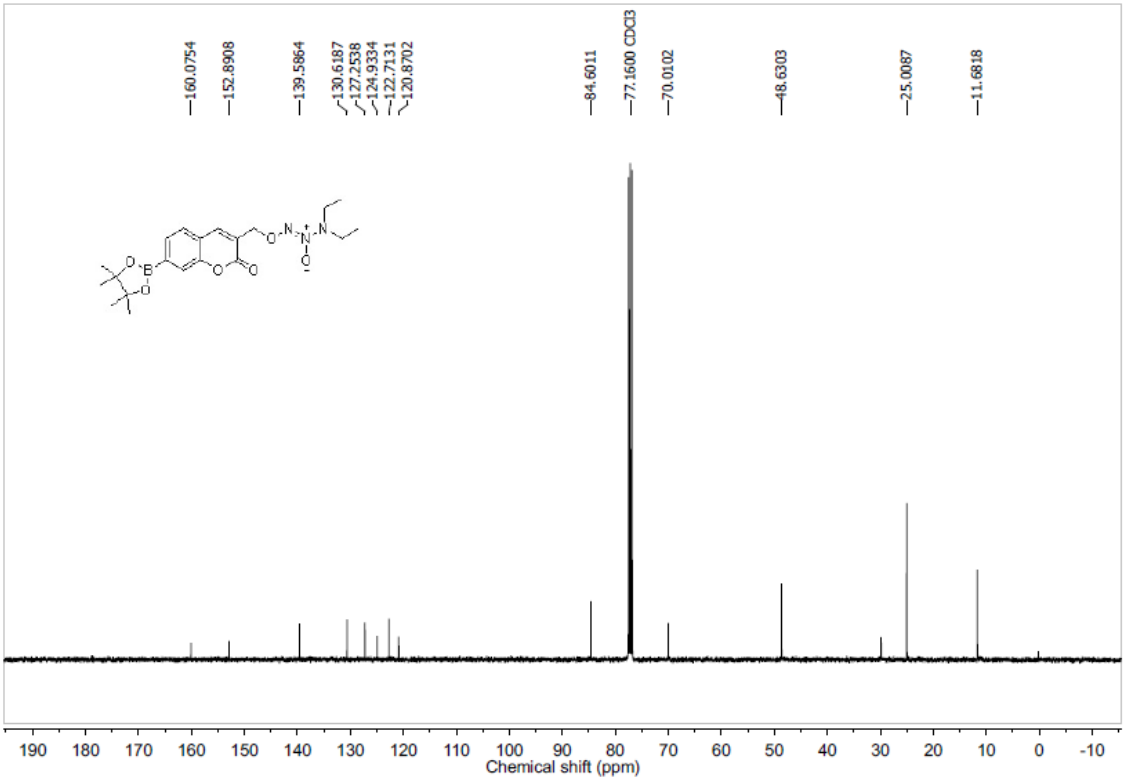

4.6. References

(1) Ravikumar, G.; Bagheri, M.; Saini, D. K.; Chakrapani, H. *ChemBioChem* **2017**, *18*, 1529.

(2) Szatrowski, T. P.; Nathan, C. F. *Cancer Res.* **1991**, *51*, 794.

(3) Antunes, F.; Cadenas, E. *FEBS Lett.* **2000**, *475*, 121.

(4) Trachootham, D.; Alexandre, J.; Huang, P. *Nat. Rev. Drug Discov.* **2009**, *8*, 579.

(5) Khandrika, L.; Kumar, B.; Koul, S.; Maroni, P.; Koul, H. K. *Cancer Lett.* **2009**, *282*, 125.

(6) Lim, S. D.; Sun, C.; Lambeth, J. D.; Marshall, F.; Amin, M.; Chung, L.; Petros, J. A.; Arnold, R. S. *Prostate* **2005**, *62*, 200.

(7) Kuang, Y.; Balakrishnan, K.; Gandhi, V.; Peng, X. *J. Am. Chem. Soc.* **2011**, *133*, 19278.

(8) Hagen, H.; Marzenell, P.; Jentzsch, E.; Wenz, F.; Veldwijk, M. R.; Mokhir, A. *J. Med. Chem.* **2012**, *55*, 924.

(9) Kim, E.-J.; Bhuniya, S.; Lee, H.; Kim, H. M.; Cheong, C.; Maiti, S.; Hong, K. S.; Kim, J. S. *J. Am. Chem. Soc.* **2014**, *136*, 13888.

(10) Dickinson, B. C.; Chang, C. J. *J. Am. Chem. Soc.* **2008**, *130*, 9638.

(11) Chen, W.; Balakrishnan, K.; Kuang, Y.; Han, Y.; Fu, M.; Gandhi, V.; Peng, X. *J. Med. Chem.* **2014**, *57*, 4498.

(12) Leonetti, F.; Favia, A.; Rao, A.; Aliano, R.; Paluszcak, A.; Hartmann, R. W.; Carotti, A. *J. Med. Chem.* **2004**, *47*, 6792.

(13) Khodade, V. S.; Kulkarni, A.; Gupta, A. S.; Sengupta, K.; Chakrapani, H. *Org. Lett.* **2016**, *18*, 1274.

(14) Dharmaraja, A. T.; Ravikumar, G.; Chakrapani, H. *Org. Lett.* **2014**, *16*, 2610.

(15) Steffen, D.; Viktor, R. M. S.; Miroslav, S.; Tetyana, D.; D., L. M.; Rostyslav, B.; Evgenia, B.; Christina, J.; Christoph, A.; Martin, H.; Leopold, S.; Andriy, M. *Angew. Chem. Int. Ed.* **2017**, *56*, 15545.

(16) A., T.; T., K.; B., G.; T., B. U. *IUBMB Life* **2006**, *58*, 531.

(17) Imlay, J. A. *Annu. Rev. Biochem.* **2008**, *77*, 755.

(18) Kiziltepe, T.; Hideshima, T.; Ishitsuka, K.; Ocio, E. M.; Raje, N.; Catley, L.; Li, C.-Q.; Trudel, L. J.; Yasui, H.; Vallet, S.; Kutok, J. L.; Chauhan, D.; Mitsiades, C.

S.; Saavedra, J. E.; Wogan, G. N.; Keefer, L. K.; Shami, P. J.; Anderson, K. C. *Blood* **2007**, *110*, 709.

(19) Zgheib, O.; Pataky, K.; Brugger, J.; Halazonetis, T. D. *Mol. Cell. Biol.* **2009**, *29*, 1050.

(20) Bagheri, M.; Nair, R. R.; Singh, K. K.; Saini, D. K. *Biochim. Biophys. Acta Mol. cell Res.* **2017**, *1864*, 177.

(21) Weinstain, R.; Segal, E.; Satchi-Fainaro, R.; Shabat, D. *Chem. Commun.* **2010**, *46*, 553.

(22) Nair, R. R.; Bagheri, M.; Saini, D. K. *J. Cell Sci.* **2015**, *128*, 342.

CHAPTER 5: Esterase Sensitive ROS Generator with a Fluorescence Reporter

5.1. Introduction

In addition to NO, a number of other redox active reactive species have important biological roles. Controlled generation as well as reliable detection of these species is challenging. In order to assess the generality of the method developed herein, we aimed to develop a ROS generator with a fluorescence reporter. Due to the short half-life of reactive oxygen species (ROS) such as a superoxide radical, controlled and localized generation of ROS is challenging. Previously, our lab designed and synthesised a series of 1, 4-naphthoquines derivatives, from the library, compound **28** was identified as an efficient ROS generator in buffer as well as cells. This compound undergoes a keto-enol tautomerism to react with molecular oxygen to produce ROS such as superoxide, H_2O_2 and OH radical mediated by Fe^{2+} (Scheme 5.1).[1-4]

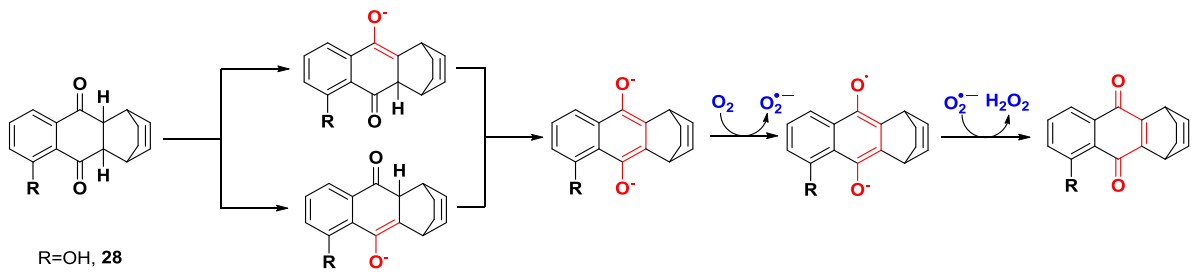

Scheme 5.1. Proposed mechanism for generation of ROS during incubation of 2,3-dihydro-1,4-benzoquinones in pH 7.4 buffer.

Mycobacterium tuberculosis (*Mtb)*, is one of the highly challenging pathogens to treat. Due to its thick waxy cell wall, many of the drug candidates have compromised cell permeability in *Mtb*. Since, *Mtb* has been shown to be sensitive to ROS. Compound **28** was able to generate extracellular and intracellular ROS in *Mtb*. It was found to be a highly potent compound against *Mtb* (MIC 0.76 µg/mL).[1,5] Although compound **28** could enhance the level of intracellular ROS in bacteria an extracellular decomposition of **28** to generate ROS is unavoidable. Furthermore, with this compound controlled and localized generation of ROS is not possible.

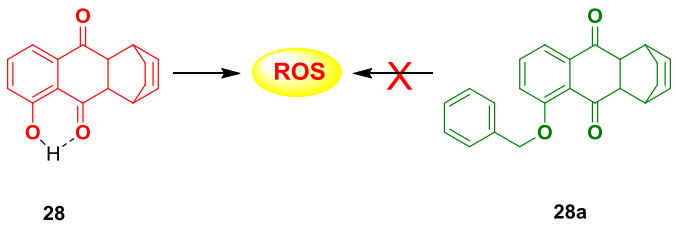

Scheme 5.2. Capability of ROS generation by **28** and **28a**

When the hydroxyl group of **28** was protected with benzyl group (**28a**), no ROS generation was observed under similar condition (Scheme 5.2), which suggests that, the hydroxyl group of **28** is crucial for ROS generation.[1] Recently, protection of 5-OH group of **28** with a self-immolative linker attached with a substrate for an enzyme that is expressed intracellularly, was designed for selective enhancement of intrabacterial ROS (Scheme 5.3).[6] Here, hydroxyl group of **28** was protected with 4-nitro benzyl group and this group is a known substrate for *E. coli* nitroreductase (NTR), a commonly expressed oxygen-insensitive bacterial enzyme that reduces a broad range of aromatic nitro compounds to amines. This compound is stable in buffer and generates ROS only in the presence of NTR.

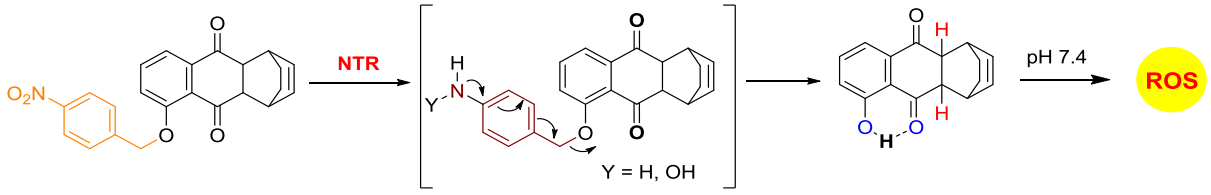

Scheme 5.3. Design of NTR activated ROS donor

Due to the short half-life of reactive oxygen species (ROS) such as a superoxide radical, controlled and localized generation of ROS is challenging, furthermore in order to infer the production of ROS from these donors, several independent secondary assays are required. For this purpose number of fluorescence probes have been reported and used.[7,8] The secondary dyes are typically destructive in nature and further cellular experiments are typically not possible. It is therefore necessary to develop a reporter linked ROS generator, which would report ROS release immediately without the need for secondary assays for detection.

As a proof of concept, first we have designed an esterase activated ROS donor without fluorescence reporter and studied first. Upon activation of **29** by esterase, self-immolation occurs and produces **28**, which dissociates at pH 7.4 to produce superoxide (Scheme 5.4).

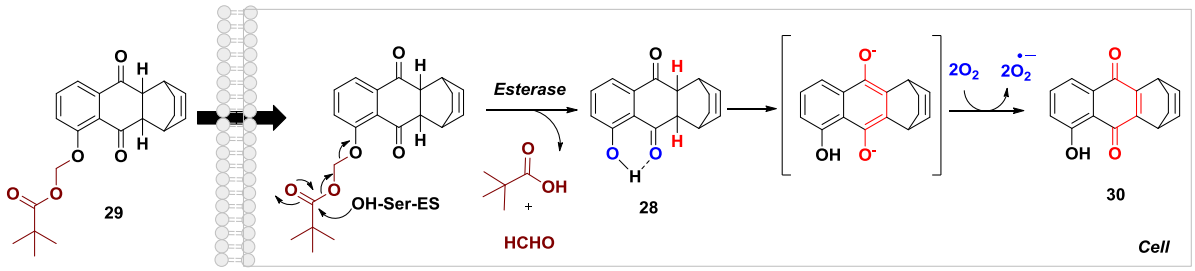

Scheme 5.4. Proposed mechanism for esterase activated ROS generation from **29**

5.2. Results and Discussion

5.2.1. Synthesis

In order to test this hypothesis, esterase activated ROS donor **29** was synthesized. Compound **2** and **28** were synthesized using previously reported methodology.[1,6] Reaction of **28** with **2** in the presence of Ag_2O produced desired compound **29**, in 19% yield (Scheme 5.5).

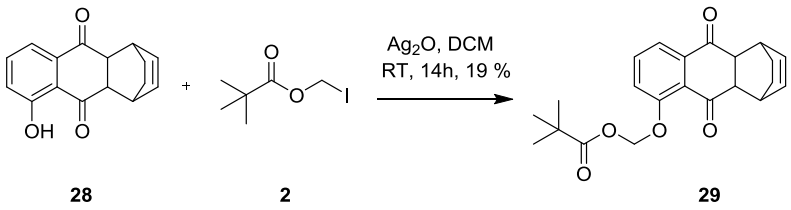

Scheme 5.5. Synthesis of ROS donor (**29**)

In addition compound **31** was synthesized as a negative control compound for ROS generation. Treatment of **1-Naphthol** with **2** afforded **31** in 93% yield (Scheme 5.6).

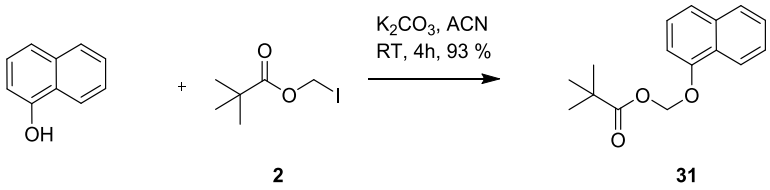

Scheme 5.6. Synthesis of control compound **31**

5.2.2. Activation of 29 and 31 by esterase

First, the conversion of **29** to active ROS donor (**28)** by esterase was monitored using HPLC analysis. Compound **29** was incubated with esterase for 30 min in pH 7.4 buffer at 37 °C, and an aliquot was injected into HPLC, nearly complete disappearance of the peak for **29** was observed with concomitant formation of a new peak for **28** (Figure 5.1). Compound **28** and **29** was used as an authentic material to verify the release of **28** from **29** by esterase. When similar experiment was performed with **31** (Figure 5.2), decomposition of **31** by esterase and formation of new peak attributable to 1-Naphthol was observed (Figure 5.2). These

experiments suggest that, upon esterase activity, **29** and **31** produced **28**, and 1-naphthol respectively.

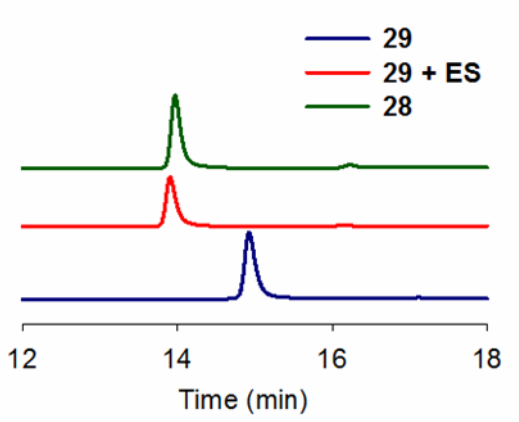

Figure 5.1. The decomposition of **29** (100 µM, red trace) in the presence of esterase (0.5 U/mL) in pH 7.4 phosphate buffer at 37 °C was assessed by HPLC analysis. **28** (100 µM, green trace) and **29** (100 µM, blue trace) were used as an authentic standards to verify the release of **28** from **29**. All absorbance was monitored at 315 nm. The HPLC analysis was done in triplicates with reproducible results.

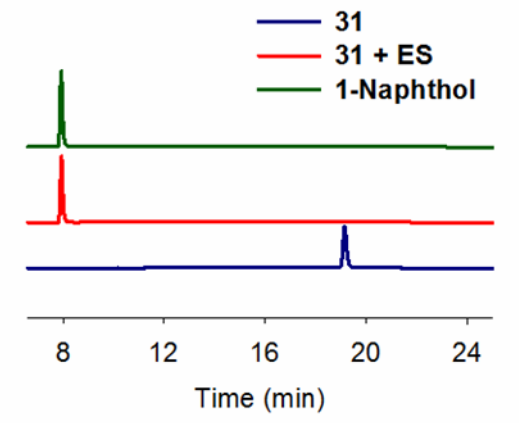

Figure 5.2. The decomposition of **31** (100 µM, red trace) in the presence of esterase (0.5 U/mL) in pH 7.4 phosphate buffer at 37 °C was assessed by HPLC analysis. 1-naphthol (100 µM, green trace) and **31** (100 µM, blue trace) were used as an authentic standards to verify the release of 1-naphthol from **31**. All absorbance was monitored at 280 nm. The HPLC analysis was done in triplicates with reproducible results.

5.2.3. ROS generation studies in buffer

Due to short half-life of ROS under physiological conditions, multiple assays were conducted to conform the ROS generation from the ROS donors. For example, i) a luminol-based chemiluminescence assay[9] and HPLC based dihydroethidium (DHE) assay[10,11] were used to conform the superoxide generation in buffer, ii) H_2DCF-DA assay was used to conform the ROS generation in cells.

5.2.3.1. Luminol assay for superoxide generation in buffer

The ability of **29** to generate superoxide was tested using a luminol based chemiluminescence assay.[9] In this assay, the reaction of luminol with superoxide leads to nitrogen extrusion and simultaneous formation of excited state species of 3-aminobenzene-1,2-dicarboxylate (Scheme 5.7). Returning of the excited state species to ground state emits light (luminescence) and the emission is recorded as a measure of superoxide generated during the reaction. Compound **29** was incubated with luminol in phosphate buffer (50 mM, pH 8.0), no evidence for superoxide generation was found. Whereas in the presence of esterase a chemiluminescence signal for superoxide was observed (Figure 5.3) and the superoxide generation from **29** was comparable to the authentic ROS donor **28**. When, a similar experiment was conducted with control compound **31**, which is a substrate for esterase, which should not produce ROS, as expected no signal was observed (Figure 5.3).

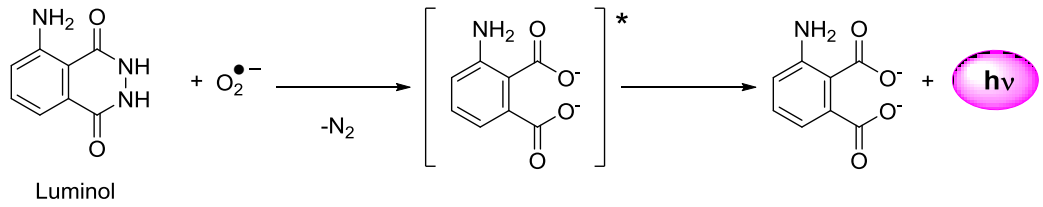

Scheme 5.7. Reaction of luminol with superoxide radical ($O_2^{\bullet-}$)

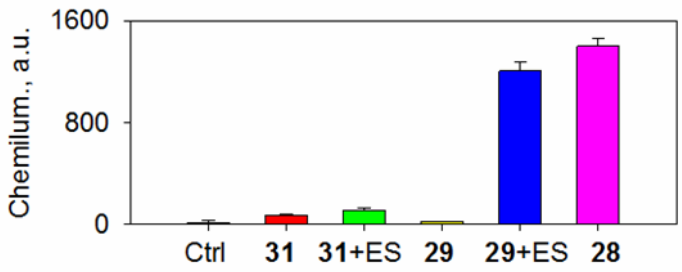

Figure 5.3. Superoxide generated during incubation of **ROS donors** (25 µM) in pH 8.0 buffer at 37 ºC for 30 min was estimated by a luminol-based chemiluminescence assay. Ctrl: only luminol in buffer; ES: Esterase (1U/mL).

Next, **29** was incubated in buffer and co-treated with esterase and superoxide dismutase (SOD, an enzyme that converts superoxide into H_2O_2), the signal for superoxide is nearly completely disappeared (Figure 5.4). Similarly in the presence of esterase inhibitor, fluorophosphonate-alkyne (FPA, a broad spectrum SH inhibitor), again reduction in the signal was observed (Figure 5.4). Together, these experiments suggest that, both ester functional group and ROS donating molecule **28** were required for the ROS generation.

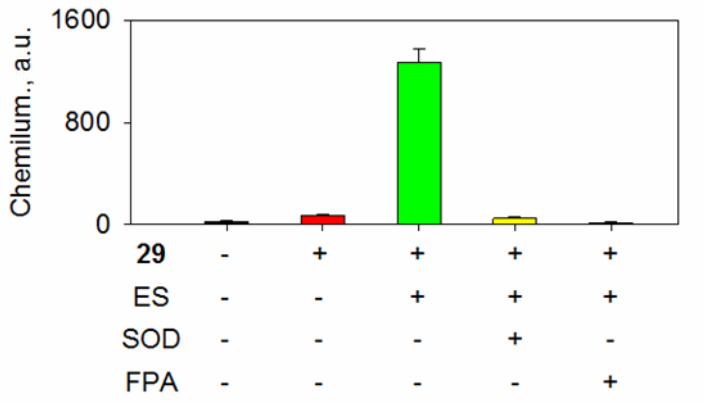

Figure 5.4. Superoxide generated during incubation of **ROS donors** (25 µM) in pH 8.0 buffer at 37 ºC for 30 min was estimated by a luminol-based chemiluminescence assay. ES: esterase (1U/mL); SOD: superoxide dismutase (2U/mL); FPA: fluorophosphonate-alkyne (25 µM, 30 min pre-treated with esterase).

Next, a similar experiment was conducted with **29** and compared with a known xenobiotics (e.g. artemisinin, cisplatin, menadione) and ROS generators (**30**) in buffer, we found **29** was the best ROS generator compared to the xenobiotics or ROS producers (Figure 5.5).

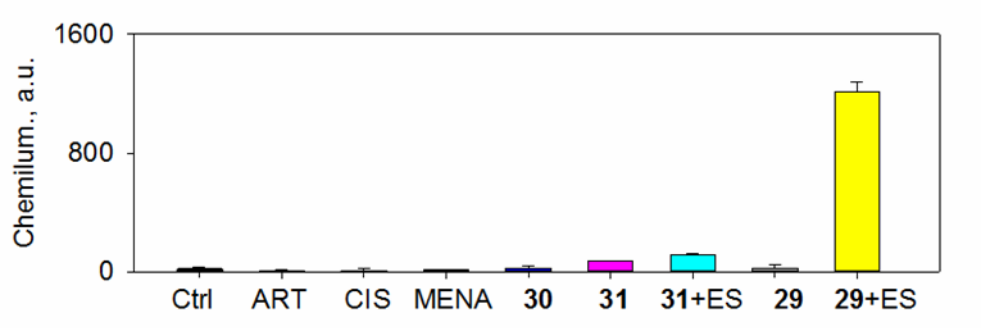

Figure 5.5. Superoxide generated during incubation of ROS donors (25 µM) in pH 8.0 buffer at 37 ºC for 60 min was estimated by a luminol-based chemiluminescence assay. Ctrl: only luminol in buffer; ES: esterase (1U/mL); ART: artemisinin; CIS: cisplatin; MENA: menadione (2-Methyl-1,4-naphthoquinone).

5.2.3.2. DHE assay for superoxide generation in buffer

Next, a HPLC-based dihydroethidium (DHE) assay was used to infer the superoxide generation independently. In this assay, $O_2^{\bullet-}$ specifically reacts with DHE to produce 2-hydroxyethidium (2-OH-E^+). DHE also reacts non-specifically with other ROS and forms ethidium (E^+) dye (Scheme 5.8).[10,11] Both of these oxidized products can be detected using HPLC attached with a fluorescence detector. This fluorescence based HPLC method is widely used for the detection of superoxide as well as other oxidative species generation.

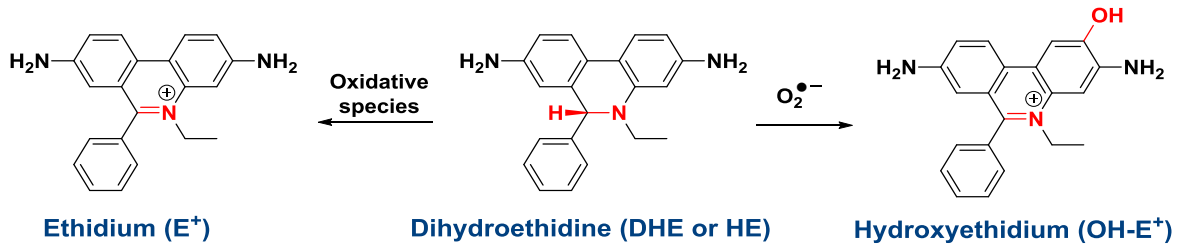

Scheme 5.8. A scheme for formation of 2-OH-E^+ and E^+ during reaction of DHE with ROS

An authentic sample of DHE (50 μM) in buffer was injected into HPLC and we observed a peak at 20.7 min corresponding to DHE (Figure 5.6). When compound **29** (25 μM) was incubated with DHE under comparable conditions, chromatogram indicated superoxide and ROS were not generated in the absence of esterase. However, when **29** and DHE were incubated with esterase (1 U/mL) in pH 8.0 phosphate buffer (50 mM), a new peak at 29.9 min corresponding to 2-OH-E^+ was observed indicating the superoxide is a major product formed under these conditions, and a small peak at 30.2 min was identified as E^+ as an evidence for the formation of other oxidative species in minor proportions (Figure 5.6). The signal at 29.9 min corresponding to 2-OH-E^+ was nearly completely disappeared when the reaction mixture was co-treated with superoxide dismutase (SOD). Compound **28** was used as a positive control for this assay (Figure 5.6). Together, these experiments confirmed the superoxide generation from **29** under physiological conditions.

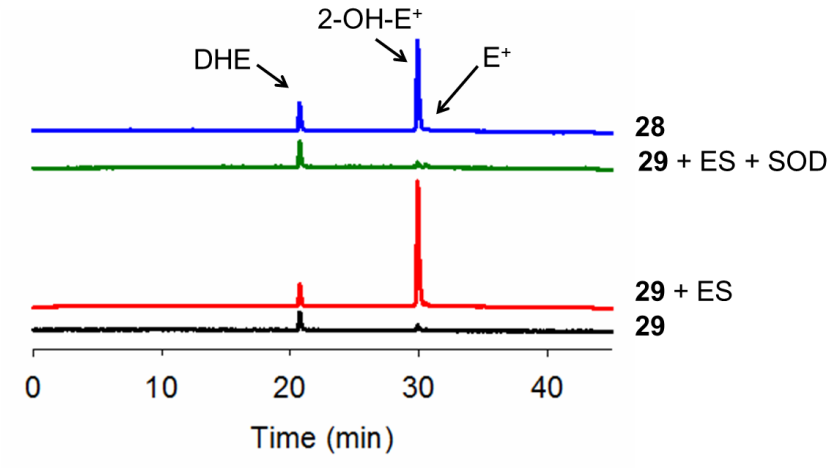

Figure 5.6. A high performance liquid chromatograph (HPLC)-based dihydroethidium (DHE) assay was used to infer the generation of superoxide after incubation of compounds (25 μM) in pH 8.0 buffer for 2 h. ES: esterase (1 U/mL).

Next, using the coumarin-based strategy, an esterase sensitive ROS donor with a fluorescence reporter **32** was designed (Scheme 5.9). Here, **32** is expected to permeate cells to be cleaved by esterases to produce the highly fluorescent **12** and the ROS releasing **28**. Using the turn on fluorescence signal we can real-time monitor the ROS release without any secondary assays.

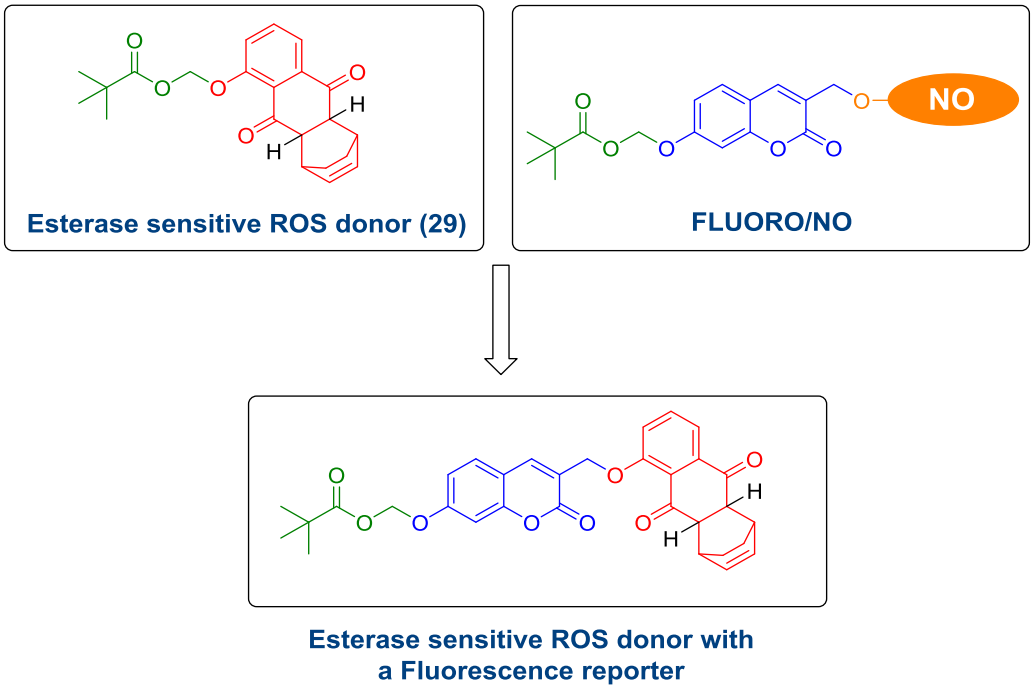

Scheme 5.9. Proposed model for the real-time monitoring of ROS generation in cells

The proposed mechanism of activation of the reporter probe, **32** is as follows. Upon activation of **32** by esterase, self-immolation and reaction with water produces **12** and **28**, which dissociates at pH 7.4 to produce ROS (Scheme 5.10).

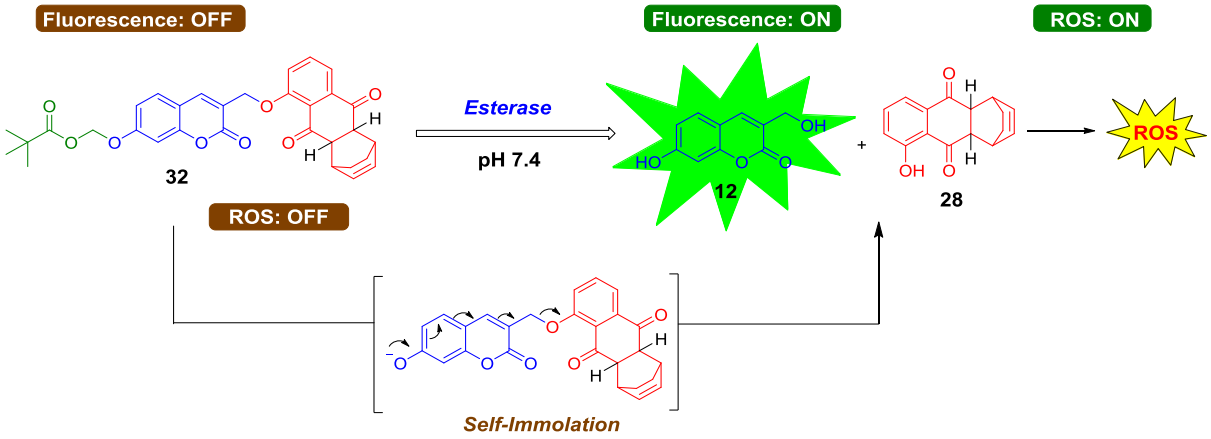

Scheme 5.10. Proposed mechanism of activation of **32** to produce **12** and **ROS**

In order to test this hypothesis, **32** was synthesized. Compound **4** and **28** were synthesized using previously reported methodology. Reaction of **28** with **4** in the presence of Ag_2O produced desired compound **32** (Scheme 5.11).

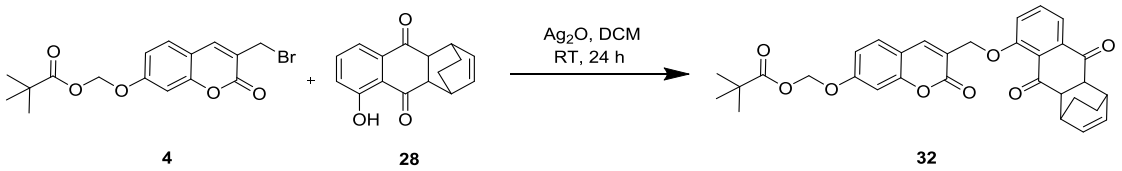

Scheme 5.11. Synthesis of compound **32**

5.2.4. ROS generation and fluorescence emission in Buffer

Next, the ability of the compound **32** to generate ROS and fluorescence signal in phosphate buffer was evaluated. Compound **32** was treated with esterase and the fluorescence signal attributable to **12** as well as ROS was independently monitored. The fluorescence signal at 460 nm was measured using a micro-well plate reader while ROS generation was measured by luminol assay. In the presence of esterase, a gradual increase in fluorescence signal attributable to **12** was observed during 60 min (Figure 5.7.a). However under similar conditions, there is no significant fluorescence signal was seen from **32** in the absence of esterase. Similarly, when ROS was monitored, we found that the compound generated ROS only in the presence of esterase (Figure 5.7.b).

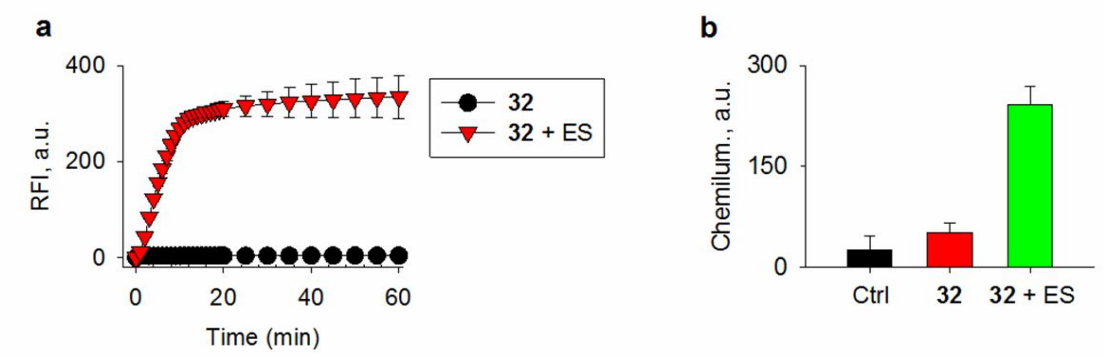

Figure 5.7. (a) Fluorescence response of **32** (25 µM) in the absence and presence of ES (0.5 U/mL) in pH 7.4 buffer. (b) Superoxide generation from **32** (25 µM) in pH 8.0 buffer at 37 ºC after 60 min was estimated by a luminol-based chemiluminescence assay.

5.2.5. ROS enhancement and fluorescence emission in cells

In order to study the capability of compound **32** to enhance fluorescence signal as well as ROS within the cells, A549 cells were treated with 25 µM of compounds (**4**, **32**, and **29**). After 30 min, the fluorescence signal at 460 nm was measured using a micro-well plate reader, while ROS enhancement was measured by 2,7-dichlorodihydrofluorescein-diacetate (H_2DCF-DA)-based fluorescence assay. H_2DCF-DA is a weakly fluorescent cell permeable dye, which reacts efficiently with hydroxyl radical and to some extent with H_2O_2, and the fluorescence turns on when H_2DCF-DA is oxidized by these ROS (Scheme 5.12).[7,12]

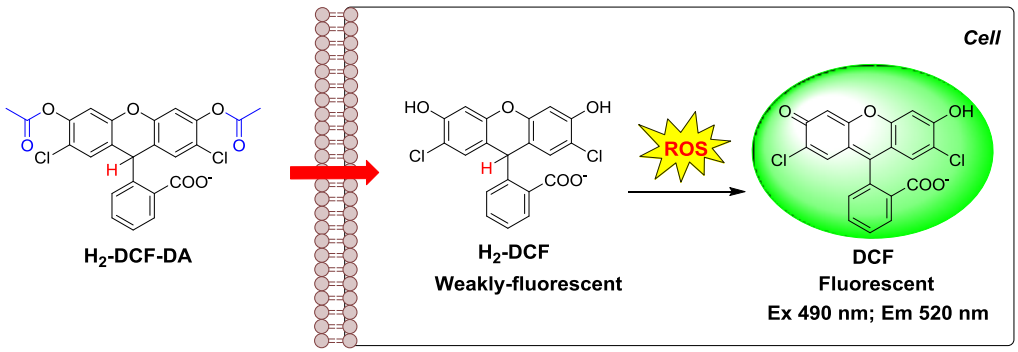

Scheme 5.12. Oxidation of non-fluorescent H_2DCF-DA by ROS to fluorescent dye, DCF

With a control compound **4** (does not contain diazeniumdiolate), an increase in the fluorescence signal was seen but no significant ROS enhancement (Figure 5.8.a, 5.8.b); and with a control compound **29** (does not contain coumarin), an increase in ROS was observed with no significant fluorescence signal (Figure 5.8.a, 5.8.b). Whereas, compound **32** is able to enhance both fluorescence signal as well as ROS was observed (Figure 5.8.a, 5.8.b). When

the incubation time and dose of **32** was varied, as expected, a dose-dependent increase in fluorescence signal was observed (Figure 5.8.c), thus supporting the suitability of **32** to enhance ROS as well as fluorescence within cells. Thus, when cells are treated with **32** and the fluorescence signal at 460 nm is a reporter for ROS generated.

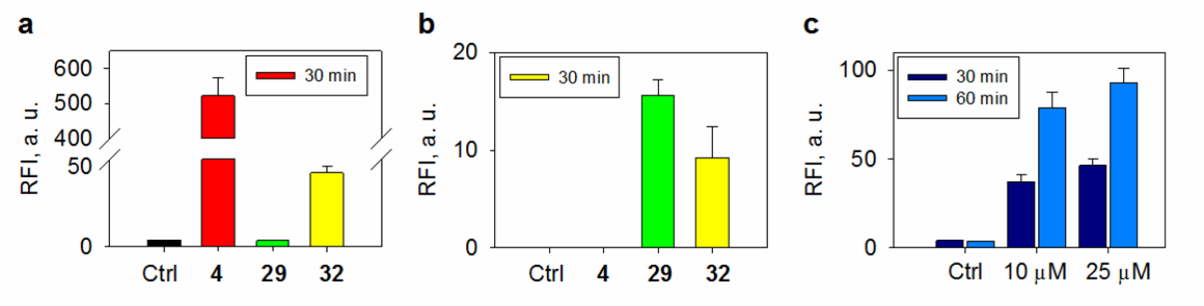

Figure 5.8. Comparison of fluorescence intensity attributable to **12** (a) and (b) ROS generation upon incubation of A549 cells with 25 μM of **4**, **29** or **32**. (c) Fluorescence intensity attributable to **12** during incubation of A549 cells with **32** at 0, 10 and 25 μM with different time at 37 °C (excitation 320 nm; emission 460 nm). Intracellular ROS enhancement was measured using a $DCFH_2$-DA assay (excitation 490 nm; emission 520 nm).

5.2.6. Cellular uptake of 32

In order to study the cellular uptake of **32**, A549 cells were treated with **32** for 60 min and the fluorescence signal attributable to the formation of **12** at 460 nm was monitored by confocal microscopy. An increase in fluorescence signal was observed (Figure 5.9). The fluorescence signal was nearly uniformly distributed within cells, possibly due to the ubiquitous nature of esterase. These results supporting that, the compound **32** permeate cells and get activated by cellular esterase to produce fluorescence signal attributable to **12**.

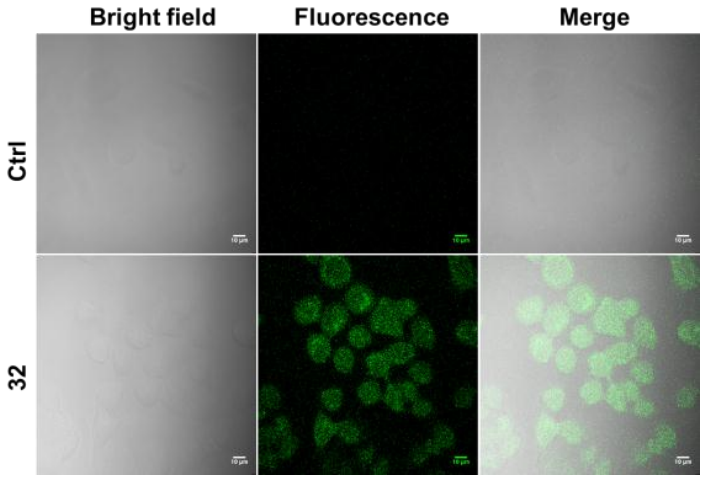

Figure 5.9. Confocal microscopy images of A549 cells treated with **32** (25 μM) for 60 min at 37 °C. Images were taken using DAPI channel and pseudocolored (green) for better visualisation. Scale bar = 10 μm.

5.2.7. Intracellular generation of ROS

Next, we investigated the capability of **32** to produce ROS in cells was evaluated using DCF assay. A549 lung carcinoma cells were treated with **32** (25 μM) for 1h and followed by cells were stained with H_2DCF-DA dye (10 μM) for 10 min and the fluorescence signal attributable to DCF was monitored in GFP channel. In this assay, Compound **4** was used as negative control and **29** was used as positive control for ROS generation. As expected we found increase in the DCF fluorescence signal for compound **29** and **32** (Figure 5.10). Together these results provide the evidence for the ability of **32** to enhance ROS in cells.

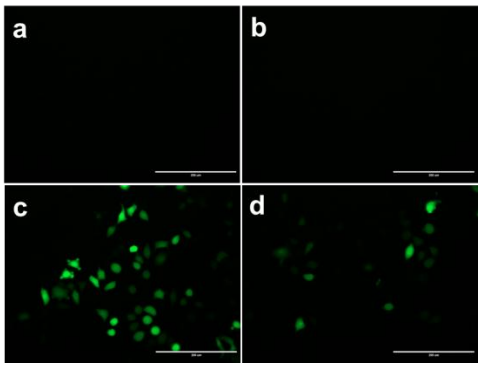

Figure 5.10. Fluorescence microscopy images of A549 cells treated with a) H_2DCF-DA dye alone (10 μM) b) **4** (25 μM) c) **29** (25 μM) d) **32** (25 μM) for 60 min at 37 °C. Images were taken using GFP channel. Scale bar = 200 μm.

5.3. Summary

The method developed for real-time monitoring of NO could be extended to ROS as well. As a prototype, **32** was synthesised and in the presnce of esterase, an increase in fluorescence as well as ROS was observed. Using independent assays, the cell permiability and ROS genrating capability was demonstrated. Further modification of the trigger can facilitate directed delivery of ROS.

5.4. Experimental Section

5.4.1. Synthesis and characterization

Compounds **2**[13], **4**[14] and **28**[1] were synthesized using previously reported procedures, and the analytical data that we collected were consistent with the reported values.

((9,10-dioxo-1,4,4a,9,9a,10-hexahydro-1,4-ethanoanthracen-5-yl)oxy)methyl pivalate (29):

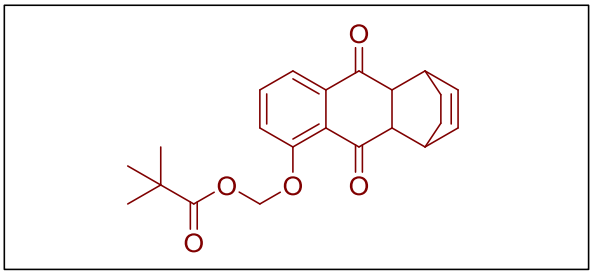

To a solution of **2** (88 µL, 0.59 mmol) in dry DCM (5 mL), **28** (100 mg, 0.39 mmol) and Ag_2O (273 mg, 1.18 mmol) was added. The reaction mixture was stirred for 14 h under nitrogen atmosphere. The solvent was removed under reduced pressure. This crude was initially purified by silica gel column chromatography using EtOAc/pet ether (0 → 40 %) as the eluent. The resulting mixture was further purified using preparative HPLC with C-18 preparative column (21.2 mm × 250 mm, 10 µm; Kromasil C18), using a gradient of ACN and water (60 – 80 %), under ambient temperature with a flow rate of 20 mL/min to obtain **29** (27 mg, 19%) as a yellow solid; FT-IR (ν_{max}, cm^{-1}): 2966, 1747, 1687, 1588, 1467; ^{1}H NMR ($CDCl_3$, 400 MHz): δ 7.65 (dd, *J* = 7.8, 1.2 Hz, 1H), 7.58 (t, *J* = 7.9 Hz, 1H), 7.33 (dd, *J* = 8.2, 1.1 Hz, 1H), 6.21-6.10 (m, 2H), 5.80 (dd, *J* = 18.2, 6.4 Hz, 2H), 3.31 (d, *J* = 4.7 Hz, 2H), 3.26-3.20 (m, 2H), 1.71 (d, *J* = 8.4 Hz, 2H), 1.39 (d, *J* = 8.5 Hz, 2H), 1.21 (s, 9H); ^{13}C NMR ($CDCl_3$, 100 MHz): δ 197.7, 196.0, 177.2, 155.5, 138.6, 134.3, 134.1, 133.5, 127.6, 123.0, 121.6, 87.4, 52.2, 51.1, 39.0, 34.4, 33.7, 27.0, 24.8, 24.7; HRMS (ESI) for $C_{22}H_{24}O_5$ $[M+Na]^+$: Calcd., 391.1521, Found, 391.1523.

(naphthalen-1-yloxy)methyl pivalate (31):

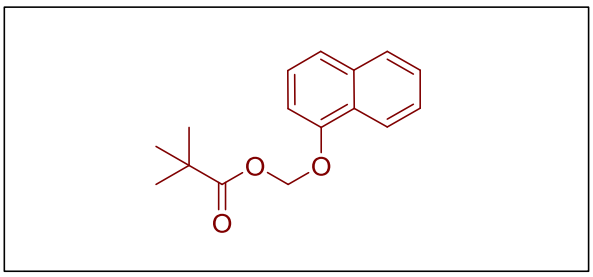

To a solution of **1-Naphthol** (200 mg, 1.39 mmol) in ACN (5 mL), K_2CO_3 (575 mg, 4.16 mmol) was added followed by a solution of **2** (312 µL, 2.08 mmol) in ACN (1mL). The reaction mixture was stirred for 4 h under nitrogen atmosphere at room temperature. Upon completion of reaction (TLC analysis), the solvent was evaporated under reduced pressure, diluted with 10 mL of water and the aqueous solution was extracted with EtOAc (3×5 mL). The combined organic layer was washed with brine, dried over Na_2SO_4 (5 g), filtered and the filtrate was concentrated to

give a crude compound. The residue was purified by silica gel column chromatography using EtOAc/pet ether (0 → 10 %) as the eluent to obtain **31** (332 mg, 93 %) as a yellowish oil; FT-IR (ν_{max}, cm^{-1}): 2972, 1746, 1584, 1469; ^1H NMR ($CDCl_3$, 400 MHz): δ 8.26-8.24 (m, 1H), 7.83-7.81 (m, 1H), 7.55 (d, *J* = 8.3 Hz, 1H), 7.53-7.47 (m, 2H) 7.40 (t, *J* = 8.0 Hz, 1H), 7.09 (d, *J* = 7.7 Hz, 1H), 5.99 (s, 2H), 1.21 (s, 9H); ^{13}C NMR ($CDCl_3$, 100 MHz): δ 177.6, 153.0, 134.7, 127.6, 126.7, 126.0, 125.8, 125.7, 122.5, 122.2, 108.1, 86.3, 39.1, 27.1; HRMS (ESI) for $C_{16}H_{18}O_3$ $[M+Na]^+$: Calcd., 281.1153, Found, 281.1147.

((3-(((9,10-dioxo-1,4,4a,9,9a,10-hexahydro-1,4-ethanoanthracen-5-yl)oxy)methyl)-2-oxo-2H-chromen-7-yl)oxy)methyl pivalate (32):

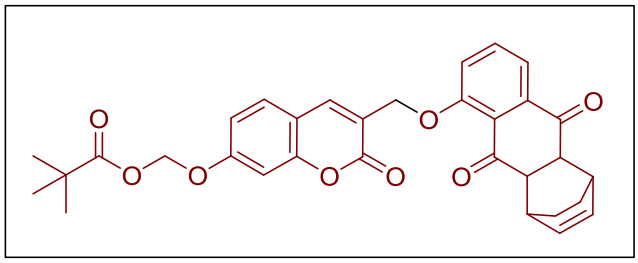

To a solution of compound **4** (200 mg, 0.54 mmol) in dry DCM (10 mL), **28** (275 mg, 1.08 mmol) and Ag_2O (377 mg, 1.62 mmol) was added. The reaction mixture was stirred for 48 h under a nitrogen atmosphere. The solvent was removed under reduced pressure. Then the residue was purified by column chromatography using EtOAc/Pet ether (0 → 30 %) as the eluent to obtain **32** (22 mg, 7 %) as a yellow solid: mp 124 – 126 °C; FT-IR (ν_{max}, cm^{-1}): 1720, 1681, 1617, 1586; ^1H NMR ($CDCl_3$, 400 MHz): δ 8.34 (s, 1H), 7.69-7.57 (m, 3H), 7.31 (dd, *J* = 8.0, 1.3 Hz, 1H), 7.05 (d, *J* = 2.3 Hz, 1H), 7.01, (dd, *J* = 8.6, 2.4 Hz, 1H), 6.23-6.14 (m, 2H), 5.83 (s, 2H), 5.07 (s, 2H), 3.38-3.33 (m, 2H), 3.25 (s, 2H), 1.79-1.71 (m, 2H), 1.46-1.38 (m, 2H), 1.22 (s, 9H) ; ^{13}C NMR ($CDCl_3$, 100 MHz): δ 198.0, 196.4, 177.2, 160.5, 159.7, 156.9, 154.6, 139.9, 138.8, 134.8, 134.1, 133.8, 129.8, 125.7, 121.5, 119.6, 118.2, 114.5, 113.9, 103.3, 85.1, 65.7, 52.3, 51.0, 39.1, 34.6, 34.1, 27.1, 24.9, 24.7; HRMS (ESI) for $C_{32}H_{30}O_8$ $[M+H]^+$: Calcd., 543.2019, Found., 543.2015.

5.4.2. HPLC decomposition study

A 10 mM stock solution of compounds (**28**, **29**, **31** and **1-Naphthol**) in DMSO and 1U/mL stock solution of porcine liver esterase enzyme (Sigma Aldrich) in phosphate buffer pH 7.4 were prepared. In the control experiment, 5 µL of respective compound (**28** or **29** or **31** or **1-Naphthol**, 100 µM) was added to 495 µL of phosphate buffer pH 7.4 (10 mM). In another set serving as esterase activated set 5 µL of **29** or **31** (100 µM), 250 µL of esterase (0.5 U/ mL) was added to 245 µL of phosphate buffer pH 7.4 (10 mM) at 37 ºC. After 30 min, the reaction mixture was filtered (0.22 µm) and injected (50 µL) in an Agilent high performance liquid chromatography (HPLC) attached with a diode-array detector (detection wavelength was 315

nm for **29** and 280 nm for **31**) and C-18 reversed phase column (4.6 mm × 250 mm, 5 µm). A mobile phase of water: ACN was used with a run time of 25 min: multistep gradient technology with a flow rate of 1 mL/min – starting with 70:30 % → 0 min, 50:50 % → 0-5 min, 40:60 % → 5-7 min, 30:70 % → 7-10 min, 20:80 % → 10-15 min, 40:60 % → 15-18 min, 60:40 % → 18-20 min, 70:30 % → 20-25 min (H_2O: ACN).

5.4.3. Generation of Reactive Oxygen Species from compounds in buffer

5.4.3.1. Superoxide estimation by Luminol assay

A luminol stock solution (4 mM) was prepared by dissolving 7.1 mg of luminol in 10 mL of 30 mM sodium hydroxide solution and stored under ice. 2.5 mM stock solutions of compounds were prepared in DMSO. In the control experiment, 2.0 µL of compound (25 µM), 5 µL of luminol was added to 193 µL of phosphate buffer pH 8.0 (50 mM). In another set serving as esterase activated set 2.0 µL of compound (25 µM), 5 µL of luminol and 2 µL of esterase (1U/ mL) was added to 191 µL of phosphate buffer pH 8.0 (50 mM). In an esterase inhibition experiment, FPA (25 µM) was pretreated with esterase for 30 min. For the experiment with superoxide dismutase (SOD from bovine erythrocytes, 2U/mL) was co-treated with the reaction mixture. The resulting mixture was incubated at 37 °C and luminescence from reaction mixture was measured using a Thermo Scientific Varioskan Flash microwell plate reader. The data represented here is average of 3 repeats.

5.4.3.2. Superoxide estimation by Dihydroethidium (DHE) assay

10 mM stock solution of dihydroethidium (10 mM) was prepared in DMSO and stored in the dark at -4 °C until its use. 10 mM stocks of compounds (**28** and **29**) was prepared in DMSO and stored at -4 °C until its use. A solution of the **29** (1.25 µL of 10 mM) and DHE (2.5 µL of 10 mM) and esterase (5 µL of 100 U/mL) were reacted in phosphate buffer of pH 8 (50 mM, final volume 500 µL) for 2 h at 37 °C. As a control, same reaction was done in the absence of esterase enzyme. The reaction mixture was filtered (0.45 µm) and injected (50 µL) in an Agilent high performance liquid chromatograph (HPLC) attached with a fluorescence detector (excitation at 480 nm; emission at 580 nm). The column used was Agilent1260-infinity with Phenomenex®C-18 reverse phase column (250 mm × 4.6 mm, 5 µm), the mobile phase was H_2O: ACN containing 0.1% trifluoroacetic acid and a gradient starting with 90: 10 % → 0 min, 10: 90 to 44: 56 → 0 – 35 min, 0: 100 → 35 – 37 min, 0: 100 → 37 – 40 min, 10: 90 → 40 – 42 min, 10: 90 → 42 – 45 was used with a flow rate of 0.5 mL/min. **28**, a known superoxide generator (1.25 µL of 10 mM) were mixed in phosphate buffer (pH 8.0, 50 mM) along with DHE (2.5 µL of 10 mM) for 2 h and served as a positive control.

5.4.4. Fluorescence measurement from 32

A 50 μM stock solution of compound **32** and a 1 U/mL stock solution of porcine liver esterase (Sigma-Aldrich) in phosphate buffer pH 7.4 (10 mM) were prepared. The experiment was performed in 96 well plates. In the control experiment, 50 μL of compound (50 μM) was diluted with 50 μL phosphate buffer pH 7.4. In another set serving as enzyme activated set 50 μL of compound (50 μM) was added to 50 μL of esterase enzyme (final concentration of **32** was 25 μM in both blank and reaction; esterase used was 0. 5 U/mL). Fluorescence was measured using a Thermo Scientific Varioscan microwell plate reader (excitation 320 nm; emission 460 nm).

5.4.5. ROS generation and fluorescence emission in cells

A549 Cells were suspended in PBS (1X) and plated in a 96-well plate (0.5 x 10^5 cells/100 μL). Compound **4**, **29** and **32** in DMSO was added to the cell suspension. Cells were incubated at 37 ºC for 30 min and fluorescence emission was measured using a Thermo Scientific Varioscan microwell plate reader (excitation 320 nm; emission 460 nm). For ROS measurement, after 30 min incubation, H_2DCF-DA (10 μM) fluorescence probe was added, and incubated 30 min at 37 ºC and fluorescence signal for DCF was measured at excitation at 490 nm and emission at 520 nm using a Thermo Scientific Varioscan microwell plate reader. The data represented here is average of 3 repeats.

5.4.6. Confocal Image of A549 cells with 32

A549 cells were seeded at 1×10^5 cells/well in 4-well chamber for overnight in RPMI medium supplemented with 10% FBS (fetal bovine serum) and 1% antibiotic solution in an atmosphere of 5% CO_2 at 37 °C. After incubation, old media was removed and the cells were washed with 500 μL of PBS (1X) buffer. Then 500 μL of fresh DMEM media was added along with compound **32** (25 μM) and cells were incubated for 60 minutes at 37 °C. After 60 minutes, old media was removed, cells were washed twice with 200 μL of PBS (1X) and then cells were imaged on a Zeiss LSM 710 confocal microscopy with 405 nm laser lines at 2.5% power using a 63X oil immersion objective. Images were analysed by ImageJ software.

5.4.7. Measurements of intracellular ROS with H_2DCFDA dye

A549 cells were seeded at 1×10^5 cells/well in 12-well corning plate for overnight in RPMI medium supplemented with 10% FBS (fetal bovine serum) and 1% antibiotic solution in an atmosphere of 5% CO_2 at 37 °C. After incubation, media was removed and the cells were washed with 1 mL of PBS (1X) buffer. Then 1 mL of fresh RPMI media was added along with compound (25 μM) and cells were incubated for 60 min at 37 °C. After 60 minutes,

media was removed, cells were washed twice with 200 µL of PBS (1X). Then 1 mL fresh media was added along with H_2DCF-DA probe (10µM) and cells were incubated for further 10 minutes at 37 °C. After 10 minutes, media was removed, cells were washed twice with 1mL of PBS (1X) and then were imaged on a EVOS fluorescence microscopy with 20 X GFP filter.

5.5. Spectral charts

^{1}H-NMR Spectrum (400 MHz, $CDCl_3$) of Compound **29**

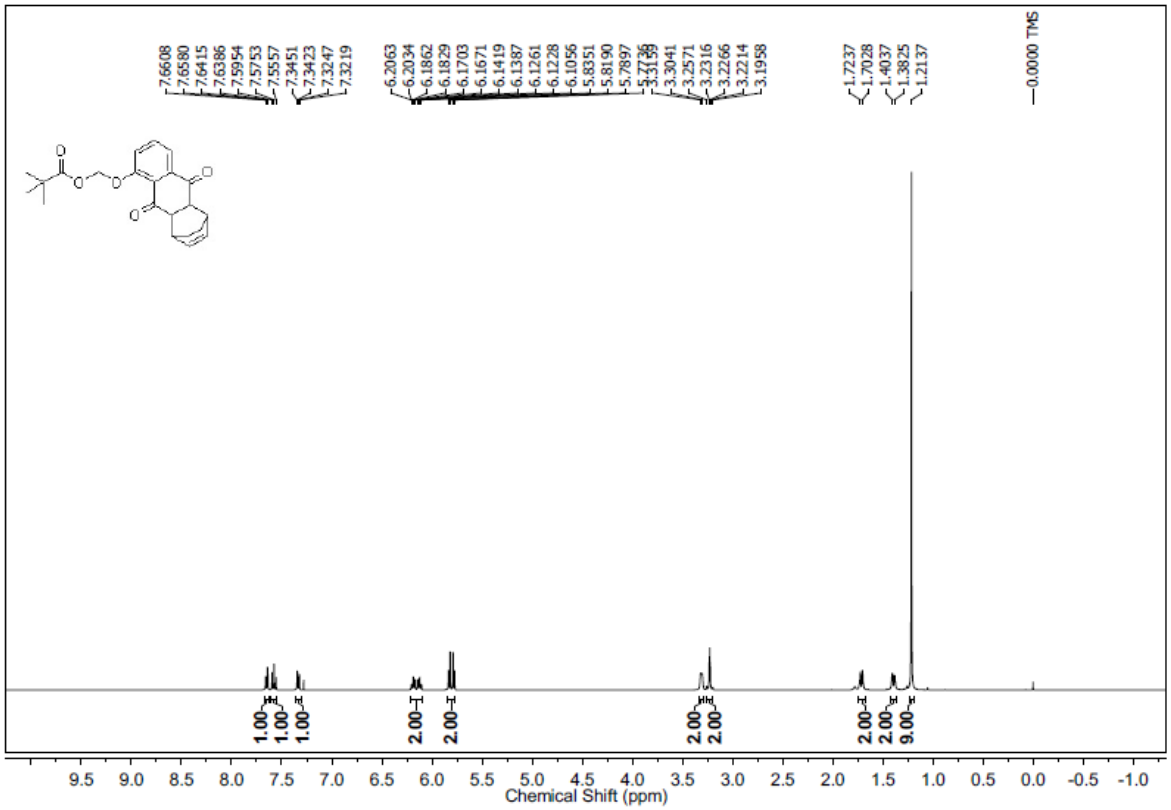

^{13}C NMR Spectrum (100 MHz, $CDCl_3$) of Compound **29**

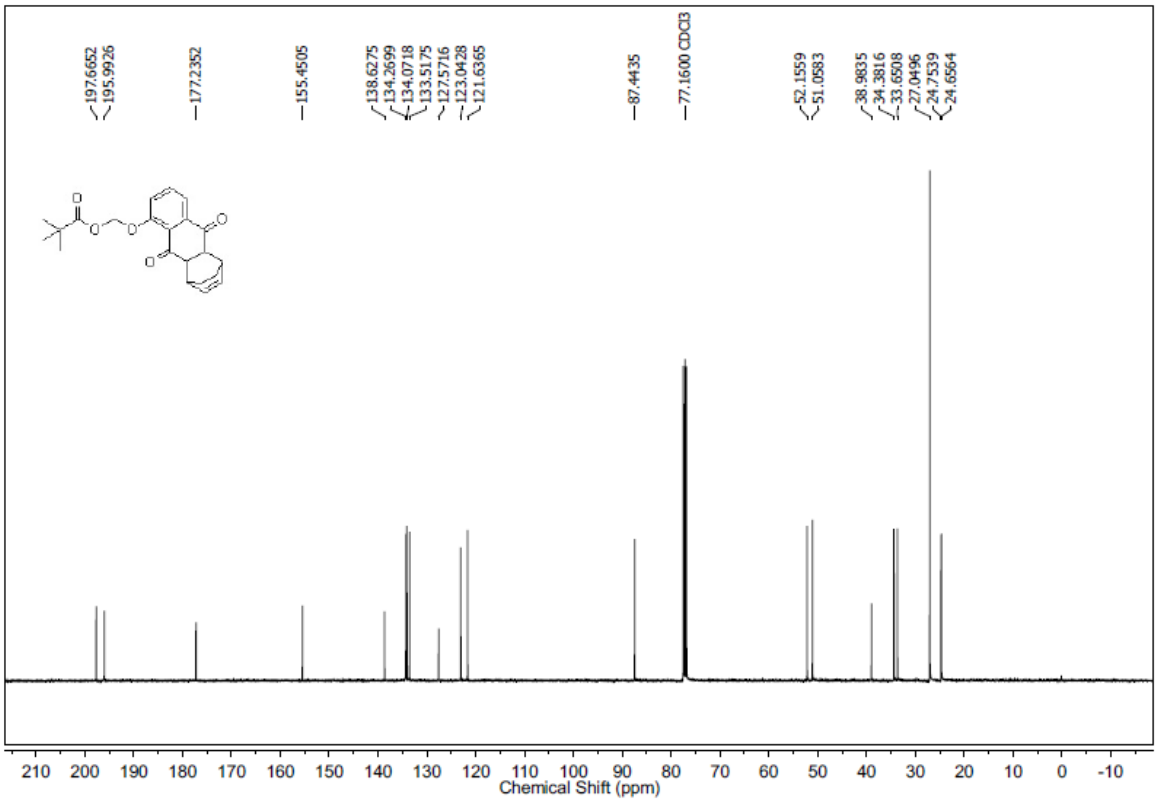

^{1}H-NMR Spectrum (400 MHz, $CDCl_3$) of Compound **31**

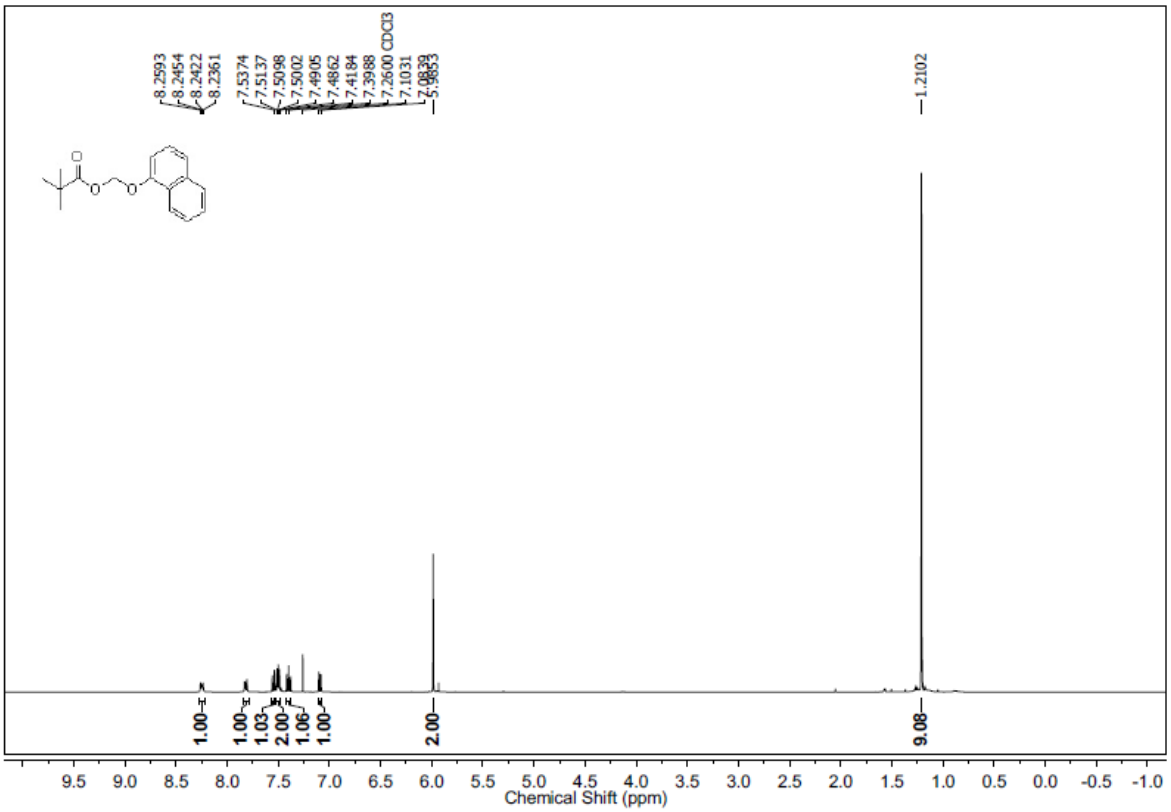

^{13}C NMR Spectrum (100 MHz, $CDCl_3$) of Compound **31**

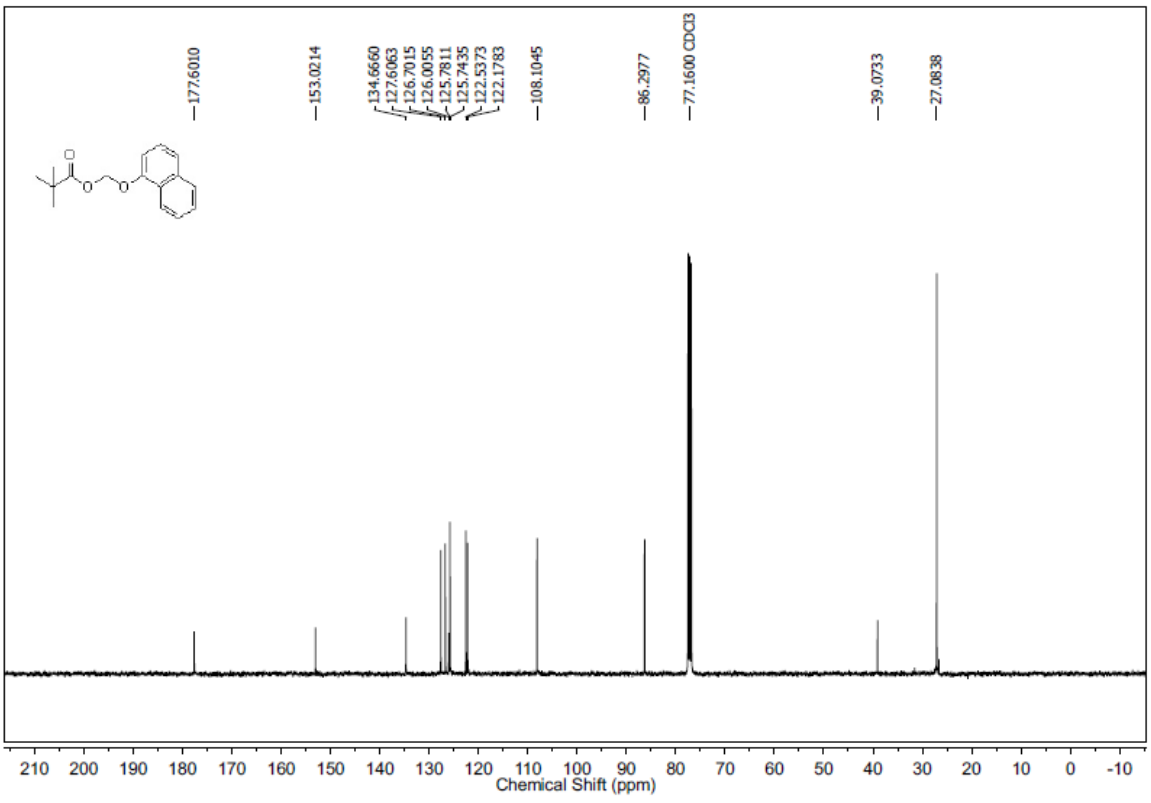

^{1}H-NMR Spectrum (400 MHz, $CDCl_3$) of Compound **32**

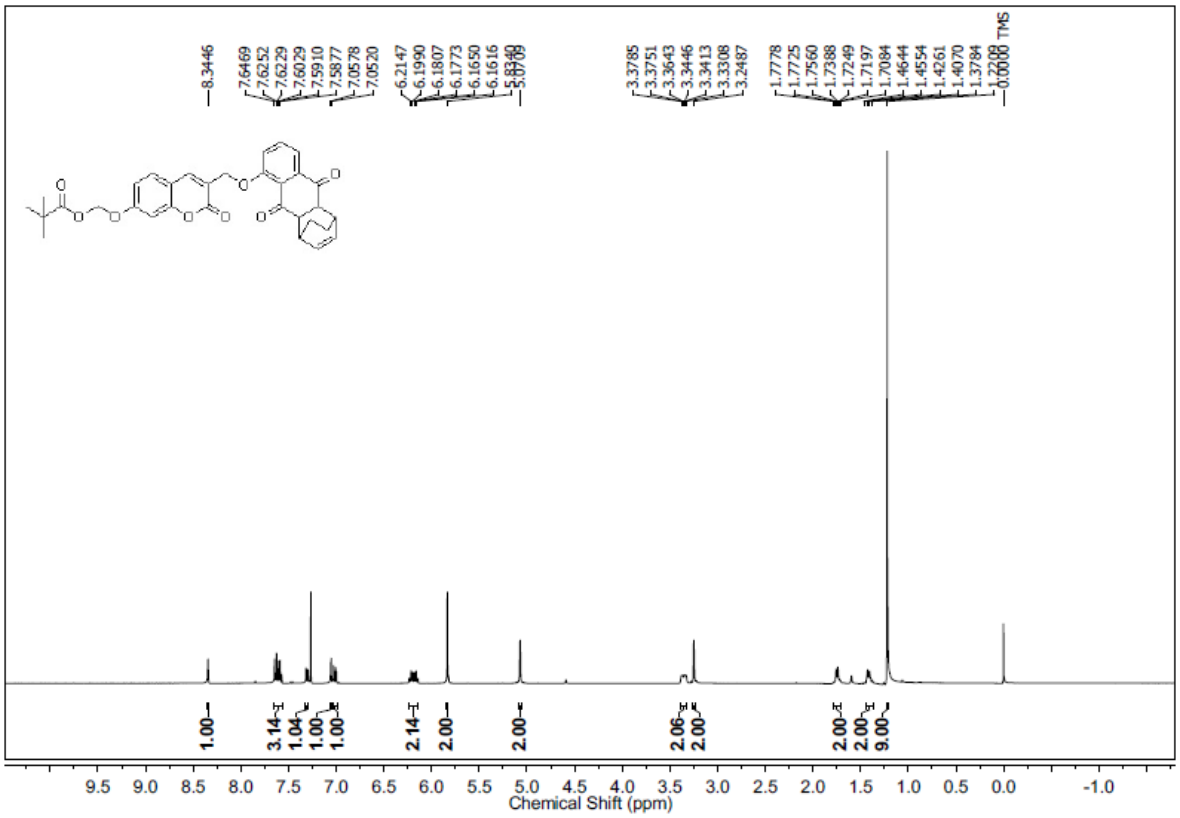

^{13}C NMR Spectrum (100 MHz, $CDCl_3$) of Compound **32**

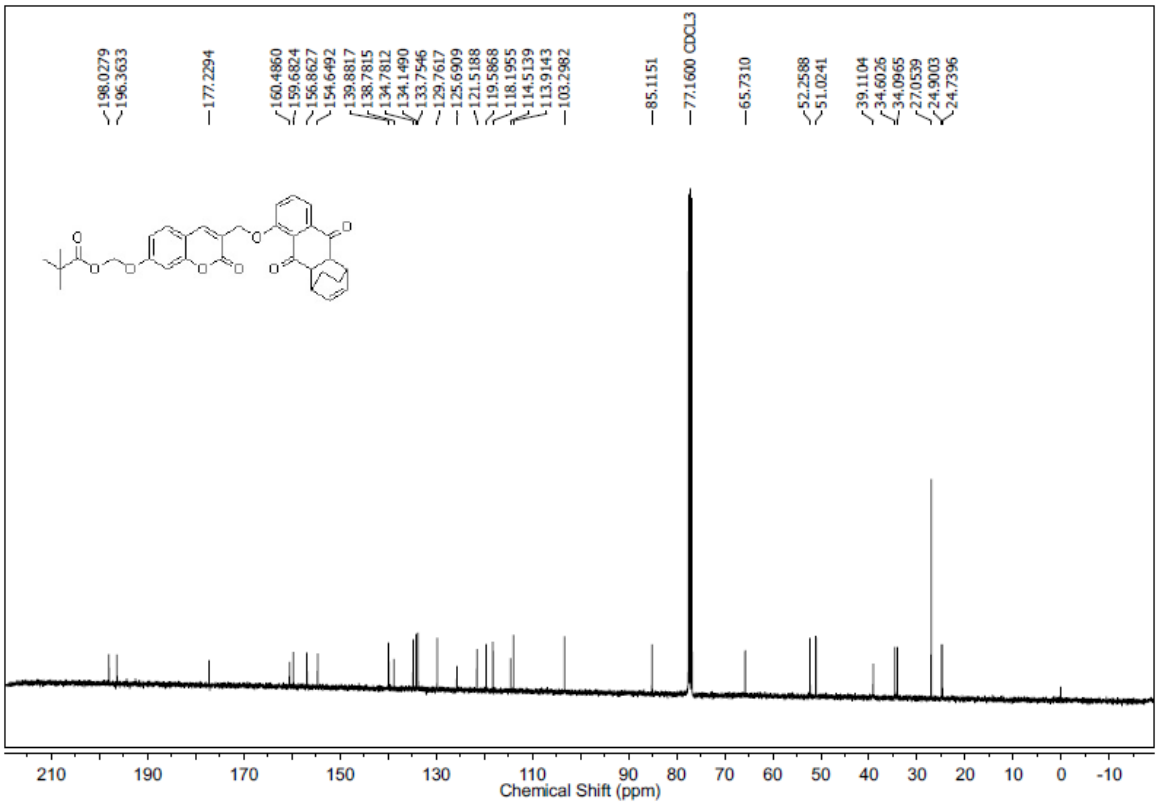

5.6. References

(1) Dharmaraja, A. T.; Alvala, M.; Sriram, D.; Yogeeswari, P.; Chakrapani, H. *Chem. Commun.* **2012**, *48*, 10325.

(2) Dharmaraja, A. T.; Dash, T. K.; Konkimalla, V. B.; Chakrapani, H. *Med. Chem. Commun.* **2012**, *3*, 219.

(3) Dharmaraja, A. T.; Jain, C.; Chakrapani, H. *J. Org. Chem.* **2014**, *79*, 9413.

(4) Khodade, V. S.; Dharmaraja, A. T.; Chakrapani, H. *Bioorg. Med. Chem. Lett.* **2012**, *22*, 3766.

(5) Tyagi, P.; Dharmaraja, A. T.; Bhaskar, A.; Chakrapani, H.; Singh, A. *Free Radic. Biol. Med.* **2015**, *84*, 344.

(6) Dharmaraja, A. T.; Chakrapani, H. *Org. Lett.* **2014**, *16*, 398.

(7) Wardman, P. *Free Radic Biol Med.* **2007**, *43*, 995.

(8) Miller, E. W.; Tulyathan, O.; Isacoff, E. Y.; Chang, C. J. *Nat. Chem. Biol.* **2007**, *3*, 263.

(9) Trung Pham, H.; Marquetty, C.; Pasquier, C.; Hakim, J. *Anal. Biochem.* **1984**, *142*, 467.

(10) Zhao, H.; Joseph, J.; Fales, H. M.; Sokoloski, E. A.; Levine, R. L.; Vasquez-Vivar, J.; Kalyanaraman, B. *Proc. Natl. Acad. Sci. U.S.A.* **2005**, *102*, 5727.

(11) Zielonka, J.; Vasquez-Vivar, J.; Kalyanaraman, B. *Nat. Protoc.* **2008**, *3*, 8.

(12) Wrona, M.; Patel, K.; Wardman, P. *Free Radic. Biol. Med.* **2005**, *38*, 262.

(13) Bandgar, B. P.; Sarangdhar, R. J.; Viswakarma, S.; Ahamed, F. A. *J. Med. Chem.* **2011**, *54*, 1191.

(14) Ravikumar, G.; Bagheri, M.; Saini, D. K.; Chakrapani, H. *ChemBioChem* **2017**, *18*, 1529.

Synopsis

Real-time Monitoring of Nitric oxide Release

Chapter 1: Introduction

Nitric oxide (NO) is a key biomolecule that is produced in nearly all cells and can mediate numerous cellular processes including vasodilation, neurotransmission and immune response.[1] It is endogenously synthesized by a class of enzyme called nitric oxide synthases (NOS), through the stepwise oxidation of L-arginine into L-citrulline, during this process NO is produced (Scheme 1). In mammalian cells, there are three major distinct isoforms of NOS are present: endothelial NOS (eNOS or NOS 3), neuronal NOS (nNOS or NOS 1) and inducible NOS (iNOS or NOS 2). The eNOS and nNOS are constitutively expressed in the endothelial cells and in the neuronal cells, respectively and release NO in nanomolar range (calcium-dependent isoforms). Whereas, iNOS is expressed upon stimulation of immune cells and produce a burst of NO in micromolar range for long time (calcium-independent isoform).[2]

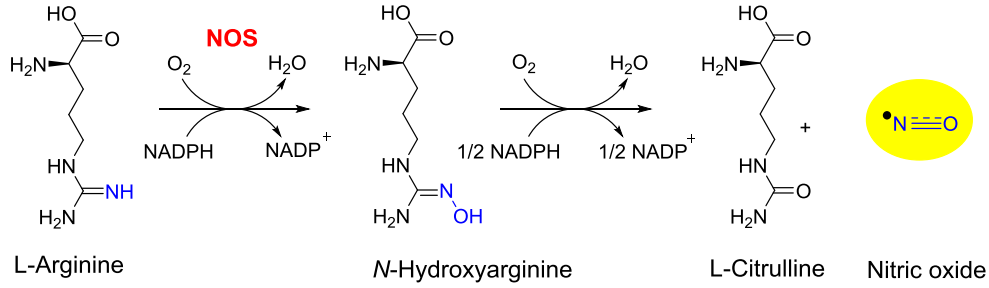

Scheme 1. Biosynthesis of NO from L -arginine

NO mediates various physiological processes in the body, and its effects are largely concentration-dependent.[3] The biological effects of NO are divided into direct and indirect effects, which highly rely on the concentration of NO (Figure 1). At low concentrations, NO exerts direct effects on cellular systems. One of the most important biochemical effects of NO is the activation of soluble guanylate cyclase (sGC), which catalyzes the conversion of GTP to cGMP, a secondary messenger. This, in turn, leads to the activation of cGMP-dependent protein kinases, phosphodiesterases and cyclic nucleotide gated ion channels, which ultimately promote the main biological functions of NO, including vasodilation, inhibition of platelet aggregation and smooth muscle relaxation. In contrast, at higher

concentration, NO reacts with various reactive oxygen species (ROS) to produce reactive nitrogen species (RNS), which exert indirect effects on biomacromolecules such as, oxidation, nitration and nitrosation (Figure 1).[3]

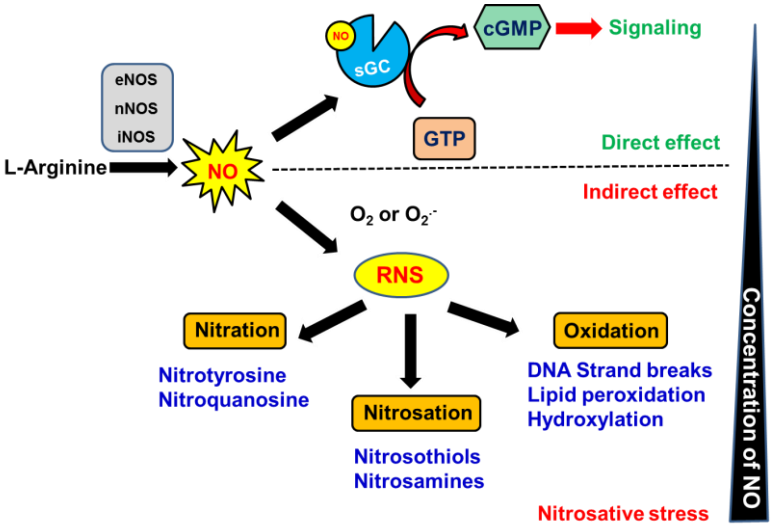

Figure 1. Concentration dependent biological effects of NO

The importance of nitric oxide (NO) in mediating numerous cellular processes is by now well established. The relationship between NO and cancer is complex and is largely dependent on the location, concentration, duration of release as well as the presence or lack thereof of other reactive entities.[4] Several investigations have shown that low levels of NO promote cancer growth, while higher concentrations of NO induce cancer cell death. Numerous studies have shown that cancers have elevated levels of NO in comparison with paired normal cells. So, the tumour cells required an optimal concentration of NO for its proliferation. However, very low levels of NO or very high levels of NO is toxic to tumour cells. This provide a therapeutic opportunity to target cancer either by lowering the concentration of NO using NOS inhibitors to inhibit tumor growth or by increasing the level of NO using NO donors to induce tumor cell death (Figure 2). Thus, a number of studies have focused on dissipating NO within tumours by using inhibitors of NOS such as L-NAME.[5] Due to the decreased levels of NO, tumour growth is slowed. However, the use of NOS inhibitors requires long term, systemic administration that may result in hypertension and tumour regrowth if treatment is come to end prior to complete eradication.

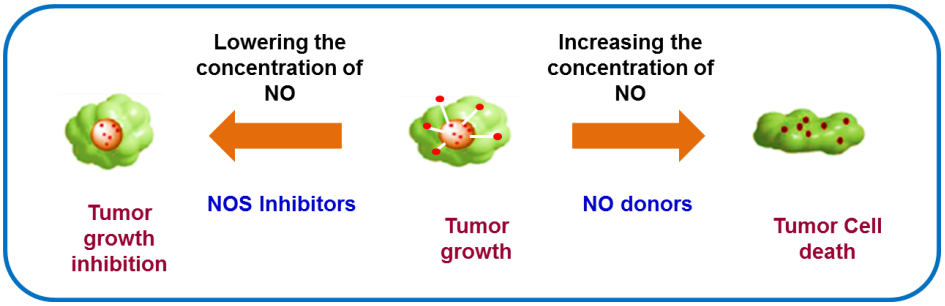

Figure 2. Concentration dependent effect of NO in tumor

Meanwhile, numerous parallel studies focused on increasing NO concentrations at the tumor site to induce tumor cell death. Due to increased metabolism associated with rapidly dividing cells, tumors also have elevated levels of reactive oxygen species (ROS) including superoxide radical anion. Thus, enhancement of NO within cancers is expected to produce peroxynitrite ($ONOO^-$), a product of rapid combination of NO and superoxide anion radical, that may be highly toxic to cancers (Figure 3). Furthermore, Multidrug resistance (MDR) is the one of the major problems associated with failure of cancer chemotherapy. Cancer cells are known to overexpress efflux pumps that reduce the intracellular accumulation of a drug, which leads to MDR. P-glycoprotein (P-gp), multidrug resistance related proteins (MRPs) and breast cancer resistance proteins (BCRP-1) are the primary efflux pumps involved in this process.[6,7] Extensive studies confirm that the antitumor effect of cancer chemotherapy agents was enhanced by the use of NO donors.[8-10] The major reason is that NO donors generate reactive nitrogen species, which nitrate tyrosine residue of the efflux pumps which leads to increased intracellular drug accumulation and enhanced anticancer effect against drug resistant cancer cells (Figure 3). Solid tumours have significant regions where oxygen concentration is diminished, hypoxia. This condition is rather difficult to treat and hypoxic cells have an increased propensity to develop resistance to doxorubicin, for example NO can reverse this resistance. Furthermore, NO can also act as a hypoxic radiosensitizer, due to low oxygen concentrations, solid tumors becomes less sensitivity towards radiation therapy. NO mimics the oxygen role and sensitize solid tumors to the radiation therapy.[11]

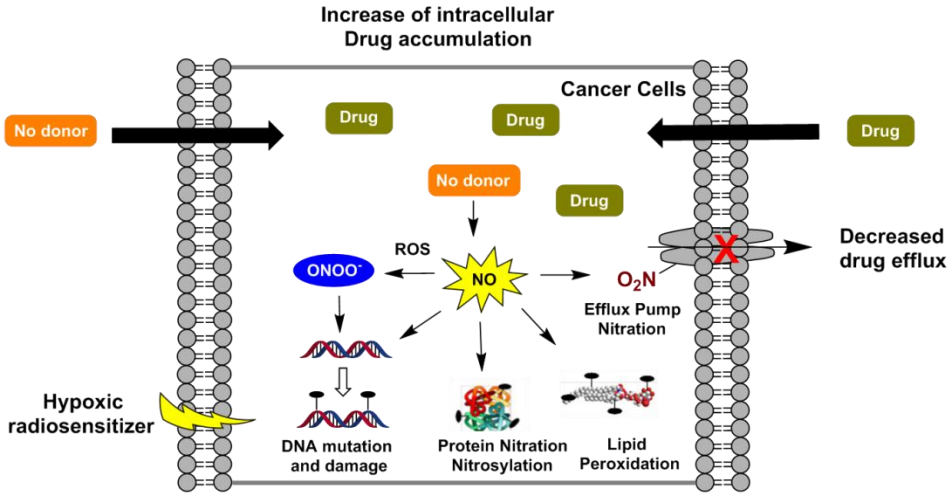

Figure 3. Cellular effects of nitric oxide

The therapeutic value of NO is well documented, and a complete realisation of its potential relies on precise spatiotemporal control over NO generation.[12] Exogenous sources of NO ("NO donors") are used for this.[13,14] Some NO donors spontaneously dissociate to produce NO, whereas others are triggered intracellularly and dissociate to produce NO (Scheme 2.a).[15-20] However, in order to infer the production of NO, secondary assays are used, typically fluorescence-based cellular assays for reactive nitrogen species (Scheme 2.a).[21-23] Since, NO is a free radical and highly reactive species, once released inside the cell, it can react with different molecules that are present inside cell, as a result of which measurement of NO by secondary assays might be inaccurate.[24,25] All the secondary dyes are used to detect only free NO (unbound) in living cells and treatment of cells with these secondary dyes often renders them unsuitable for further study. Furthermore, measurement of NO with these secondary dyes invariably associated with consumption of NO. Enhancement of NO within cells as well as simultaneous detection is cumbersome. So real-time monitoring of NO in cells is challenging. One possibility to address this task is to introduce a fluorescent reporter in the NO donor. Thus, a strategy where a small molecule can generate NO along with a fluorescence reporter, for the produced NO would be useful (Scheme 2.b), which will eliminates the need for the secondary assays to monitor the release of NO.

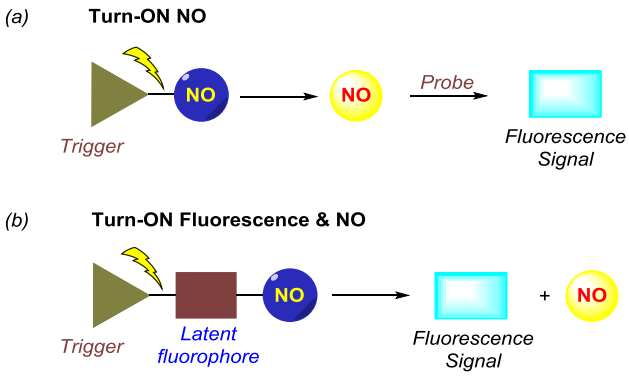

Scheme 2. (a) Stimuli responsive nitric oxide generation by a NO donor requires a secondary probe for detection of NO produced. (b) Incorporation of a latent fluorophore in the donor eliminates the need for the secondary probe for monitoring of NO.

It is therefore necessary to develop a reporter linked NO donors. A photochemical trigger offers a high degree of spatiotemporal control over NO generation and useful for ON-Demand NO generation. A number of methodologies for light-activated generation of NO with a fluorescence reporter are known. For example, Mascharak and coworkers have developed a light-triggered ruthenium based NO donors with fluorescencent reporter (resorufin or dansyl chromophores) to track NO in cells (Figure 4).[26,27] However, this system displays turn-OFF fluorescence signal upon NO release.

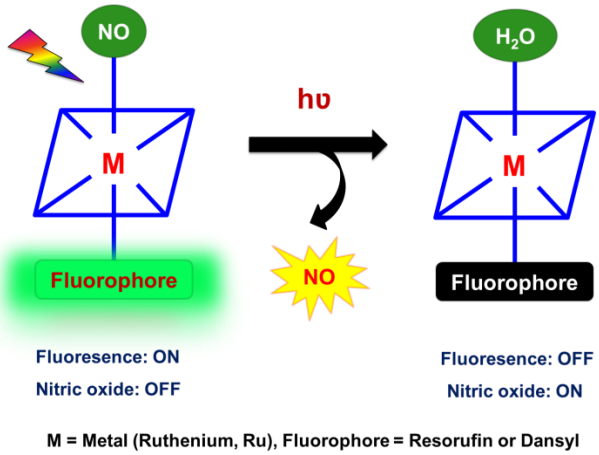

Figure 4. Photosensitive Metal-based NO donor with a fluorescence reporter

For real-time monitoring of NO, turn ON fluorescence signal would be useful. Same group developed a turn ON system to track NO release in cells.[28] But because of the fluorescence bands (metal bound and free dye) overlapping, monitoring of NO in cells is difficult with this method. Next, Sortino and coworkers have developed a light activated NO donor with fluorescence reporter.[29,30] Although, this system is

fluorescence turn ON type, nitroaniline derivative was used as a NO donor, which is not an efficient NO donor. Recently, a nanoplatform for light triggered target specific NO delivery methods also reported but this system generates NO as well as singlet oxygen. Several materials-based methods for NO generation are known, but they have limitations, such as consumption of NO or being a turn-off fluorescence methodology. However, all the above methods required light as a trigger, most optically triggered approaches utilize UV light, which limits tissue permeability and triggers toxic side effects. A nitric oxide delivery system with a fluorescence reporter for broad applicability is not yet available.

Therefore, we need a new NO donor, which should have the following characteristics,

1) It should be a triggerable NO donor
2) The trigger should be cancer selective
3) Fluorescence reporter signal should be turn ON type
4) Fluorophore should not consume NO during its detection
5) It should release NO in a controlled and sustained manner at a cancer site

Weinstein *et al*. reported real-time monitoring of drug release using a reporting drug delivery system (RDDS) where a 7-hydroxycoumarin linker was used as a fluorescent reporter.[31] 7- hydroxylcoumarin derivative was attached to the peptidase substrate to one end and to the drug molecule on the other end. Upon activation of RDDS, a spontaneous 1, 8- elimination reaction takes place and release the drug and reporter molecule (Figure 5).

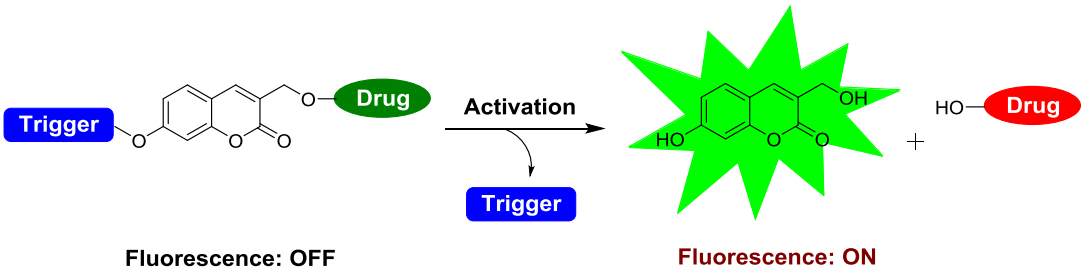

Figure 5. 7-Hydroxycoumarin was used as a fluorescence reporter for real time monitoring of drug release

Therefore, based on the above strategy of real-time monitoring of drug release, in **Chapter 2**, we propose FLUORO/NO, a nitric oxide donor with fluorescence reporter. In the presence of esterase it produces NO and fluorescence signal without consumption of NO during its detection. The trigger that we had is esterase, which is

present in nearly all cells, and therefore the compound will be suitable for a range of cell biology studies. In order to study the precise role of NO in cancer, we need a cancer specific trigger. Since cancer cells produce higher level of H_2O_2 compared with normal cells, as a proof of concept in **Chapter 3**, we propose BORO/NO, a NO donor without fluorescence reporter, which are capable of generating NO when triggered by H_2O_2. Next, in **Chapter 4**, we propose Thera/NO, a H_2O_2 activated NO donor that can be used for selectively delivering and monitoring the release of NO in cancer cells.

The versatility of this scaffold for real-time monitoring of NO release was demonstrated by incorporating two distinct triggers and can, in principle, be extended to other stimuli of interest as well. Altogether, the results presented in this thesis address important problems associated with site-specific delivery of NO and real-time monitoring of NO release in cells as well. It is anticipated that these tools will find use in interrogating NO biology, which is yet to be completely understood.

Finally, In addition to NO, a number of other redox active reactive species have important biological roles. Controlled generation as well as reliable detection of these species is challenging.[12] In order to assess the generality of the method developed herein, we aimed to develop a ROS generator with a fluorescence reporter and discussed in **chapter 5**. This tool would be useful to deliver and real-time monitor ROS release in cells without the need for secondary assays.

Chapter 2: FLUORO/NO: A Nitric Oxide Donor with a Fluorescence Reporter

Using the coumarin-based strategy, FLUORO/NO (**5**) was designed the compound was expected to permeate cells to be cleaved by esterase to produce the highly fluorescent **12** and the nitric oxide-releasing **DEA/NO** (Scheme 3). If the release of NO and the fluorescent **12** is nearly concurrent, a secondary assay for NO would not be necessary to monitor NO generation. The triggers that we chose were metabolically relevant, esterases are present in nearly all cells, and therefore the trigger would have broad relevance.

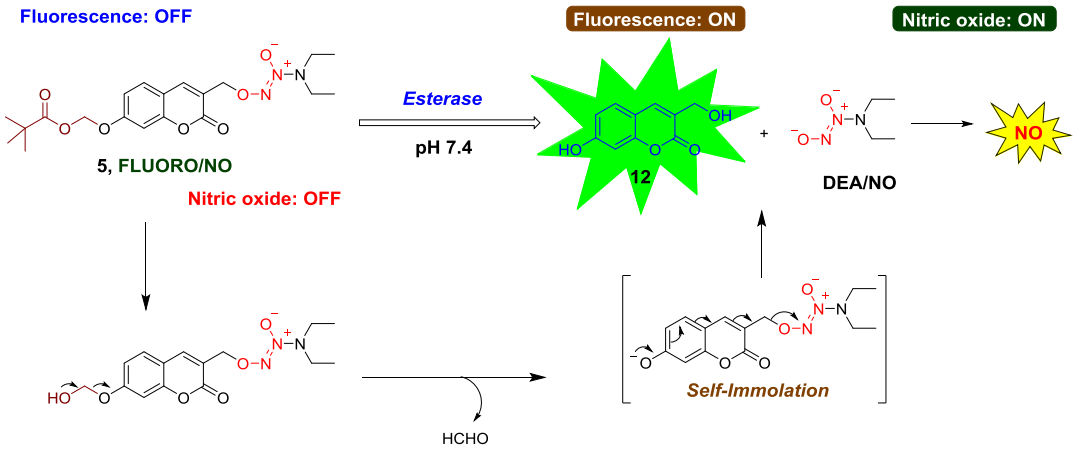

Scheme 3. FLUORO/NO (**5**), a class of triggerable nitric oxide donors with an in-built fluorescence reporter. FLUORO/NO is expected to have diminished fluorescence. Upon activation by esterase, followed by self-immolation and reaction with water will produce **12**, which is highly fluorescent and DEA/NO, which dissociates in pH 7.4 buffer to produce NO.

First, the ability of the compound **5** to generate NO and fluorescence signal in phosphate buffer (pH 7.4, 10 mM) was evaluated. Compound **5** was treated with esterase (ES) and the fluorescence signal attributable to **12** was measured using a micro-well plate reader while nitric oxide released was measured by nitric oxide analyser (NOA). The time course of NO generation corresponded well with the time course of fluorescence enhancement (Figure 6), thus suggesting that once the pivaloyl group is cleaved, the rearrangement of the ensuing intermediate to produce DEA/NO and **12** is rapid (Scheme 3). Hence, once the fluorescence signal is seen, NO generation can be expected nearly instantaneously.

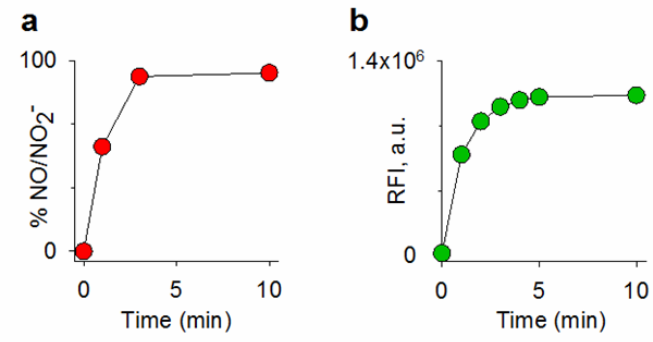

Figure 6. (a) Time-course of NO generation from **5** with ES (0.5 U/mL) in buffer (b) Time-course of fluorescence enhancement from **5** with ES (0.5 U/mL) in buffer (All the experiments were conducted in phosphate buffer pH 7.4 at 37 °C, excitation 315 nm; emission 325 to 460 nm).

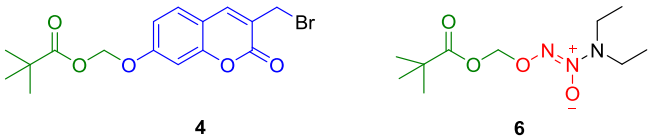

Scheme 4. Structure of **4** and **6**

Next, we study the capability of compound **5** to enhance fluorescence signal as well as NO within the cells, HeLa cells were treated with 25 µM of compounds (**4**, **5** and **6**). After 30 min, the fluorescence signal at 460 nm was measured using a micro-well plate reader, while nitrite release was measured by Griess assay (Figure 7). With a control compound **4** (does not contain diazeniumdiolate, Scheme 4), an increase in the fluorescence signal was seen but no significant NO generation (Figure 7.a, 7.b); and with a control compound **6** (does not contain coumarin, Scheme 4), an increase in extracellular nitrite was observed with no significant fluorescence signal (Figure 7.a, 7.b). Whereas, compound **5** is able to enhance both fluorescence signal as well as NO was observed (Figure 7.a, 7.b). When the dose of **5** was varied, as expected, a dose-dependent increase in fluorescence signal as well as nitrite was observed (Figure 7.c), thus supporting the suitability of **5** to enhance NO as well as fluorescence within cells.

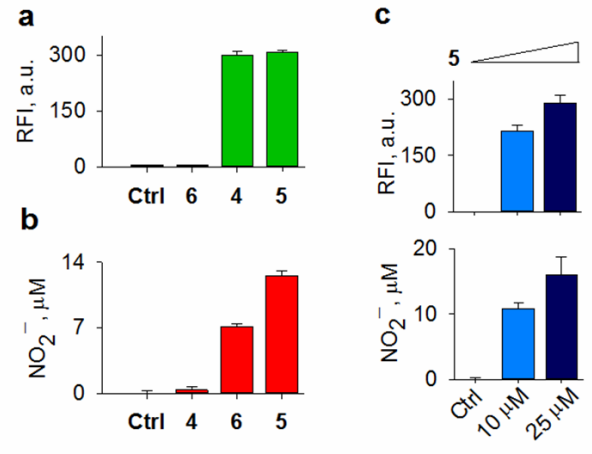

Figure 7. Comparison of fluorescence intensity attributable to **12** (a) and (b) extracellular nitrite release upon incubation of HeLa cells with 25 µM of **4**, **5** or **6**. (c) Comparison of fluorescence intensity attributable to **12** and extracellular nitrite release during incubation of HeLa cells with **5** at 0, 10 and 25 µM after 30 min at 37 °C (excitation 315 nm; emission 460 nm).

Having established that **5** is a reliable source of NO within cells, the fluorescence signal at 460 nm can now be used as a surrogate for NO generation. In order to study

the cellular uptake of **5**, HeLa cells were treated with different concentrations of **5** for 30 min and the fluorescence signal attributable to the formation of **12** at 460 nm was monitored by confocal microscopy. A dose-dependent increase in fluorescence signal was observed (Figure 8). These results supporting that, the compound **5** permeate cells and get activated by cellular esterase to produce fluorescence signal attributable to **12**.

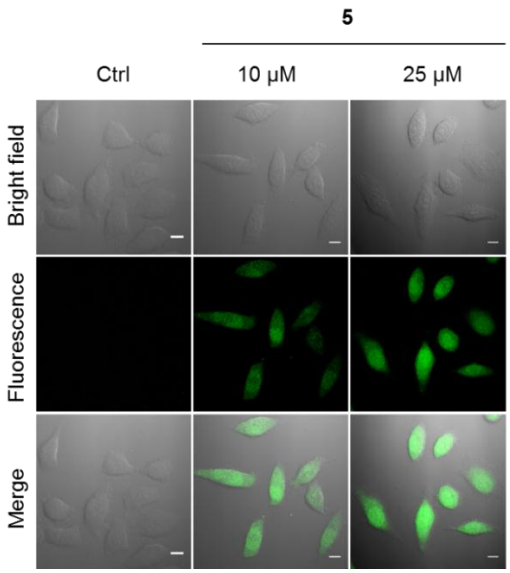

Figure 8. Confocal microscopy images of HeLa cells treated with **5** (10 and 25 µM) after 30 min at 37 °C. The excitation and emission channels were 405 nm and 460 nm respectively. Scale bar = 10 µm.

One of the most important biological roles of NO is activation of soluble guanylate cyclase (sGC), which results in the production of secondary messenger cGMP from GTP, which ultimately promotes the main biological functions of NO, including smooth muscle relaxation, platelet aggregation and gene expression. In order to test if **5** was capable of activating sGC within cells, cGMP levels were measured by using a bioluminescence resonance energy transfer (BRET) assay in human embryonic HEK293T cells.[32] First, a known NO donor, sodium nitroprusside (SNP, 50 µM) was tested as the positive control and a significant enhancement in cGMP levels was observed (Figure 9). When a similar assay was conducted with **5** (25 µM), as expected, a signal for cGMP was observed. This assay was conducted with the negative control compound **4** and as expected no significant enhancement in cGMP levels was observed (Figure 9). Thus, other than NO, the by-products produced during decomposition of **5** were incapable of inducing NO-like signalling. This result suggesting that **FLUORO/NO** (**5**) was suitable for use as a tool to enhance NO for cellular signalling studies.

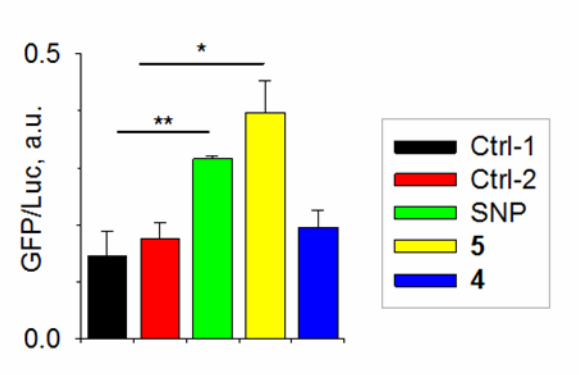

Figure 9. Formation of NO in cells was inferred by measurement of cyclic GMP, a secondary messenger for NO, by a BRET assay at 37 °C. *p value = 0.022; **p value = 0.007. Control 1=cells only, Control 2=cells containing DeepBlueC (luciferase substrate) without any treatment. Data provided by Meisam Bagheri & Deepak Saini, IISc Bangalore.

Chapter 3: BORO/NO, a Class of Hydrogen Peroxide Inducible Nitric Oxide (NO) Donors

In chapter 2, we have reported FLUORO/NO, a nitric oxide donor with fluorescence reporter. In the presence of esterase it produces NO and fluorescence signal without consumption of NO during its detection. The trigger that we had is esterase, which is present in nearly all cells, and therefore the compound will be suitable for a range of cell biology studies. In order to study the precise role of NO in cancer, we need a specific trigger to target cancer. The tumour micro environment is different from normal tissues; one feature that has been widely reported is the high levels of reactive oxygen species (ROS). These are reduced forms of oxygen that mediate certain signalling events within the cell but are harmful at elevated concentrations and damage bio-macromolecules including DNA, proteins and RNA. The most common ROS include superoxide anion ($O_2^{\bullet -}$), hydrogen peroxide (H_2O_2), and hydroxyl radical ($HO^{\bullet}$). Among these, H_2O_2 was found to be more stable due to its uncharged in nature and generation of H_2O_2 in several cancer cell lines has been estimated to be 0.5 nM per 10^4 cells per h, which are significantly higher than those in normal cells.[33] Keeping this in mind, H_2O_2 has been used as a specific agent to activate prodrugs[34-36] and latent fluorophores[37,38] (as imaging agents) in cancers. A functional group that has been widely used is the arylboronate ester, which is known to react with H_2O_2 to produce phenol. Hence, this functional group was chosen as a substrate for the metabolic stimulus, *i.e.* H_2O_2 to specifically generate NO in cancer cells.

As a proof of concept, first we have designed a H_2O_2 activated NO donor without fluorescence reporter and studied in this chapter. Arylboronate ester based diazeniumdiolates (BORO/NO), a class of diazeniumdiolate derivatives that are attached to a pinacolboronate ester through a self-immolative aryl linker were considered as H_2O_2 activated NO donors (Scheme 5). Reaction of BORO/NO with H_2O_2 should produce the phenolate intermediate **I**, which could rearrange to produce the diazeniumdiolate anion, which in pH 7.4 releases NO (Scheme 5).

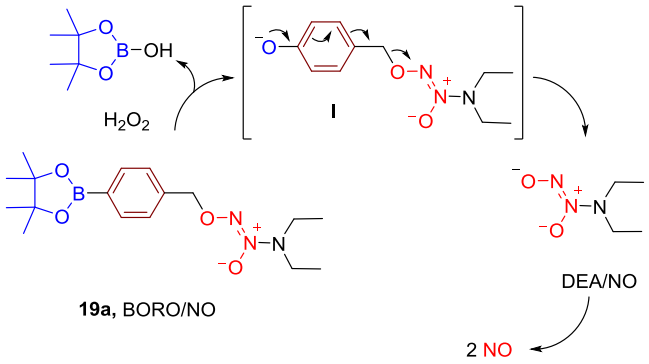

Scheme 5. Proposed mechanism of activation of **19a** by hydrogen peroxide to produce nitric oxide

In order to deliver NO selectively to cancer over normal cells, the compound should be selectively activated by H_2O_2 over other common reactive species that are present in cells. To verify that, selectivity of **19a** towards activation by H_2O_2 was investigated in the presence of number of biologically relevant nucleophiles, reductants and oxidants. The compound **19a** was incubated in buffer and treated with 10 equivalents of different reactive species and an aliquot was analysed by NOA for NO. The compound **19a** generates NO only in the presence of H_2O_2 and no significant levels of NO generation was observed in the presence of biologically relevant thiols, metal ions, antioxidants and other common reactive oxygen species (Figure 10), which suggesting the selectivity of the functional group towards activation by H_2O_2 in a physiological condition. The observed specificity of boronate ester functional group towards H_2O_2 was consistent with previous reports.[35,37]

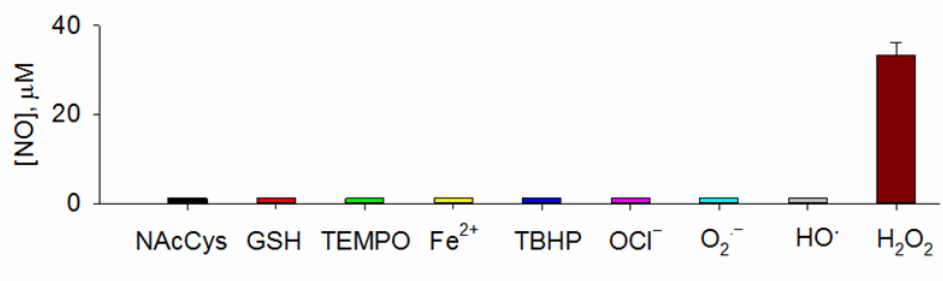

Figure 10. Nitric oxide analysis of **19a** (25 µM) with various reactive species (250 µM) at 37 °C in pH 7.4 phosphate buffer after 10 min incubation, NAcCys: N-acetyl cysteine; GSH: glutathione; TEMPO: 2,2,6,6-tetramethylpiperidinyloxy; Fe (II): $FeCl_2$; TBHP: *tert*-butyl hydroperoxide; OCl^-: sodium hypochlorite; $O_2^{\bullet-}$: generated using hypoxanthine/xanthine oxidase; $HO^{\bullet}$ was generated using H_2O_2 and Fe(II) mixed at a 1:10 ratio; H_2O_2.

Having established that compound **19a** was capable of generating NO when triggered by H_2O_2, a series of an arylboronate ester based diazeniumdiolates (BORO/NO) was synthesized. After confirmation of products, the ability of all analogues of BORO/NO derivatives **19b-19d** and **24a-24d** to produce NO was investigated. The compounds **19b-19d** and **24a-24d** (25 µM) were independently incubated with H_2O_2 (250 µM) in pH 7.4 buffer for 10 min and an aliquot was analysed by NOA for NO. We found all the compounds were stable and generated nitric oxide only when exposed to H_2O_2 and the yields of NO (Figure 11) were comparable or lower than the yield of NO produced during incubation of **19a** under similar conditions.

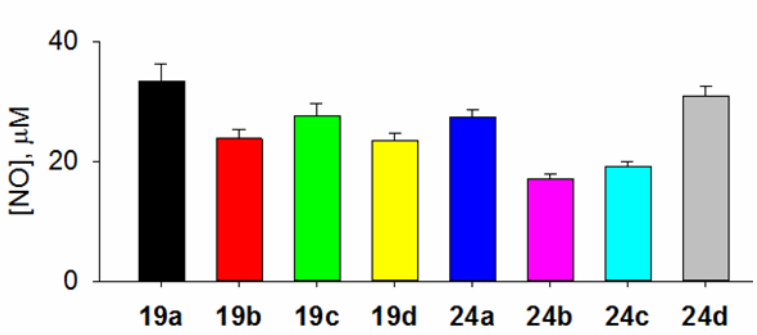

Figure 11. Nitric oxide analysis of BORO/NO derivatives **19a-19d** and **24a-24d** (25 µM) in the presence of H_2O_2 (10 eq.) in buffer after 10 min incubation (Experiments were conducted in 10 mM pH 7.4 phosphate buffer containing 100 µM of diethylene triamine pentaacetic acid (DTPA), a metal ion chelating agent at 37 ºC).

Chapter 4: Hydrogen peroxide Activated NO Donor with a Fluorescence Reporter

In chapter 3, we designed and synthesized a series of arylboronate ester based diazeniumdiolates (**BORO/NO**), established that **BORO/NO** derivatives are capable of generating NO when triggered by H_2O_2. Next, we have designed Thera/NO (**27**), a H_2O_2 activated NO donor that can be used for selectively delivering and monitoring the release of NO in cancer cells (Scheme 6).

The proposed mechanism of activation of the reporter probe, **27** is as follows. Upon activation of **27** by H_2O_2, self-immolation and reaction with water produces **12** and DEA/NO, which rapidly dissociates at pH 7.4 to produce NO (Scheme 6).

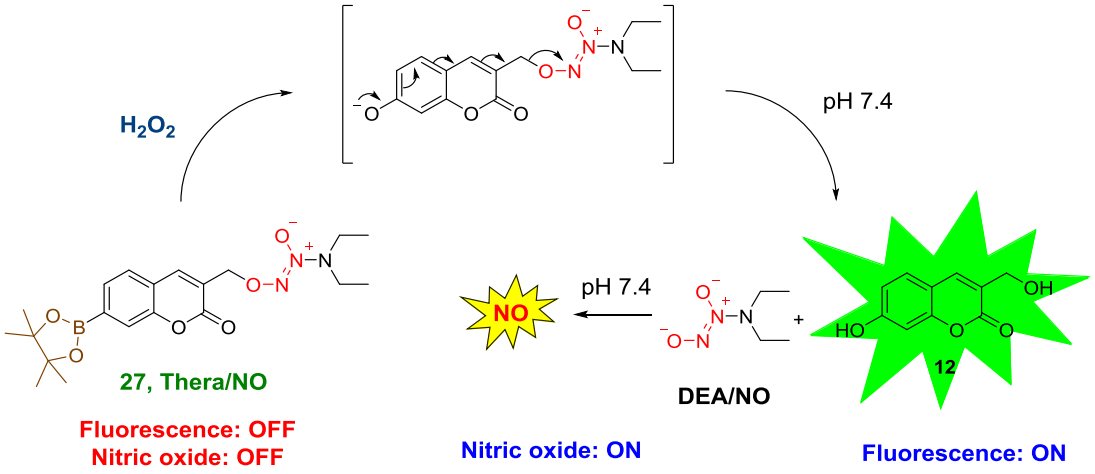

Scheme 6. Proposed mechanism of activation of **27** by hydrogen peroxide to produce **12** and NO

First, the ability of the compound **27** to generate NO and fluorescence signal in phosphate buffer (pH 7.4, 10 mM) was evaluated. Compound **27** was treated with 10 eq. H_2O_2 and the fluorescence signal attributable to **12** as well as nitric oxide was independently monitored. The fluorescence signal at 460 nm was measured using a micro-well plate reader while nitric oxide released was measured by nitric oxide analyser (NOA). A close correlation between these two parameters was observed (Figure 12), suggesting that the aforementioned fluorescence signal and NO generation were nearly concurrent.

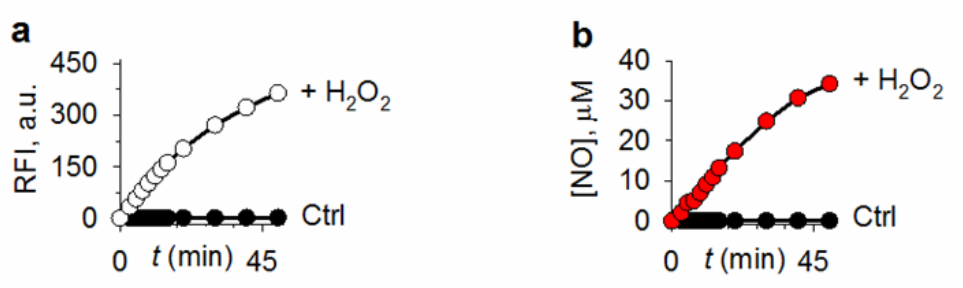

Figure 12. (a) Time course of enhancement of fluorescence signal (excitation 315 nm, emission 460 nm) attributable to **12** upon incubation of **27** (25 μM) with and without H_2O_2 (10 eq). (b) Time course of enhancement of NO upon incubation of **27** (25 μM) with and without H_2O_2 (10 eq). (All the experiments were conducted in phosphate buffer pH 7.4 at 37 °C, excitation 315 nm; emission 460 nm).

In order to study the capability of compound **27** to enhance fluorescence signal as well NO within the cells, HeLa cells were treated with **27** and exogenously H_2O_2 was added. The fluorescence signal at 460 nm was measured using a micro-well plate reader while nitrite released was measured by Griess assay and an increase in fluorescence and nitrite was observed (Figure 13). These results indicate that, the compound **27** gets activated by H_2O_2 within cells and produces NO and fluorescence signal.

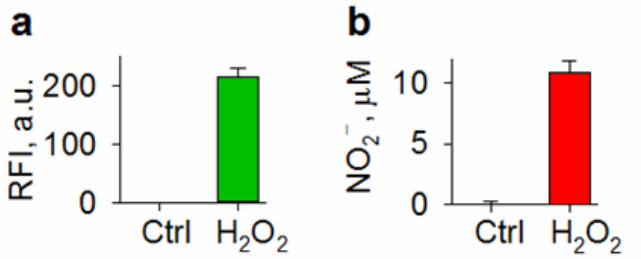

Figure 13. Comparison of the fluorescence signal attributable to **12** (a) and extracellular nitrite release (b) during incubation of HeLa cells when incubated with **27** (25 μM) alone (Ctrl) or HeLa cells pre-treated with H_2O_2 (100 μM) for 30 min followed by addition of **27** (25 μM) (excitation 315 nm; emission 460 nm).

Catalases are the highly efficient antioxidant enzymes, found in nearly all living organisms. It catalyses the conversion of hydrogen peroxide to water and molecular oxygen. Catalases protect the cells from oxidative stress by maintaining a safe level of H_2O_2 in cells. In order to simulate increased ROS intracellularly, a catalase knockdown HeLa cell line (KD) was used. Here, due to the low level of catalase, an

increased level of ROS is expected. When intracellular ROS level was measured by $DCFH_2$-DA assay (fluorescence indicator for reactive oxygen species in cells), the catalase knockdown cell line (KD) showed higher DCF fluorescence (Figure 14.a) when compared with wild-type (WT). Both these cell lines were independently exposed to **27** and fluorescence signal corresponding to **12** was measured. We found that the relative increase in fluorescence signal was much higher in the case of KD when compared with WT (Figure 14.b). Thus, when encountered with cellular situations with varying ROS levels, **27** is preferentially activated in cell lines where ROS levels are relatively higher.

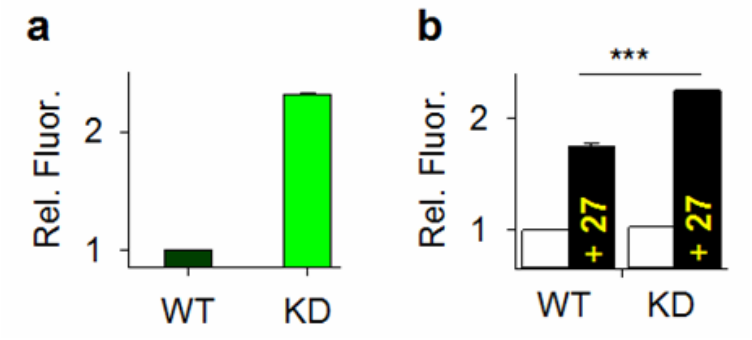

Figure 14. (a) Intracellular ROS enhancement was measured using a $DCFH_2$-DA assay in wild type (WT) and catalase expression knockdown (KD) cells. (b) Comparison of the relative fluorescence signal attributable to **12** in wild type (WT) and catalase expression knockdown (KD) cells after treatment with **27**. ***p-value = 0.006. Data provided by Meisam Bagheri & Deepak Saini, IISc Bangalore.

Since cancer cells produce higher level of H_2O_2 compared with normal cells, selective activation of **27** was expected in cancer cells than the normal cells. To validate it, compound **27** was treated with MRC5 (normal fibroblast) and cancer cell lines: A549, HeLa, MDA-MB-231 and the fluorescence response was evaluated by fluorescence microscopy imaging. As expected, we found enhancement in the fluorescence signal attributable to **12** in cancer cells compared with normal cells (Figure 15). Together these experiments suggest that **27** get selectively activated in cancer cells over normal cells.

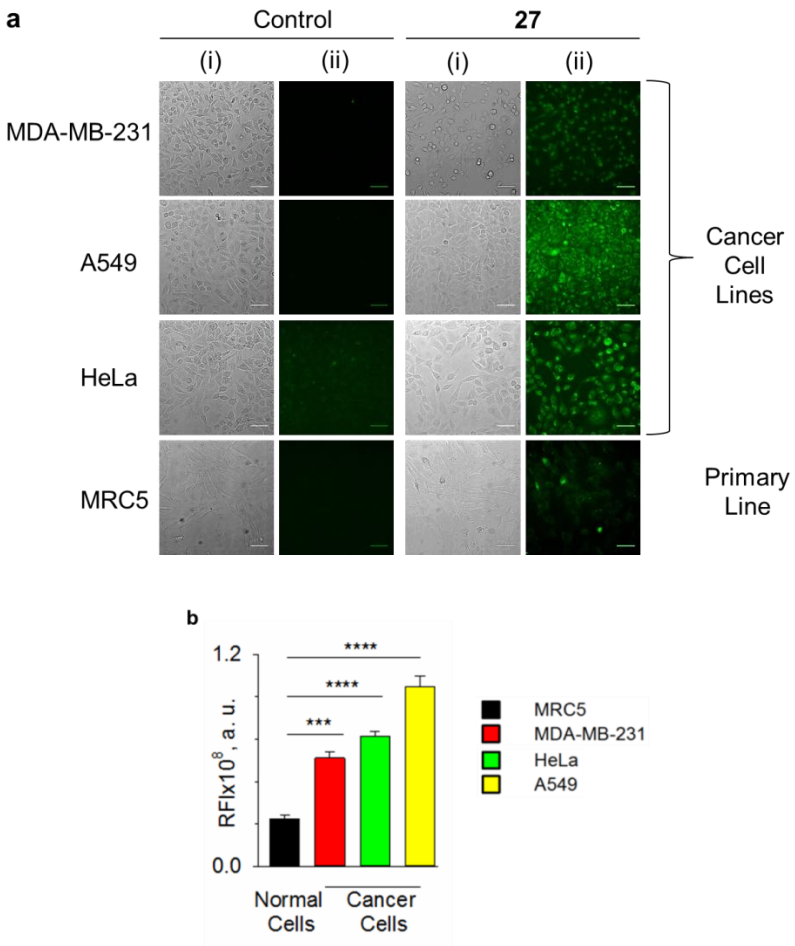

Figure 15. (a) Fluorescence images of different cells treated with **27** (25 µM) after 6 h at 37 °C. Images were taken using DAPI channel and pseudocolored (in green) for better visualisation. (i) Bright field image, (ii) Fluorescence image. Scale bar = 100 µm. All images were acquired with identical parameters (gain 3, intensification 200 and ND: 75). (b) Quantification of fluorescence intensity was done using ImageJ software and statistical analysis was done using t-test. ***p-value 0.0002, ****p-value < 0.0001. Data provided by Meisam Bagheri & Deepak Saini, IISc Bangalore.

Nitric oxide and reactive nitrogen species (RNS) are well known to induce DNA damage, especially double strand breaks (DSBs). Therefore, we monitored the ability of **27** to induce DNA damage by monitoring 53BP1 foci, which are markers of double strand breaks and accumulate as nuclear foci. HeLa cells stably expressing 53BP1 fused to GFP were seeded on glass-bottom dishes and independently treated with **27** and imaged 6 h post-treatment. As expected, we found an increase in DNA damage induced by **27** as evidenced by increased foci, increased foci are indicative of enhanced DNA damage response suggesting the involvement of reactive nitrogen species (RNS) in the observed phenotype. When the concentration of **27** was varied, a

dose-dependent increase in 53BP1 foci was observed (Figure 16). Under similar conditions, an increase in the fluorescence signal attributable to **12** in DAPI channel was also observed (Figure 16) suggesting the suitability of Thera/NO for real-time monitoring of NO.

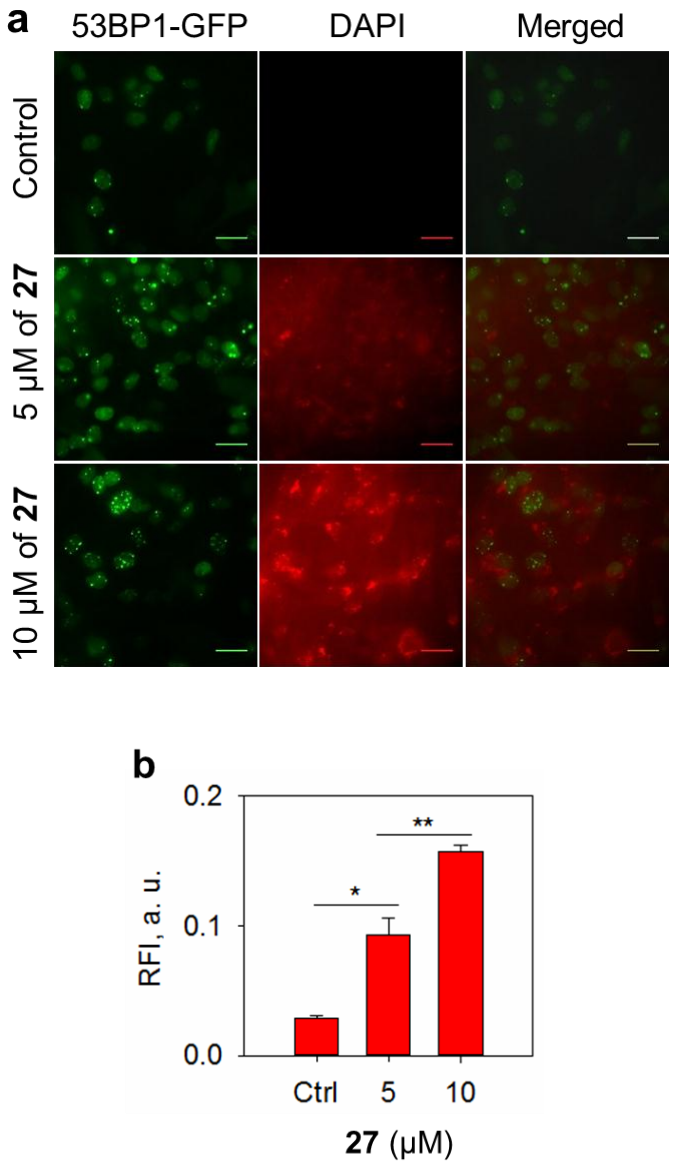

Figure 16. (a) Formation of 53BP1 foci and enhancement of fluorescence signal attributable to **12** upon exposure of **27** in HeLa cells. Images were taken in GFP channel (for foci) and DAPI channel (for **12**) with fixed acquisition settings. DAPI images have been pseudocolored (red) for better visualization. Scale bar 100 µm. All images were acquired with identical image acquisition parameters. (b) Quantification of fluorescence intensity was done using ImageJ software and statistical analysis was done using t-test. *p-value 0.0112, **p-value 0.0086. Data provided by Meisam Bagheri & Deepak Saini, IISc Bangalore.

Finally, the cytotoxic effect of compound **27** was evaluated with MRC5 (normal fibroblast) and cancer cell lines: A549, HeLa, MDA-MB-231 by an Alamar blue assay, as expected we found compound **27** showed significant cytotoxic effect towards cancer cells compared with normal cells (Figure 17).

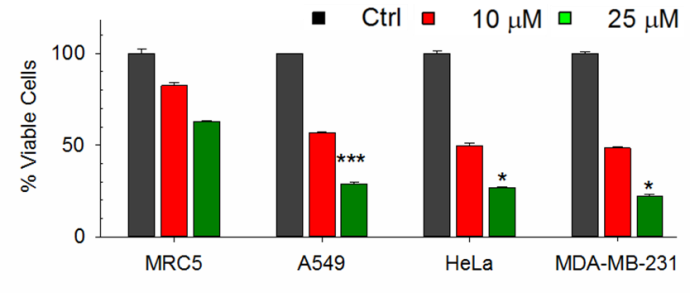

Figure 17. Comparison of cytotoxic effect of **27** (10 and 25 µM) on primary cell (MRC5) versus cancer cells (A549, HeLa and MDA-MB 231 cells) after incubation for 12 h. Statistical analysis at 25 µM: A549 vs MRC5, p-value 0.0096; HeLa vs MRC5, p-value 0.014; MDA-MB-231 vs MRC5, p-value 0.028. Data provided by Meisam Bagheri & Deepak Saini, IISc Bangalore.

Chapter 5: Esterase Sensitive ROS generator with a Fluorescence Reporter

In addition to NO, a number of other redox active reactive species have important biological roles. Controlled generation as well as reliable detection of these species is challenging. In order to assess the generality of the method developed herein, we aimed to develop a ROS generator with a fluorescence reporter (**28**). Upon activation of **32** by esterase, self-immolation and reaction with water produces **12** and **28**, which dissociates at pH 7.4 to produce ROS (Scheme 7).

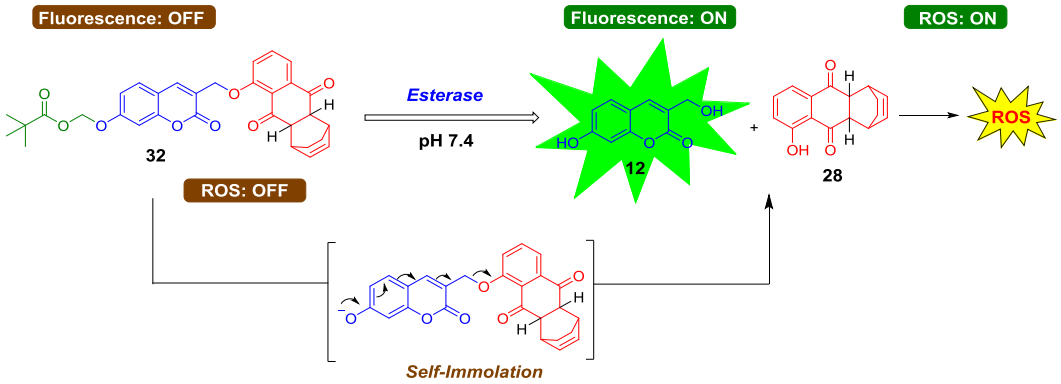

Scheme 7. Proposed mechanism of activation of **32** to produce **12** and **ROS**

First, the ability of the compound **32** to generate ROS and fluorescence signal in phosphate buffer was evaluated. Compound **32** was treated with esterase and the

fluorescence signal attributable to **12** as well as ROS was independently monitored. The fluorescence signal at 460 nm was measured using a micro-well plate reader while ROS generation was measured by luminol assay. In the presence of esterase, a gradual increase in fluorescence signal attributable to **12** was observed during 60 min (Figure 18.a). However under similar conditions, there is no significant fluorescence signal was seen from **32** in the absence of esterase. Similarly, when ROS was monitored, we found that the compound generated ROS only in the presence of esterase (Figure 18.b).

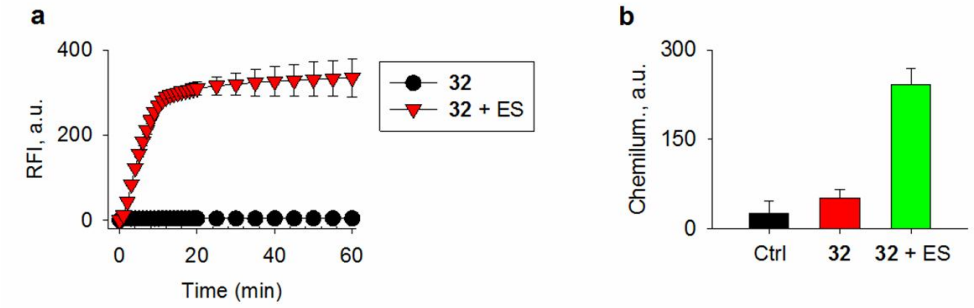

Figure 18. (a) Fluorescence response of **32** (25 µM) in the absence and presence of ES (0.5 U/mL) in pH 7.4 buffer. (b) Superoxide generation from **32** (25 µM) in pH 8.0 buffer at 37 ºC after 60 min was estimated by a luminol-based chemiluminescence assay.

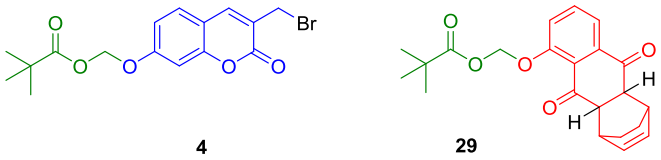

Scheme 8. Structure of **4** and **29**

Next, we studied the capability of compound **32** to enhance fluorescence signal as well as ROS within the cells, A549 cells were treated with 25 µM of compounds (**4**, **32**, and **29**). After 30 min, the fluorescence signal at 460 nm was measured using a micro-well plate reader, while ROS enhancement was measured by 2,7-dichlorodihydrofluorescein-diacetate (H_2DCF-DA)-based fluorescence assay. With a control compound **4** (does not contain diazeniumdiolate, Scheme 8), an increase in the fluorescence signal was seen but no significant ROS enhancement (Figure 19.a, 19.b); and with a control compound **29** (does not contain coumarin, Scheme 8), an increase in ROS was observed with no significant fluorescence signal (Figure 19.a, 19.b). Whereas, compound **32** is able to enhance both fluorescence signal as well as ROS

was observed (Figure 19.a, 19.b). When the incubation time and dose of **32** was varied, as expected, a dose-dependent increase in fluorescence signal was observed (Figure 19.c), thus supporting the suitability of **32** to enhance ROS as well as fluorescence within cells. Thus, when cells are treated with **32** and the fluorescence signal at 460 nm is a reporter for ROS generated.

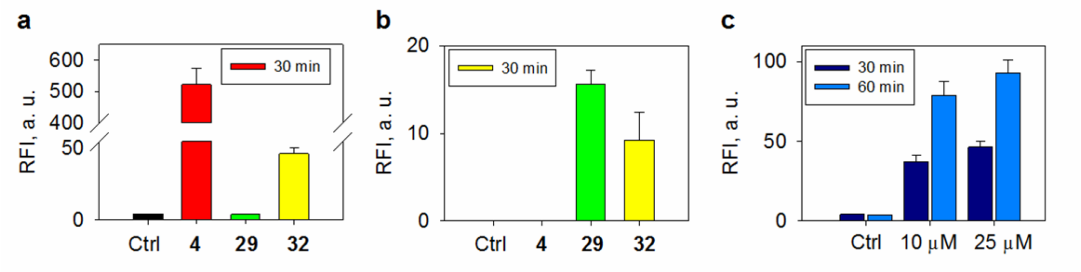

Figure 19. Comparison of fluorescence intensity attributable to **12** (a) and (b) ROS generation upon incubation of A549 cells with 25 µM of **4**, **29** or **32**. (c) Fluorescence intensity attributable to **12** during incubation of A549 cells with **32** at 0, 10 and 25 µM with different time at 37 °C (excitation 320 nm; emission 460 nm). Intracellular ROS enhancement was measured using a $DCFH_2$-DA assay (excitation 490 nm; emission 520 nm).

In order to study the cellular uptake of **32**, A549 cells were treated with **32** for 60 min and the fluorescence signal attributable to the formation of **12** at 460 nm was monitored by confocal microscopy. An increase in fluorescence signal was observed (Figure 20). These results supporting that, the compound **32** permeate cells and get activated by cellular esterase to produce fluorescence signal attributable to **12**.

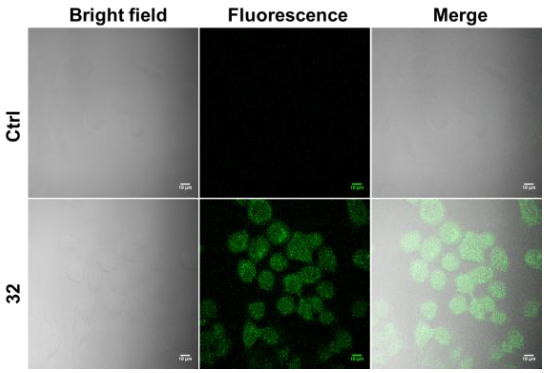

Figure 20. Confocal microscopy images of A549 cells treated with **32** (25 µM) for 60 min at 37 °C. Images were taken using DAPI channel and pseudocolored (green) for better visualisation. Scale bar = 10 µm.

Next, we investigated the capability of **32** to produce ROS in cells was evaluated using DCF assay. A549 lung carcinoma cells were treated with **32** (25 μM) for 1h and followed by cells were stained with H_2DCF-DA dye (10 μM) for 10 min and the fluorescence signal attributable to DCF was monitored in GFP channel. In this assay, Compound **4** was used as negative control and **29** was used as positive control for ROS generation. As expected we found increase in the DCF fluorescence signal for compound **29** and **32** (Figure 21). Together these results provide the evidence for the ability of **32** to enhance ROS in cells.

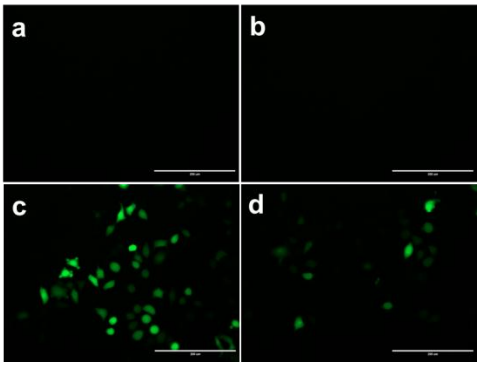

Figure 21. Fluorescence microscopy images of A549 cells treated with a) H_2DCF-DA dye alone (10 μM) b) **4** (25 μM) c) **29** (25 μM) d) **32** (25 μM) for 60 min at 37 °C. Images were taken using GFP channel. Scale bar = 200 μm.

References

(1) Ignarro, L. J. *Angew. Chem. Int. Ed.* **1999**, *38*, 1882.

(2) Wink, D. A.; Hines, H. B.; Cheng, R. Y.; Switzer, C. H.; Flores-Santana, W.; Vitek, M. P.; Ridnour, L. A.; Colton, C. A. *J. Leukoc. Biol.* **2011**, *89*, 873.

(3) Thomas, D. D.; Ridnour, L. A.; Isenberg, J. S.; Flores-Santana, W.; Switzer, C. H.; Donzelli, S.; Hussain, P.; Vecoli, C.; Paolocci, N.; Ambs, S.; Colton, C. A.; Harris, C. C.; Roberts, D. D.; Wink, D. A. *Free Radic. Biol. Med.* **2008**, *45*, 18.

(4) Huang, Z.; Fu, J.; Zhang, Y. *J. Med. Chem.* **2017**, *60*, 7617.

(5) Tozer, G. M.; Prise, V. E.; Chaplin, D. J. *Cancer research* **1997**, *57*, 948.

(6) Doyle, L. A.; Yang, W.; Abruzzo, L. V.; Krogmann, T.; Gao, Y.; Rishi, A. K.; Ross, D. D. *PNAS* **1998**, *95*, 15665.

(7) Eckford, P. D. W.; Sharom, F. J. *Chem. Rev.* **2009**, *109*, 2989.

(8) Riganti, C.; Miraglia, E.; Viarisio, D.; Costamagna, C.; Pescarmona, G.; Ghigo, D.; Bosia, A. *Cancer research* **2005**, *65*, 516.

(9) Chegaev, K.; Riganti, C.; Lazzarato, L.; Rolando, B.; Guglielmo, S.; Campia, I.; Fruttero, R.; Bosia, A.; Gasco, A. *ACS Med. Chem. Lett.* **2011**, *2*, 494.

(10) Riganti, C.; Rolando, B.; Kopecka, J.; Campia, I.; Chegaev, K.; Lazzarato, L.; Federico, A.; Fruttero, R.; Ghigo, D. *Mol. Pharmaceutics* **2013**, *10*, 161.

(11) Sharma, K.; Chakrapani, H. *Nitric Oxide* **2014**, *43*, 8.

(12) Szabo, C. *Nat. Rev. Drug. Discov.* **2016**, *15*, 185.

(13) Wang, P. G.; Xian, M.; Tang, X.; Wu, X.; Wen, Z.; Cai, T.; Janczuk, A. J. *Chem. Rev.* **2002**, *102*, 1091.

(14) Keefer, L. K. *ACS Chem. Biol.* **2011**, *6*, 1147.

(15) Cai, T. B.; Lu, D. N.; Landerholm, M.; Wang, P. G. *Org. Lett.* **2004**, *6*, 4203.

(16) Saavedra, J. E.; Shami, P. J.; Wang, L. Y.; Davies, K. M.; Booth, M. N.; Citro, M. L.; Keefer, L. K. *J. Med. Chem.* **2000**, *43*, 261.

(17) Chakrapani, H.; Maciag, A. E.; Citro, M. L.; Keefer, L. K.; Saavedra, J. E. *Org. Lett.* **2008**, *10*, 5155.

(18) Chakrapani, H.; Showalter, B. M.; Kong, L.; Keefer, L. K.; Saavedra, J. E. *Org. Lett.* **2007**, *9*, 3409.

(19) Chakrapani, H.; Showalter, B. M.; Citro, M. L.; Keefer, L. K.; Saavedra, J. E. *Org. Lett.* **2007**, *9*, 4551.

(20) Sharma, K.; Iyer, A.; Sengupta, K.; Chakrapani, H. *Org. Lett.* **2013**, *15*, 2636.

(21) Nagano, T.; Yoshimura, T. *Chem. Rev.* **2002**, *102*, 1235.

(22) Chan, J.; Dodani, S. C.; Chang, C. J. *Nat Chem* **2012**, *4*, 973.

(23) Li, H.; Wan, A. *Analyst* **2015**, *140*, 7129.

(24) Coneski, P. N.; Schoenfisch, M. H. *Chem. Soc. Rev.* **2012**, *41*, 3753.

(25) Hunter, R. A.; Storm, W. L.; Coneski, P. N.; Schoenfisch, M. H. *Anal. Chem.* **2013**, *85*, 1957.

(26) Rose, M. J.; Fry, N. L.; Marlow, R.; Hinck, L.; Mascharak, P. K. *J. Am. Chem. Soc.* **2008**, *130*, 8834.

(27) Rose, M. J.; Mascharak, P. K. *Chem. Commun.* **2008**, 3933.

(28) Fry, N. L.; Wei, J.; Mascharak, P. K. *Inorg. Chem.* **2011**, *50*, 9045.

(29) Vittorino, E.; Sciortino, M. T.; Siracusano, G.; Sortino, S. *ChemMedChem* **2011**, *6*, 1551.

(30) Vittorino, E.; Sciortino, M. T.; Siracusano, G.; Sortino, S. *ChemMedChem.* **2011**, *6*, 1551.

(31) Weinstain, R.; Segal, E.; Satchi-Fainaro, R.; Shabat, D. *Chem. Commun.* **2010**, *46*, 553.

(32) Biswas, K. H.; Sopory, S.; Visweswariah, S. S. *Biochemistry* **2008**, *47*, 3534.

(33) Szatrowski, T. P.; Nathan, C. F. *Cancer research* **1991**, *51*, 794.

(34) Hagen, H.; Marzenell, P.; Jentzsch, E.; Wenz, F.; Veldwijk, M. R.; Mokhir, A. *J. Med. Chem.* **2012**, *55*, 924.

(35) Kuang, Y.; Balakrishnan, K.; Gandhi, V.; Peng, X. *J. Am. Chem. Soc.* **2011**, *133*, 19278.

(36) Kumar, R.; Han, J.; Lim, H.-J.; Ren, W. X.; Lim, J.-Y.; Kim, J.-H.; Kim, J. S. *J. Am. Chem. Soc.* **2014**, *136*, 17836.

(37) Dickinson, B. C.; Chang, C. J. *J. Am. Chem. Soc.* **2008**, *130*, 9638.

(38) Miller, E. W.; Tulyanthan, O.; Isacoff, E. Y.; Chang, C. J. *Nat. Chem. Biol.* **2007**, *3*, 263.

List of Figures

List of Schemes

List of Tables

List of Publications

1. **Ravikumar, G**.; † Bagheri, M.; † Saini, D. K.; Chakrapani, H. "A Small Molecule for TheraNOstic Targeting of Cancer Cells" *Chemical Communications*, **2017**, *53*, 13352-13355 († Equal Contribution).

2. **Ravikumar, G**.; Bagheri, M.; Saini, D. K.; Chakrapani, H. "FLUORO/NO, a Nitric Oxide Donor with a Fluorescence Reporter" *ChemBioChem* **2017**, *18*, 1529-1534.

3. Dharmaraja, A. T.; † **Ravikumar, G**.; † Chakrapani, H. "Arylboronate ester based diazenium diolates (BORO/NO), a class of hydrogen peroxide inducible nitric oxide donors" *Organic Lett*ers, **2014**, *16*, 2610-2613 († Equal Contribution).

4. Chauhan, P.; Bora, P.; **Ravikumar, G**.; Jos, S.; Chakrapani, H. "Esterase Activated Carbonyl Sulfide/Hydrogen Sulfide (H_2S) Donors" *Organic Letters*, **2017**, *19*, 62-65.

5. Pardeshi, K. A.; **Ravikumar, G**.; Chakrapani, H. "Esterase Sensitive Self-Immolative Sulfur Dioxide (SO_2) Donors" Organic *Letters*, **2017**, *20*, 4-7.

6. **Ravikumar, G**.; Chakrapani, H. "Synergistic Activities of Nitric Oxide and Various Drugs" in NITRIC OXIDE DONORS, Novel Biomedical Applications and Perspectives **2017** Academic Press 293-307.

Manuscripts in Preparation

1. Kelkar, D. S.; † **Ravikumar, G**.; † Mehendale, N.; † Singh, S.; † Joshi, A.; Sharma, A. K.; Mhetre, A.; Rajendren, A.; Chakrapani, H.; Kamat, S. S. "A Chemical Genetic Screen Identifies ABHD12 as an Oxidized Phosphatidylserine Lipase" († Equal Contribution).
2. **Ravikumar, G**.; Chakrapani, H. "Reat-time Monitoring of ROS generator with a fluorescence reporter"

Organic LETTERS

Letter

pubs.acs.org/OrgLett

Arylboronate Ester Based Diazeniumdiolates (BORO/NO), a Class of Hydrogen Peroxide Inducible Nitric Oxide (NO) Donors

Allimuthu T. Dharmaraja,[†] Govindan Ravikumar,[†] and Harinath Chakrapani*

Indian Institute of Science Education and Research Pune, Dr. Homi Bhabha Road, Pashan, Pune 411 008, Maharashtra, India

Supporting Information

ABSTRACT: Here, we report the design, synthesis, and evaluation of arylboronate ester based diazeniumdiolates (BORO/NO), a class of nitric oxide (NO) donors activated by hydrogen peroxide (H_2O_2), a reactive oxygen species (ROS), to generate NO. We provide evidence for the NO donors' ability to permeate bacteria to produce NO when exposed to H_2O_2 supporting possible applications for BORO/NO to study molecular mechanisms of NO generation in response to elevated ROS.

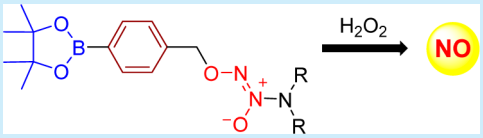

Although reactive oxygen species (ROS) such as hydrogen peroxide (H_2O_2) mediate numerous physiological processes,[1] elevated levels of ROS can cause oxidative stress leading to cell death.[2−6] Similarly, nitric oxide (NO), a reactive nitrogen species (RNS), has multifarious functions and effects in cells, but increased NO has been associated with nitrosative stress and growth inhibition.[7−10] Both ROS and RNS are generated during immune response to counter infectious pathogens, presumably due to their ability to synergize[11,12] leading to increased damaging effects.[13−15] However, due to its antioxidant capability,[16,17] NO has also been implicated in protecting bacteria from oxidative stress and may hence contribute to bacterial drug resistance.[18−20] Thus, the precise effects of NO when generated in the presence of elevated ROS are yet to be completely understood.

Due to its diverse roles, NO for use in biological studies must be generated in a controlled manner and preferably in response to a stimulus.[21,22] A number of nitric oxide donors are available, but among these, sodium salts of diazeniumdiolates (such as DEA/NO **1a**, Scheme 1) are reliable sources of NO.[23] However, these NO donor salts lack specificity and would generate NO in the absence of H_2O_2 as well. Diazeniumdiolate anions can, however, be derivatized into "protected" forms, which can be activated in the presence of a specific metabolic trigger to generate NO.[24,25] Numerous methodologies[11,12,26−33] for cleavage of otherwise stable diazeniumdiolate derivatives are known, but to our knowledge a nitric oxide donor that is selectively activated by ROS is not available.

Boronate ester protecting groups are highly specific to cleavage by H_2O_2 and have been extensively used in imaging[34−37] as well as in drug delivery.[38−41] For mechanistic studies with bacteria, elevated H_2O_2 is frequently used to simulate conditions of oxidative stress.[2,42] Arylboronate ester based diazeniumdiolates (BORO/NO), a class of diazeniumdiolate derivatives that are attached to a pinacolboronate ester through a self-immolative aryl linker, were considered as H_2O_2 activated NO donors (Scheme 1). Reaction of BORO/NO with H_2O_2 should produce the phenolate intermediate **I**, which could rearrange to produce the diazeniumdiolate anion, which in pH 7.4 releases NO (Scheme 1.).

Following a reported procedure, compound **5** was synthesized by bromination of **4**[43,44] (Figure 1) and reacted with DEA/NO **1a** to obtain **2a** (Scheme 2). A similar procedure was used to synthesize **2b−2d** by the reaction of

Scheme 1. BORO/NO, H_2O_2 Activated NO Donors

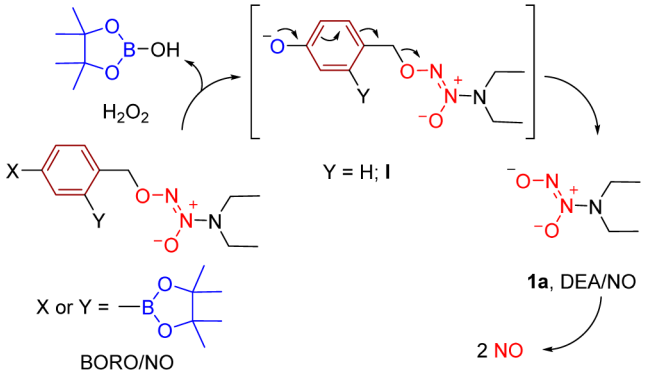

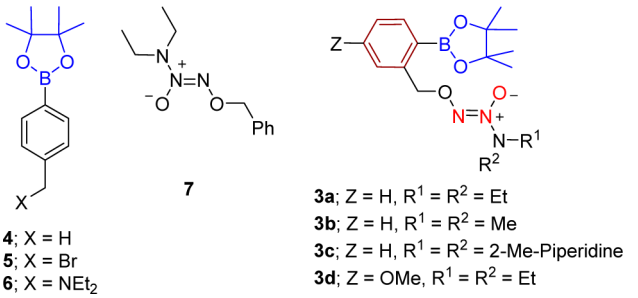

Figure 1. Structure of compounds **4−7** and **3a−3d**.

Received: March 11, 2014
Published: May 5, 2014

dx.doi.org/10.1021/ol5010643 | Org. Lett. 2014, 16, 2610−2613

Scheme 2. Synthesis of 4-BORO/NO Derivatives

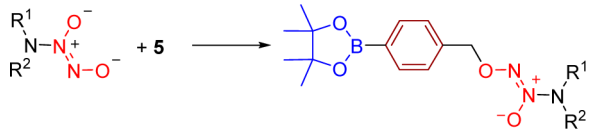

1a; $R^1 = R^2 = Et$ **2a**; $R^1, R^2 = Et$
1b; $R^1 = R^2 = Me$ **2b**; $R^1, R^2 = Me$
1c; R^1R^2N = pyrrolidine **2c**; R^1R^2N = pyrrolidine
1d; R^1R^2N = 2-Me-piperidine **2d**; R^1R^2N = 2-Me-piperidine

the bromide **5** with the corresponding diazeniumdiolate salts, **1b**–**1d** (Scheme 2).[45] In order to study possible differences in 1,4- versus 1,2-elimination[38] of the phenolate intermediate generated during hydrogen peroxide activated NO release from this class of compounds, derivatives **1a**, **1b**, and **1d** were reacted with the corresponding 2-(pinacol boronate ester)benzyl bromides to produce **3a**–**3d** (Figure 1).

The 4-BORO/NO derivative **2a** was incubated in pH 7.4 buffer, and no evidence for NO production in the headspace was found as determined by a chemiluminescence-based assay that is selective for NO (Figure 2a). In the presence of H_2O_2,

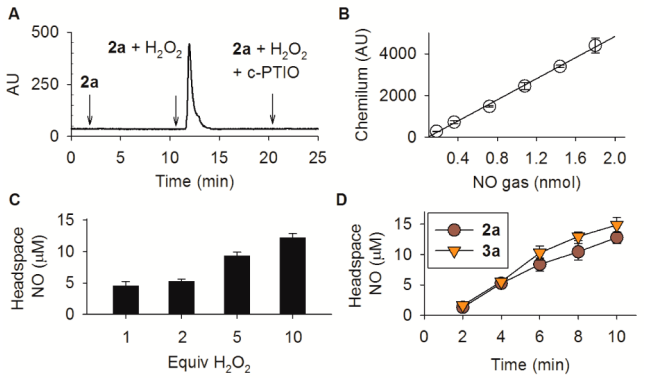

Figure 2. Nitric oxide analysis in the headspace[a] using a chemiluminescence detector: (a) Traces for **2a** alone, in the presence of H_2O_2 with and without a NO scavenger;[b] (b) Calibration curve generated using NO gas; (c) NO generated by **2a** with increasing equivalents of H2O2; (d) Time course of NO generated during incubation of **2a** and **3a** in the presence of 10 equiv H_2O_2. [a] Experiments were conducted in 10 mM pH 7.4 phosphate buffer containing 100 μM of diethylene triamine pentaacetic acid (DTPA), a metal ion chelating agent at 37 °C. Reaction mixtures from headspace of reaction vial were injected into a chemiluminescene-based nitric oxide analyzer using argon as the carrier gas. [b] Arrow indicates injection of sample.

we found significant levels of NO produced (Figure 2a). When **2a** was incubated in the presence of H_2O_2 and (2-(4-carboxyphenyl)-4,4,5,5-tetramethyl imidazoline-1-oxyl-3-oxide (c-PTIO), a scavenger for NO, we found nearly complete abrogation of signal attributable to NO in the headspace confirming NO generation by **2a** (Figure 2a). A calibration curve with nitric oxide gas was generated using authentic NO gas (linear regression analysis coefficient, R^2 = 0.998, Figure 2b).

Next, hydrogen peroxide induced NO generation in solution was analyzed. First, a calibration curve with sodium nitrite in a reducing mixture, which converts nitrite to NO, was generated (linear regression analysis coefficient, R^2 = 0.999, Figure 3a). We found evidence for nitric oxide production during

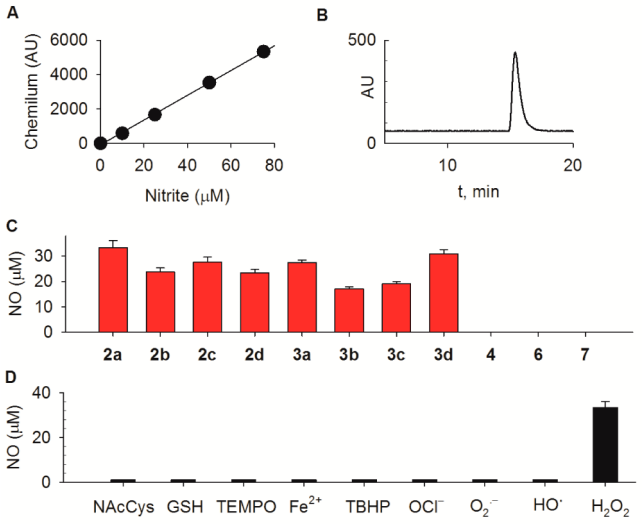

Figure 3. Solution phase nitric oxide analysis using a chemiluminescence detector: (a) Calibration curve generated using sodium nitrite; (b) Representative spectrum when a solution of **2a** in H_2O_2 was analyzed; (c) Nitric oxide analysis of BORO/NO derivatives and **4**, **6**, and **7**; (d) NO generated in solution when incubated with various biologically relevant species. Aliquots from the solution phase of the reaction vial were injected into a chemiluminescene-based nitric oxide analyzer using argon as the carrier gas containing a reducing mixture. Under these conditions, values of NO reported are NO + nitrite. NAcCys: *N*-acetyl cysteine; GSH: glutathione; TEMPO: 2,2,6,6-tetramethylpiperidinyloxy; Fe^{2+}; TBHP: *tert*-butyl hydroperoxide; OCl^-: sodium hypochlorite; $O_2^{-\bullet}$: generated using hypoxanthine/xanthine oxidase; $HO^\bullet$ was generated using H_2O_2 and Fe(II) mixed at a 1:10 ratio; here, DTPA was not added.

incubation of **2a** in the presence of H_2O_2 in buffer (Figure 3b; see Supporting Information Figure S3). When **2a** (25 μM) was incubated with varying equivalents of H_2O_2, we found a dose-dependent increase in nitric oxide produced after 10 min (Figure 2c; see Supporting Information, Table S6) and 10 equiv of H_2O_2 were chosen for further studies.

A time course of headspace NO produced during incubation of **2a** (25 μM) in the presence of H_2O_2 (10 equiv) showed a gradual increase of NO during 10 min, and the yield of NO was nearly 12 μM (Figure 2d). When the other analogues **2b**–**2d** and **3a**–**3d** were tested, we found nitric oxide production only when exposed to H_2O_2 and the yields of NO (see Supporting Information, Table S1 and Figure 3c) were comparable or lower than the yield of NO produced during incubation of **2a** under similar conditions. A time course of NO production during incubation of the 2-BORO/NO derivative **3a** in the presence of H_2O_2 showed no major difference in the rate of NO release possibly because 1,2- and 1,4-eliminations occurred at comparable rates (Figure 2d).

Compound **4** (Figure 1) which contained the boronate ester but no capability to generate NO did not produce significant levels of NO during incubation with H_2O_2 (Figure 3c). Next, the diethylamino derivative **6** and benzyl derivative of DEA/NO, **7** (Figure 1), were prepared using reported procedures (see Supporting Information). During incubation with H_2O_2 (10 equiv), as expected, we found no evidence for NO generation by these compounds suggesting the requirement for the boronate ester functionality as well as the diazeniumdiolate for NO production (Figure 3c).

dx.doi.org/10.1021/ol5010643 | *Org. Lett.* 2014, 16, 2610–2613

Having established that BORO/NO derivatives were capable of generating NO when triggered by H_2O_2, a number of biologically relevant nucleophiles, reductants, and oxidants were utilized to study the selectivity of activation of **2a** to produce NO (Figure 3d). The NO donor **2a** was found to be highly specific toward activation by H_2O_2 and did not generate significant levels of NO in the presence of biologically relevant thiols, metal ions, antioxidants, and other common ROS (Figure 3d). The observed specificity is consistent with previously published data on reactivity of boronate esters toward H_2O_2.[36,46]

In order to study if BORO/NO was capable of generating NO in bacteria, *Escherichia coli* (*E. coli*) cells were incubated with **2a** (25 μM). The ability of this compound to enhance NO was studied by measuring extracellular nitrite using a Griess assay. We found negligible NO during incubation of **2a** alone, but under similar conditions, when **2a** was cotreated with H_2O_2, we found a significant increase in extracellular nitrite, a marker for increased NO (Figure 4a). The amount of nitrite

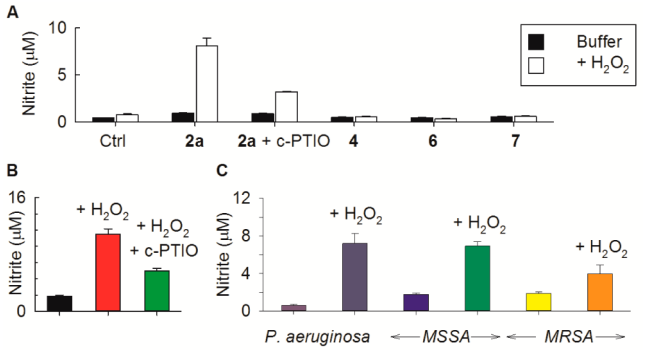

Figure 4. (a) Extracellular nitrite in *E. coli* after 1 h; (b) Intracellular NO from **2a** in *E. coli*; (c) Extracellular nitrite release upon incubation of **2a** in the presence of Gram-positive and Gram-negative bacteria.

generated was diminished when cotreated with c-PTIO, a scavenger for NO. Compounds **4**, **6**, and **7**, which did not generate NO upon reaction with H_2O_2 in buffer (Figure 3c), were incapable of enhancing nitrite when incubated with bacteria and H_2O_2 (Figure 4a).

We next studied the ability of **2a** to enhance intracellular NO levels in *E. coli* in the presence of elevated levels of H_2O_2.[47] Bacteria were incubated with **2a** (100 μM) for 30 min followed by centrifugation of the bacterial suspension to aspirate out any excess **2a** in the medium. The collected bacterial pellet was resuspended with buffer and plated in a 96-well microplate, and cells were incubated with and without added H_2O_2 at 37 °C. Any NO that is produced must be due to **2a** that has permeated bacteria. After 30 min, Griess reagent was added and we found significantly increased NO in bacteria treated with H_2O_2 in comparison with untreated cells (Figure 4b). Under similar conditions, when bacterial cells were treated with H_2O_2 and c-PTIO, a NO scavenger, we found diminished nitrite supporting the intermediacy of NO during decomposition of **2a** (Figure 4b). Taken together, our data support **2a** as a cell permeable hydrogen peroxide activated NO donor.

The capability of **2a** to enhance NO in other Gram-negative and Gram-positive bacteria, *Pseudomonas aeruginosa* (*P. aeruginosa*), methicillin-sensitive *Staphylococcus aureus* (MSSA), and methicillin-resistant *Staphylococcus aureus* (MRSA), was studied. We found that incubation of these bacteria with **2a** resulted in increased nitrite (see Supporting Information) in the presence of hydrogen peroxide (Figure 4c).

Taken together, we report BORO/NO, a novel class of cell permeable H_2O_2 activated NO donors. Antibiotic resistance is emerging as a major global health problem with millions affected each year, and the role of NO in bacteria developing drug resistance remains unclear. NO has been reported to synergize with silver(I) sulfadiazine, an oxidative stress inducing antimicrobial, against a host of bacteria including *S. aureus* suggesting the possible use of NO in combination therapy. In contrast, NO generated by bacterial nitric oxide synthase (bNOS) has been proposed as a possible cellular antioxidant that protects MRSA from oxidative stress,[18−20] and specific bNOS inhibitors are in development as possible drug candidates.[48] Thus, molecular mechanisms of NO-derived protective effects (or otherwise)[16,17] remain to be elucidated and it is anticipated that BORO/NO will be useful in deciphering such mechanisms.[42] The use of BORO/NO for localized delivery of NO to cancers,[24,25] which are known to have elevated ROS as a phenotype, and other applications are currently under investigation.[24,25,49,50]

■ ASSOCIATED CONTENT

Supporting Information

Synthesis, characterization data, assay protocols and associated data. This material is available free of charge via the Internet at http://pubs.acs.org.

■ AUTHOR INFORMATION

Corresponding Author

*E-mail: harinath@iiserpune.ac.in.

Author Contributions

†These authors contributed equally.

Notes

The authors declare no competing financial interest.

■ ACKNOWLEDGMENTS

The authors thank IISER Pune and the Department of Biotechnology, Ministry of Science and Technology, India (DBT, BT/PR6798/MED/29/636/2012) for financial support. A.T.D. and G.R. acknowledge research fellowships from Council for Scientific and Industrial Research (CSIR). Diazeniumdiolate salts were a gift from Dr. Larry Keefer and Dr. Joseph Saavedra (Chemical Biology Laboratory, National Cancer Institute).

■ REFERENCES

(1) Imlay, J. A. *Nat. Rev. Microbiol.* **2013**, *11*, 443.
(2) Brynildsen, M. P.; Winkler, J. A.; Spina, C. S.; MacDonald, I. C.; Collins, J. J. *Nat. Biotechnol.* **2013**, *31*, 160.
(3) Foti, J. J.; Devadoss, B.; Winkler, J. A.; Collins, J. J.; Walker, G. C. *Science* **2012**, *336*, 315.
(4) Kohanski, M. A.; Dwyer, D. J.; Hayete, B.; Lawrence, C. A.; Collins, J. J. *Cell* **2007**, *130*, 797.
(5) Ruben Morones-Ramirez, J.; Winkler, J. A.; Spina, C. S.; Collins, J. J. *Sci. Transl. Med.* **2013**, *5*, 190ra81.
(6) Dharmaraja, A. T.; Alvala, M.; Sriram, D.; Yogeeswari, P.; Chakrapani, H. *Chem. Commun.* **2012**, *48*, 10325.
(7) Hirst, D.; Robson, T. *J. Pharm. Pharmacol.* **2007**, *59*, 3.
(8) Huerta, S.; Chilka, S.; Bonavida, B. *Int. J. Oncol.* **2008**, *33*, 909.
(9) Lu, Y.; Slomberg, D. L.; Shah, A.; Schoenfisch, M. H. *Biomacromolecules* **2013**, *14*, 3589.

(10) Sun, B.; Slomberg, D. L.; Chudasama, S. L.; Lu, Y.; Schoenfisch, M. H. *Biomacromolecules* **2012**, *13*, 3343.
(11) Kiziltepe, T.; Hideshima, T.; Ishitsuka, K.; Ocio, E. M.; Raje, N.; Catley, L.; Li, C.-Q.; Trudel, L. J.; Yasui, H.; Vallet, S.; Kutok, J. L.; Chauhan, D.; Mitsiades, C. S.; Saavedra, J. E.; Wogan, G. N.; Keefer, L. K.; Shami, P. J.; Anderson, K. C. *Blood* **2007**, *110*, 709.
(12) Maciag, A. E.; Chakrapani, H.; Saavedra, J. E.; Morris, N. L.; Holland, R. J.; Kosak, K. M.; Shami, P. J.; Anderson, L. M.; Keefer, L. K. *J. Pharmacol. Exp. Ther.* **2011**, *336*, 313.
(13) Fang, F. C. *Nat. Rev. Microbiol.* **2004**, *2*, 820.
(14) Nathan, C.; Cunningham-Bussel, A. *Nat. Rev. Immunol.* **2013**, *13*, 349.
(15) Privett, B. J.; Deupree, S. M.; Backlund, C. J.; Rao, K. S.; Johnson, C. B.; Coneski, P. N.; Schoenfisch, M. H. *Mol. Pharmaceutics* **2010**, *7*, 2289.
(16) Hummel, S. G.; Fischer, A. J.; Martin, S. M.; Schafer, F. Q.; Buettner, G. R. *Free Radical Biol. Med.* **2006**, *40*, 501.
(17) Joshi, M. S.; Ponthier, J. L.; Lancaster, J. R., Jr. *Free Radical Biol. Med.* **1999**, *27*, 1357.
(18) Van Sorge, N. M.; Beasley, F. C.; Gusarov, I.; Gonzalez, D. J.; Von Köckritz-Blickwede, M.; Anik, S.; Borkowski, A. W.; Dorrestein, P. C.; Nudler, E.; Nizet, V. *J. Biol. Chem.* **2013**, *288*, 6417.
(19) Gusarov, I.; Nudler, E. *Proc. Natl. Acad. Sci. U.S.A.* **2005**, *102*, 13855.
(20) Gusarov, I.; Shatalin, K.; Starodubtseva, M.; Nudler, E. *Science* **2009**, *325*, 1380.
(21) Wang, P. G.; Xian, M.; Tang, X.; Wu, X.; Wen, Z.; Cai, T.; Janczuk, A. J. *Chem. Rev.* **2002**, *102*, 1091.
(22) Chakrapani, H.; Bartberger, M. D.; Toone, E. J. *J. Org. Chem.* **2009**, *74*, 1450.
(23) Hrabie, J. A.; Keefer, L. K. *Chem. Rev.* **2002**, *102*, 1135.
(24) Keefer, L. K. *Annu. Rev. Pharmacol. Toxicol.* **2003**, *43*, 585.
(25) Keefer, L. K. *ACS Chem. Biol.* **2011**, *6*, 1147.
(26) Chakrapani, H.; Kalathur, R. C.; Maciag, A. E.; Citro, M. L.; Ji, X.; Keefer, L. K.; Saavedra, J. E. *Bioorg. Med. Chem.* **2008**, *16*, 9764.
(27) Chakrapani, H.; Maciag, A. E.; Citro, M. L.; Keefer, L. K.; Saavedra, J. E. *Org. Lett.* **2008**, *10*, 5155.
(28) Chakrapani, H.; Showalter, B. M.; Kong, L.; Keefer, L. K.; Saavedra, J. E. *Org. Lett.* **2007**, *9*, 3409.
(29) Nandurdikar, R. S.; Maciag, A. E.; Hong, S. Y.; Chakrapani, H.; Citro, M. L.; Keefer, L. K.; Saavedra, J. E. *Org. Lett.* **2010**, *12*, 56.
(30) Cai, T. B.; Lu, D. N.; Landerholm, M.; Wang, P. G. *Org. Lett.* **2004**, *6*, 4203.
(31) Saavedra, J. E.; Shami, P. J.; Wang, L. Y.; Davies, K. M.; Booth, M. N.; Citro, M. L.; Keefer, L. K. *J. Med. Chem.* **2000**, *43*, 261.
(32) Sharma, K.; Sengupta, K.; Chakrapani, H. *Bioorg. Med. Chem. Lett.* **2013**, *23*, 5964.
(33) Sharma, K.; Iyer, A.; Sengupta, K.; Chakrapani, H. *Org. Lett.* **2013**, *15*, 2636.
(34) Chung, C.; Srikun, D.; Lim, C. S.; Chang, C. J.; Cho, B. R. *Chem. Commun.* **2011**, *47*, 9618.
(35) Au-Yeung, H. Y.; New, E. J.; Chang, C. J. *Chem. Commun.* **2012**, *48*, 5268.
(36) Chang, M. C. Y.; Pralle, A.; Isacoff, E. Y.; Chang, C. J. *J. Am. Chem. Soc.* **2004**, *126*, 15392.
(37) Miller, E. W.; Tulyanthan, O.; Isacoff, E. Y.; Chang, C. J. *Nat. Chem. Biol.* **2007**, *3*, 263.
(38) Cao, S.; Christiansen, R.; Peng, X. *Chem.—Eur. J.* **2013**, *19*, 9050.
(39) Stone, J. R. *Arch. Biochem. Biophys.* **2004**, *422*, 119.
(40) Hagen, H.; Marzenell, P.; Jentzsch, E.; Wenz, F.; Veldwijk, M. R.; Mokhir, A. *J. Med. Chem.* **2012**, *55*, 924.
(41) Marzenell, P.; Hagen, H.; Sellner, L.; Zenz, T.; Grinyte, R.; Pavlov, V.; Daum, S.; Mokhir, A. *J. Med. Chem.* **2013**, *56*, 6935.
(42) Yadav, R.; Samuni, Y.; Abramson, A.; Zeltser, R.; Casap, N.; Kabiraj, T. K.; L. Banach, M.; Samuni, U. *Free Radical Biol. Med.* **2014**, *67*, 248.
(43) Kuang, Y.; Balakrishnan, K.; Gandhi, V.; Peng, X. *J. Am. Chem. Soc.* **2011**, *133*, 19278.
(44) White, J. R.; Price, G. J.; Schiffers, S.; Raithby, P. R.; Plucinski, P. K.; Frost, C. G. *Tetrahedron Lett.* **2010**, *51*, 3913.
(45) Chakrapani, H.; Showalter, B. M.; Citro, M. L.; Keefer, L. K.; Saavedra, J. E. *Org. Lett.* **2007**, *9*, 4551.
(46) Chan, J.; Dodani, S. C.; Chang, C. J. *Nat. Chem.* **2012**, *4*, 973.
(47) Dharmaraja, A. T.; Chakrapani, H. *Org. Lett.* **2014**, *16*, 398.
(48) Holden, J. K.; Li, H.; Jing, Q.; Kang, S.; Richo, J.; Silverman, R. B.; Poulos, T. L. *Proc. Natl. Acad. Sci. U.S.A.* **2013**, *110*, 18127.
(49) Weinstain, R.; Savariar, E. N.; Felsen, C. N.; Tsien, R. Y. *J. Am. Chem. Soc.* **2013**, *136*, 874.
(50) Ballard, R. A.; Truog, W. E.; Cnaan, A.; Martin, R. J.; Ballard, P. L.; Merrill, J. D.; Walsh, M. C.; Durand, D. J.; Mayock, D. E.; Eichenwald, E. C.; Null, D. R.; Hudak, M. L.; Puri, A. R.; Golombek, S. G.; Courtney, S. E.; Stewart, D. L.; Welty, S. E.; Phibbs, R. H.; Hibbs, A. M.; Luan, X.; Wadlinger, S. R.; Asselin, J. M.; Coburn, C. E. *New Engl. J. Med.* **2006**, *355*, 343.

ChemPubSoc Europe

DOI: 10.1002/cbic.201700155

CHEMBIOCHEM Full Papers

FLUORO/NO: A Nitric Oxide Donor with a Fluorescence Reporter

Govindan Ravikumar,[a] Meisam Bagheri,[b] Deepak Kumar Saini,[b] and Harinath Chakrapani*[a]

Nitric oxide (NO) plays significant signalling roles in cells; the controlled generation of NO is of therapeutic relevance. Although a number of methods for the delivery and detection of NO are available, these events are typically mutually exclusive. Furthermore, the efficiency of delivery of NO can be compromised by detection technologies that consume NO. Here, we report FLUORO/NO, an esterase-activated diazeniumdiolate-based NO donor with an in-built fluorescence reporter. We demonstrate that this compound is capable of enhancing NO within cells in a dose-dependent manner, accompanied by a similar increase in fluorescence. The compatibility of this tool to study NO-mediated signalling as well as NO-mediated stress is demonstrated. FLUORO/NO is a convenient tool that shows NO-like activity and allows monitoring of NO release. This tool will help interrogate the redox biology of NO.

Introduction

Nitric oxide (NO) is a key biomolecule that is produced in nearly all cells and can mediate numerous cellular processes[1] including vasodilation, neurotransmission and immune response.[2] The therapeutic value of NO is well documented, and a complete realisation of its potential relies on precise spatiotemporal control over NO generation.[3] Exogenous sources of NO ("NO donors") are used for this.[4] Some NO donors spontaneously dissociate to produce NO, whereas others are triggered intracellularly and dissociate to produce NO (Scheme 1 A).[5] However, in order to infer the production of NO, assays are used, typically fluorescence-based cellular assays for reactive nitrogen species (Scheme 1 A).[6] As NO and its derivatives are short lived and highly reactive towards biomolecules, precise detection of NO in biological systems is highly challenging. Furthermore, the measurement of NO is invariably associated with consumption of NO.[7] Thus, a strategy where a small molecule can generate NO along with a reporter, preferably fluorescent, for the produced NO would be useful (Scheme 1 B). This eliminates the need for monitoring released NO, and the fluorescence signal that is produced suffices. A number of methodologies for light-activated generation of NO with a fluorescence reporter are known.[8] A photochemical trigger offers spatiotemporal control and is useful for imaging experiments.[8d,9] A possible limitation of these methodologies, however, is the requirement of exposure to a specific wavelengths of light: modification of cell culture conditions to incorporate a light source to achieve NO release might be necessary. Several materials-based methods for NO generation are known, but they might have similar limitations, such as consumption of NO[10] or being a turn-off fluorescence methodology.[11] An NO delivery system with a fluorescence reporter and broad applicability is not yet available.

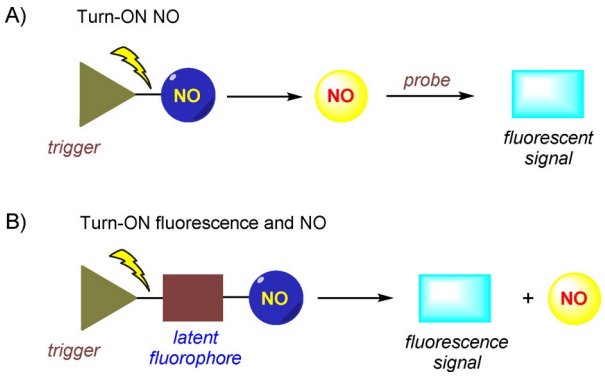

Scheme 1. A) Stimulus-responsive nitric oxide generation by an NO donor requires a secondary probe for detection of NO produced and is associated with collateral consumption of NO. B) Incorporation of a latent fluorophore in the donor eliminates the need for the secondary probe for monitoring of NO.

Derivatives of 7-hydroxycoumarins have been used as latent fluorophores suitable for drug delivery and imaging (Scheme 2).[12] When substituted by an alkyl or aryl group, the compound's fluorescence is diminished. However, upon cleavage of the group to produce a free alcohol, a significant increase in fluorescence is seen. When the 3-position has a methylene functionality containing a suitable leaving group, upon formation of the 7-hydroxycoumarin a rearrangement occurs to release the leaving group (Scheme 2).[12a] We therefore designed FLUORO/NO, which is expected to permeate cells to be cleaved and to produce a highly fluorescent compound (**2**)

[a] G. Ravikumar, Dr. H. Chakrapani
Department of Chemistry
Indian Institute of Science Education and Research
Dr. Homi Bhabha Road, Pune 411008, Maharashtra(India)
E-mail: harinath@iiserpune.ac.in

[b] M. Bagheri, Dr. D. K. Saini
Department of Molecular Reproduction
Development and Genetics, Indian Institute of Science
Bangalore 560012, Karanataka (India)

Supporting information and the ORCID identification numbers for the authors of this article can be found under https://doi.org/10.1002/cbic.201700155.

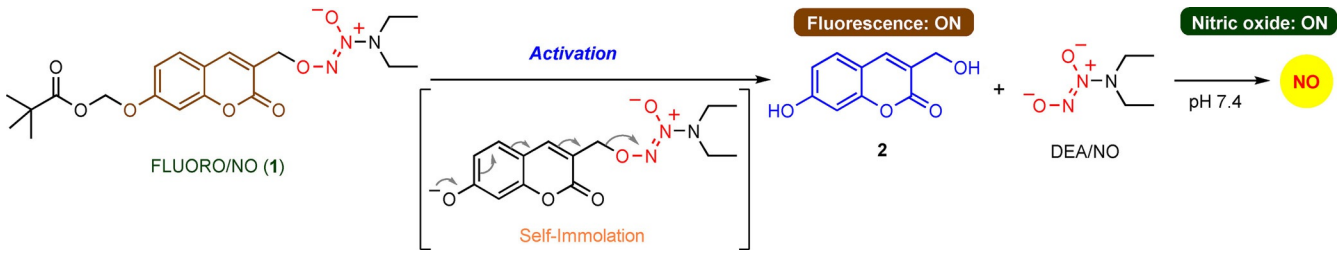

Scheme 2. FLUORO/NO (**1**) is an enzyme-triggerable nitric oxide donor with an in-built fluorescence reporter. FLUORO/NO is expected to have low fluorescence. Upon activation by a suitable trigger, self-immolation and reaction with water produces **2** (highly fluorescent) and DEA/NO, which rapidly dissociates at pH 7.4 to produce NO.

and the NO-releasing diazeniumdiolate[5d–g,13] (DEA/NO; Scheme 2). If the release of NO and **2** is nearly concurrent, a secondary assay for NO is not necessary to monitor NO release. The mechanism of NO release from diazeniumdiolates is well documented.[2b,14] Furthermore, the release from DEA/NO is rapid, and the yield of NO is nearly quantitative. Thus, efficient generation of NO within cells in a short time is anticipated by the use of FLUORO/NO.

Results and Discussion

FLUORO/NO (**1**) was synthesised in three steps from 3-methylumbelliferone (**3**; Scheme 3), which was prepared by a reported method.[15] Reaction of **3** with iodomethylpivalate **4** in the presence of K_2CO_3 produced **5** in excellent yield (Scheme 3). Next, **5** was reacted with *N*-bromosuccinamide (NBS) in the presence of a radical initiator azobisisobutyronitrile (AIBN) in carbon tetrachloride to produce the corresponding bromide **6**, which was then reacted with DEA/NO to give the desired compound **1**. The esterase-activated NO donor (**7**; Scheme 4) was synthesised by a reported protocol.[16]

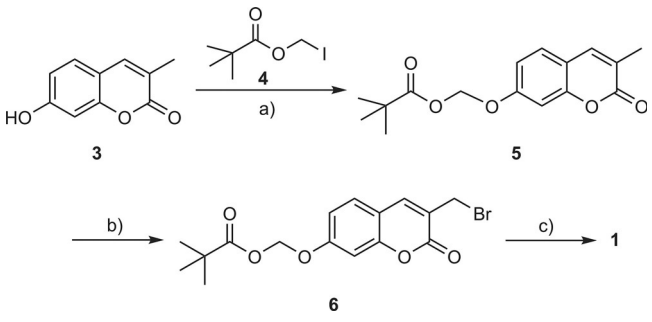

Scheme 3. Synthesis of **1**. a) K_2CO_3, ACN, RT, 3 h (89%); b) NBS, AIBN, CCl_4, reflux, 3 h (75%); c) DEA/NO, THF, DMF, [15]crown-5, 0 °C–RT, 3 h (24%).

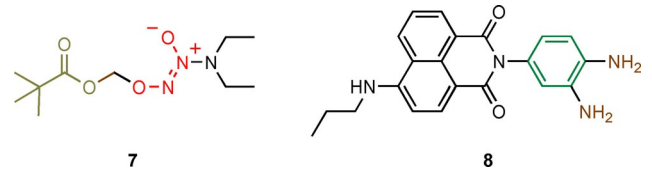

Scheme 4. Compounds **7** and **8**.

Compound **1** was dissolved in phosphate buffer (10 mM, pH 7.4), and an aliquot was analysed by a chemiluminescence-based detector for NO. As expected, no NO was detected (Figure 1 A). When ES was added, a signal attributable to NO was observed (Figure 1 A). The yield of NO was 93%. This signal was nearly completely abrogated when a similar experiment was conducted with 2-(4-carboxyphenyl)-4,4,5,5-tetramethyl-

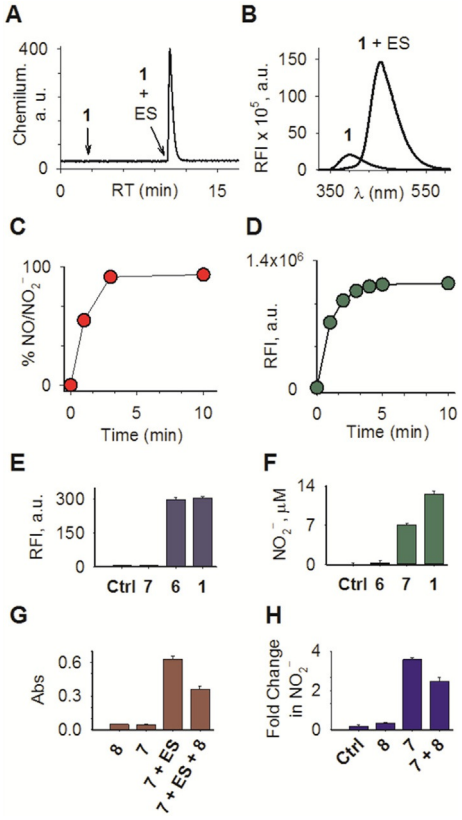

Figure 1. A) Nitric oxide analysis of **1** in buffer (pH 7.4) by a chemiluminescence-based detector for NO, and upon addition of esterase (ES). B) Fluorescence emission spectra at (λ_{ex} = 315 nm) of **1** in pH 7.4 buffer and **1** + ES. C) Time-course of NO generation from **1** with ES in buffer (pH 7.4). D) Time-course of fluorescence enhancement from **1** with ES in buffer (pH 7.4). Comparison of fluorescence intensity attributable to E) **2** and F) extracellular nitrite release upon incubation of HeLa cells with 25 μM **1**, **6** or **7**. G) Griess assay for the formation of nitrite upon incubation of **7** in the presence/absence of ES, and with and without NO dye **8** in buffer (pH 7.4). H) Griess assay for the formation of nitrite upon incubation of **7** with and without NO dye **8** in HeLa cells. All experiments were carried out at 37 °C.

imidazoline-1-oxyl-3-oxide potassium salt (c-PTIO, NO quencher), thus supporting the generation of NO by **1** (Figure S1 in the Supporting Information). Next, the fluorescence emission spectra of **1** in the presence/absence of ES were recorded (Figure 1 B). The expected product following cleavage by ES is **2**; this compound was independently synthesised and was found to be highly fluorescent ($\lambda_{ex}=315$ nm, $\lambda_{em}=460$ nm; Figure S2 and Table S1).

When **1** was incubated in buffer, no significant fluorescence emission at 460 nm was observed, but in the presence of esterase (**1** + ES), an emission profile (Figure 1 B) nearly identical to that of authentic **2** (Figure S2) was observed. The time-course of NO generation (Figure 1 C) corresponded well with the-time course of fluorescence enhancement (Figure 1 D), thus suggesting that once the pivaloyl group is cleaved, the rearrangement of the ensuing intermediate to produce DEA/NO and **2** (Scheme S1) is rapid (Scheme 2).

In order to study the ability of **1** to enhance fluorescence within cells and whether this signal correlates with NO release, HeLa cells were treated with 10 or 25 μM **1**. The fluorescence signal at 460 nm was measured in a micro-well plate reader; nitrite release was measured by Griess assay, and a dose-dependent increase in fluorescence was observed (Figure 2 A).

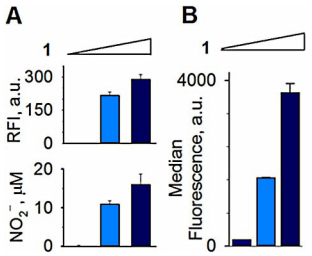

Figure 2. A) Comparison of fluorescence intensity attributable to **2** and extracellular nitrite release during incubation of HeLa cells with **1** at 0, 10 and 25 μM after 30 min at 37 °C. B) Flow cytometry analysis of HeLa cells incubated with 0, 10 and 25 μM **1** after 30 min at 37 °C ($\lambda_{ex}=355$ nm, $\lambda_{em}=460$ nm).

When extracellular nitrite was measured, a similar result was recorded, thus supporting the suitability of **1** to enhance NO as well as fluorescence within cells (Figure 2 A). When a similar experiment was carried out with **6**, we found increased fluorescence but no significant NO generation (Figure 1 E and F); and with **7**, an increase in extracellular nitrite was recorded with no significant fluorescence (Figure 1 E and F). NO donor **1** was incubated with medium, and no significant decomposition was observed, thus supporting the stability of **1** in media (Figure S3).

The most common problem during NO delivery and concomitant detection is consumption of NO during detection (Scheme 1 A). This consumption was demonstrated by the use of the NO donor **7** and an *o*-diamine based, lysosome-specefic two-photon fluorogenic probe **8** (Schemes 4 and S2). Here, **7** was incubated in buffer (pH 7.4), and ES was added. A signal attributable to NO was seen (Figure 1 G). The same experiment was conducted in the presence of NO-sensitive fluorophore **8** (Figure 1 G).[17] Although a distinct fluorescence signal (presumably from the formation of the triazole adduct) was observed (Figure S4), a diminished colorimetric signal was recorded for nitrite when compared with **7** + ES (Figure 1 G). In a cellular assay, the use of **7** along with **8** resulted in diminished yield of nitrite when compared with a similar concentration of **7** alone (Figure 1 H). Together, these data show that using a NO donor along with a probe for NO invariably leads to collateral consumption of NO during detection. This major limitation is overcome by the use of FLUORO/NO as NO is released along with a fluorescence signal at 460 nm in buffer (pH 7.4), without collateral consumption of NO (Scheme 1 B).

Having established that **1** is a reliable source of NO within cells, the fluorescence signal at 460 nm can now be used as a surrogate for NO generation. Confocal microscopy analysis of HeLa cells treated with **1** showed a distinct dose-dependent signal at 460 nm (Figure S5). The fluorescence signal was nearly uniformly distributed within the cell, possibly because of the wide distribution of ES within cells (Figure 3). As coumarin-based fluorophores are compatible with two-photon excitation microscopy, we carried out a confocal live-cell imaging experiment with **1**. As expected, we found a dose-dependent increase in the fluorescence signal at 460 nm ($\lambda_{ex}=740$ nm; Figure S5).

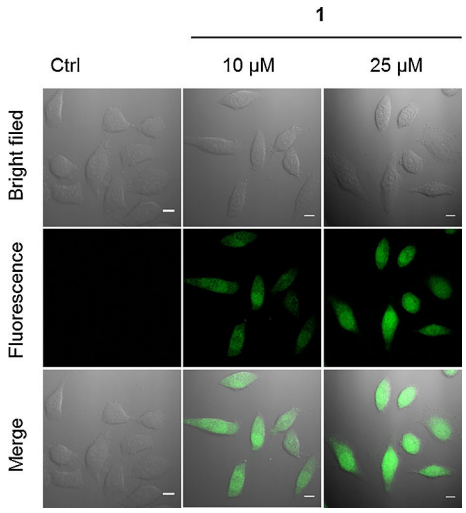

Figure 3. Confocal microscopy images of HeLa cells treated with **1** (10 and 25 μM) after 30 min at 37 °C. The excitation and emission channels were 405 and 460 nm, respectively. Scale bar: 10 μm.

Thus, this compound is expected to have deep tissue penetration and reduced phototoxicity during imaging. Flow cytometry analysis in HeLa cells incubated with **1** similarly showed a dose-dependent increase in fluorescence at 460 nm (Figure 2 B). These results suggest the suitability of FLUORO/NO for use in flow-cytometry as well as live-cell imaging experiments.

Activation of soluble guanylate cyclase (sGC) by NO results in the production of secondary messenger cyclic guanosine monophosphate (cGMP) from guanosine triphosphate (GTP). This signalling cascade promotes the biological functions of NO, including smooth muscle relaxation, platelet aggregation

and gene expression. In order to test if **1** was capable of activating sGC within cells, cGMP levels were measured by using a bioluminescence resonance energy transfer (BRET) assay in human embryonic HEK 293T cells.[18] The ratio of green fluorescence protein (GFP) fluorescence (BRET efficiency) to chemiluminescence (luciferase level) was determined. When sodium nitroprusside (SNP, 50 μM) was used (positive control), a significant enhancement in cGMP level was observed (Figure 4).

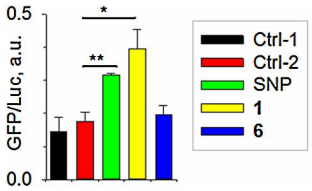

Figure 4. Formation of NO in cells was inferred by measurement of cyclic GMP, a secondary messenger for NO, by a BRET assay at 37 °C. * p value = 0.022; ** p value = 0.007. Control 1 = cells only, Control 2 = cells containing DeepBlueC (luciferase substrate) without any treatment.

When a similar assay was conducted with **1** (25 μM), as expected, a signal for cGMP was observed. This assay was conducted with **6** as a negative control, and as expected no significant enhancement in cGMP level was observed (Figure 4). Thus, other than NO, the by-products produced during decomposition of **1** were incapable of inducing NO-like signalling.

Lastly, we monitored the ability of **1** to induce DNA damage by monitoring 53BP1 foci,[19] which are markers of double-strand breaks and accumulate in nuclear foci. HeLa cells stably expressing 53BP1 fused to GFP were seeded on glass-bottom dishes and independently treated with **1** and **6**, and imaged 24 h post-treatment. As expected, we found a dose-dependent increase in DNA damage induced by **1** as evidenced by increased foci (Figure 5). Furthermore, **6** did not induce the same level of damage, thus suggesting the involvement of reactive nitrogen species (RNS) in the observed phenotype (Figure 5).

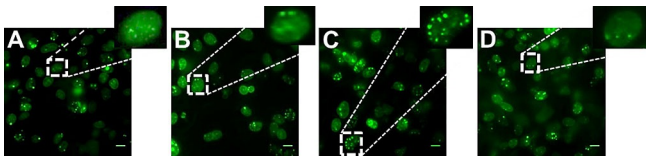

Figure 5. Formation of 53BP1 foci at 37 °C upon exposure of A) control, B) 5 μM **1**, C) 10 μM **1**, or D) 10 μM **6**. Scale bar: 10 μm. Increased foci are indicative of enhanced DNA damage response.

In summary, we report a new tool for studying NO biology. It eliminates the need for secondary assays to report the formation of NO. The collateral consumption of NO associated with NO delivery and concomitant detection can be avoided by the use of FLUORO/NO. Although excellent correlation between NO and fluorescence in cell-free conditions was observed, this cannot necessarily be extended to cellular systems. The dependence on pH and local microenvironment have significant effects on fluorescence intensity. In addition, the potential for toxicity of the quinone-methide-type intermediate might be a limitation when applied in vivo. These limitations will need to be addressed. The by-products of decomposition did not show NO-like activity in signalling (Figure 4) or DNA damage assays (Figure 5), thus suggesting the suitability of this compound for NO delivery. To the best of our knowledge, this is the first example of a small molecule that, when incubated in the presence of an enzyme, simultaneously produces NO as well as a fluorescence signal without collateral NO consumption. It is anticipated that this tool will find use in interrogating NO biology, which is yet to be completely understood.

Experimental Section

Compounds **2**,[12a] **3**,[15] **4**,[20] **7**[16] and **8**[21] were synthesised by using previously reported procedures, and the analytical data that we collected were consistent with the reported values.

(*Z*)-3,3-Diethyl-1-((2-oxo-7-((pivaloyloxy)methoxy)-2*H*-chromen-3-yl)methoxy)triaz-1-ene 2-oxide (1): 15-crown-5 (12 μL) was added to DEA/NO (100 mg, 0.65 mmol) in THF (3 mL) under ice, and the mixture was stirred at 0 °C for 5 min under nitrogen. A solution of **6** (200 mg, 0.54 mmol) in DMF (1 mL) was added to the reaction mixture at 0 °C and stirred at room temperature for 3 h. The solvent was evaporated under reduced pressure and diluted with of water (10 mL), then the aqueous solution was extracted with EtOAc (3×5 mL). The combined organic layer was washed with brine, dried over Na_2SO_4 (5 g), filtered and the filtrate was concentrated to give a crude compound. This was initially purified by silica gel column chromatography with EtOAc/petroleum ether (0→40%) as the eluent. The resulting mixture was further purified by semi-preparative HPLC with a ZORBAX ODS C_{18} semi-preparative column (9.4 mm×250 mm, 5 μm) by eluting with a gradient of ACN/water (60:40→80:20) at a flow rate of 2.5 mL min^{-1} and at room temperature to obtain **1** (55 mg, 24%) as a white solid: m.p. 81–83 °C; ^{1}H NMR ($CDCl_3$, 400 MHz): δ = 7.71 (s, 1H), 7.40 (d, J = 8.6 Hz, 1H), 7.02 (d, J = 2.4 Hz, 1H), 6.96 (dd, J = 8.7, 2.5 Hz, 1H), 5.81 (s, 2H), 5.22 (d, J = 1.1 Hz, 2H), 3.16 (q, J = 7.2 Hz, 4H), 1.20 (s, 9H), 1.09 ppm (t, J = 7.1 Hz, 6H); ^{13}C NMR ($CDCl_3$, 100 MHz): δ = 177.2, 160.2, 159.9, 155.0, 140.2, 129.2, 121.2, 114.0, 113.9, 103.2, 85.0, 70.0, 48.6, 39.1, 27.0, 11.6 ppm; FTIR (ν_{max}, cm^{-1}): 2980, 1752, 1726, 1614, 1571, 1508, 1392; HRMS (ESI) calcd for $C_{20}H_{27}N_3O_7$: 444.1746 $[M+Na]^+$, found: 444.1743.

((3-Methyl-2-oxo-2*H*-chromen-7-yl)oxy)methyl pivalate (5): K_2CO_3 (118 mg, 0.85 mmol) was added to **3** (50 mg, 0.28 mmol) in ACN (3 mL), followed by **4** (103 mg, 0.42 mmol) in ACN (1 mL). The reaction mixture was stirred for 3 h under nitrogen at room temperature. Upon completion of reaction (TLC analysis), the solvent was removed under reduced pressure. The residue was purified by silica gel column chromatography by using EtOAc/pet ether (0→25%) as the eluent to obtain **5** (73 mg, 89%) as a white solid: m.p. 98–100 °C; ^{1}H NMR ($CDCl_3$, 400 MHz): δ = 7.46 (s, 1H), 7.34 (d, J = 8.6 Hz, 1H), 7.00 (d, J = 2.4 Hz, 1H), 6.92 (dd, J = 8.4, 2.4 Hz, 1H), 5.79 (s, 2H), 2.18 (d, J = 1.3 Hz, 3H), 1.20 ppm (s, 9H); ^{13}C NMR ($CDCl_3$, 100 MHz): δ = 177.3, 162.4, 158.9, 154.6, 139.2, 128.1, 123.5, 114.8, 113.6, 103.2, 85.2, 39.1, 27.0, 17.2 ppm; FTIR (ν_{max}, cm^{-1}): 2969, 1755, 1709, 1615, 1505; HRMS (ESI) calcd for $C_{16}H_{18}O_5$: 291.1232 $[M+H]^+$, found: 291.1234.

((3-(Bromomethyl)-2-oxo-2*H*-chromen-7-yl)oxy)methyl pivalate (6): NBS (34 mg, 0.19 mmol) with a trace amount of AIBN was added to **5** (50 mg, 0.17 mmol) in CCl_4 (6 mL). The reaction mixture was refluxed for 3 h under nitrogen. After cooling to room temperature, the solvent was removed under reduced pressure. Then the residue was purified by column chromatography by using EtOAc/Pet ether (0→30%) as the eluent to obtain **6** (48 mg, 75%) as a white solid: m.p. 124–126 °C; ^{1}H NMR ($CDCl_3$, 400 MHz): δ = 7.80 (s, 1H), 7.44 (d, J = 8.6 Hz, 1H), 7.02 (d, J = 2.4 Hz, 1H), 6.97 (dd, J = 8.6, 2.5 Hz, 1H), 5.81 (s, 2H), 4.42 (s, 2H), 1.20 ppm (s, 9H); ^{13}C NMR ($CDCl_3$, 100 MHz): δ = 177.2, 160.2, 160.1, 155.3, 142.0, 129.4, 123.1, 114.1, 114.0, 103.2, 84.9, 39.1, 28.0, 27.0 ppm; FTIR (ν_{max}, cm^{-1}): 2978, 1751, 1725, 1612, 1502; HRMS (ESI) calcd for $C_{16}H_{17}BrO_5$: 369.0337 $[M+H]^+$, found: 369.0336.

Nitric oxide detection from 1:[13a] Stock solutions of **1** (1 mM) were prepared in DMSO and of porcine liver esterase (1 U mL^{-1}; Sigma–Aldrich) in phosphate buffer (pH 7.4). A typical reaction mixture consisted of **1** (25 μM) and esterase (0.5 U mL^{-1}) prepared by mixing **1** (12.5 μL of stock) and esterase (250 μL of stock) with phosphate buffer (237.5 μL, 10 mM, pH 7.4) at 37 °C. An aliquot of the reaction mixture (10 μL) was injected into a Sievers NOA 280i nitric oxide analyzer (GE Instruments) in argon as the carrier gas. For the experiment with c-PTIO (250 μM, 10 equiv compared to **1**), an aliquot of the reaction mixture (10 μL) was injected into the NOA chamber.

Nitric oxide collateral consumption assay: NO donor **7** and NO-sensitive fluorophore **8** was used to demonstrate collateral consumption of NO during detection. Compounds **7** (25 μM) and **8** (75 μM) were incubated in buffer (pH 7.4) at 37 °C for 15 min with and without ES (0.5 U mL^{-1}). Fluorescence emission was measured in a Varioscan microwell plate reader (excitation 430 nm; emission 530 nm; Thermo Fisher Scientific). For nitrite measurement, after 15 min incubation, Griess' reagent (14 μL for 200 μL reaction mixture, Sigma–Aldrich) was added, and incubated at 37 °C for 25 min before measuring the OD at 535 nm in the Varioscan reader.

Fluorescence emission and nitrite release in cells: Cells were suspended in PBS and placed in a 96-well plate (5×10^4 cells, 100 μL). Compounds **1**, **6** and **7** in DMSO was added to the cell suspension. Cells were incubated at 37 °C for 30 min, and fluorescence emission was measured in a Varioscan plate reader (λ_{ex} = 315 nm, λ_{em} = 460 nm). For nitrite measurement, after 30 min incubation, Griess' reagent (14 μL for 200 μL reaction mixture, Sigma–Aldrich) was added, and incubated at 37 °C for 25 min before measuring OD at 535 nm in a Varioscan plate reader. The amount of nitrite release was estimated from a standard calibration curve (R^2 = 0.998). The data represented here are averages of 3 repeats.

Confocal imaging of HeLa cells with 1: HeLa cells in Dulbecco's modified Eagle's medium (DMEM) supplemented with foetal bovine serum (FBS, 10%) and penicillin (5000 U mL^{-1})–streptomycin (5000 μg U mL^{-1}) antibiotic solution (1%) were seeded (10^5 cells per well) in four-well chamber and incubated overnight in an atmosphere of 5% CO_2 at 37 °C. The medium was removed, and the cells were washed with PBS (500 μL). Then fresh DMEM (500 μL) was added along with **1** (10 or 25 μM), and the cells were incubated for 30 min at 37 °C. The medium was removed, cells were washed twice with PBS (200 μL), and then cells were imaged on an LSM 710 confocal microscope (Zeiss) with 405 nm (740 nm was used for two photon) laser lines at 2% power and a 63× oil immersion objective. Images were analysed by ImageJ software.

FACS analysis for 1: HeLa cells in DMEM supplemented with FBS (10%) and antibiotic (1 mL per 100 mL DMEM) were seeded (10^5 cells per well) in six-well plate and incubated overnight in an atmosphere of 5% CO_2 at 37 °C. The medium was removed, and the cells were washed with PBS (1 mL). Then fresh DMEM (1 mL) was added along with **1** (10 or 25 μM), and cells were incubated for 30 min at 37 °C. After 30 min, the medium was removed, the cells were washed with PBS (1 mL), and cells were detached by trypsination. Cells were centrifuged (1000 rpm (Eppendorf 5810 R, A-4-81 rotor), 22 °C, 5 min). The supernatant was removed, and PBS (500 μL) was added to the cell pellet. Samples were illuminated with a UV laser at 355 nm on an LSRFortessa SORP cell analyser (BD Biosciences).

cGMP measurement:[18] HEK 293T cells were maintained in DMEM with foetal calf serum (10%), penicillin (100 mg L^{-1}) and streptomycin (100 mg L^{-1}) at 37 °C in a 5% CO_2 humidified incubator. Transfection was performed with Turbofect (Thermo Fisher Scientific) according to the manufacturer's protocol. HEK 293T cells were transfected with pGFP2-GAFa-Rluc in a 12-well plate. After 48 h, cells were harvested, and cells were seeded (10^5 cells per well) in a 96-well plate in Live Cell Imaging Solution (Invitrogen) and treated with various analytes. After 10 min, DeepBlueC (5 μM, Thermo Fisher) was added. BRET measurements were made in an Infinite M1000 PRO plate reader (TECAN) at the channel of BLUEI (luminescence) and Green1 (fluorescence).

53BP1 foci formation assay:[22] HeLa cells stably expressing GFP-53BP1[22] were used for live imaging experiments. The cells were treated with different concentrations of **1** and/or **6** for 5 days and imaged prior to and after treatment. For imaging, cells were seeded in a glass-bottomed dish and treated with the indicated compounds and imaged in an IX83 inverted fluorescence microscope (Olympus) with Slidebook 6.0 software (Intelligent Imaging Innovations, Denver, CO) in the GFP-specific excitation and emission channel. The excitation and emission wavelengths were 478 and 505 nm, respectively.

Acknowledgements

The authors thank IISER Pune and the Department of Science and Technology (DST, Grant number EMR/2015/000668) and Council for Scientific and Industrial Research (CSIR) for financial support.

Conflict of Interest

The authors declare no conflict of interest.

Keywords: diazeniumdiolate · esterase · fluorescence · nitric oxide · prodrugs

[1] L. J. Ignarro, *Angew. Chem. Int. Ed.* **1999**, *38*, 1882–1892; *Angew. Chem.* **1999**, *111*, 2002–2013.
[2] a) D. A. Wink, H. B. Hines, R. Y. S. Cheng, C. H. Switzer, W. Flores-Santana, M. P. Vitek, L. A. Ridnour, C. A. Colton, *J. Leukocyte Biol.* **2011**, *89*, 873–891; b) N. Barraud, B. G. Kardak, N. R. Yepuri, R. P. Howlin, J. S. Webb, S. N. Faust, S. Kjelleberg, S. A. Rice, M. J. Kelso, *Angew. Chem. Int. Ed.* **2012**, *51*, 9057–9060; *Angew. Chem.* **2012**, *124*, 9191–9194.
[3] C. Szabo, *Nat. Rev. Drug. Discovery* **2016**, *15*, 185–203.
[4] a) P. G. Wang, M. Xian, X. Tang, X. Wu, Z. Wen, T. Cai, A. J. Janczuk, *Chem. Rev.* **2002**, *102*, 1091–1134; b) L. K. Keefer, *ACS Chem. Biol.* **2011**, *6*, 1147–1155.

[5] a) T. B. Cai, D. Lu, M. Landerholm, P. G. Wang, *Org. Lett.* **2004**, *6*, 4203 – 4205; b) J. E. Saavedra, P. J. Shami, L. Y. Wang, K. M. Davies, M. N. Booth, M. L. Citro, L. K. Keefer, *J. Med. Chem.* **2000**, *43*, 261 – 269; c) H. Chakrapani, A. E. Maciag, M. L. Citro, L. K. Keefer, J. E. Saavedra, *Org. Lett.* **2008**, *10*, 5155 – 5158; d) H. Chakrapani, B. M. Showalter, L. Kong, L. K. Keefer, J. E. Saavedra, *Org. Lett.* **2007**, *9*, 3409 – 3412; e) H. Chakrapani, B. M. Showalter, M. L. Citro, L. K. Keefer, J. E. Saavedra, *Org. Lett.* **2007**, *9*, 4551 – 4554; f) K. Sharma, A. Iyer, K. Sengupta, H. Chakrapani, *Org. Lett.* **2013**, *15*, 2636 – 2639; g) K. Sharma, K. Sengupta, H. Chakrapani, *Bioorg. Med. Chem. Lett.* **2013**, *23*, 5964 – 5967.

[6] J. Chan, S. C. Dodani, C. J. Chang, *Nat. Chem.* **2012**, *4*, 973 – 984.

[7] R. A. Hunter, W. L. Storm, P. N. Coneski, M. H. Schoenfisch, *Anal. Chem.* **2013**, *85*, 1957 – 1963.

[8] a) A. Fraix, S. Sortino, *Chem. Asian J.* **2015**, *10*, 1116 – 1125; b) A. Fraix, N. Kandoth, R. Gref, S. Sortino, *Asian J. Org. Chem.* **2015**, *4*, 256 – 261; c) E. Deniz, N. Kandoth, A. Fraix, V. Cardile, A. C. E. Graziano, D. Lo Furno, R. Gref, F. M. Raymo, S. Sortino, *Chem. Eur. J.* **2012**, *18*, 15782 – 15787; d) T. Horinouchi, H. Nakagawa, T. Suzuki, K. Fukuhara, N. Miyata, *Chem. Eur. J.* **2011**, *17*, 4809 – 4813; e) E. Vittorino, E. Cicciarella, S. Sortino, *Chem. Eur. J.* **2009**, *15*, 6802 – 6806.

[9] a) N. Ieda, Y. Hotta, N. Miyata, K. Kimura, H. Nakagawa, *J. Am. Chem. Soc.* **2014**, *136*, 7085 – 7091; b) H. Nakagawa, K. Hishikawa, K. Eto, N. Ieda, T. Namikawa, K. Kamada, T. Suzuki, N. Miyata, J.-i. Nabekura, *ACS Chem. Biol.* **2013**, *8*, 2493 – 2500.

[10] L. Tan, A. Wan, H. Li, *Analyst* **2013**, *138*, 879 – 886.

[11] a) S. Liu, T. Gu, J. Fu, X. Li, I. S. Chronakis, M. Ge, *Mater. Sci. Eng. C* **2014**, *45*, 37 – 44; b) S. Liu, L. Jin, I. S. Chronakis, X. Li, M. Ge, *Mater. Lett.* **2014**, *123*, 104 – 106.

[12] a) R. Weinstain, E. Segal, R. Satchi-Fainaro, D. Shabat, *Chem. Commun.* **2010**, *46*, 553 – 555; b) E.-J. Kim, S. Bhuniya, H. Lee, H. M. Kim, C. Cheong, S. Maiti, K. S. Hong, J. S. Kim, *J. Am. Chem. Soc.* **2014**, *136*, 13888 – 13894.

[13] a) A. T. Dharmaraja, G. Ravikumar, H. Chakrapani, *Org. Lett.* **2014**, *16*, 2610 – 2613; b) V. S. Khodade, A. Kulkarni, A. S. Gupta, K. Sengupta, H. Chakrapani, *Org. Lett.* **2016**, *18*, 1274 – 1277.

[14] K. M. Davies, D. A. Wink, J. E. Saavedra, L. K. Keefer, *J. Am. Chem. Soc.* **2001**, *123*, 5473 – 5481.

[15] F. Leonetti, A. Favia, A. Rao, R. Aliano, A. Paluszcak, R. W. Hartmann, A. Carotti, *J. Med. Chem.* **2004**, *47*, 6792 – 6803.

[16] N. Bensel, M. T. Reymond, J.-L. Reymond, *Chem. Eur. J.* **2001**, *7*, 4604 – 4612.

[17] Y. Xiao, H. Yu, Y. Zhang, X. Zhang (Dalian University of Technology) CN102617467 A, **2012**.

[18] K. H. Biswas, S. Sopory, S. S. Visweswariah, *Biochemistry* **2008**, *47*, 3534 – 3543.

[19] O. Zgheib, K. Pataky, J. Brugger, T. D. Halazonetis, *Mol. Cell. Biol.* **2009**, *29*, 1050 – 1058.

[20] B. P. Bandgar, R. J. Sarangdhar, S. Viswakarma, F. A. Ahamed, *J. Med. Chem.* **2011**, *54*, 1191 – 1201.

[21] H. Yu, Y. Xiao, L. Jin, *J. Am. Chem. Soc.* **2012**, *134*, 17486 – 17489.

[22] M. Bagheri, R. R. Nair, K. K. Singh, D. K. Saini, *Biochim. Biophys. Acta Mol. Cell Res.* **2017**, *1864*, 177 – 190.

Manuscript received: March 17, 2017

Accepted manuscript online: May 4, 2017

Version of record online: June 26, 2017

ChemComm

COMMUNICATION

View Article Online
View Journal | View Issue

Cite this: *Chem. Commun.*, 2017, **53**, 13352

Received 6th November 2017,
Accepted 20th November 2017

DOI: 10.1039/c7cc08526e

rsc.li/chemcomm

A small molecule for theraNOstic targeting of cancer cells†

Govindan Ravikumar,‡[a] Meisam Bagheri,‡[b] Deepak Kumar Saini *[b] and Harinath Chakrapani *[a]

Thera/NO – a small molecule that is activated by hydrogen peroxide to generate nitric oxide (NO) and a fluorescence signal is reported. Using cancer and primary cells, we show that Thera/NO preferentially releases NO in cancer cells, which can trigger DNA damage and cell death in them. The coupled fluorescence signal facilitated tracking the NO release in living cells without collateral consumption of NO.

Nitric oxide (NO) is an endogenously produced signaling molecule that mediates numerous cellular processes. The relationship between NO and cancer is complex and depends on the concentration of NO, and its duration of release.[1,2] A number of efforts towards delivering NO to cancer cells as a tumoristatic agent are in development. For example, expression of inducible nitric oxide synthase (iNOS) has been attempted wherein a gene encoding NOS was transfected in cancer cells, and when expressed, NO levels within cells increased. This methodology is highly effective in localizing NO but may have problems associated with selectivity, toxicity and the requirement of cofactors for NOS.[3–7] Other strategies use exogenous donors to generate NO within cancer cells, which spontaneously dissociate to generate NO, and have limited utility. That can be overcome using a cleavage trigger which offers both spatial and temporal control in localized generation of NO. A commonly used cleavage methodology is light, which offers a high degree of spatiotemporal control over NO generation.[8–12] However, the selectivity of NO generation only within cancers will depend on the ability to focus the light source on the site of interest. Furthermore, most optically triggered approaches utilize UV light, which limits tissue permeability and triggers toxic side effects. Enzymatic NO prodrug activation has been developed but has limited selectivity for cancer cells. For example, NO donors that are activated by esterase,[13] β-galactosidase,[14–16] and DT-diaphorase[17] are known (Fig. 1a).

Although some of these enzymes are over-expressed in tumours, cancer-selectivity data for these NO donors are not available. Lastly, glutathione/glutathione *S*-transferase (GSH/GST) NO prodrugs such as JS-K[18] and PABA/NO[19] are reported. Although these thiol-activated NO donors have limited cancer specificity, they have potent anti-proliferative activity in animal models, supporting the further development of NO as a tumoristatic agent.

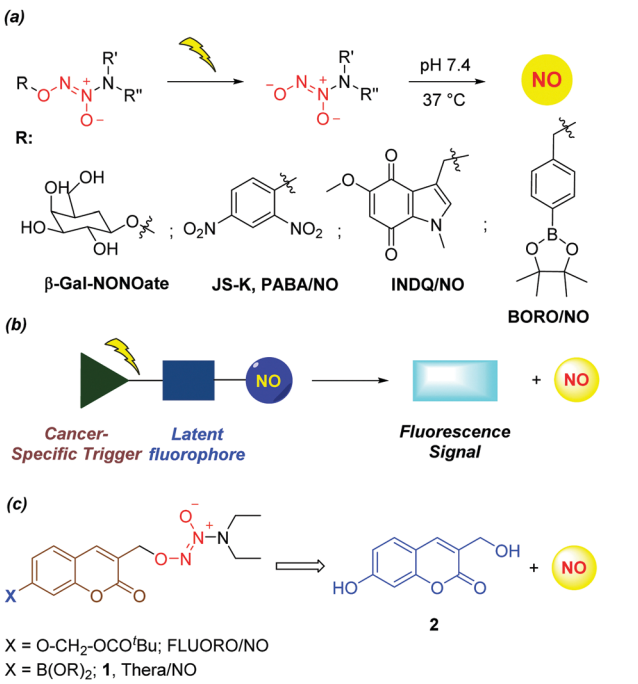

Fig. 1 (a) Selective examples of diazeniumdiolate based NO donors R′ and R″ = various groups. (b) Strategy for NO-based theraNOstics: if the trigger is cancer-specific, localized NO release along with a fluorescence reporter is possible. (c) FLUORO/NO, a reported strategy for esterase activated NO generation triggered by esterase, and boronate-ester-based NO delivery (Thera/NO) towards a theraNOstic agent.

[a] *Department of Chemistry, Indian Institute of Science Education and Research, Pune, India. E-mail: harinath@iiserpune.ac.in*
[b] *Department of Molecular Reproduction, Development and Genetics, Indian Institute of Science, Bangalore, India. E-mail: deepaksaini@iisc.ac.in*

† Electronic supplementary information (ESI) available. See DOI: 10.1039/c7cc08526e

‡ These authors contributed equally.

Furthermore, the absence of a methodology for real-time monitoring of NO release in the above examples is a major limitation. Since detection of NO is invariably associated with collateral consumption of NO,[20] a reporter for activation would be useful which can report the quantum of NO release. Such a strategy may lay a platform for NO-based theranostics (Fig. 1b). Here, we report a new small molecule NO donor attached with a fluorescence reporter that is activated selectively in cancers.

Cancers are complex in their phenotypes,[21] but one feature that has been widely reported is the high levels of reactive oxygen species (ROS). These are reduced forms of oxygen that mediate certain signalling events within the cell but are harmful at elevated concentrations and damage biomacromolecules including DNA, proteins and RNA. Hydrogen peroxide (H_2O_2) generation in several cancer cell lines has been estimated to be 0.5 nM per 10^4 cells per h.[22] Other studies estimate H_2O_2 levels in cancers to be 5 μM to 1 mM, which are significantly higher than those in normal cells.[23–26] Keeping this in mind, H_2O_2 has been used as a specific agent to activate prodrugs[27–30] and latent fluorophores[31] (as imaging agents) in cancers. A functional group that has been widely used is the arylboronate ester, which is known to react with H_2O_2 to produce an aryl alcohol.[30,32] This functional group was hence chosen as a substrate for the metabolic stimulus, *i.e.* H_2O_2 to specifically generate NO in cancer cells. Furthermore, due to the complexity associated with the detection of NO, the presence of a "turn on" fluorescence reporter for NO would be an additional feature which will be useful for studying possible cancer therapeutic outcomes of NO in a systematic manner.

Recently, our laboratory has reported FLUORO/NO, a diazeiniumdiolate-based NO donor with a fluorescence reporter (Fig. 1c).[20] Here, esterase was used as the activating enzyme, and NO generation from the donor correlated well with fluorescence enhancement. Using this template, we designed **1**, a ROS-sensitive NO donor that can be used for selectively delivering and monitoring the release of NO in cancer cells (Fig. 1c).

Compound **1** was synthesized in two steps from **3** (Scheme 1), which was prepared using a reported methodology.[32,33] Compound **3** was reacted with *N*-bromosuccinimide (NBS) in the presence of a radical initiator azobisisobutyronitrile (AIBN) in carbon tetrachloride to produce the corresponding bromide, which was then reacted with sodium (*Z*)-1-(*N*,*N*-diethylamino)diazen-1-ium-1,2-diolate (DEA/NO) to give the desired compound **1**.

We first investigated the ability of the compound **1** to generate NO and a fluorescence signal in the presence of H_2O_2 in phosphate buffer (pH 7.4, 10 mM). Compound **1** was exposed to 10 eq. of H_2O_2, and the fluorescence signal attributable to **2** and NO were independently monitored. The fluorescence signal at 460 nm was measured using a micro-well plate reader, while nitric oxide released was measured using a nitric oxide analyser (a chemiluminescence-based detector for NO). We found a gradual increase in the fluorescence signal attributable to **2** only in the presence of the stimulus, H_2O_2, during 50 min (see the ESI,† Fig. S3a).

Similarly, when NO was monitored, we found that the compound generated NO only in the presence of H_2O_2 (see the ESI,† Fig. S3b). The rate constant for the fluorescence signal k_{Fluor} was found to be 4×10^{-4} s^{-1}, while the rate constant for the formation of NO, k_{NO}, under similar conditions was found to be comparable in magnitude: 2×10^{-4} s^{-1}. Next, through a calibration curve of relative fluorescence intensity and authentic **2**, the % **2** formed upon treatment of **1** with H_2O_2 could be calculated (see the ESI,† Fig. S2). Using these quantitative data, the time course for formation of **2** was monitored by its fluorescence signal at 460 nm, and independently, the formation of NO was also monitored under similar conditions. A close correlation between these two parameters was observed (Fig. 2a), suggesting that the aforementioned fluorescence signal and NO generation were nearly concurrent.

In order to study the responsiveness of **1** to elevated ROS, the fluorescence signal and NO generated were monitored (Fig. 2b) by first exposing the compound to 5 eq. (first arrow) of H_2O_2

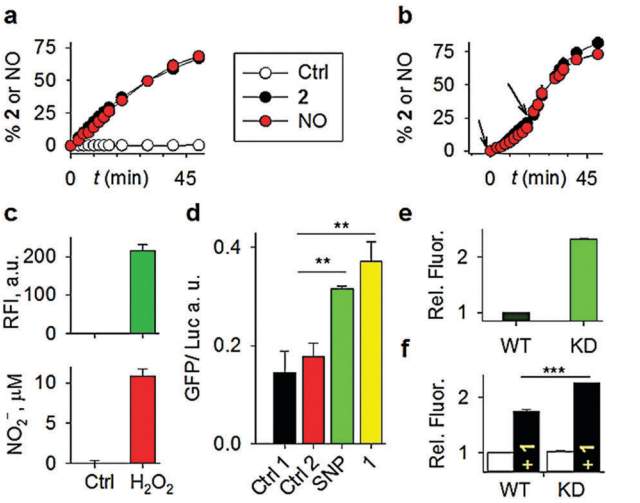

Fig. 2 (a) Time course of the enhancement of the fluorescence signal attributable to **2** and time course of the enhancement of NO upon incubation of **1** (25 μM) with and without H_2O_2 (10 eq.) (Ctrl = **1** without H_2O_2). (b) Stimuli responsive fluorescence (black circle) and NO (red circle) generation during exposure to 5 and 20 eq. of H_2O_2. (c) Comparison of the fluorescence intensity attributable to **2** and extracellular nitrite release during incubation of HeLa cells when incubated with **1** (25 μM) alone (Ctrl) or HeLa cells pre-treated with H_2O_2 (100 μM) for 30 min followed by addition of **1** (25 μM). (d) Formation of NO in cells was confirmed by measurement of cyclic GMP, a secondary messenger for NO, using a BRET assay; $^{**}p$-value = 0.004, $^{**}p$-value = 0.007. Control 1 = cells only, Control 2 = cells containing DeepBlueC (luciferase substrate) without any treatment. (e) Intracellular ROS enhancement was measured using a $DCFH_2$-DA assay in wild type (WT) and catalase expression knockdown (KD) cells. (f) Comparison of the relative fluorescence signal attributable to **2** in wild type (WT) and catalase expression knockdown (KD) cells after treatment with **1**. $^{***}p$-value = 0.006.

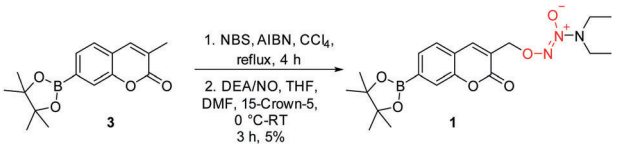

Scheme 1 Synthesis of **1**.

followed by exposure to 20 eq. of H_2O_2 (second arrow). Again, as a testament to its stimuli-responsiveness, a close correlation between NO and fluorescence signal at 460 nm was observed (Fig. 2b). Next, the selectivity of **1** for H_2O_2 over other biologically relevant reactive species was evaluated and no significant increase in fluorescence was seen except when **1** was treated with H_2O_2 (see the ESI,† Fig. S4a). The selectivity of the boronate ester functional group towards oxidative cleavage was found to be along the lines of previous reports.[27,29,31,32] Next, when **1** was treated with increasing concentrations of H_2O_2, we found a dose-dependent increase in the fluorescence signal at 460 nm (see the ESI,† Fig. S4b). The fluorescence intensity attributable to **2** was not affected by the increasing concentration of hydrogen peroxide (see the ESI,† Fig. S5). Together, these results suggest the responsiveness and selectivity of the functional group towards activation by H_2O_2.

In order to study the capability of compound **1** to generate fluorescence and NO in cells, HeLa cells were exposed to **1** and exogenously H_2O_2 was added. The fluorescence signal at 460 nm was measured using a micro-well plate reader, while nitrite released was measured using a Griess assay and an increase in fluorescence and nitrite was observed (Fig. 2c).

Having established that **1** is a reliable source of NO within cells, the fluorescence signal at 460 nm can now be used as a surrogate for NO generation. Fluorescence microscopy images of HeLa cells pretreated with **1** (25 μM) for 30 min and exposed to the increasing concentration of exogenous H_2O_2 for 30 min showed a dose-dependent increase in the fluorescence signal at 460 nm (see the ESI,† Fig. S7). Similar results were obtained using flow cytometry analysis (see the ESI,† Fig. S8), supporting the cell-permeability of **1**.

In order to study the cellular uptake and intracellular localization of **1** using confocal microscopy, HeLa cells were treated with **1** followed by incubation with H_2O_2. A significant enhancement in the fluorescence signal, which overlapped with the fluorescence signal of LysoTracker Green (fluorescence marker for lysosomes) (see the ESI,† Fig. S9), was observed. This result suggested the preferential activation of **1** in lysosomes, which is along the lines of previous reports.[29]

NO is known to activate soluble guanylate cyclase (sGC) which catalyzes the conversion of GTP to cGMP and promotes many biological functions of NO. In order to test whether **1** was capable of activating sGC within cells, cGMP levels were measured using a BRET-based assay in HEK cells.[34] Here, the ratio between GFP fluorescence and chemiluminescence was determined. Sodium nitroprusside (SNP) was used as the positive control (50 μM) and a significant enhancement in cGMP levels was observed (Fig. 2d). When a similar assay was conducted with **1** (25 μM), as expected, a signal for cGMP was observed.

Elevated levels of H_2O_2 were found in numerous cancer cells compared with normal cells. In a separate experiment, in order to simulate increased ROS intracellularly, a catalase knockdown HeLa cell line (KD) was used. Here, due to low levels of catalase, which was confirmed by quantitative real time PCR to check the mRNA levels (see the ESI,† Fig. S10), an increased level of ROS was expected. As predicted, the $DCFH_2$-DA (fluorescence indicator for reactive oxygen species in cells) assay revealed that the catalase knockdown cell line (KD) showed higher DCF fluorescence (Fig. 2e) when compared with wild-type (WT). Both these cell lines were independently exposed to **1** and fluorescence corresponding to **2** was measured. We found that the relative increase in fluorescence attributable to the formation of **2** was much higher in the case of KD when compared with WT (Fig. 2f). Thus, when encountered with cellular situations with varying ROS levels, **1** was preferentially activated in cell lines where ROS levels were relatively higher.

In order to further validate it, we tested **1** in MRC5 (normal fibroblast) and cancer cell lines A549, HeLa, and MDA-MB-231 and evaluated the fluorescence response by fluorescence microscopy imaging. As expected, we found an enhancement in the fluorescence signal attributable to **2** in cancer cells compared with normal cells (see the ESI,† Fig. S11). Together, these data suggest that **1** gets selectively activated in cancer cells which have relatively higher ROS levels.

Next we monitored the ability of **1** to induce DNA damage by monitoring 53BP1 foci, which marks double-strand breaks and accumulate as nuclear foci.[35] HeLa cells stably expressing 53BP1 fused to GFP were seeded onto glass-bottom dishes, independently treated with **1** and imaged 6 h post-treatment. Increased foci indicative of DNA damage was observed (Fig. 3a), suggesting the involvement of reactive nitrogen species (RNS) in the observed phenotype.[20,36] Under similar conditions, an increase in the

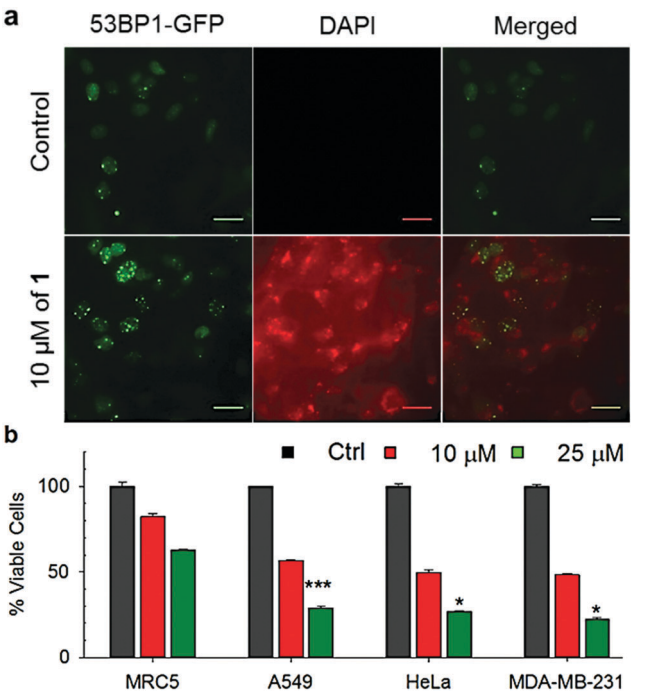

Fig. 3 (a) Formation of 53BP1 foci and the enhancement of the fluorescence signal attributable to **2** upon exposure of **1** in HeLa cells. Images were taken in the GFP channel (for foci) and the DAPI channel (for **2**). DAPI images have been pseudocolored (red) for better visualization. Scale bar: 100 μm. (b) Comparison of the cytotoxic effects of **1** (10 and 25 μM) on primary cells (MRC5) and cancer cells (A549, HeLa and MDA-MB 231 cells) after incubation for 12 h. Statistical analysis at 25 μM: A549 *vs.* MRC5, $p = 0.0096$; HeLa *vs.* MRC5, $p = 0.014$; MDA-MB-231 *vs.* MRC5, $p = 0.028$.

fluorescence signal attributable to **2** in the DAPI channel was also observed (Fig. 3a). When the dose of Thera/NO was varied, a dose-dependent increase in 53BP1 foci (see the ESI,† Fig. S12) as well as fluorescence signal attributable to **2** (see the ESI,† Fig. S13) were recorded, suggesting the suitability of Thera/NO for real-time monitoring of NO.

Finally, the cytotoxic effect of compound **1** was evaluated with MRC5 (normal fibroblast) and cancer cell lines (A549, HeLa, and MDA-MB-231) using an Alamar Blue assay. As expected, we found that compound **1** showed a significant cytotoxic effect on cancer cells compared with normal cells (Fig. 3b and see the ESI,† Fig. S14).

Taken together, we report a new strategy for selectively generating NO in cancer cells. Previous reports have established H_2O_2 as a biomarker for cancers and have validated drug delivery to cancers using the boronate ester functional group. The boronate ester group is also known to react with peroxynitrite ($ONOO^-$), a reactive nitrogen species at a much faster rate than H_2O_2.[37] Thus, the activation of **1** in cells with higher levels of $ONOO^-$ might occur. However, the estimated half-life of $ONOO^-$ at physiological pH is $\sim$10 ms, while H_2O_2 is relatively more stable.[38] Previous reports with a similar boronate ester-based fluorescent probe have shown that activation of the fluorophore occurs only upon exogenous addition of $ONOO^-$.[39] Lastly, nanoparticle-based carriers, which use pH, thermal and light activation strategies; and a few decorated with cancer-targeting functional groups including folate have been reported.[40–45] The use of a boronate ester functional group for triggering NO release with a fluorescent reporter can be adapted to such carrier systems as well.

The potential for use of NO in cancers is multifarious: (a) the vasodilatory effects of NO may improve blood circulation in the proximity of tumours; (b) the ability of NO to synergize with certain cancer drugs, especially, by inhibition of drug efflux pumps may be highly beneficial; and (c) NO can be a radiosensitizer facilitating radiation therapy. Thera/NO will lay the platform for exploiting the unique properties of NO in cancer therapy.

Funding for this work is by the Department of Science and Technology (DST, grant number EMR/2015/000668 and EMR/2014/000997).

Conflicts of interest

There are no conflicts to declare.

Notes and references

1 Z. Huang, J. Fu and Y. Zhang, *J. Med. Chem.*, 2017, **60**, 7617–7635.
2 K. Sharma and H. Chakrapani, *Nitric Oxide*, 2014, **43**, 8–16.
3 S. Ambs, W. G. Merriam, M. O. Ogunfusika, W. P. Bennett, N. Ishibe, S. P. Hussain, E. E. Tzeng, D. A. Geller, T. R. Billiar and C. C. Harris, *Nat. Med.*, 1998, **4**, 1371–1376.
4 E. Tzeng, T. Yoneyama, K. Hatakeyama, L. L. Shears and T. R. Billiar, *Surgery*, 1996, **120**, 315–321.
5 S. Lehrman, *Nature*, 1999, **401**, 517–518.
6 W. Xu, L. Z. Liu, M. Loizidou, M. Ahmed and I. G. Charles, *Cell Res.*, 2002, **12**, 311–320.
7 S. Mocellin, V. Bronte and D. Nitti, *Med. Res. Rev.*, 2007, **27**, 317–352.
8 P. H. Ruane, K. M. Bushan, C. M. Pavlos, R. A. D'Sa and J. P. Toscano, *J. Am. Chem. Soc.*, 2002, **124**, 9806–9811.
9 K. Kitamura, M. Kawaguchi, N. Ieda, N. Miyata and H. Nakagawa, *ACS Chem. Biol.*, 2016, **11**, 1271–1278.
10 M. J. Rose, N. L. Fry, R. Marlow, L. Hinck and P. K. Mascharak, *J. Am. Chem. Soc.*, 2008, **130**, 8834–8846.
11 K. Chegaev, A. Fraix, E. Gazzano, G. E. F. Abd-Ellatef, M. Blangetti, B. Rolando, S. Conoci, C. Riganti, R. Fruttero, A. Gasco and S. Sortino, *ACS Med. Chem. Lett.*, 2017, **8**, 361–365.
12 K. K. Behara, Y. Rajesh, Y. Venkatesh, B. R. Pinninti, M. Mandal and N. D. P. Singh, *Chem. Commun.*, 2017, **53**, 9470–9473.
13 J. E. Saavedra, P. J. Shami, L. Y. Wang, K. M. Davies, M. N. Booth, M. L. Citro and L. K. Keefer, *J. Med. Chem.*, 2000, **43**, 261–269.
14 C. Chen, Y. Shi, S. Li, Q. Qi, L. Gu, J. Song and P. G. Wang, *Arch. Pharm. Pharm. Med. Chem.*, 2006, **339**, 366–371.
15 C. A. Valdez, J. E. Saavedra, B. M. Showalter, K. M. Davies, T. C. Wilde, M. L. Citro, J. J. Barchi, J. R. Deschamps, D. Parrish, S. El-Gayar, U. Schleicher, C. Bogdan and L. K. Keefer, *J. Med. Chem.*, 2008, **51**, 3961–3970.
16 X. Wu, X. Tang, M. Xian and P. G. Wang, *Tetrahedron Lett.*, 2001, **42**, 3779–3782.
17 K. Sharma, A. Iyer, K. Sengupta and H. Chakrapani, *Org. Lett.*, 2013, **15**, 2636–2639.
18 P. J. Shami, J. E. Saavedra, L. Y. Wang, C. L. Bonifant, B. A. Diwan, S. V. Singh, Y. Gu, S. D. Fox, G. S. Buzard, M. L. Citro, D. J. Waterhouse, K. M. Davies, X. Ji and L. K. Keefer, *Mol. Cancer Ther.*, 2003, **2**, 409–417.
19 J. E. Saavedra, A. Srinivasan, G. S. Buzard, K. M. Davies, D. J. Waterhouse, K. Inami, T. C. Wilde, M. L. Citro, M. Cuellar, J. R. Deschamps, D. Parrish, P. J. Shami, V. J. Findlay, D. M. Townsend, K. D. Tew, S. Singh, L. Jia, X. Ji and L. K. Keefer, *J. Med. Chem.*, 2006, **49**, 1157–1164.
20 G. Ravikumar, M. Bagheri, D. K. Saini and H. Chakrapani, *ChemBioChem*, 2017, **18**, 1529–1534.
21 A. T. Dharmaraja, *J. Med. Chem.*, 2017, **60**, 3221–3240.
22 T. P. Szatrowski and C. F. Nathan, *Cancer Res.*, 1991, **51**, 794–798.
23 S. D. Lim, C. Sun, J. D. Lambeth, F. Marshall, M. Amin, L. Chung, J. A. Petros and R. S. Arnold, *Prostate*, 2005, **62**, 200–207.
24 L. Khandrika, B. Kumar, S. Koul, P. Maroni and H. K. Koul, *Cancer Lett.*, 2009, **282**, 125–136.
25 D. Trachootham, J. Alexandre and P. Huang, *Nat. Rev. Drug Discovery*, 2009, **8**, 579–591.
26 F. Antunes and E. Cadenas, *FEBS Lett.*, 2000, **475**, 121–126.
27 Y. Kuang, K. Balakrishnan, V. Gandhi and X. Peng, *J. Am. Chem. Soc.*, 2011, **133**, 19278–19281.
28 H. Hagen, P. Marzenell, E. Jentzsch, F. Wenz, M. R. Veldwijk and A. Mokhir, *J. Med. Chem.*, 2012, **55**, 924–934.
29 E.-J. Kim, S. Bhuniya, H. Lee, H. M. Kim, C. Cheong, S. Maiti, K. S. Hong and J. S. Kim, *J. Am. Chem. Soc.*, 2014, **136**, 13888–13894.
30 W. Chen, K. Balakrishnan, Y. Kuang, Y. Han, M. Fu, V. Gandhi and X. Peng, *J. Med. Chem.*, 2014, **57**, 4498–4510.
31 B. C. Dickinson and C. J. Chang, *J. Am. Chem. Soc.*, 2008, **130**, 9638–9639.
32 A. T. Dharmaraja, G. Ravikumar and H. Chakrapani, *Org. Lett.*, 2014, **16**, 2610–2613.
33 V. S. Khodade, A. Kulkarni, A. S. Gupta, K. Sengupta and H. Chakrapani, *Org. Lett.*, 2016, **18**, 1274–1277.
34 K. H. Biswas, S. Sopory and S. S. Visweswariah, *Biochemistry*, 2008, **47**, 3534–3543.
35 O. Zgheib, K. Pataky, J. Brugger and T. D. Halazonetis, *Mol. Cell. Biol.*, 2009, **29**, 1050–1058.
36 M. Bagheri, R. R. Nair, K. K. Singh and D. K. Saini, *Biochim. Biophys. Acta, Mol. Cell Res.*, 2017, **1864**, 177–190.
37 A. Sikora, J. Zielonka, M. Lopez, J. Joseph and B. Kalyanaraman, *Free Radical Biol. Med.*, 2009, **47**, 1401–1407.
38 C. Szabo, H. Ischiropoulos and R. Radi, *Nat. Rev. Drug Discovery*, 2007, **6**, 662–680.
39 J. Kim, J. Park, H. Lee, Y. Choi and Y. Kim, *Chem. Commun.*, 2014, **50**, 9353–9356.
40 J. Kim, G. Saravanakumar, H. W. Choi, D. Park and W. J. Kim, *J. Mater. Chem. B*, 2014, **2**, 341–356.
41 D. A. Riccio and M. H. Schoenfisch, *Chem. Soc. Rev.*, 2012, **41**, 3731–3741.
42 J. F. Quinn, M. R. Whittaker and T. P. Davis, *J. Controlled Release*, 2015, **205**, 190–205.
43 A. B. Seabra, R. de Lima and M. Calderon, *Curr. Top. Med. Chem.*, 2015, **15**, 298–308.
44 H.-J. Xiang, M. Guo, L. An, S.-P. Yang, Q.-L. Zhang and J.-G. Liu, *J. Mater. Chem. B*, 2016, **4**, 4667–4674.
45 H.-J. Xiang, L. An, W.-W. Tang, S.-P. Yang and J.-G. Liu, *Chem. Commun.*, 2015, **51**, 2555–2558.

Organic LETTERS

Letter

pubs.acs.org/OrgLett

Esterase Activated Carbonyl Sulfide/Hydrogen Sulfide (H_2S) Donors

Preeti Chauhan, Prerona Bora, Govindan Ravikumar, Swetha Jos, and Harinath Chakrapani*

Department of Chemistry, Indian Institute of Science Education and Research Pune, Dr. Homi Bhabha Road, Pashan Pune 411 008, Maharashtra, India

Supporting Information

ABSTRACT: Hydrogen sulfide (H_2S) is a mediator of a number of cellular processes, and modulating cellular levels of this gas has emerged as an important therapeutic area. Localized generation of H_2S is thus very useful but highly challenging. Here, we report pivaloyloxymethyl-based carbonothioates and carbamothioates that are activated by the enzyme, esterase, to generate carbonyl sulfide (COS), which is hydrolyzed to H_2S.

Gaseous entities such as nitric oxide (NO),[1] carbon monoxide (CO),[2,3] sulfur dioxide (SO_2)[4−6] and hydrogen sulfide (H_2S)[7] have emerged as major mediators of cellular processes and have therapeutic applications.[3] For example, H_2S is involved in regulating the homeostasis of various physiological systems which include−cardiovascular, neuronal, gastrointestinal, renal, liver and reproductive systems.[8−11] Modulating levels of H_2S within cells has tremendous impact on disease biology.[10,12,13] Thus, methodologies for controlled generation as well as dissipation assume importance.[14] Due to its gaseous nature, site-specific delivery of H_2S is challenging. A common strategy to deliver gaseous species is to mask them as organic or inorganic compounds that dissociate to generate the gas.[15] These compounds, known as H_2S donors, are widely used to generate this gas within cells and in animal models.[10,15,16] Due to the ubiquitous targets of H_2S, localized delivery of H_2S is highly desirable but remains a major hurdle. Site-directed delivery requires installation of a structural trigger in the H_2S donor which is cleaved by a metabolic stimulus to generate H_2S.[17−24]

Carbonyl sulfide (COS) is a naturally occurring gas that hydrolyzes to H_2S. This reaction is accelerated by the widely prevalent enzyme, carbonic anhydrase (CA).[25] Thus, generating COS within cells is a newly emerging and an attractive strategy to localize H_2S within cells. Recently, Pluth and co-workers reported a new class of H_2S generating small molecules that are triggered by H_2S.[26] These thiocarbamates generate COS, which undergoes hydrolysis to produce H_2S (Figure 1a).[27] Thiocarbamates were proposed as analytical tools for detection of H_2S and may aid in analyte homeostasis. Matson and co-workers, more recently, reported *N*-thiocarboxyanhydride (NTA) as a nucleophile activated COS/H_2S donor (Figure 1b).[25] Here, a nucleophile, such as an amine reacts with NTA to generate COS/H_2S. However, due to the ubiquitous nature of nucleophiles in various biological media, selectivity of this donor may be compromised. Our laboratory considered the possibility of using enzyme-activated donors of COS/H_2S. The use of enzymes to deliver drugs, latent fluorophores (for imaging), or biological species[28,29] has been widely used and

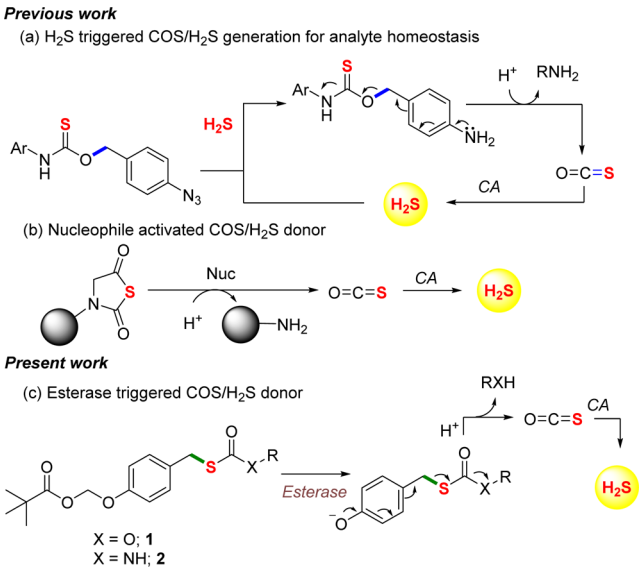

Figure 1. (a) Analyte homeostasis during H_2S detection is possible using azide-based thiocarbamates. (b) Nucleophile-activated COS/H_2S donors and their corresponding polymeric analogue. (c) Proposed enzyme-activated carbonothioate (**1**) and carbamothioate (**2**) COS/H_2S donors.

presents distinct advantages.[30] We considered carbonothioates (Figure 1c, **1**; X = O) as well as carbamothioates (Figure 1c, **2**; X = NH) as enzyme activated COS/H_2S donors. The significantly lower bond dissociation energy of a typical C−S bond (shown in green, Figure 1c) when compared with a C−O bond (shown in blue, Figure 1a) might facilitate the process of self-immolation.[31] It is anticipated that, upon activation, a carbonothioate (X = O) will dissociate rapidly in pH 7.4 buffer to produce COS and an alcohol (Figure 1c).

Received: November 7, 2016
Published: December 20, 2016

DOI: 10.1021/acs.orglett.6b03336
Org. Lett. 2017, 19, 62−65

In order to test if the nature of the leaving group X affects the rate of decomposition, carbamothioates (X = NH) were also considered (Figure 1c). Together, these compounds will offer an enzymatic trigger for H_2S generation and a better understanding of the nature of COS/H_2S donors. The enzyme that we chose was esterase (ES). Due to its wide occurrence in nearly all cells, this metabolic trigger will find broad use for the study of H_2S biology. The choice of a pivaloyloxymethyl group as the protective group will ensure rapid activation of the donor and help with localization of the bioactive molecule.[32]

In order to test this hypothesis, the thiol **4** was synthesized from **3** (Scheme 1). Reaction of **4** independently with **5a**, **5b**, and **5c** gave the desired compounds **1a**, **1b**, and **1c** (Table 1). Next, carbamothioates **2a**, **2b**, and **2c** were synthesized from the corresponding 4-nitrophenolates **6a**, **6b**, and **6c**, respectively by reaction with the thiol **4** (Table 1).[33]

Scheme 1. Synthesis of Thiol 4

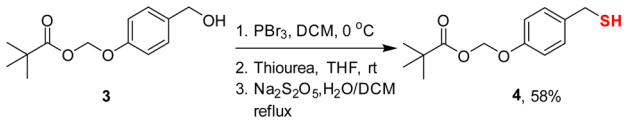

Table 1. Synthesis of Carbonothioates and Carbamothioates

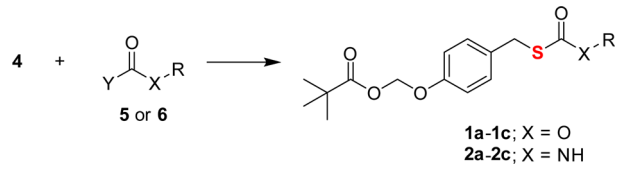

X	Y	R	reactant	prod	yield, %[a]
O	Cl	4-NO_2Ph	**5a**	**1a**	77
O	Cl	Ph	**5b**	**1b**	64
O	Cl	CH_2Ph	**5c**	**1c**	16
NH	OAr[b]	Ph	**6a**	**2a**	11
NH	OAr[b]	4-OMePh	**6b**	**2b**	44
NH	OAr[b]	CH_2Ph	**6c**	**2c**	37

[a]Unoptimized isolated yields. [b]Ar = 4-NO_2Ph.

(4-((4-Nitrophenoxy)methyl)phenoxy)methyl pivalate **7** was prepared and used as a negative control. This compound should be cleaved by esterases but will not produce COS. The formation of 4-nitrophenol (as in the case of **1a**) will serve as a colorimetric indicator for mechanistic investigations.

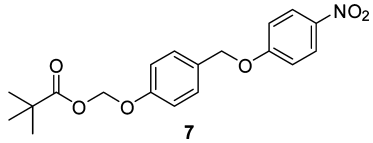

Using Dansyl-Azide (Dn-N_3), a H_2S-sensitive fluorogenic dye, the formation of H_2S was assessed. This probe is known to react with HS^- to produce dansylamine (Dn-NH_2), which has a distinct fluorescence signal at 535 nm (excitation 340 nm). When authentic H_2S was treated with Dn-N_3, we find a fluorescence signal at 535 nm (excitation 340 nm) for Dn-NH_2 (Figure 2a).[34] Compound **1a** was incubated in the presence of ES and CA for 1 h, followed by addition of Dn-N_3. A fluorescence signal at 535 nm was indicative of the capability of this compound to generate H_2S under these conditions (Figure 2a). All other compounds **1**–**2** were similarly found to generate H_2S under these conditions (Figure 2a). Compound **7**, which is expected to dissociate in the presence of ES but does not generate H_2S, did not show a significant signal attributable to Dn-NH_2 in this assay (Figure 2a). The formation of the Dn-NH_2 fluorophore (see Supporting Information (SI), Figures S1, S2) was also independently confirmed by HPLC analysis of a reaction mixture containing **1c**, ES, CA, and Dn-N_3 (Figure 2b). The formation of H_2S during decomposition was also inferred by a lead acetate assay.[35] Here, incubation of **1c** with ES and CA followed by addition of an aliquot to lead acetate paper showed a distinct dark coloration that is indicative of the formation of lead sulfide (see SI, Figure S3).

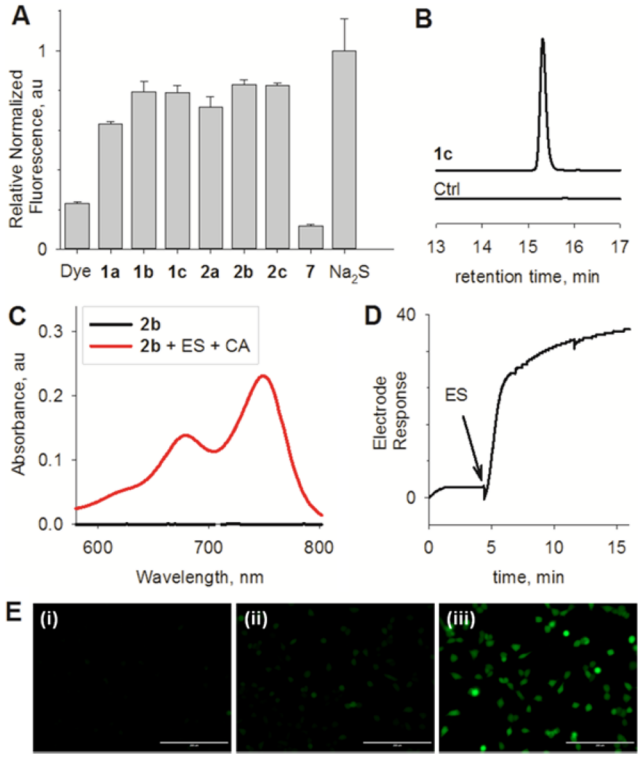

Figure 2. (a) H_2S yields were measured using a Dn-N_3-based assay. Compounds were incubated with ES and CA in pH 7.4 buffer for 60 min followed by addition of Dn-N_3. Fluorescence intensity at 535 nm (excitation 340 nm) was measured. (b) HPLC analysis of a reaction mixture consisting of **1c**, ES, CA, and Dn-N_3. Ctrl is Dn-N_3. Fluorescence detector was used: excitation 340 nm; emission 535 nm. Positive control: Na_2S (see SI, Figure S2). (c) Formation of methylene blue as determined by spectrophotometry during incubation of **2b** in the presence of ES and CA. Na_2S was used as the positive control in this experiment. (d) Representative trace for H_2S detection using a H_2S-sensitive electrode: **1a** was incubated in pH 7.4 buffer in the presence of CA. After 5 min, ES was added to the reaction mixture. (e) Representative images of MCF-7 cells. The H_2S-sensitive fluorogenic probe NBD-fluorescein (10 μM) was cotreated with (i) DMSO; (ii) **2b**, 50 μM; (iii) **2b**, 100 μM, for 40 min followed by imaging using a fluorescence microscope. Scale bar is 200 μm.

Independent verification of H_2S release from this class of compounds was carried out by a colorimetric assay where methylene blue formation is monitored (Figure 2c; see SI, Figure S5).[25] An absorbance profile that correlated well with authentic Na_2S was observed (see SI, Figure S4). When this experiment was carried out with acetazolamide, a known inhibitor of CA, we find nearly complete abrogation of the absorbance for methylene blue formation (see SI, Figure

DOI: 10.1021/acs.orglett.6b03336
Org. Lett. 2017, 19, 62−65

S6).[24,26] Lastly, carbonothioate **1a** was incubated with CA and a H_2S-selective electrode was used for detection of H_2S (Figure 2d). The formation of COS was verified by a reported mass spectrometry methodology, and a profile that is consistent with COS was recorded (see SI, Figure S7).[36]

The H_2S donors prepared herein were evaluated for their ability to inhibit proliferation of human breast cancer MCF-7 cells using a standard cell viability assay. We find no significant cytotoxicity at 25 μM (see SI, Figure S13). The H_2S generating capability of **2b** within cells was evaluated using a fluorogenic probe NBD-Fluorescein for H_2S (see SI, Figure S14).[37] Upon incubation of MCF-7 cells with this probe and subsequent treatment of cells with **2b**, we find a distinct fluorescence signal suggesting increased intracellular H_2S (Figure 2e). Together, these data support the formation of COS/H_2S under the assay conditions from donors prepared in this study and their compatibility for use in cellular studies.

Next, the kinetics of H_2S release from these compounds was studied. Using the Dn-N_3 method, the time course of Dn-NH_2 formation, which is a proxy for H_2S release, was monitored. A representative curve for H_2S release from **1a** is shown (see SI, Figure S1). The rate constant for H_2S release was found by fitting the initial rate data to first-order kinetics (see SI, Figure S1). The rate constants for H_2S release from **1a**, **1b**, and **1c** were found to be similar in magnitude suggesting no major dependence on the nature of the leaving group (see SI, Table S1, entries 1−3). In order to better understand the mechanism of decomposition (Scheme 2), the decomposition of **1a** was monitored by HPLC (see SI, Figure S8).

Scheme 2. Proposed Mechanism for Decomposition of Carbonothioates and Carbamothioates in the Presence of ES and CA

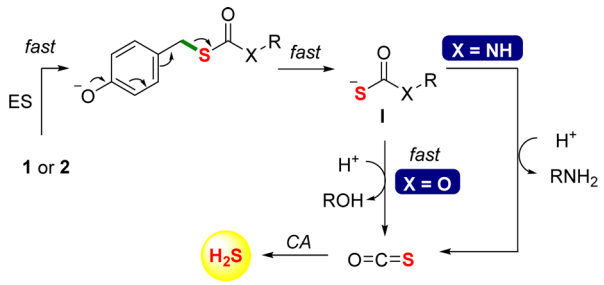

Upon addition of esterase, nearly complete disappearance of **1a** within 15 min was recorded suggesting that cleavage of the pivaloyloxymethyl group is fast.[32] During this study, concomitant formation of 4-nitrophenol was observed, which was confirmed by using an authentic sample of this compound (see SI, Figure S8). The time course of 4-nitrophenol formation during decomposition of **1a** was next independently recorded by spectrophotometry by monitoring the absorbance of 4-nitrophenol at 405 nm (see SI, Figure S9). The rate constant was found as 0.14 min^{-1}. When a similar experiment was conducted with **7** where 4-nitrophenol release does not involve the formation of COS, a comparable rate constant of 0.15 min^{-1} was recorded. Together, these data suggest the short-lived nature of intermediate I in the case of **1a**. Although the rate of 4-nitrophenol formation is faster than H_2S release as determined by Dn-NH_2 formation, these relatively small differences do not support significant accumulation of intermediate I (Scheme 2).[38] Next, H_2S release profiles of carbamothioates **2a**, **2b**, and **2c** in pH 7.4 buffer in the presence of ES and CA were recorded by using a similar Dn-N_3 assay. The relative rates for Dn-NH_2 formation during incubation of **2a** and **2b** were found to be comparable with those of **1a**−**1c** (see SI, Table S1, entries 4−5); it is thus likely that a similar mechanism is operational. The rate of H_2S release from **2b** was monitored by a methylene blue formation assay (see SI, Figure S5), and we found a similar rate when compared with the dansyl azide method.[39] HPLC analysis of the decomposition of **2b** (see SI, Figure S10) showed the formation of an intermediate (possibly I, Scheme 2) that decomposed to produce *p*-anisidine. Thus, rapid cleavage of the pivaloyloxymethyl group followed by self-immolation produces a short-lived intermediate I, which dissociates to produce COS. Hydrolysis of COS in the presence of CA produces H_2S.

When H_2S release from **2c** was monitored by the Dn-N_3 assay as well as methylene blue formation, we found a slower rate of release when compared with other compounds tested (see SI, Table S1 and Figure S5).[39] Decomposition of **2c** in the presence of ES was carried out: HPLC analysis revealed nearly complete disappearance of **2c** within 15 min suggesting the triggerable nature of this donor in the presence of the stimulus, esterase (see SI, Figure S11). An intermediate (possibly I, Scheme 2) was observed which gradually disappeared during the course of the reaction (see SI, Figure S12). We were unable to characterize this intermediate, but it appears that the rate of COS release may, in part, depend on the decomposition of this intermediate. Hence, the use of carbamothioates such as the ones developed in this work may offer distinct advantages in modulating H_2S release through stereoelectronic effects on the nitrogen.[40] Although these offer mechanistic insight, the differences among the release profiles are small, and in cellular experiments, the concentrations of these enzymes will, in part, determine the kinetics of H_2S release. Wang and co-workers reported an esterase triggered small molecule with tunable H_2S generating capability.[21] Here, the nature of the ester was modified to attain differences in rates of H_2S generation. The compounds prepared in our study can perhaps similarly be modified to achieve tunability. Furthermore, this scaffold is also amenable to incorporation of other triggers of interest that facilitate localized delivery of H_2S: Pluth and co-workers have reported a hydrogen peroxide inducible H_2S donor based on the thiocarbamate scaffold.[40] However, carbonothioates and carbamothioates prepared in this study, to our knowledge, have thus far not been reported as H_2S donors.[41]

In summary, we show that carbonothioates as well as carbamothioates can be suitably modified to be triggered to generate COS under physiologically relevant conditions. The importance of gaseous species in mediating cellular processes as well as close association with pathophysiological conditions has been widely studied. In order to better understand the precise roles of these gases, new and improved tools are necessary. While these tools are being developed, they are also being evaluated for their therapeutic potential. Numerous investigations have shown that H_2S has enormous potential but is limited by its toxicity. Therefore, being able to trigger H_2S generation intracellularly in a site of interest is of fundamental importance. Our data reveal that the cleavage of these compounds by esterase is rapid followed by generation of COS/H_2S. Although esterases are widely present in numerous cell types, this study lays the foundation for site-directed delivery of COS/H_2S.

DOI: 10.1021/acs.orglett.6b03336
Org. Lett. 2017, 19, 62−65

■ ASSOCIATED CONTENT

Supporting Information

The Supporting Information is available free of charge on the ACS Publications website at DOI: 10.1021/acs.orglett.6b03336.

Preparative procedures, characterization data, and spectra (PDF)

■ AUTHOR INFORMATION

Corresponding Author

*E-mail: harinath@iiserpune.ac.in.

ORCID

Harinath Chakrapani: 0000-0002-7267-0906

Notes

The authors declare no competing financial interest.

■ ACKNOWLEDGMENTS

The authors thank the Department of Science and Technology (DST, Grant No. EMR/2015/000668) and Council for Scientific and Industrial Research (CSIR) for financial support.

■ REFERENCES

(1) Heinrich, T. A.; da Silva, R. S.; Miranda, K. M.; Switzer, C. H.; Wink, D. A.; Fukuto, J. M. *Br. J. Pharmacol.* **2013**, *169*, 1417.
(2) Wu, L.; Wang, R. *Pharmacol. Rev.* **2005**, *57*, 585.
(3) Szabo, C. *Nat. Rev. Drug Discovery* **2015**, *15*, 185.
(4) Malwal, S. R.; Gudem, M.; Hazra, A.; Chakrapani, H. *Org. Lett.* **2013**, *15*, 1116.
(5) Day, J. J.; Yang, Z.; Chen, W.; Pacheco, A.; Xian, M. *ACS Chem. Biol.* **2016**, *11*, 1647.
(6) Malwal, S. R.; Sriram, D.; Yogeeswari, P.; Konkimalla, V. B.; Chakrapani, H. *J. Med. Chem.* **2012**, *55*, 553.
(7) Gadalla, M. M.; Snyder, S. H. *J. Neurochem.* **2010**, *113*, 14.
(8) Wang, R. *Physiol. Rev.* **2012**, *92*, 791.
(9) Wang, R. *Antioxid. Redox Signaling* **2003**, *5*, 493.
(10) Wallace, J. L.; Wang, R. *Nat. Rev. Drug Discovery* **2015**, *14*, 329.
(11) Ianaro, A.; Cirino, G.; Wallace, J. L. *Pharmacol. Res.* **2016**, *111*, 652.
(12) Chegaev, K.; Rolando, B.; Cortese, D.; Gazzano, E.; Buondonno, I.; Lazzarato, L.; Fanelli, M.; Hattinger, C. M.; Serra, M.; Riganti, C.; Fruttero, R.; Ghigo, D.; Gasco, A. *J. Med. Chem.* **2016**, *59*, 4881.
(13) McCune, C. D.; Chan, S. J.; Beio, M. L.; Shen, W.; Chung, W. J.; Szczesniak, L. M.; Chai, C.; Koh, S. Q.; Wong, P. T. H.; Berkowitz, D. B. *ACS Cent. Sci.* **2016**, *2*, 242.
(14) Shatalin, K.; Shatalina, E.; Mironov, A.; Nudler, E. *Science* **2011**, *334*, 986.
(15) Zhao, Y.; Biggs, T. D.; Xian, M. *Chem. Commun.* **2014**, *50*, 11788.
(16) Caliendo, G.; Cirino, G.; Santagada, V.; Wallace, J. L. *J. Med. Chem.* **2010**, *53*, 6275.
(17) Zhao, Y.; Kang, J.; Park, C.-M.; Bagdon, P. E.; Peng, B.; Xian, M. *Org. Lett.* **2014**, *16*, 4536.
(18) Devarie-Baez, N. O.; Bagdon, P. E.; Peng, B.; Zhao, Y.; Park, C.-M.; Xian, M. *Org. Lett.* **2013**, *15*, 2786.
(19) Zhao, Y.; Wang, H.; Xian, M. *J. Am. Chem. Soc.* **2011**, *133*, 15.
(20) Kang, J.; Li, Z.; Organ, C. L.; Park, C.-M.; Yang, C.-t.; Pacheco, A.; Wang, D.; Lefer, D. J.; Xian, M. *J. Am. Chem. Soc.* **2016**, *138*, 6336.
(21) Zheng, Y.; Yu, B.; Ji, K.; Pan, Z.; Chittavong, V.; Wang, B. *Angew. Chem., Int. Ed.* **2016**, *55*, 4514.
(22) Fukushima, N.; Ieda, N.; Kawaguchi, M.; Sasakura, K.; Nagano, T.; Hanaoka, K.; Miyata, N.; Nakagawa, H. *Bioorg. Med. Chem. Lett.* **2015**, *25*, 175.
(23) Foster, J. C.; Powell, C. R.; Radzinski, S. C.; Matson, J. B. *Org. Lett.* **2014**, *16*, 1558.
(24) Fukushima, N.; Ieda, N.; Sasakura, K.; Nagano, T.; Hanaoka, K.; Suzuki, T.; Miyata, N.; Nakagawa, H. *Chem. Commun.* **2014**, *50*, 587.
(25) Powell, C. R.; Foster, J. C.; Okyere, B.; Theus, M. H.; Matson, J. B. *J. Am. Chem. Soc.* **2016**, *138*, 13477.
(26) Steiger, A. K.; Pardue, S.; Kevil, C. G.; Pluth, M. D. *J. Am. Chem. Soc.* **2016**, *138*, 7256.
(27) Smeulders, M. J.; Pol, A.; Venselaar, H.; Barends, T. R. M.; Hermans, J.; Jetten, M. S. M.; Op den Camp, H. J. M. *J. Bacteriol.* **2013**, *195*, 4046.
(28) Sharma, K.; Chakrapani, H. *Nitric Oxide* **2014**, *43*, 8.
(29) Sharma, K.; Iyer, A.; Sengupta, K.; Chakrapani, H. *Org. Lett.* **2013**, *15*, 2636.
(30) Saavedra, J. E.; Shami, P. J.; Wang, L. Y.; Davies, K. M.; Booth, M. N.; Citro, M. L.; Keefer, L. K. *J. Med. Chem.* **2000**, *43*, 261.
(31) Hadad, C. M.; Rablen, P. R.; Wiberg, K. B. *J. Org. Chem.* **1998**, *63*, 8668.
(32) Leroy, E.; Bensel, N.; Reymond, J.-L. *Bioorg. Med. Chem. Lett.* **2003**, *13*, 2105.
(33) Sankar, R. K.; Kumbhare, R. S.; Dharmaraja, A. T.; Chakrapani, H. *Chem. Commun.* **2014**, *50*, 15323.
(34) Peng, H.; Cheng, Y.; Dai, C.; King, A. L.; Predmore, B. L.; Lefer, D. J.; Wang, B. *Angew. Chem., Int. Ed.* **2011**, *50*, 9672.
(35) Megraud, F.; Bonnet, F.; Garnier, M.; Lamouliatte, H. *J. Clin. Microbiol.* **1985**, *22*, 1007.
(36) Tanc, M.; Carta, F.; Scozzafava, A.; Supuran, C. T. *ACS Med. Chem. Lett.* **2015**, *6*, 292.
(37) Wei, C.; Zhu, Q.; Liu, W.; Chen, W.; Xi, Z.; Yi, L. *Org. Biomol. Chem.* **2014**, *12*, 479.
(38) Elliott, S.; Lu, E.; Rowland, F. S. *Environ. Sci. Technol.* **1989**, *23*, 458.
(39) Morcos, E. F.; Kussrow, A.; Enders, C.; Bornhop, D. *Electrophoresis* **2010**, *31*, 3691. Although Dn-NH_2 is known to inhibit CA, we find that the rate of H_2S release from **2b** as independently determined by the Dn-N_3 and methylene blue methods are comparable (see SI, Figure S5). The origin of this effect is not clear, but as expected, a known CA inhibitor (acetazolamide) slows down H_2S release from **2b** (see SI, Figure S6).
(40) Zhao, Y.; Pluth, M. D. *Angew. Chem.* **2016**, *128*, 14858.
(41) The formation of a *p*-quinone-methide intermediate may potentially limit the utility of the compounds reported here as well as the ones reported in ref 40.

DOI: 10.1021/acs.orglett.6b03336
Org. Lett. 2017, 19, 62−65

Organic LETTERS

Letter

Cite This: Org. Lett. 2018, 20, 4−7

pubs.acs.org/OrgLett

Esterase Sensitive Self-Immolative Sulfur Dioxide Donors

Kundansingh A. Pardeshi, Govindan Ravikumar, and Harinath Chakrapani*

Department of Chemistry, Indian Institute of Science Education and Research Pune, Dr. Homi Bhabha Road, Pune 411 008, Maharashtra, India

Supporting Information

ABSTRACT: A series of cell-permeable esterase-sensitive sulfonates that undergo self-immolation to produce sulfur dioxide (SO_2), a gaseous pollutant with new and emerging biological roles, is reported. These compounds should facilitate the study SO_2 biology and will lay the platform for newer stimuli-responsive donors of this gas.

Gaseous signaling molecules derived from nitrogen, carbon, and sulfur are ubiquitous in nature and are emerging as major modulators of diverse physiological processes.[1] For example, hydrogen sulfide (H_2S) has numerous roles in neuromodulation, pathogen response to antibiotics,[2] and blood vessel relaxation. Sulfur dioxide (SO_2),[3] a potential product of oxidation of H_2S, similarly has recently assumed importance as a mediator of cellular processes.[4] SO_2 is widely used in the food industry as a preservative and as an antibacterial agent.[5] At diminished concentrations, SO_2 can mediate signaling such as vasodilation.[6] However, at elevated concentrations, SO_2 can damage biomacromolecules such as DNA, especially in the presence of metal ions.[7−9] Thus, controlled generation of this gaseous molecule has enormous potential but is challenging.

Biochemical and cellular experiments carried out with gaseous SO_2 are somewhat unreliable, associated with potential variations, and have limited therapeutic potential. The most commonly used inorganic donor of sulfite, which is a mixture of sulfite and bisulfite has limited permeability and is thus used in high millimolar concentrations.[5,6] These elevated concentrations may compromise appropriate interpretations regarding the effects of SO_2. Thus, small molecule donors of this gas assume importance.[10] Our laboratory reported benzosultines as donors of SO_2 under ambient physiological pH conditions (Figure 1).[11] These donors spontaneously undergo retro Diels−Alder to generate SO_2 with moderately tunable rates. Binghe Wang and co-workers have recently shown a "click and release" strategy for generation of sulfur dioxide (Figure 1).[12,13] These donors have the unique advantage of having a wide range of rates of SO_2 generation. However, these donors are more akin to spontaneous donors of SO_2 and again, incorporation of a trigger will help in controlling delivery of this gas. Xian and co-workers have recently reported a sulfinate which undergoes hydrolysis to produce SO_2.[14] They have also shown the vasodilatory effects of this molecule underscoring the importance of controlled generation of SO_2. However, this donor does not contain a physiological trigger and this may be a limitation for further exploitation of therapeutic potential of this gas.

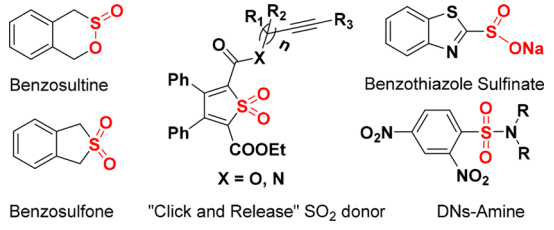

Figure 1. Representative examples of sulfur dioxide donors.

Photolabile SO_2 donors have also been reported. Benzosulfones were found to be photolabile under ultraviolet irradiation conditions to produce SO_2.[15] A similar class of phototriggerable SO_2 donors were reported by Uchida and co-workers.[16] The use of ultraviolet light, however, has limited utility and may be harmful to cells due to phototoxicity. Our laboratory has reported 2,4-dinitrophenylsulfonamides (DNs-Amine) as thiol-activated sulfur dioxide donors (Figure 1).[17−19] While these donors have triggerable SO_2 donation, the use of thiols, which are a major antioxidant within cells, as triggers may not be useful to study SO_2, a redox-active gaseous species. It is thus desirable to have a relatively innocuous stimulus such as esterase (ES) to trigger SO_2 generation within cells.

In order to design a new class of esterase-sensitive SO_2 donors, we considered the chemistry associated with decomposition of carbonates, which have been extensively used for drug delivery and they operate by generation of carbon dioxide (CO_2), which presumably is an irreversible reaction. An appropriately placed trigger and subsequent self-immolation can produce CO_2 from a carbonate (Scheme 1a). The key bond that breaks is the C−O bond shown by an arrow, whose estimated bond dissociation energy (BDE) is 68 kcal·mol^{-1}. Similarly, it was envisaged that cleavage of a C−S bond in sulfonates (shown by an arrow) will similarly trigger generation of SO_2 and an alcohol. The BDE of this bond is estimated to be 57 kcal·mol^{-1}, which is comparable with the C−O bond.[20] If successful, such a method may have broad relevance as a probe for SO_2 biology as well as a methodology for codelivery of an alcohol-based drug. Further-

Received: August 17, 2017
Revised: December 2, 2017
Published: December 13, 2017

DOI: 10.1021/acs.orglett.7b02544
Org. Lett. 2018, 20, 4−7

Scheme 1. (a) Esterase-Cleavable Carbonate Should Generate CO_2 and an Alcohol (1a, R = Umbelliferone (Figure 2)); (b) Proposed Esterase Cleavable Sulfonates That Are Expected To Generate SO_2 and an Alcohol

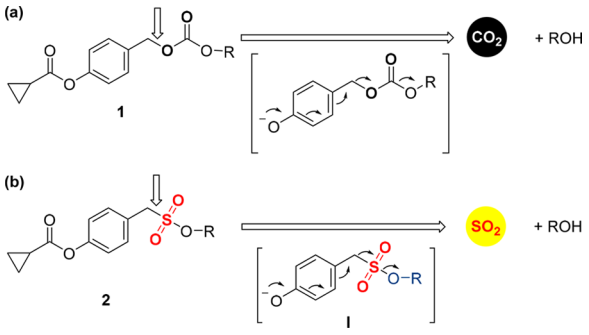

more, the nature of the leaving group i.e. the alcohol may determine the SO_2 generation capability.

In order to test this hypothesis, first, the fluorophore umbelliferone (Umb, Figure 2) was derivatized. The carbonate

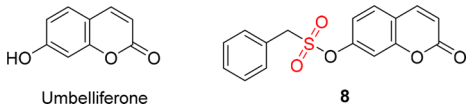

Figure 2. Structures of umbelliferone and **8**.

1a (Scheme 1a) was synthesized (see the SI). Due to the improved hydrolytic stability of cyclopropyl esters when compared with other aliphatic esters, this ester was chosen.[21,22] The pivaloyloxymethyl group was not considered as sulfite is known to react with formaldehyde, a byproduct of decomposition.[23] In order to synthesize the sulfonate **2a**, first, the aldehyde **3** was synthesized from 4-hydroxybenzaldehyde (Scheme 2) Reduction with sodium borohydride gave **4**, which

Scheme 2. Synthesis of the Sulfonyl Chloride 6

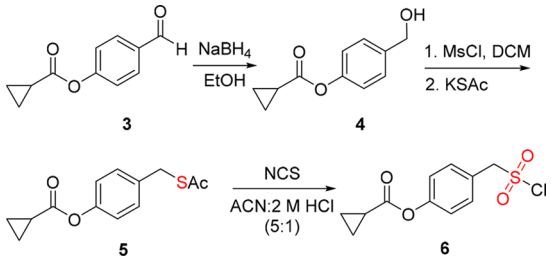

was then converted to the thioacetate **5** in two steps. The thioacetate was treated with *N*-chlorosuccinamide to afford the sulfonyl chloride **6**.[24] Treatment of **6** with umbelliferone (Figure 2) gave **2a** (Table 1). The structure of **2a** was confirmed by X-ray diffraction analysis of crystalline material (see Figure S1).

The carbonate **1a** and the sulfonate **2a** were independently treated with esterase.[22,25] HPLC analysis of the reaction mixture after 10 min revealed complete disappearance of the **1a** (see Figure S2). The disappearance of **2a** (Figure 3a) was somewhat slower when compared with **1a** (0.54 ± 0.08 min^{-1}). The rate constant was found to be 0.13 min^{-1} and the half-life was 5 min. This rate is comparable with the formation of umbelliferone, 0.18 min^{-1} monitored under similar conditions (Figure 3b). The yield

Table 1. Synthesis of Sulfonates 2a−k

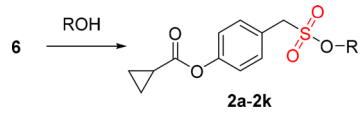

R	pK_a of ROH[a]	product	yield (%)
umbelliferone	7.7	**2a**	50
Ph	9.9	**2b**	75
4-OMePh	10.2	**2c**	65
4-NO_2Ph	7.1	**2d**	70
(2-*tert*-b	10.2	**2e**	65
(3,5-dimethyl-4-Cl)Ph	9.4	**2f**	72
Bn	15.4	**2g**	23
allyl	15.5	**2h**	27
propargyl	13.6	**2i**	24
n-butyl	16.0	**2j**	53
*i*Pr	17.0	**2k**	44

[a]Values are from literature and are either for the compound itself or analogues with similar structures. References 27−31.

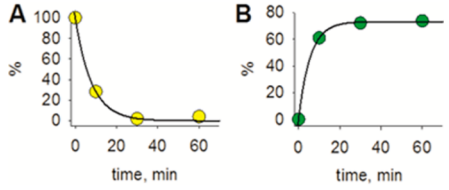

Figure 3. (a) HPLC analysis of **2a**. Compound **2a** (50 μM) in PBS (pH 7.4, 10 mM) at 37 °C was incubated in the presence of esterase showed the disappearance of **2a**. Rate constant for disappearance was found as 0.13 ± 0.01 min^{-1}. (b) HPLC analysis of the reaction mixture for Umb. Rate constant for appearance of Umb was found as 0.18 ± 0.006 min^{-1} (for a detailed protocol, see the SI).

of Umb was 80% suggesting an efficient conversion of **2a** to Umb in the prescence of esterase.

A coumarin−hemicyanine dye **7** (Scheme 3),[26] for colorimetric as well as fluorescence-based detection of sulfite (SO_3^{2-}), the

Scheme 3. Dye 7 and the Adduct It Forms upon Reaction with Sulfite

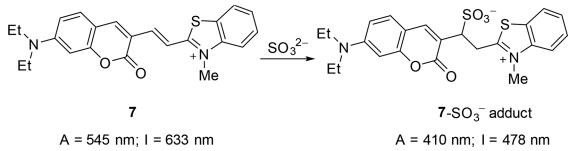

hydrated form of SO_2, was synthesized using reported procedures. This probe has been found to be useful in in vitro as well as cellular studies to detect SO_2. The dye **7** reacts with sulfite to produce a covalent adduct (Scheme 3). This results in a characteristic decrease in absorbance at 545 nm with concomitant increase in the absorbance signal at 410 nm (Figure 4a). In the presence of **2a** and esterase, a decrease in the absorbance at 545 nm was seen (Figure 4b). Due to the significant absorbance of Umb at 410 nm, the use of **7** to accurately determine sulfite is not possible. However, based on the diminution of the absorbance at 545 nm, the generation of sulfite during decomposition of **2a** in the presence of esterase was inferred (see Figure S6).

In the absence of esterase, no significant decomposition of **1a** or **2a** was observed (see Figure S3), suggesting that the cyclopropylester is not susceptible to hydrolysis. When **2a** was

DOI: 10.1021/acs.orglett.7b02544
Org. Lett. 2018, 20, 4−7

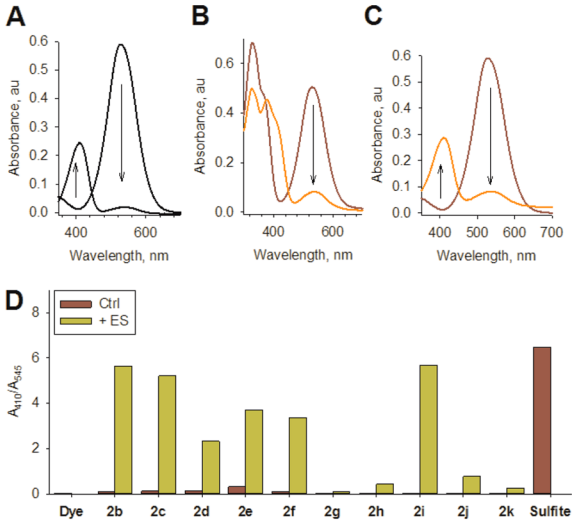

Figure 4. (a) Incubation of **7** (10 μM) in the presence of $NaHSO_3$ (50 μM) for 15 min shows a decrease in absorbance at 545 nm and a corresponding increase in absorbance at 410 nm.; (b) Incubation of **2a** + ES in the presence of **7** (10 μM) for 15 min. Disappearance of the 545 nm signal was observed and is indicative of sulfite formation. Concentration of **2a** was 50 μM. This experiment was carried out in the presence of Umb (see Figure S6). (c) Incubation of **7** (10 μM) in the presence of **2e** + ES for 15 min shows an absorbance profile comparable with $NaHSO_3$. (d) Ratio of absorbance at 410 nm (A_{410}) to the absorbance at 545 nm (A_{545}) during incubation of **7** with various compounds (Ctrl) and in the presence of ES (see Figure S7). Concentration of **2e** was 50 μM. All of the experiments were conducted in PBS (pH 7.4, 10 mM) at 37 °C (for a detailed protocol, see the SI).

pretreated with an esterase inhibitor (phenylmethanesulfonyl fluoride, PMSF)[32] and subsequent exposure to ES, a diminished signal for Umb was observed (see Figure S4). Preincubation of ES with PMSF and subsequent addition of **2a** showed a dose-dependent decrease in fluorescence, again supporting catalysis by esterase is necessary for activation of **2a** (see Figure S4, inset). In the presence of common biological nucleophiles, **2a** was found to be stable (see Figure S4). In basic pH (9.2), significant formation of Umb from the hydrolysis of the carbonate was observed; while the sulfonate remained stable. This enhanced stability of the sulfonate may present opportunities for delivering SO_2-based hybrid drugs.

In order to study the reactivity of the sulfonate functional group toward esterase, compound **8** (Figure 2) was synthesized. When treated with esterase, no significant fluorescence signal corresponding to Umb formation was recorded (see Figure S4). A similar result was observed in human cervical cancer HeLa cell lysate during 1 h suggesting that the sulfonate group is stable under cellular conditions (see Figure S5). Incubation of **2a**, as expected, produced a fluorescence signal confirming the production of Umb. Taken together, our data supports the selectivity of cleavage by esterase and the broad-range stability of the sulfonate group to cellular nucleophiles.

Having established that **2a** was capable of undergoing self-immolation in the presence of esterase to generate SO_2, we next proceeded to study the effect of the leaving group on this process. A series of aromatic alcohols were independently reacted with **6** to produce the corresponding sulfonates **2b**–**f** (Table 1). Again, the SO_2-sensitive dye **7** was used to assess the capability of these compounds to generate SO_2. These compounds were next exposed to esterase in the presence of the dye **7**. A representative absorbance profile for **2e** is shown in Figure 4c. The ratio of absorbance at 410 nm (A_{410}) to the absorbance at 545 nm (A_{545}) provides an estimate of the ability of the compound to produce SO_2. Colorimetric analysis revealed that all the aforementioned compounds were capable of generating sulfite. The dye **7** is also used as a sulfite-sensitive fluorescence probe: the free probe displayed a red emission with the maximum at 633 nm (excitation at 545 nm). In the presence of sulfite, the fluorescence signal at this wavelength is diminished with a concomitant increase in a new blue emission peak at 478 nm (excitation at 410 nm). I_{478}/I_{633} is hence a measure of SO_2 donating capability. The fluorescence data corroborated the absorbance data that was obtained with the donors. Together, our data supports a mechanism of ester hydrolysis leading to formation of intermediate I, which undergoes self-immolation to produce an alkoxide and a quinone methide (Scheme 4).

Scheme 4. Mechanism of Generation of SO_2 from Sulfonates[a]

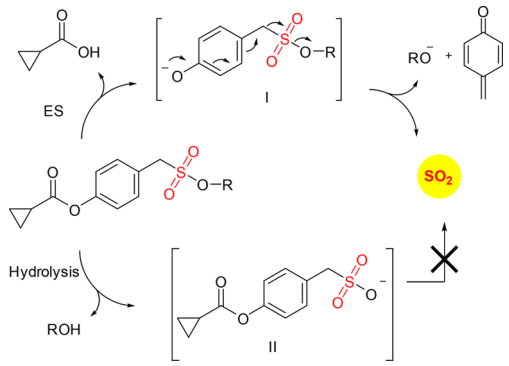

[a]For sulfonates derived from aromatic alcohols, SO_2 generation is dominant. Certain sulfonates derived from aliphatic alcohols were susceptible to hydrolysis (through II) and were poor SO_2 donors or are possibly trapped as intermediate I.

Next, sulfonates **2g**–**k**, which are derived from aliphatic alcohols were synthesized. When estimated for SO_2 in the presence of esterase, **2g**, **2h**, and **2k** did not show a significant shift in the absorbance profile, and accordingly, the ratio of A_{410}/A_{545} was diminished (Figure 4d). This data suggests that these compounds are poor donors of SO_2 when compared with their counterparts. Being aliphatic alcohols (Scheme 4), their leaving group ability is significantly lower than aromatic alcohols and this may contribute to diminished yield (see Table 1 for pK_a values). Prolonged incubation in buffer of these reaction mixtures also did not produce significant levels of sulfite. Since the cyclopropyl ester is stable toward hydrolysis in pH 7.4 buffer, the propensity for the sulfonate group to undergo hydrolysis to produce II was next examined. Compounds **2g**–**k** were independently incubated in pH 7.4 buffer, and we found that all compounds except for the benzyl and allyl compounds were stable toward hydrolysis (see Figure S12). When the benzyl derivative was incubated in buffer, nearly complete disappearance in 30 min was seen. While partial hydrolysis was observed in the case of the allyl derivative, this data suggested that certain sulfonates were susceptible to hydrolysis. Thus, among aliphatic alcohol-derived sulfonates, SO_2 generation after activation by esterase is possible provided the sulfonate is not susceptible to hydrolysis and if the alcohol was a good leaving group (such as propargyl alcohol).

Next, we investigated the capability of the SO_2 donors to permeate cells and generate SO_2. Accordingly, the dye **7** was used

DOI: 10.1021/acs.orglett.7b02544
Org. Lett. 2018, 20, 4–7

in A549 lung carcinoma cells. In the presence of sulfite (200 μM), a distinct increase in the signal in the blue channel with concomitant decrease in signal in the red channel was observed (Figure 5 and Figure S13). The SO_2 donors **2c** was similarly found

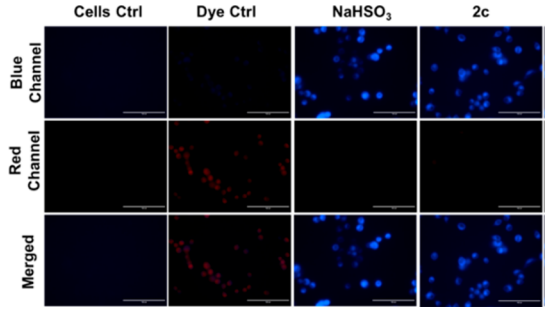

Figure 5. Fluorescence microscopy images of A549 cells treated with dye for 30 min and followed by treatment of the compound for 30 min in PBS (pH 7.4, 10 mM) at 37 °C. Fluorescence signal was monitored in red channel (**7**) and the blue channel (**7**-SO_3^- adduct). Final concentrations of dye **7** was 10 μM; $NaHSO_3$, 200 μM; sulfonates, 25 μM. Scale bar = 200 μm (for a detailed protocol, see the SI).

to fluoresce in the blue channel but at a much lower concentration (25 μM) suggesting their superior capability to generate sulfite within cells. Compounds **2g** and **2h**, which were poor SO_2 donors in the presence of esterase were similarly found to be incapable of generating SO_2 within cells. Lastly, the cytotoxicity of these compounds was estimated using two different cell lines and a majority of these compounds were not significantly cytotoxic (see Figure S14 for A549 cells and Figure S15 for HeLa cells). The likely byproducts that were produced during decomposition of SO_2 donors **2c** and **2i** were not cytotoxic either (see Figure S16). Thus, the SO_2 donors prepared in this study are cell-permeable and appear to be well tolerated by cells and should facilitate a better understanding of the biology of this gas.[33]

■ ASSOCIATED CONTENT

Supporting Information

The Supporting Information is available free of charge on the ACS Publications website at DOI: 10.1021/acs.orglett.7b02544.

Synthesis, characterization data, protocols for assays, and X-ray data for **2a** (PDF)

Accession Codes

CCDC 1585422 contains the supplementary crystallographic data for this paper. These data can be obtained free of charge via www.ccdc.cam.ac.uk/data_request/cif, or by emailing data_request@ccdc.cam.ac.uk, or by contacting The Cambridge Crystallographic Data Centre, 12 Union Road, Cambridge CB2 1EZ, UK; fax: +44 1223 336033.

■ AUTHOR INFORMATION

Corresponding Author

*E-mail: harinath@iiserpune.ac.in.

ORCID

Harinath Chakrapani: 0000-0002-7267-0906

Notes

The authors declare no competing financial interest.

■ ACKNOWLEDGMENTS

We thank the Department of Science and Technology (DST, Grant No. EMR/2015/000668) and the Council for Scientific and Industrial Research (CSIR) for financial support.

■ REFERENCES

(1) Wang, R. *Physiol. Rev.* **2012**, *92*, 791.
(2) Shukla, P.; Khodade, V. S.; SharathChandra, M.; Chauhan, P.; Mishra, S.; Siddaramappa, S.; Pradeep, B. E.; Singh, A.; Chakrapani, H. *Chem. Sci.* **2017**, *8*, 4967.
(3) Li, L.; Rose, P.; Moore, P. K. *Annu. Rev. Pharmacol. Toxicol.* **2011**, *51*, 169.
(4) Meng, Z.; Li, J.; Zhang, Q.; Bai, W.; Yang, Z.; Zhao, Y.; Wang, F. *Inhalation Toxicol.* **2009**, *21*, 1223.
(5) Garcia-Alonso, B.; Pena-Egido, M. J.; Garcia-Moreno, C. *J. Agric. Food Chem.* **2001**, *49*, 423.
(6) Yao, Q.; Huang, Y.; Liu, A. D.; Zhu, M.; Liu, J.; Yan, H.; Zhang, Q.; Geng, B.; Gao, Y.; Du, S.; Huang, P.; Tang, C.; Du, J.; Jin, H. *Am. J. Physiol. Regul. Integr. Comp. Physiol.* **2016**, *310*, R1073.
(7) Meng, Z.; Qin, G.; Zhang, B.; Bai, J. *Mutagenesis* **2004**, *19*, 465.
(8) Shi, X. *J. Inorg. Biochem.* **1994**, *56*, 155.
(9) Shi, X. L.; Mao, Y. *Biochem. Biophys. Res. Commun.* **1994**, *205*, 141.
(10) Bisseret, P.; Blanchard, N. *Org. Biomol. Chem.* **2013**, *11*, 5393.
(11) Malwal, S. R.; Gudem, M.; Hazra, A.; Chakrapani, H. *Org. Lett.* **2013**, *15*, 1116.
(12) Ji, X.; El-labbad, E. M.; Ji, K.; Lasheen, D. S.; Serya, R. A. T.; Abouzid, K. A.; Wang, B. *Org. Lett.* **2017**, *19*, 818.
(13) Wang, W.; Ji, X.; Du, Z.; Wang, B. *Chem. Commun.* **2017**, *53*, 1370.
(14) Day, J. J.; Yang, Z.; Chen, W.; Pacheco, A.; Xian, M. *ACS Chem. Biol.* **2016**, *11*, 1647.
(15) Malwal, S. R.; Chakrapani, H. *Org. Biomol. Chem.* **2015**, *13*, 2399.
(16) Kodama, R.; Sumaru, K.; Morishita, K.; Kanamori, T.; Hyodo, K.; Kamitanaka, T.; Morimoto, M.; Yokojima, S.; Nakamura, S.; Uchida, K. *Chem. Commun.* **2015**, *51*, 1736.
(17) Malwal, S. R.; Sriram, D.; Yogeeswari, P.; Chakrapani, H. *Bioorg. Med. Chem. Lett.* **2012**, *22*, 3603.
(18) Malwal, S. R.; Sriram, D.; Yogeeswari, P.; Konkimalla, V. B.; Chakrapani, H. *J. Med. Chem.* **2012**, *55*, 553.
(19) Pardeshi, K. A.; Malwal, S. R.; Banerjee, A.; Lahiri, S.; Rangarajan, R.; Chakrapani, H. *Bioorg. Med. Chem. Lett.* **2015**, *25*, 2694.
(20) Yu, H.-Z.; Fu, F.; Zhang, L.; Fu, Y.; Dang, Z.-M.; Shi, J. *Phys. Chem. Chem. Phys.* **2014**, *16*, 20964.
(21) Leroy, E.; Bensel, N.; Reymond, J.-L. *Bioorg. Med. Chem. Lett.* **2003**, *13*, 2105.
(22) Zheng, Y.; Yu, B.; Ji, K.; Pan, Z.; Chittavong, V.; Wang, B. *Angew. Chem., Int. Ed.* **2016**, *55*, 4514.
(23) Kovacs, K.; McIlwaine, R.; Gannon, K.; Taylor, A. F.; Scott, S. K. *J. Phys. Chem. A* **2005**, *109*, 283.
(24) Nishiguchi, A.; Maeda, K.; Miki, S. *Synthesis* **2006**, *2006*, 4131.
(25) Chauhan, P.; Bora, P.; Ravikumar, G.; Jos, S.; Chakrapani, H. *Org. Lett.* **2017**, *19*, 62.
(26) Sun, Y.-Q.; Liu, J.; Zhang, J.; Yang, T.; Guo, W. *Chem. Commun.* **2013**, *49*, 2637.
(27) Albert, A.; Serjeant, E. P. *The Determination of Ionization Constants: A Laboratory Manual*; Chapman and Hall: London, 1984.
(28) Nakagawa, Y.; Uehara, K.; Mizuno, N. *Inorg. Chem.* **2005**, *44*, 9068.
(29) Perrin, D. D. *Dissociation Constants of Organic Bases in Aqueous Solution*; Butterworths: London, 1965.
(30) Perrin, D. D.; Dempsey, B.; Serjeant, E. P. *pK_a Prediction for Organic Acids and Bases*; Chapman and Hall: London; New York, 1981.
(31) Williams, M. *Drug Dev. Res.* **2006**, *67*, 870.
(32) Smith, P. C.; McDonagh, A. F.; Benet, L. Z. *J. Pharmacol. Exp. Ther.* **1990**, *252*, 218.
(33) Wang, W.; Wang, B. *Chem. Commun.* **2017**, *53*, 10124.

DOI: 10.1021/acs.orglett.7b02544
Org. Lett. 2018, 20, 4−7